THE UNIVERSITY
of EDINBURGH

BMP-SMAD1/4 upregulates HNF4α in a subset of heterogeneous mouse pancreatic cancer cells while under metabolic stress

By Man-Yeung Heung

Doctor of Philosophy

College of Medicine and Veterinary Medicine

The University of Edinburgh

2013

Declaration

I declare that all the work in this thesis was performed personally unless stated otherwise. No part of this work has been submitted for consideration as part of any other degree or award.

Man-Yeung Heung

22 January 2013 (submission for viva)
14 August 2013 (with post-viva corrections)

ABSTRACT

It is not known whether pancreatic cancers evolve from a single or multiple cells, or from a particular pancreatic lineage. However, in the *Pdx1*-Cre; *LSL-Kras*^{G12D}; *LSL-Tp53*^{R172H} mouse model of pancreatic cancer, all pancreatic lineages are susceptible to express mutant KRas and p53. Hence, such mouse model implies a scenario of maximal heterogeneity of cancer cell origins. On this basis, I isolated seven sub-clones of heterogeneous mouse pancreatic cancer cells from a single tumour; each of them had a distinct morphology and gene expression profile. Notably, they possessed different intrinsic phospho-SMADs downstream of the TGFβ receptor (phospho-SMAD2/3) or the BMP receptor (Phospho-SMAD1/5/8). I discovered that SMAD4, a co-SMAD which is frequently found to be lost in pancreatic caner tissues, upregulated HNF4α via the classical BMP-SMAD1 pathway, when cells were experiencing metabolic stress upon deprivation of serum, or in the presence of excess thymidine. Under serum starvation at a hypoglycemic-like glucose concentration, the HNF4α-expressing sub-clones appeared to be more able to sustain an unstressed morphology than other non-HNF4α-expressing sub-clones. Immunohistochemical staining on pancreatic cancer sections revealed nuclear co-localization of SMAD4 and HNF4α in human (half of the cases) and in mouse samples. As a secondary project conducted during characterization of cells, I also found that three of the sub-clones more robustly proliferated under anchorage independent conditions, and they relied on the MEK-ERK pathway and the canonical Wnt pathway, to a different degree. Both studies demonstrate for the first time in primary cell culture that pancreatic cancer cells within a tumour could be highly heterogeneous in terms of both morphology and signaling pathways.

ACKNOWLEDGEMENTS

First of all, I would like to thank my supervisors, Margaret Frame and Valerie Brunton for offering me the chance to work in the lab and on pancreatic cancer such an important topic in current cancer research, as well as their continuous support and guidance.

Thank you to all the members of the Frame and Brunton laboratory, as well as people in the Edinburgh Cancer Research Centre, for their swift assistance from time to time, without which my project would have been a little bit more difficult. I want to thank Bryan Serrels for his guidance and his initial opinion on the possible co-existence of mesenchymal and epithelial cells in the primary culture. I want to thank Hitesh Patel and Arek Welman for their insightful opinions, in particular, Tesh's opinions on the main part (TGFβ/BMP) of my project.

I want to thank Kenny Macleod for his patience and sharing with me techniques in doing experiments and handling different equipments. I want to thank Alan Serrels for advice on how to use the lentiviral system for knockdowns; Morwenna Muir for conducting subcutaneous injection and teaching me how to handle mice in the animal house; Andrew Kinnaird and Jing Zhou for their advices on immunohistochemistry. I want to thank Mark Duxbury for inviting me to the operating theatre in the Royal Infirmary, and sharing with me his some of his clinical experience in pancreatic cancer research.

I also want to thank Elizabeth Fryer for her excellent help with flow cytometry; Joe Rainger and David Fitzpatrick for generously offering phospho-SMADs antibodies as well as suggestions on inhibiting the BMP pathway.

I am also indebted to my undergraduate tutors in the University of Birmingham: Stephen Dove, Klaus Fütterer, and Laura Machesky. They have brought me to the wonderful yet stringent world of science. And also Nancy Ip (and her lab's colleagues in 2007) of the Hong Kong University of Science and Technology, currently serving as Dean of Science; I learnt a wide range of techniques while working as a research assistant in her lab.

This thesis is dedicated to my wife, Zhao Xiaofei, my parents, Heung Kam-Ching and Tsoi Yin- Chu, and my sister Heung Man-Kuen.

And I am grateful to the College of Medicine and Veterinary Medicine for awarding me a scholarship to do a PhD.

Post-viva addendum:

Thanks to David Melton and Gareth Inman for being my thesis examiners, and providing valuable suggestions and comments on my thesis.

TABLE OF CONTENTS

2 MATERIALS AND METHODS

3 RESULTS

3.1 Characterization of heterogeneity of mouse pancreatic cancer cells

3.2 The MEK-ERK pathway and anchorage independent proliferation

3.3 The canonical Wnt pathway

3.4 The-SMAD4-HNF4α pathway & metabolic stress

4 DISCUSSION

5 FUTURE PERSPECTIVES

*****Results 3.2 (MEK-ERK pathway) and 3.3 (the canonical Wnt pathway) have been presented as a short talk and poster in an American Association for Cancer Research (AACR) conference titled “Frontiers in Basic Cancer Research”, on 19, San Francisco, USA.

LIST OF FIGURES

ABBREVIATIONS

21G 21 gauge

-/- Null

Ab Antibody

ALK Activin receptor-Like Kinase

APC Adenomatous Polyposis Coli

APS Ammonium persulphate

ATCC American Type Culture Collection

BCA Bicinchoninic acid assay

BMP Bone Morphogenetic Proteins

BSA Bovine serum albumin

DMEM Dulbecco's modified eagle's medium

DMSO Dimethyl sulfoxide

DNA Deoxyribonucleic acid

E-cadherin Epithelial-cadherin

ECL Enhanced chemiluminescence

EDTA Ethylene diamine tetra-acetic acid

EGFR Epidermal growth factor receptor

EGTA Ethylene glycol tetra-acetic acid

EMT Epithelial-to-Mesenchymal Transition

ERK Extracellular regulated kinase

FAK Focal Adhesion Kinase

FACS Fluorescence-activated cell sorting

FBS Foetal bovine serum

H_2O Water (Dihydrogen monoxide)

HER2 Human Epidermal growth factor Receptor 2

HNF4α Hepatocyte Nuclear Factor 4 alpha

LEF-1 Lymphoid Enhancer Factor-1

mAb Monoclonal antibody

MAP kinase Mitogen-activated protein kinase

$MgCl_2$ Magnesium chloride

ml Millilitres

mm Millimetre

mTOR Mammalian Target Of Rapamycin

Na_3VO_4 Sodium orthovanadate

$Na_4P_2O_7$ Sodium pyrophosphate

NaCl Sodium chloride

N-cadherin Neural-cadherin

PBS Phosphate buffered saline

pH The Potential of Hydrogen

PI3K Phosphatidylinositol-3-kinase

PMSF Phenylmethylsulphonyl fluoride

PTEN Phosphatase and Tensin homologue

RT Reverse transcription

RT-PCR Reverse transcription polymerase chain reaction

S Serine

SDS Sodium dodecyl sulphate

SDS-PAGE Sodium dodecyl sulphate-polyacrylamide gel electrophoresis

SRB Sulforhodamine B

T Threonine

TCA Trichloroacetic acid

TEMED Tetramethylethylenediamine

TGFβ Transforming growth factor-beta

Y Tyrosine

ZO Zona Occludens

1 INTRODUCTION

1.1 Overview of pancreatic cancer

1.1.1 Risk factors of sporadic pancreatic cancer

Pancreatic cancer in most cases interchangeably refers to pancreatic adenocarcinoma (Hruban et al., 2006). It is one of the most lethal types of cancer, with an overall 5-year survival rate below 5% (reviewed by Hidalgo, 2010). In the UK, pancreatic cancer ranks fifth for the deaths caused among other cancers (Figure 1A). Another type of cancer in the pancreas is insulinoma, which is rare, non-ductal and arises in the beta cells of the endocrine pancreas.

One main reason for the deadliness of pancreatic cancer is the difficulties in early detection. Owing to the retroperitoneal location of the pancreas, the pancreas is largely inaccessible for routine sampling, or radiographic and endoscopic screening (reviewed by Leach 2004) (Figure 1B). Moreover, since pancreatic cancer causes few symptoms at early stages, diagnosis is often found when patients have undergone abdominal computed tomography (CT) scans for other reasons. Hence, people who show symptoms attributable to pancreatic cancer, such as mid-back pain, obstructive jaundice and weight loss, may have reached more advanced, metastatic stages of the disease (reviewed by Vincent et al., 2011). In addition, metastases are very common in regional lymph nodes, the liver, and other distant sites (Hruban et al., 2006).

Pancreatic cancer is predominantly a disease of the elderly that it is rare before the age of 40, and the median age at diagnosis is 73 years (Villeneuve et al., 2000). So far, only cigarette-smoking has been identified as a preventable and statistically important cause (reviewed by Li et al., 2004), and as many as one in four cases of pancreatic cancer may be attributable to smoking (Lowenfels et al., 2006). Other risk factors include diets high in meats and fat, low serum folate levels, obesity, chronic pancreatitis and long-standing diabetes mellitus (Lowenfels et al., 2006; Michaud et al., 2002, 2001; Everhart et al., 2006). About 25% of patients with pancreatic cancer have diabetes mellitus at diagnosis and roughly another 40%

Figure 1

(A)

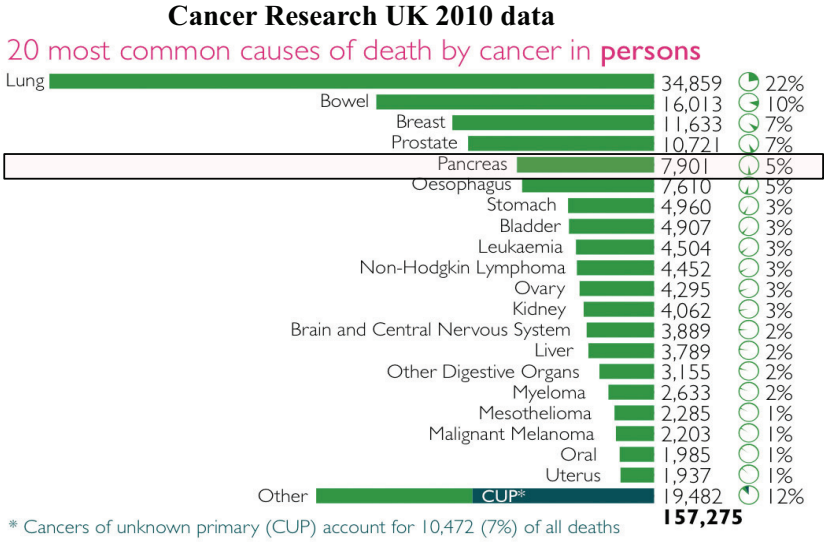

(B)

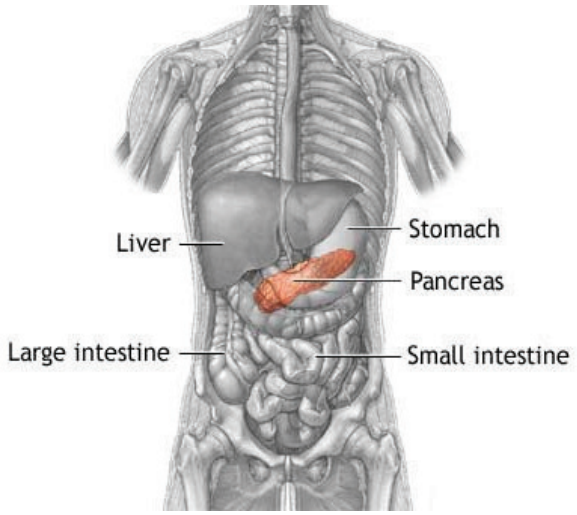

(C)

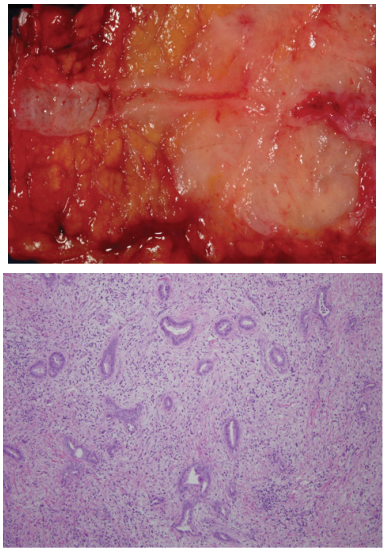

Figure 1 (A) Ranking by the number of deaths caused by different cancer types in 2010 (Source: Cancer Research UK website). **(B)** - Location of the pancreas in the human body (Source: the New York Times). **(C)** - Top: Gross appearance of pancreatic cancer excised from a surgery. bottom: low magnification of H&E staining of pancreatic cancer (Source: Johns Hopkins University Pancreatic Cancer Center website).

have impaired glucose tolerance (Chari et al 2008; Pannala et al., 2008; reviewed by Vincent et al., 2011).

1.1.2 Familial pancreatic cancer

Familial pancreatic cancer is defined as a patient having at least a pair of first-degree relatives diagnosed with the disease. It accounts for up to 10% of pancreatic cancer cases (reviewed by Vincent et al., 2011). Screenings do identify precancerous lesions in many individuals with strong family histories of pancreatic cancer (Szafranska et al., 2008; Li et al., 2010; reviewed by Vincent et al., 2011). The risk for developing pancreatic cancer increases with the number of first-degree relatives diagnosed with pancreatic cancer, potentially attributed to autosomal dominant inheritance of a rare allele (Klein et al. 2004). A number of genes alterations have been found to be more closely related to familial than to sporadic pancreatic cancer, such as *Brca2* (reviewed by Maitra & Hruban 2008).

Nevertheless, individuals with germ-line *Brca2* gene mutations do not always have a strong family history of cancer. A demographic study reveals that in 41 patients with apparently sporadic pancreatic cancer, 4 patients have a *Brca2* mutation but none has a family history of pancreatic cancer (Goggins et al., 1996). This suggests the presence of additional modifiers in determining an individual's susceptibility to familial pancreatic cancer. In one family, the *4q32-34* locus has been linked to the development of diabetes, pancreatic exocrine insufficiency, and pancreatic cancer with a penetrance approaching 100% (Eberle et al. 2002). However, it is not yet known which gene is associated with this syndrome.

1.1.3 Clinical pathology and precursor lesions

Pancreatic cancer is clinically classified into resectable (without spread to the nearby blood vessels or any distant tissues), borderline resectable, locally advanced (tumour cells present in nearby blood vessels) and metastatic disease (distant metastasis often with ascites). Most of the primary tumours develop in the head of the pancreas (reviewed by Hidalgo 2011).

In the operating theatre, pancreatic cancer often appears to be a firm, highly sclerotic mass (Hruban et al., 2006) (Figure 1C). The edges of these cancers are poorly defined, with long tongues of carcinoma extending beyond the main tumour (Hruban et al., 2006). At the light-

microscopic level, pancreatic cancer is composed of an infiltrating gland-forming neoplastic epithelium with an intense desmoplastic reaction. This desmoplastic reaction is usually so intense that only a minority of the cells in the mass formed by pancreatic cancer are actually neoplastic cells (Hruban et al., 2006).

1.1.4 Precursor lesions

Three types of pre-malignant lesions are believed to be the tipping points of pancreatic cancer progression, including the frequently observed Pancreatic Intraepithelial Neoplasia (PanIN), the intraductal papillary mucinous neoplasm (IPMN) and the mucinous cystic neoplasm (MCN). PanINs are neoplastic lesions in the small (<5 mm) pancreatic ducts (Hruban et al., 2001; 2004). They are observed in about 30% of specimens from clinical pancreatic samples of elderly patients (reviewed by Hezel et al., 2006).

PanINs look like dyplastic growth of the pancreatic ducts, and are classified into three stages, starting with stage-I having the appearance of a columnar, mucinous epithelium and with increasing architectural disorganization and nuclear atypia through stages II and III (Figure 2A, B). The high-grade PanINs eventually transform into pancreatic cancer with invasion of tumour cells into the basement membrane (reviewed by Hezel et al., 2006).

Patients with PanINs often end up with pancreatic cancer, and PanINs are frequently found in the pancreatic parenchyma adjacent to infiltrating adenocarcinomas (Bart et al., 1998). Consistent with this, PanINs harbour many of the gene mutations found in pancreatic cancer (Maitra et al., 2005, 2006, reviewed by Maitra & Hruban 2008). These mutations will be discussed in the next section. Furthermore, telomere shortening occurs early in PanIN-1 lesions, and this may contribute to the accumulation of chromosomal abnormalities (van Heek et al., 2002; reviewed by Maitra & Hruban 2008).

In contrast, MCNs and IPMNs lesions are less frequently observed. MCNs are large mucin-producing epithelial cystic lesions that harbour an “ovary-like” stroma with dysplasia and focal regions of invasion. The vast majority of MCNs arise in women (reviewed by Hruban et al., 2006; reviewed by Maitra & Hruban 2008). The genetic basis of MCN has not been defined. IPMNs resemble PanINs at the cellular level but grow into larger cystic and

Figure 2

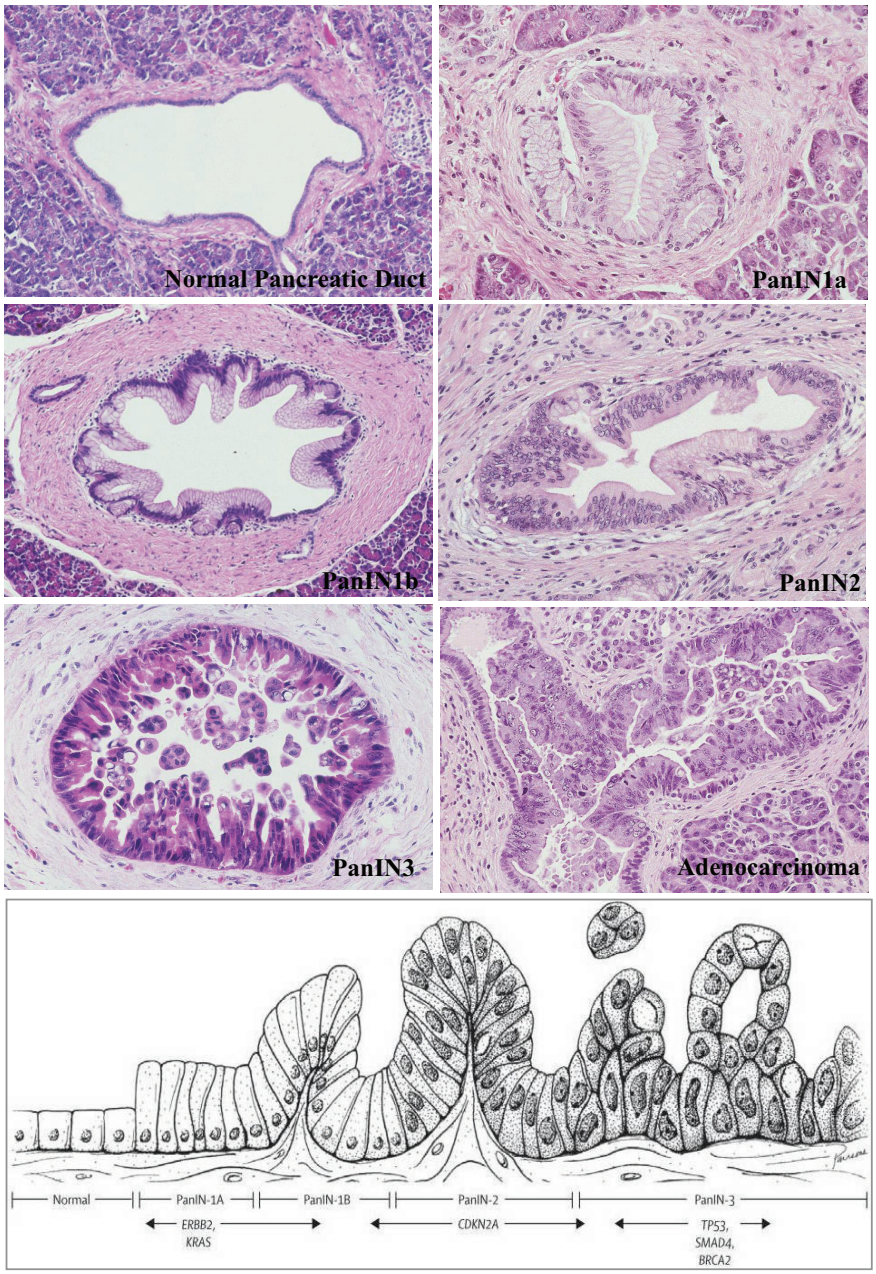

Figure 2 (H&E staining, top) - Morphology of early-to-late grade PanIN lesions, compared with normal pancreatic ducts and adenocarcinoma **(Bottom) -** An Illustration of pancreatic cancer progression, corresponding to the H&E staining shown in (A), and with respect to the timing of most frequently altered genes (Source: Johns Hopkins University Pancreatic Cancer Center, http://www.path.jhu.edu/pancreas/professionals/DuctLesions.php)

sometimes papillary structures (reviewed by Hezel et al., 2006). Loss of the *Stk11* gene product (Liver Kinase B1, LKB1) is very common (reviewed by Maitra & Hruban 2008).

1.1.5 Genetic alterations in PanIN lesions

Much effort has been spent in investigating the underlying genetic aberrations in patients and in detecting these lesions in patients. *Kras* activating-mutations (more than 90% of patients) and telomere shortening occur early in low-grade PanIN (van Heek et al., 2002), whereas inactivations of *Cdkn2a* (more than 90%), *Tp53* (more than 90%), *Dpc4* (about 50%), and *Brca2* (in familial pancreatic cancer) occur in advanced PanINs and invasive carcinomas (Hruban et al., 2002, 2008). Many of these hot-spot mutations have been knocked into mouse models, resulting in tumour formation (to be discussed in later chapters). Progress has also been made recently using improved endoscopic ultrasound to detect lesions as small as 1cm diameter. In a clinical trial in the USA (NCT00438906), both improved endoscopic ultrasound (93%) and MRI (81%) demonstrated much stronger detection frequency in patients than CT (27%) (Canto et al., 2010, reviewed by Vincent et al., 2011).

1.1.6 Current and potential drugs against pancreatic cancer

Gemcitabine is the current routine treatment for patients with advanced pancreatic cancer. It is a nucleoside analogue in which the hydrogen atoms on the 2' carbon of deoxycytidine are replaced by fluorine atoms, hence, being able to block DNA replication. However, Gemcitabine alone alleviates symptoms only in a few patients with advanced tumours (reviewed by Vincent et al., 2011). Therefore, many additional drugs in combination with Gemcitabine have been used to increase elimination of pancreatic cancer cells in patients.

Since pancreatic tumours are often poorly vascularized and bounded by a relatively thicker stroma than other cancers, one treatment strategy is to increase cancer cells' exposure to drugs, such as controllably increasing vasculature within the cancer, which has been shown effective in a mouse model study by using a hedgehog pathway inhibitor (Olive et al., 2009). To date, the hedgehog pathway inhibitor GDC-0449 (Genentech Inc., USA) is on phase-2 clinical trial in the USA, in combination with Gemcitabine and the nanoparticle formulation of paclitaxel, in patients with metastatic pancreatic cancer (NCT01088815) (reviewed by Vincent et al., 2011).

1.1.7 Heterogeneity and clonal evolution

Several studies using DNA sequencing and mathematical modelling with patient samples have shown that pancreatic cancer cells within a tumour are highly heterogeneous. The major driver genes are mutated before the development of invasive adenocarcinoma, and further heterogeneity arises in different metastases due to continuing genetic instability (Campbell et al., 2010). The metastatic cells evolve at about one in a million pancreatic cancer cells in the primary tumour (Haeno et al., 2012).

Pancreatic cancer grows at an exponential rate (Haeno et al., 2012); a precursor neoplastic clone may take 10 years to become a malignant clone, plus five more years to acquire metastatic potential, and patients often die in two years thereafter (Yachida et al., 2010). Nevertheless, the studies also revealed that 13.8% patients died with only locally advanced tumour; if these patients did not die of obstructions, physiological problems or exaggerated responses to therapies, their primary tumours may intrinsically lack the factors to acquire metastatic potential (Haeno et al., 2012; reviewed by Tuveson 2012).

1.1.8 Possible origins of pancreatic cancer cells

Pancreatic cancer (ductal adenocarcinoma) on histology often resembles pancreatic duct cells, displaying cuboidal shape, tubular structures, and ductal antigen expression (Solcia et al. 1995). Hence, pancreatic cancer is widely thought to have arisen from neoplastic ductal cells (reviewed by Hezel et al., 2006). Despite such similarity to duct cells, the cell of origin (that receives the first oncogenic hit) for pancreatic cancer, and in fact for most solid malignant tumours, has never been directly identified.

One hypothesis is that cancer precursors arise from adult stem cells, which are thought to have unique potential to self-renew and differentiate into multiple lineages when necessary, such as when there is a need for tissue-repair under stress or upon tissue damage (reviewed by Hezel et al., 2006). However, such adult stem cell has not been identified in the pancreas, and developmental studies have found that the majority of β cells *in vivo* are generated by replication of existing β cells rather than formation of new β cells from stem cells (Dor et al. 2004).

1.1.9 Multiple pancreatic lineages are susceptible to cancer in mice

Mouse model studies have indicated that multiple cell types in the pancreas can give rise to pancreatic cancer, depending on the nature of carcinogenic stress. For example, Gidekel Friedlander et al., 2009 showed that *Pdx1*-Cre*ER*; *LSL-Kras*$^{G12D/+}$ mice develop mPanIN and ductal metaplasia as in *Pdx1*-Cre; *LSL-Kras*$^{G12D/+}$ (Hingorani et al., 2003; 2005). In contrast, the procarboxypeptidase-A1 (CPA1)-expressing acinar cells (*proCPA1*-Cre*ER*), and insulin-expressing cells (*Rip*-Cre*ER*), were inefficiently transformed by *KRas*$^{G12D/+}$ (Gidekel Friedlander et al., 2009). Nevertheless, upon induction of chronic pancreatitis and inflammation by *caerulin, the insulin-positive cells were transformed into mPanINs, and into tumours if *Tp53* or *Ink4A/Arf* was deleted simultaneously (Gidekel Friedlander et al., 2009).

This suggests that only a subpopulation of cells along the PDX1-positive acinar lineage are susceptible to transformation by mutant KRas, in the absence of prior tissue injury. While insulin-expressing endocrine β-cells may be sensitive to transformation under damaging stress. Such subpopulations of highly-susceptible PDX1-positive cells are likely to be acinar cells that do not express CPA1. This observation is supported by other mouse models showing loss of acinar cells after direct damage or apparent transdifferentiation, and accompanied by duct-like, proliferative structures (Hruban et al. 2006). Furthermore, targeting the *Kras*^{G12D} allele to the population of elastase-expressing acinar cells (mature acinar cells) resulted in formation of mPanINs and adenocarcinomas upon caerulein-induced pancreatitis (Guerra et al., 2007). On the other hand, differentiated ductal cells are unlikely to be the proximate cell of origin for pancreatic adenocarcinoma in mouse, as expression of *Kras*$^{G12D/+}$ under the control of the Cytokeratin-19 (CK-19) promoter, which includes the mature ductal epithelium lineage, did not cause mPanINs or neoplasia, but only periductal lymphocytic infiltration (Brembeck et al., 2005).

In conclusion with these mouse models, acinar cells that do not express CPA1 are more likely to be transformed by mutant KRas. Although pancreatic cancer have a duct-like appearance, pancreatic duct cells do not appear to be the source of cancer evolution; rather, if the pancreas is injured and inflamed, multiple cell types would become susceptible to cancer development.

*[Caerulin is a ten amino-acid oligopeptide that stimulates expression of intercellular adhesion molecule-1 (ICAM-1) in pancreatic cells, via increased NF-κB inflammatory activity (Zaninovic et al., 2000). Cell-surface ICAM-1 in turn promotes neutrophil adhesion onto acinar cells and enhances inflammation (Zaninovic et al., 2000).

1.2 Ras GTPases and their mutants

As $KRas^{G12D}$ is the primary driver for pancreatic cancer in the *Pdx1*-Cre mouse model used in my study, I am going to present the background and recent findings in some of the signaling pathways downstream of KRas.

1.2.1 An Overview of the Ras GTPases

The Ras proteins are monomeric GTPases that act as binary switches to regulate multiple cellular processes, such as proliferation, survival, differentiation and cell cycle entry. They lie at the cross-road of many signaling pathways. One main function of Ras is to couple, or uncouple, cell surface receptors to intracellular effector-pathways, by cycling between 'on' and 'off' conformations that are conferred by the binding to GTP or GDP, respectively (reviewed by Pylayeva-Gupta et al., 2011). Such 'on-off' transition is regulated by guanine nucleotide exchange factors (GEFs), which promote the activation of Ras proteins by stimulating GDP for GTP exchange, and by GTPase-activating proteins (GAPs), that accelerate Ras-mediated GTP hydrolysis (reviewed by Pylayeva-Gupta et al., 2011) (Figure 3A).

In many cancers, Ras has been irreversibly turned into an "ever-on" mode by mutations that severely dampen the intrinsic rate of GTP hydrolysis, making Ras insensitive to GAPs. Notably, oncogenic substitutions in residues G12 or G13 of Ras results in steric hindrance and prevents the formation of van der Waals bonds between Ras and the GAP. This consequently perturbs the proper orientation of the catalytic glutamine (Q61) in Ras, blocking GTP hydrolysis (Scheffzek et al., 1997; reviewed by Pylayeva-Gupta et al., 2011).

In humans, three *Ras* genes encode four highly homologous Ras proteins of about 21kDa: HRas, NRas, KRas4A and KRas4B (KRas4A and KRas4B are alternative splice variants of the *Kras* gene) (reviewed by Pylayeva-Gupta et al., 2011). These proteins are 90% identical

Figure 3
(A)

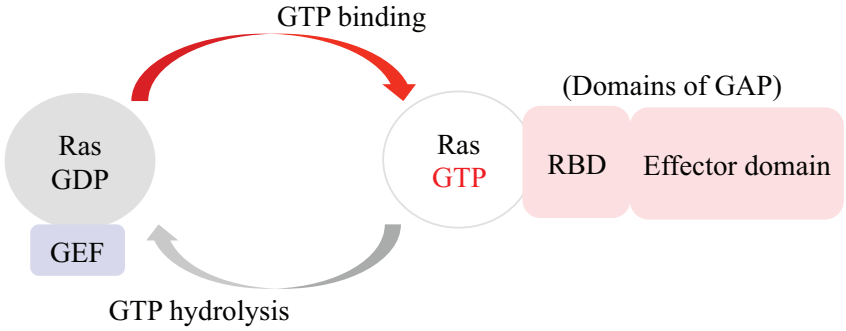

(B)

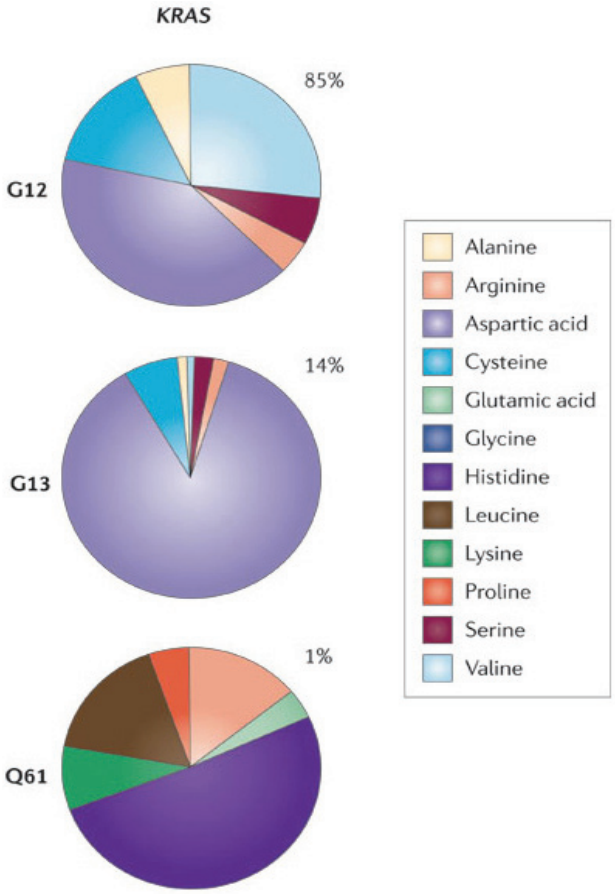

Figure 3 (A) - An Illustration of the forward and reverse mechanism in which GTP is hydrolyzed to GDP by Ras. **(B) -** Statistics of the most frequently mutated (substituted) amino acids in Kras's G12, G13 and Q61 residues (source: Pylayeva-Gupta et al., 2011).

in the first 168–169 amino acids (known as the G domain) but variable in the 20 amino acids at the carboxyl-terminus (Ahearn et al., 2012). Ras proteins are also subjected to post-translational modifications, particular in their carboxyl-terminus, and are subsequently directed to various subcellular compartments, including the Golgi apparatus and endosomes; hence they can signal from multiple membrane structures (reviewed by Ahearn et al., 2012).

1.2.2 Activating mutations of Ras

Mutations of Ras occur in a wide range of cancers in humans, in which the first known and most common are the point mutations at codon 12 (from GGT to GAT or GTT, and more rarely CGT) that results in substitution of glycine with aspartate, valine, or arginine (Figure 3B, 4A). These codon-12 mutations are present in 30% of early neoplasms and in most of the advanced pancreatic ductal adenocarcinoma in patients (Klimstra and Longnecker 1994; Rozenblum et al. 1997). KRas mutations are also frequently detected in colorectal cancers and non-small-cell lung carcinomas (NSCLC) (reviewed by Pylayeva-Gupta et al., 2011). While HRas mutations are associated with skin, head and neck cancers, NRas mutations are common in haematopoietic malignancies (reviewed by Pylayeva-Gupta et al., 2011).

KRas mutations are also found in pancreatic tissues of patients with chronic pancreatitis, of cigarrette-smokers, and of pancreatic neoplasias in patients without pancreatic cancer (Tada et al., 1993; Jimeno et al., 2006). This is consistent with findings in several mouse models that KRas mutation is an early event to potentiate aggressive adenocarcinoma. Yet different KRas mutations can cause distinct outcomes. In colorectal and lung cancers, $KRas^{G12V}$ mutation has been associated with a worse prognosis than $KRas^{G12D}$ mutation, suggesting particular amino acid substitutions may dictate specific transforming characteristics of oncogenic *Ras* alleles (reviewed by Pylayeva-Gupta et al., 2011).

Ras mutations at codons other than 12, 13 or 61 cause developmental disorders rather than cancer. For example, KRas mutations are found in some Noonan syndrome patients (a kind of dwarfism), and those mutations are restricted to targeting residues Val14, Thr58, Val152, Asp153 and Phe156, all of which are thought to cause moderate upregulation of Ras activity and are tolerated in the germline (Schubbert et al., 2006).

In mice, universal expression of $KRas^{G12D}$ is lethal to the developing embryo (Tuveson et al., 2004), indicating such oncogenic activating mutation is not tolerated during embryogenesis. Tissue-specific expression of the mutant $KRas^{G12D}$ in transgenic mouse models initiates lung hyperplasia (Jackson et al., 2001; Johnson et al., 2001), accelerates intestinal tumorigenesis that also carried a mutant allele of the adenomatous polyposis coli (*Apc*) tumour-suppressor gene (Chan et al., 2004), and induces formation of PanINs in *Pdx*-Cre or *Ptf1a*-Cre mouse pancreatic cancer models (Hingorani et al., 2003).

Among the three Ras isoforms, only KRas is essential for embryonic development. KRas-deficient mouse embryos died of anaemia, liver defects and cardiac abnormalities after two weeks of gestation (Johnson et al., 1997; Koera et al., 1997; Khalaf et al., 2005; reviewed by Schubbert et al., 2007). Deletion of HRas or NRas, or both, does not cause any malformation or survival difference (Esteban et al., 2001, Umanoff et al., 1995; reviewed by Schubbert et al., 2007). Mice are still viable when the *Kras* gene is replaced by the *Hras* gene (Potenza et al., 2005). Thus, HRas and NRas are functionally redundant in development; and the *Kras* promoter plays an exclusive role to direct Ras function in the appropriate cell compartments.

1.2.3 Downstream of KRas

The mutant KRas engages in numerous downstream pathways in pancreatic cancer. Among the most well studied are the Raf-mitogen-activated kinase (MAPK) pathway, and the phosphoinositide-3-kinase (PI3K) pathway (reviewed by Hezel et al., 2006) (Figure 4B). I am going to briefly describe these two pathways, as they are not the main focus of my project.

Along the MAPK pathway, the Raf family of serine/threonine kinases are immediately downstream of KRas. One-third of pancreatic cancers with wild-type KRas have activating mutations in B-Raf, so the downstream signaling can still be constitutively active in the absence of mutant KRas (Calhoun et al., 2003; reviewed by Maitra & Hruban 2008). The RAF kinases then phosphorylate Mitogen-Activated Protein Kinase (MEK) kinases, such as MEK1 and MEK1, resulting in their activation (reviewed Downward, 2003). Activated MEK kinases then phosphorylate Extracellular Regulated MAP Kinase (ERK), which have

Figure 4

(A)

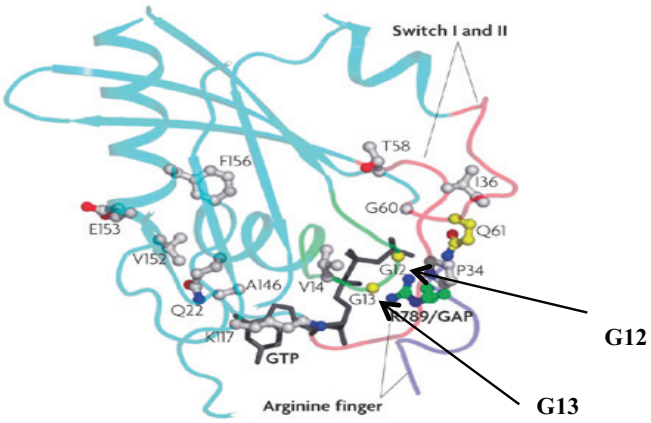

(B)

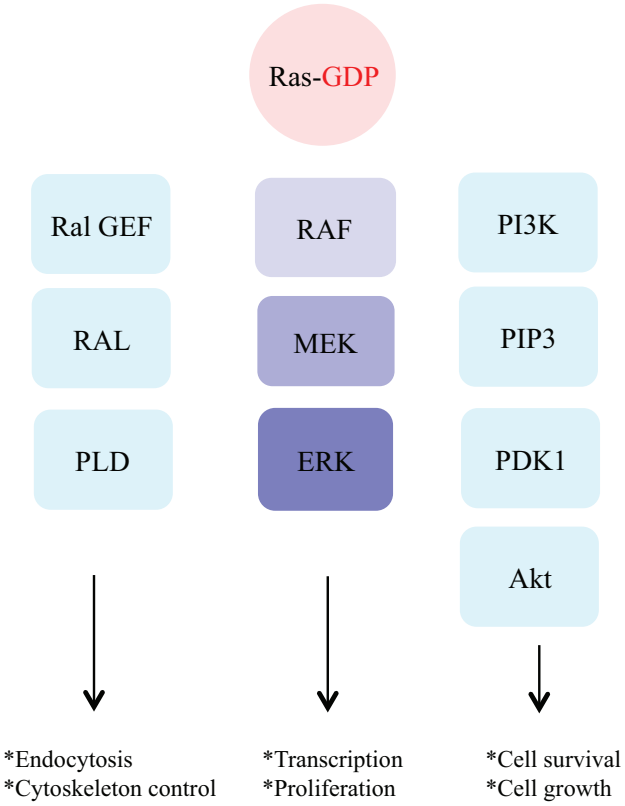

Figure 4 (A) - The crystal structure of a GTP-bound Ras, with arrows showing G12 and G13, two hotspot residues that are frequently mutated in cancer, (adapted from Schubbert et al., 2007). **(B)** – An illustration of three of the many pathways downstream of Ras, respectively Ral, Mek and PI3K, which are relatively more well studied.

numerous pro-proliferative targets in both the cytoplasm and the nucleus (reviewed by Downward, 2003).

The PI3K-AKT pathway is also constitutively activated in most pancreatic cancers (reviewed by Maitra & Hruban 2008). Preventing Ras from binding to PI3K, but not pharmacological inhibition of PI3K, was found effective in preventing mutant KRas-induced lung tumour formation (Gupta et al., 2007), providing a potential strategy to be used in treating pancreatic cancer. Although Ras certainly contributes to PI3K-AKT signaling in pancreatic cancer, the *Akt2* gene on chromosome 19q is also found to be amplified in about 15% of the cases (Cheng et al., 1996; reviewed by Maitra & Hruban 2008). Hence, targeting different downstream components of PI3K may be required in treating pancreatic cancer.

1.3 p53 and its mutants

The mutant $p53^{R172H}$ acts as the accelerator for $KRas^{G12D}$-induced pancreatic cancer in the *Pdx1*-Cre mouse model used in my study. In this section, I am going to discuss the background of and recent findings about p53 in pancreatic cancer.

1.3.1 Roles of p53 in normal cells

P53 is the central mediator of cellular responses to acute stress and has a well established role in protecting cells against cancer (reviewed by Vousden & Lane 2007) (Figure 5A). In doing so, p53 induces cell cycle arrest, senescence, or apoptotic activities upon DNA damage (Lassus et al., 1996; Gorgoulis et al., 2005) or oncogene expressions (Bartkova et al., 2005; Efeyan et al., 2006). These selective mechanisms prevent errors during DNA duplication under stress, enhance the fidelity of cell division, and prevent cancers from arising (reviewed by Riley et al., 2008).

For example, glucose starvation of normal cells causes phosphorylation at Ser15 on p53 by AMP kinase without activating additional p53-mediated transcriptions (reviewed by Riley et al., 2008). Conversely, glucose starvation of transformed cells causes p53-mediated apoptosis (Feng et al., 2007). Introduction of a mutant *Ras* oncogene into epithelial cells causes p53-mediated senescence (Yang et al., 2006), which in turn triggers production of cytokines that attract inflammatory cells, and consequently eliminate the Ras-transformed

Figure 5

(A)

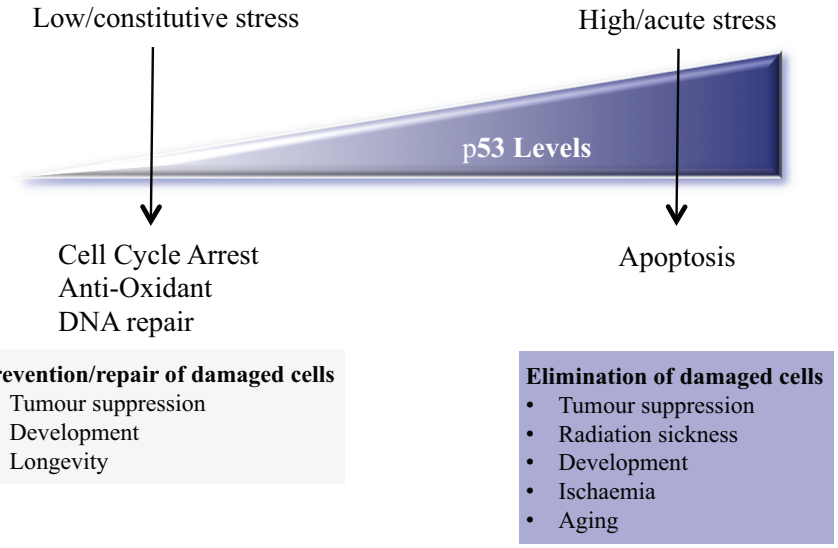

(B)

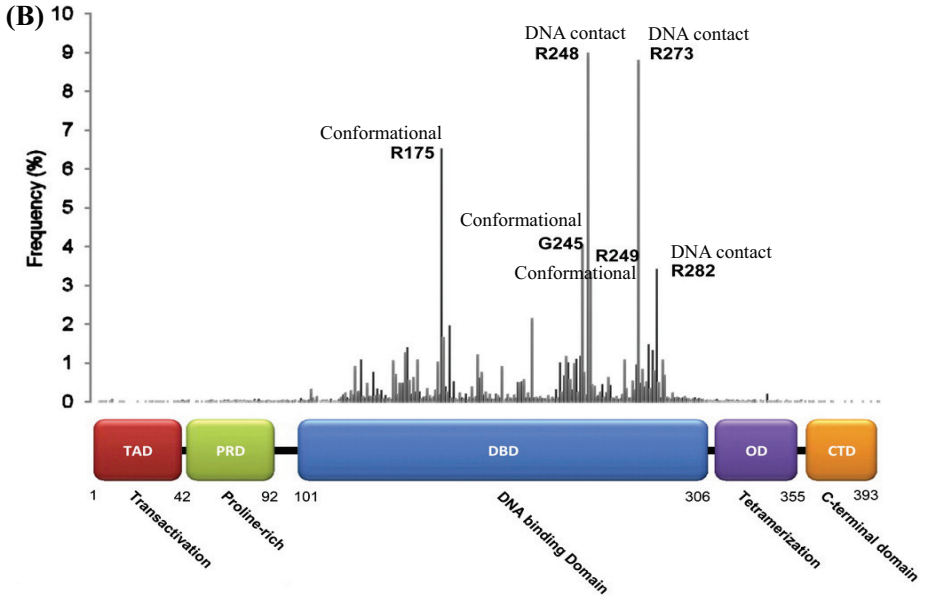

Figure 5 (A) - Levels and functions of p53 in normal cells under non-stressed and stressed conditions (Source: Vousden & Lane 2007). **(B) -** Frequency of different hotspot mutations on p53 found in human cancers (Source: Freed-Pastor & Prives 2012).

cell from the organ (Yang et al., 2006).

Hence, the "p53 network" is inter-regulated by numerous pathways, resulting in different programmes of transcription by p53 (reviewed by Riley et al., 2008). Under normal conditions with minimal stress, p53 activity is held in check by multiple mechanisms in cells. For example, HDM2 (first discovered as MDM2 in mouse) is one of the key ubiquitin ligases that negatively regulates protein levels of p53. Deletion of *Mdm2* in mice results in pre-embryonic lethality due to failure to restrain p53-mediated apoptosis (reviewed by Vousden & Lane 2010).

1.3.2 Mutant p53 and carcinogenesis

Inactivation of *Tp53* on chromosome 17p, the gene that encodes p53, is found in 50% of human cancers (reviewed by Toledo & Wahl 2006). Inactivation is most commonly in the form of intragenic mutation, combined with loss of the second allele (Redston et al., 1994). While another 50% of human cancers show overexpression of its negative regulators, such as MDM2 and MDM4 (MDMX) (reviewed by Toledo & Wahl 2006). Loss of p53 function allows cells to survive and divide even with faulty DNA, and this leads to accumulation of more and more genetic abnormalities (Vogelstein et al., 2004).

Two of the most common and well studied hotspot mutants of p53 are R172H (corresponding to R175H in mouse) and R273H (corresponding to R270H in mouse) (Figure 5B). R175H disrupts p53's DNA-binding domain and affects its overall structure (Sigal et al., 2000; Cho et al., 1994), whereas R273H still maintains a wild-type p53 conformation but is defective in DNA binding, since R273 directly binds DNA in the wild type p53 (Cho et al., 1994). Both mutants lose the ability to sensitize to cell-cycle arrest and to induce senescence, despite this there is no intrinsic survival difference between *Tp53* mutant or *Tp53* null mice (Lang et al., 2004; Olive et al., 2004).

However, mutant p53 has acquired additional or even malignant functions. Notably, p53 mutants enhance metastatic potential in multiple knock-in mouse models (Liu et al., 2000; Lang et al., 2004; Olive et al., 2004; reviewed by Donehower & Lozano, 2010), and this is not observed in the p53-null mice. Such acquired pro-metastatic function of p53 mutants

also depends on additional genetic modifiers that vary among different mouse strains (Donehower & Lozano, 2010, as unpublished data).

Mutation to different amino acids at the same site of p53 can end up with different outcomes. For example, if R175 is mutated to P instead of H, the p53 mutant still retains some tumour suppressor capacity and is rarely selected for during tumour evolution in both mouse and human (Liu et al., 2004). Furthermore, these R to H p53 mutants can induce genomic instability by inactivating Mre11/ATM-dependent DNA damage responses, causing chromosomal translocation and defects in the G2/M checkpoint (Liu et al., 2010). In addition, both wild type and mutant p53 can be extensively modified by phosphorylation, acetylation, methylation, ubiquitination, sumoylation, neddylation and even addition of N-acetyl glucosamine (reviewed by Levine & Oran 2009), each of which influences the stability and activity of p53.

1.3.3 Stability of p53 and mutant p53

Since mutant p53 is stabilised by evading MDM2-mediated degradation, it is often easily detected by immunohistochemistry; this is in contrast to wild-type p53, which is present at very low levels in unstressed normal cells (Donehower & Lozano, 2010). However, in homozygous *Tp53* mutant mice, mutant-p53 is not necessarily stable in all cell types, irrespective of the particular *Tp53* mutation they inherited (Lang et al., 2004; Olive et al., 2004; reviewed by Donehower & Lozano, 2010). This suggests that signals (such as MDM2) that keep wild-type p53 at low levels may also maintain low levels of mutant p53. Hence, additional factors are needed to stabilize mutant p53 during cancer progression (Donehower & Lozano, 2010).

One of these factors is loss of the INK4A cell cycle inhibitor (reviewed by Kim & Sharpless 2006), which occurs in 80% of human pancreatic cancer (reviewed by Tuveson 2012). Malfunctioning INK4A leads to increased Cyclin-D and CDK complexes, which in turn phosphorylate retinoblastoma protein (Rb). Phosphorylated Rb releases the transcription factor E2F1, which activates a tumour suppressor ARF (one of the gene products the *Cdkn2a* gene); ARF sequesters MDM2 and eventually stabilizes p53 (reviewed by Polager & Ginsberg 2009) (Figure 6). Selection for tumour cells with *Tp53* mutations then occurs, in a

Figure 6

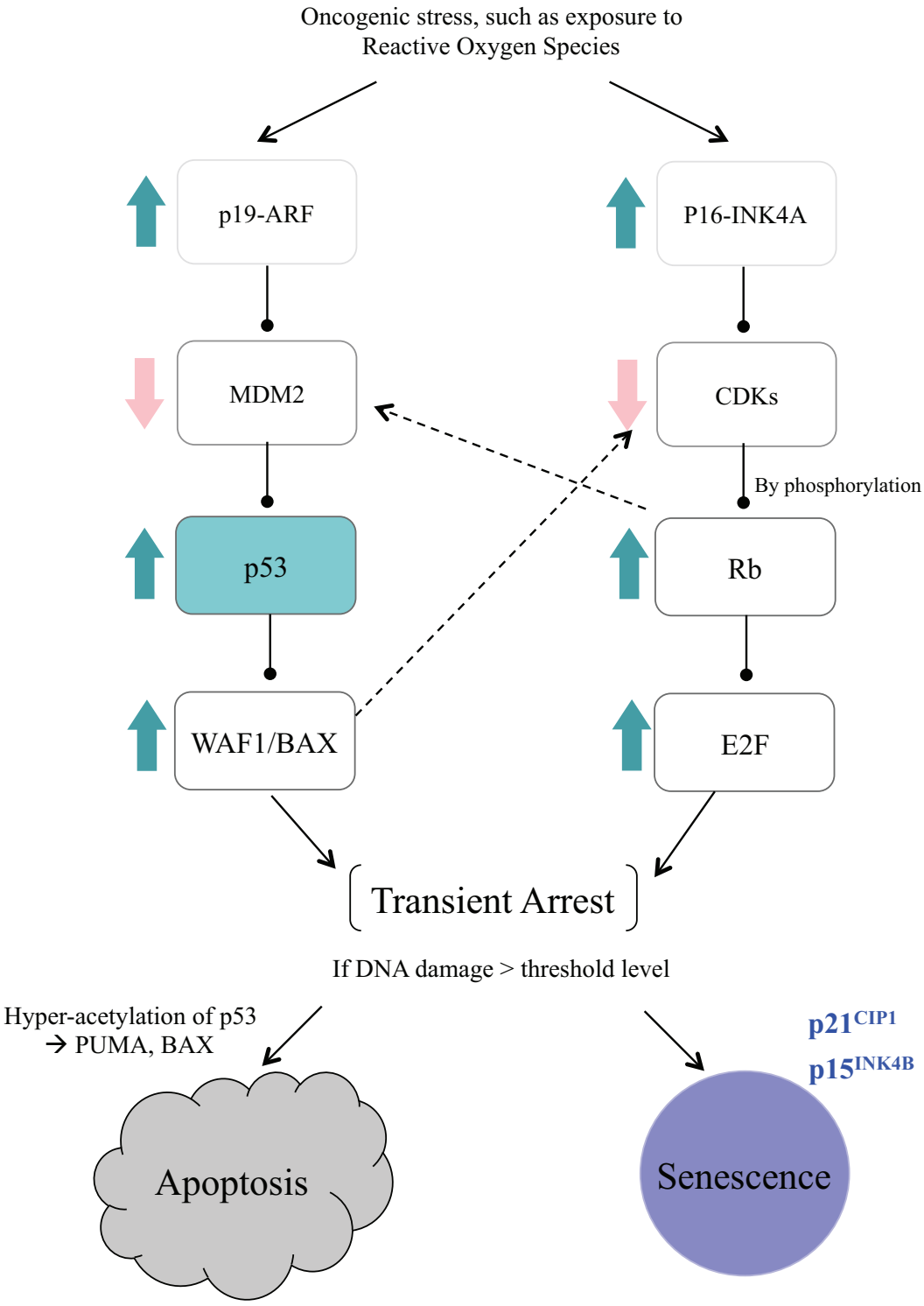

Figure 6 – An illustration of how p53 and its "network partners" regulate the activity of one another. When DNA damage is detected, the cells will undergo a transient arrest; If DNA damage exceeds certain threshold levels, cells will undergo either apoptosis or senescence. Although p21CIP and p15INK4B are now known to mark senescence, it is still not clear how cells determine which way to go; the cell type and the nature of the damage are believed to be important factors (reviewed by D'Adda di Fagagna 2008).

cell-type dependent manner, as only a subset of cell types showed stabilized mutant p53 in *Tp53*$^{R172H/R172H}$/ *Cdkn2a*$^{INK4A-/-}$ mice (Terzian et al., 2008).

1.4 The canonical Wnt pathway

The canonical Wnt pathway has been well known to be deregulated in colorectal cancer. Since the pancreas is also a part of the gastroenterological system, as a secondary project, I investigated whether or not the canonical Wnt pathway is upregulated in only a subset of the KRas-induced mouse cancer cells, despite there is little evidence for the Wnt pathway to play an important role in pancreatic cancer. In this section, I am going to present the background of the canonical Wnt pathway and the tankyrase inhibitors used in my study.

1.4.1 The central role of β-catenin

β-catenin is the central messenger of the canonical Wnt pathway; it shuttles from the cytoplasm to the nucleus to induce Wnt specific transcriptional responses. When the pathway is inactive, cytoplasmic β-catenin levels are kept low by continuous proteasome-mediated degradation, which is mediated by the β-catenin destruction complex involving GSK-3β, APC and Axin (reviewed by Logan & Nusse, 2004) (Figure 7A). GSK-3β is a serine/threonine kinase that phosphorylates β-catenin as a label for its degradation (Yost et al. 1996), whereas both Axin and APC are scaffolding proteins (Hart et al. 1998, Kishida et al. 1998) that enhance interaction between GSK-3β and β-catenin. This complex is subjected to negative regulation by tankyrase, which directs Axin to degrade through ubiquitination of Axin (Huang et al., 2009). In addition to GSK-3β, casein kinase Iα can also phosphorylate β-catenin to mediate its degradation (Amit et al. 2002, Liu et al. 2002, Yanagawa et al. 2002). Phosphorylated β-catenin is recognized by β-TrCP, targeted for ubiquitination, and eventually degraded by the proteosome (Aberle et al. 1997, Latres et al. 1999, C. Liu et al. 1999; reviewed by Logan & Nusse, 2004).

Activation of the canonical Wnt pathway is normally initiated at the cell surface upon binding of Wnt-ligands to Frizzled receptors and co-receptor (LRP5 or LRP6) complexes. Upon activation, the Frizzled receptor complexes transduce signals to stabilise β-catenin by dissociating the destruction complex, thereby allowing sufficient β-catenin to translocate into the nucleus (Figure 7A). Nuclear β-catenin interacts with transcription factors such as

Figure 7

(A)

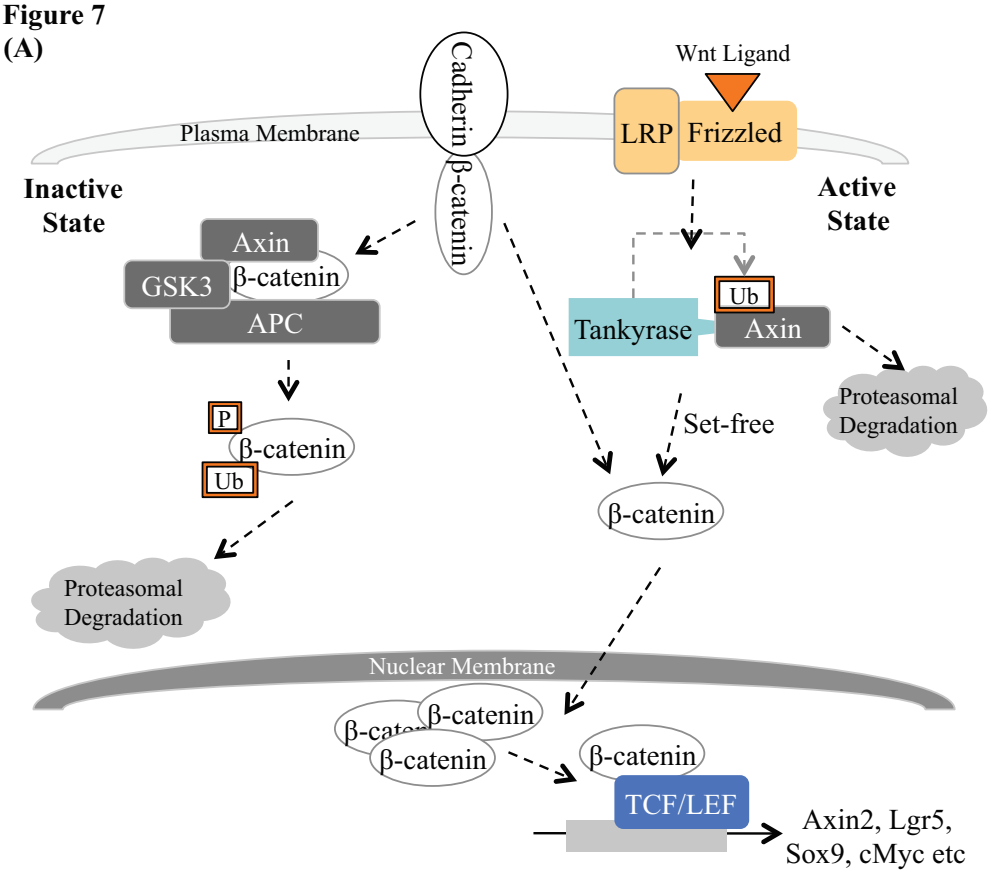

(B)

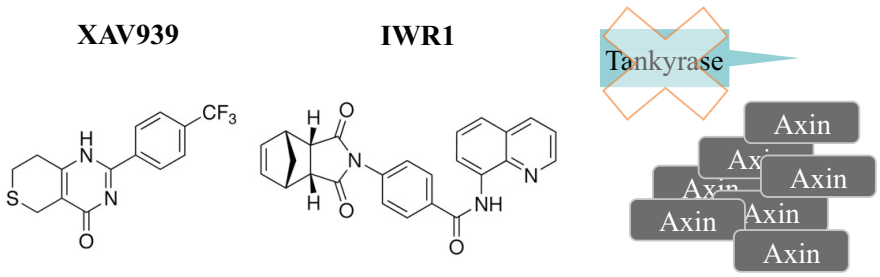

Figure 7 (A) – An illustration of the canonical Wnt pathway, featuring how β-catenin is set free or being targeted to degradation, when the pathway is active (ligand binding to receptors) and inactive (no ligand binding to receptors). **(B)** The chemical structure of two tankyrase inhibitors used in this study. Axin is stabilized as tankyrase's Axin binding site is blocked by the inhibitors, and this eventually enhances the formation of the β-catenin destruction complex, thereby suppressing the canonical Wnt pathway.

lymphoid enhancer-binding factor 1/T cell-specific transcription factor (LEF/TCF) to regulate Wnt-specific transcription. Numerous Wnt target genes have been identified, and these include components of the Wnt pathway itself, indicating that the canonical Wnt pathway is also regulated by feedback mechanisms (reviewed by Logan & Nusse, 2004).

1.4.2 Studying Wnt in the mouse pancreas

Mutations in β-catenin regulatory proteins are rare in pancreatic cancer (reviewed by Morris et al., 2010), hence the role of β-catenin in pancreatic cancer has been controversial. Moreover, deletion of APC in the mouse pancreas (*Pdx1*-Cre/ $Apc^{flox/flox}$), which resulted in constitutively activated canonical Wnt pathway, was insufficient to initiate PanIN lesions or pancreatic cancer (Strom et al., 2007). Yet, these mice showed increased post-natal pancreatic mass that correlates with enhanced proliferation of acinar cells, accumulation of nuclear β-catenin in older mice, and increased expression of β-catenin target genes (Strom et al., 2007). This suggests that the canonical Wnt pathway may contribute to proliferation of acinar cells during aging.

Furthermore, both *Pdx1*-Cre/ *LSL-Wnt1* and *Pdx1*-Cre/ *LSL-Wnt5a* mice had severe hypoplasia, suggesting these ligands of the canonical and non-canonical Wnt pathway suppress pancreas development or cell differentiation. In contrast, transgenic expression of other ligands of Wnts2, 4, 6, or 7a, caused no phenotype (reviewed by Gittes, 2008). Consistent with these findings, targeted expression of a constitutively active β-catenin (having negative regulatory phosphorylation sites removed) under the control of the *Pdx1* promoter resulted in severe hypoplasia (Heiser et al., 2006). Taken together, it appears that hyperactivation of certain aspects of the Wnt pathway potentiates proliferation and suppresses differentiation of pancreatic cells.

1.4.3 Activated Wnt pathway in colorectal cancers

Since constitutive activation of the Wnt pathway is prevalent in colorectal cancer, a large part of our understandings of the pathway has come from studying colorectal cancer. Sporadic colorectal cancer accounts for about 85% of all colorectal cancers cases, while some other colorectal cancers evolve from a genetic disease known as familial adenomatous polyposis (FAP) (Ashton-Rickardt et al., 1989; Groden et al., 1991; reviewed by Klaus &

Birchmeier 2008). Patients with FAP develop hundreds to thousands of adenomatous polyps in the colon; if the polyps are not removed, some of these polyps can progress to malignant carcinomas (reviewed by Klaus & Birchmeier 2008).

Abnormal activation of the Wnt pathway in both familial and sporadic colorectal cancers is most often attributed to truncations of APC, a key component of the β-catenin destruction complex described in the preceding section. APC mutations are commonly found to be frameshift, nonsense or splice-site mutations, which result in truncations of about 50% of the APC protein (reviewed by Polakis 2000). As an early event in colorectal cancer progression, mutation in a single APC allele is insufficient to induce adenomatous polyposis; alterations in the remaining APC allele or additional oncogenic mutations, commonly in *Kras*, *Smad2*, *Dpc4* or *Tp53*, are required (reviewed by Klaus & Birchmeier 2008).

1.4.4 Tankyrase mediates Axin to degrade and stabilize β-catenin

Tankyrase was first identified as a Poly (ADP-Ribose) Polymerase localized to human telomeres (Smith et al., 1998), and later found to have a central role in regulating the canonical Wnt pathway (Huang et al., 2009). It is expressed in adipose tissue, brain, and endocrine pancreas but scarcely in the exocrine pancreas and skeletal muscle in mouse (Yeh et al., 2009). Tankyrase-deficient mice are viable but show an increase in both fatty acid oxidation and insulin-stimulated glucose utilization, resulting in increased food intake and higher core body temperatures as compared with normal mice (Yeh et al., 2009).

Tankyrase's role in the canonical Wnt pathway is to bind Axin and to catalyze poly-ADP-ribosylation of Axin, thereby promoting Axin degradation, which results in stabilization of β-catenin (Huang et al., 2009). The co-crystal structure of 'tankyrase-binding-to-Axin' reveals two well conserved tankyrase-binding segments of Axin (amino acid 18-30 and 60-80). These two segments are each marked by a glycine residue that interacts with two parallel tyrosine side-chains on tankyrase's surface (Morrone et al., 2012). Mutation of either glycine residue abolishes bivalent binding of the corresponding Axin segment to tankyrase (Morrone et al., 2012).

Two of the earliest compounds that disrupt the interaction between tankyrase and Axin are XAV939 (Huang et al., 2009) and IWR-1 (Chen et al., 2009; Huang et al., 2009) (Figure 7B). IWR1 was found effective in a well documented, canonical Wnt-active human colon cancer cell line, DLD1. Stabilization of Axin by IWR1 in DLD1 cells did not reduce total β-catenin levels, but promoted phosphorylation of β-catenin (Chen et al., 2009). XAV939 decreases β-catenin levels, and increases β-catenin phosphorylation (S33/S37/T41) by GSK3β in SW480 cells (Huang et al., 2009). In addition, XAV939 also appears to be a more potent tankyrase inhibitor, with an IC50 of 0.004 - 0.011μM, compared with that of IWR1 between 0.78 – 1.897μM (Huang et al., 2009). Nevertheless, such high-affinity inhibition of tankyrase *in vitro* is not reflected *in vivo* in zebrafish, as both compounds are required at higher dose (between 5 – 10 μM) in order to be effective (Chen et al., 2009; Huang et al., 2009). This suggests that both XAV939 and IWR1 are inefficient to be used *in vivo*.

1.4.5 Axin2 and Lgr5 – two most commonly used *in vivo* Wnt reporter genes

Axin2 and *Lgr5* are only two of the many Wnt target genes, but they are commonly found to be more specific than many other target genes to be used as readouts of the canonical Wnt pathway *in vivo*. The Jackson Laboratory, one of the dominant suppliers of transgenic mice, is producing robust mouse strains bearing intrinsic reporter for the activity of *Axin2* and *Lgr5* to visualise Wnt activity in mouse tissues. Indeed their transcriptional levels have been a useful measurement of canonical Wnt activity in my study of anchorage independent proliferation of murine pancreatic cancer cells, but not other Wnt-target genes tested, such as *Myc* and *Tcf7*, which appeared to be less reflective of Wnt activity.

Axin2 expression is directly induced by canonical Wnt signalling. As a negative-feedback protein, its expression pattern marks the cells exposed to Wnt signals (Jho et al., 2002; Lustig et al., 2002). Similar to Axin1, which instead is ubiquitously expressed, Axin2 can inhibit and stabilize β-catenin when overexpressed in cells (Behrens et al., 1998). Despite their differences in expression pattern, Axin2 can fully replace the function of Axin1 during mouse development, when it is homozygously knocked into the *Axin1* locus (Chia & Costantini 2005). However, deletion of *Axin2* in mice resulted in defects in skull and tooth development (Yu et al., 2005), suggesting it has unique roles in development and cell differentiation.

Lgr5 (leucine-rich-repeat-containing G-protein-coupled receptor 5, also known as Gpr49) is a Wnt target gene of the TCF4 family of transcription factors (Barker et al., 2007). This G protein coupled receptor interacts with the Frizzled/lrp Wnt receptor complex upon binding of the ligand, R-spondin (de Lau et al., 2011). It was originally identified in colon cancer, and has also been shown to be overexpressed in ovarian and hepatic cancers (reviewed by Haegebarth & Clevers 2009). It is a useful marker of adult stem cells in the colon and skin (Barker et al., 2007; reviewed by Haegebarth & Clevers 2009). Lgr5 is expressed exclusively in cycling columnar cells in the crypt base; whereas in the stem cell niche of the murine hair follicle, Lgr5 is expressed in actively cycling follicle cells (reviewed by Haegebarth & Clevers 2009). Mice deficient for Lgr5 exhibit a malformation of the tongue and the lower jaw, causing newborns to swallow air, leading to early neonatal death (Morita et al., 2004).

1.5 The Transforming Growth Factor-β (TGFβ) superfamily

The TGFβ/BMP pathway is one of the implicated pathways in pancreatic cancer, in which SMAD4, the central mediator of the pathway's many upstream signals, is known to be deleted in 50% of pancreatic cancer cases. As the main focus, as well as the key discovery of my project, I am going to present the backgrounds and chemical inhibitors of the TGFβ/BMP pathway.

1.5.1 Overview of the TGFβ superfamily

The human TGFβ super family comprises more than 30 cytokines or cytokine-like ligands that can be divided into two distinct branches (Massague 2008). Activin, Nodal, Lefty, Myostatin, and TGFβ are clustered in one family branch, and bone morphogenetic proteins (BMPs), anti-muellerian hormone (AMH, also known as MIS), and various growth and differentiation factors (GDFs) are grouped into the other branch (Derynck and Akhurst, 2007; Roberts and Wakefield, 2003; Shi and Massagué, 2003; Massagué 2008). Among these branches, the TGFβ and the BMP sub-branches have been more extensively studied. Their ligands exist in multiple forms, for example, TGFβ family has TGFβ1, β2, and β3 variants, while the BMP has up to 10 variants such as BMP2, 4 and 9.

The BMP/TGFβ ligands are synthesized within the cell as dimeric pro-hormones (Gray et al., 1990). These dimeric precursors are then secreted into the extracellular matrix, where they are cleaved by furins and other convertases to become active ligands (Dubois et al., 1995; Constam et al., 1999). Active ligands bind their specific type-2 receptors, such as BMPR2 and TGFβR2. Binding of the mature ligand causes phosphorylation of the type-1 receptors (also known as Activin-receptor-link kinase, ALK) by the type-2 receptor, and the two receptors consequently form a heterotetrameric receptor complex (reviewed by Massague 2008). Both type 1 and type 2 receptors contain serine or threonine kinase domains in their intracellular portions (Heldin et al., 1993). These heterotetrameric receptor-complexes activate both SMAD-dependent and non-SMAD-dependent pathways (reviewed by Derynck & Zhang 2003). Non-SMAD-dependent pathways overlap with many other pathways, such as the PI3-kinase, p38-MAP kinase, Ras homolog gene family - member A (RhoA), and Rho-associated protein kinase (ROCK) (reviewed by Derynck & Zhang 2003).

1.5.2 Signal transduction by SMAD proteins

The SMAD proteins are mammalian homologs of the Drosophila melanogaster protein, Mothers Against Decapentaplegic (MAD), and the Caenorhabditis elegans protein SMA (from gene sma for small body size). Hence, SMAD is a portmanteau of the two. Of the five Receptor-associated SMADs (R-SMADs) in mammals, type-1 receptors of the TGFβ branch (ALKs 4, 5 and 7) phosphorylate SMADs 2 and 3, whereas those of the BMP branch (ALKs 1, 2, 3 and 6) phosphorylate SMADs 1, 5, and 8, (Piek et al., 1999; Jornvall et al., 2001) (Figure 8A). However, it is now known that TGFβ ligands can also phosphorylate SMAD1 and SMAD5 in certain cell types via TGFβR2-ALK1/5 complexes (Irwin et al., 2008; Wrighton et al., 2009). Upon phosphorylation, the R-SMADs lose affinity to their cytoplasmic retention proteins, such as SARA (SMAD anchor for receptor activation), and in turn exposing their nuclear localization signal sequences (Tsukazaki et al., 1998). These activated R-SMADs may then form heteromeric complexes with SMAD4 (also known as co-SMAD) and accumulate in the nucleus (Shi & Massague 2003).

In the nucleus, the SMADs complexes associate with additional DNA-binding co-factors to specifically regulate target gene expressions. These SMAD partners are members of various families of transcription factors, such as the forkhead, homeobox, zinc-finger, basic helix-loop-helix (bHLH), and Activator Protein-1 (AP1) families (Feng and Derynck, 2005;

Figure 8

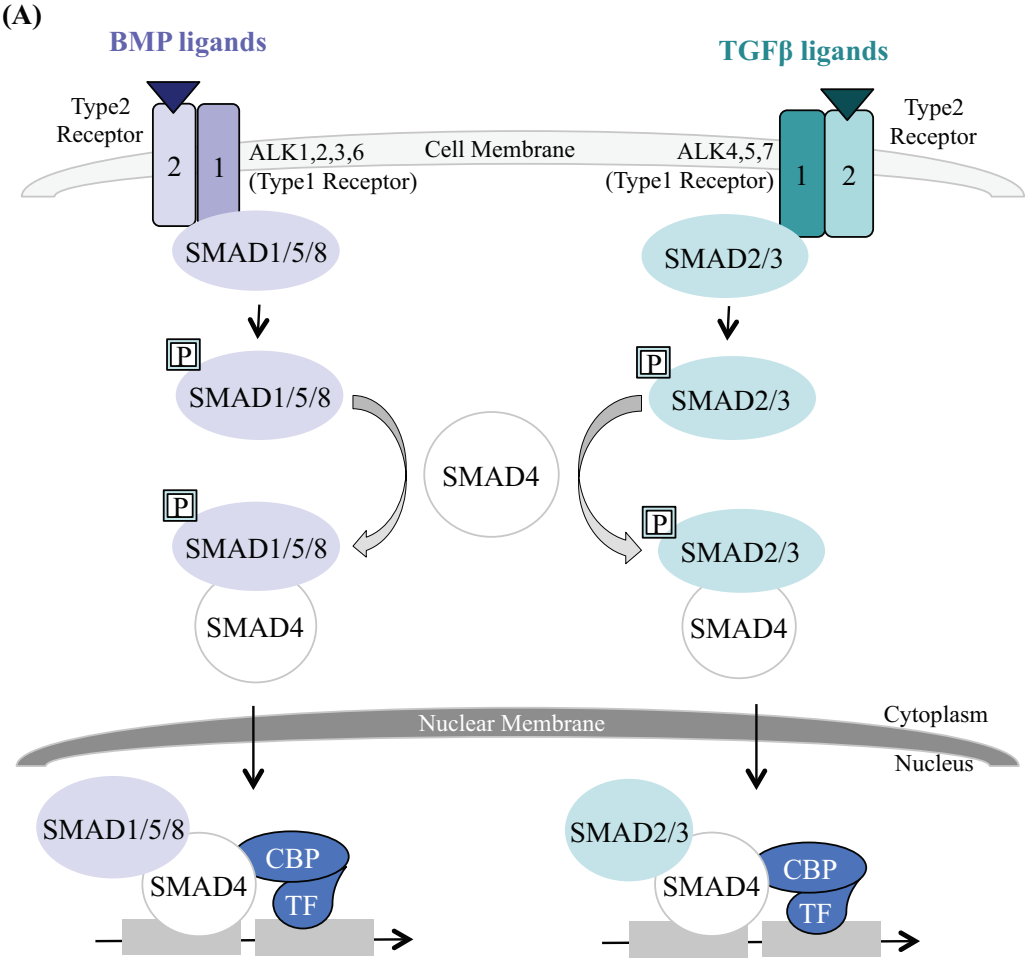

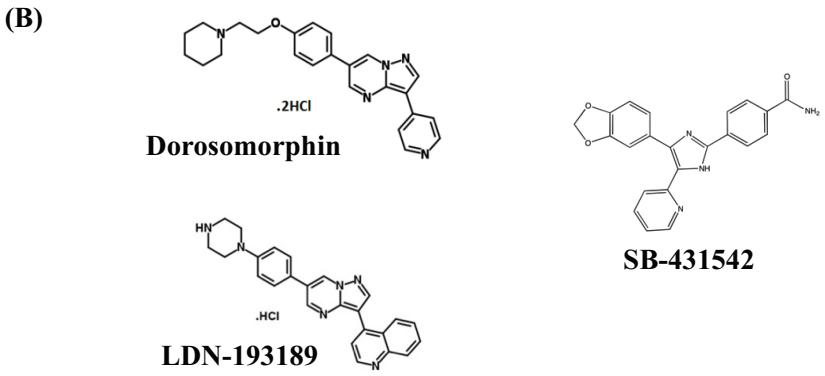

Figure 8 (A) – An illustration of the TGFβ/BMP pathway, starting from activation of receptors by ligands, to signaling through their respective R-SMADS and SMAD4, and accumulation of these complexes in the nucleus and to bind DNA to initiate transcription programs **(B)** – The chemical structure of two BMP type-I receptor inhibitors (left) and a TGFβ type-I receptor inhibitor (right) used in this study.

Massagué et al., 2005; reviewed by Massague et al., 2005). However, SMAD4 is not always required for the RSMADs to go into the nucleus. For example, Transcriptional intermediary factor 1γ (TIF1γ) competes with SMAD4 to interact with phosphorylated SMAD2/3 and mediate TGFβ-induced erythroid differentiation (He et al., 2006). Independent of SMAD4, phospho-SMAD2/3 can also bind IκB kinase α (IKKα), which negatively regulates keratinocyte proliferation by upregulating the Myc antagonists, Mads, during mouse epidermal differentiation (Descargues et al., 2007).

1.5.3 SMAD4, the co-SMAD

Dpc4 (Deleted in Pancreatic Cancer locus 4), which codes for the SMAD4 protein, is a tumour suppressor gene on chromosome 18q21. As its name implies, homozygous deletion is found in about 30% of pancreatic cancer cases, and loss of one allele coupled with an intragenic mutation in the second allele is found in another 25% of the cases (Hahn SA et al., 1996; Wilentz et al., 2000). Deletion of *Dpc4* is frequent in ductal pancreatic cancer (Hruban et al., 2006), and with a relatively low incidence in non-ductal pancreatic cancer and in other cancers, including colon, breast, and ovarian or biliary tract carcinomas (Schutte et al., 1996; Hahn et al., 1998). On immunohistochemistry, SMAD4 protein expression reflects the *Dpc4* gene status in pancreatic cancers with rare exceptions (Wilentz et al., 2000). In addition, absence of SMAD4 often correlates with higher metastatic potential in patients of pancreatic cancer (Wilentz et al., 2002). Somatic mutation of SMAD4 in pancreatic cancer usually emerges during the transition from adenoma to carcinoma (Jaffee et al., 2002; Jones et al., 2008; reviewed by Massague 2008). Hence, loss of SMAD4 in tumours is generally a late event (reviewed by Massague 2008).

Despite the fact that TGFβ receptor or SMAD4 mutations are often found in cancer, tissue-specific ablation of the gene encoding TGFβR2 alone in mouse cancer models is rarely sufficient to induce tumourigenesis (reviewed by Massague 2008). For example, no developmental or pathological changes are observed upon deletion of TGFβR2 in the epithelia of the murine oral cavity, esophagus, forestomach (Lu et al., 2006), pancreas (Ijichi et al., 2006), intestine (Muñoz et al., 2006), or skin (Guasch et al., 2007). In the mouse mammary gland, although deletion of TGFβR2 results in excessive lobular-alveolar cell proliferation (hyperplasia), it does not induce tumourigenesis (Forrester et al., 2005).

Similarly, deletion of SMAD4 does not affect normal development or cause spontaneous tumour formation in the mouse liver (Wang et al., 2005b) or mouse pancreas (Bardeesy et al., 2006, Kojima et al., 2007; Xu et al., 2010). However, it does cause spontaneous squamous cell carcinomas in the mammary gland, which shows trans-differentiation of mammary epithelium to squamous epithelium (Li et al., 2003). Overall, mouse models reveal that TGFβ is not a universal proliferation suppressor; it suppresses proliferation only under some conditions, for example, when there is tissue injury or oncogenic stress. This is demonstrated by increased rate of keratinocyte proliferation, migration, and would healing in injured mouse skin that lacks SMAD3 or TGFβR2 expression.

Both TGFβR2 and SMAD4 have been shown to accelerate cancer progression in mouse models. Deletion of TGFβR2 promotes carcinoma conversion of intestinal polyps initiated after deletion of the *Apc* gene or by chemically-induced mutagenesis (Biswas et al., 2004 and Muñoz et al., 2006). Similarly, heterozygous deletion of a single *Dpc4* allele potentiates the progression of intestinal polyps to carcinoma in APC-deficient mice with loss of the remaining wild-type *Dpc4* allele (Takaku et al., 1998). In a mouse model of pancreatic cancer, $KRas^{G12D}$-induced PanIN lesions progress to IPMN-type lesions when combined with deletion of SMAD4 (Bardeesy et al., 2006). Somatic mutation of SMAD4 in pancreatic cancer, and of TGFβR2 or SMAD4 in colorectal cancer, are selected during the adenoma to carcinoma transition (Jaffee et al., 2002 and Jones et al., 2008). Furthermore, loss of SMAD4 promotes metastasis in mouse pancreatic cancer models (reviewed in Mazur and Siveke, 2011), and loss of SMAD4 also correlates with increased metastasis in patients (Iacobuzio-Donahue et al., 2009).

1.5.4 The TGFβ-responsive R-SMADS

Despite their crucial function in connecting signalling pathways, R-SMAD mutations are infrequent in cancer (Massague 2008). Intragenic mutations in SMAD2 occur in only a small proportion (5%) of colorectal cancers (Sjoblom et al., 2006); loss of SMAD3 expression occurs in some gastric cancers and T cell lymphoblastic leukemias (Levy and Hill, 2006). However, SMAD2 may occasionally mark metastasis, as histological analysis demonstrates that 75% of human breast cancer bone metastasis biopsies show nuclear phosphorylated-SMAD2 in metastatic cancer cells (Kang et al., 2005). Mice deficient in

SMAD3 develop colon cancer after Helicobacter infection due to increased inflammation (Maggio-Price et al., 2006).

Although both SMAD2 and SMAD3 are downstream of the TGFβ branch of the pathway, they have distinct target genes (Brown et al., 2007). One important difference between SMAD2 and SMAD3 is their ability to bind DNA. The SMAD3 homodimer can form DNA-binding complexes with its MAD homology1 domain (MAD1) in the absence of SMAD4 (reviewed by Brown et al., 2007). In contrast, the SMAD2 homodimer cannot bind DNA without SMAD4, because the MH1 domain of SMAD2 has a small insert encoded by an extra exon of about 30 amino acids that blocks its way to directly bind DNA (Yagi et al., 1999). In some human pancreatic cancer cell lines that lack SMAD4, TGFβ signalling through SMAD2 and SMAD3 seem to remain intact, as both proteins are serine phosphorylated and localized to the nucleus (Fink et al., 2003; Subramanian et al., 2004). In addition, nuclear SMAD2/3 is also detected in mouse PanIN lesions by immunofluoresccence (Bardeesy et al., 2006).

1.5.5 The BMP responsive R-SMADs

Multiple mouse models indicate that the BMP-SMADs pathway acts to suppress tumourigenesis in most situations. BMPR1A-null mice died at embryonic day 8.0 (E8.0), due to lack of mesoderm formation (Mishina et al., 1995a). Similarly, heterozygous or homozygous deletion of SMAD1 or SMAD5 is embryonic lethal; in contrast, SMAD8-null mice are viable and fertile (Arnold et al., 2006; Pangas et al., 2008). If both SMAD1 and SMAD5 are homozygously deleted in ovarian granulosa cells or in testicular cells, tumours would arise and cause infertility. These mice develop peritoneal and lymphatic metastases regardless of gender, indicating that SMAD1 and SMAD5 are essential to development of germ cells, and are critical tumour suppressors with redundant functions (Pangasa et al., 2008).

Another example showing the tumour suppressor role of the BMP-SMAD pathway is Juvenile Polyposis Syndrome. It is a rare autosomal dominant disorder characterized by a predisposition to hamartomatous polyps and cancers of the gastrointestinal and colorectal tract. This syndrome is caused by germline mutation of either SMAD4 (15%–20% of the

patients) or BMPR1A (in 20%–25% of the patients) (Calva-Cerqueira et al., 2009; Friedl et al., 2002; Howe et al., 2002; van Hattem et al., 2008; reviewed by Yang & Yang 2010).

Consistent with the human disease, heterozygous deletion of SMAD4 in mice causes polyps along the gastrointestinal tract. These polyps morphologically resemble those of Juvenile Polypsosis Syndrome, and loss of heterozygosity (LOH) are frequently observed in advanced tumours of the *Dpc4*$^{+/-}$ mice (reviewed by Yang & Yang 2010). In addition, both *Bmpr1a*, and *Dpc4* are among the cancer driver genes identified in a mouse model using transposons to insert mutations in the gastrointestinal epithelium, along with *Pten* and *Apc* (Starr et al., 2009). Deletion of *Bmpr1a* under the control of a gastric epithelium promoter, *Mx1*-Cre, caused polyps in the intestinal epithelium and carcinomas in the gastrointestinal transitional zone (Bleuming et al., 2007).

1.5.6 SB-431542, a potent TGFβ receptor inhibitor used in this study

SB-431542 is a potent inhibitor against the TGFβ type-I receptors (ALK4, ALK5 and ALK7) (Inman et al., 2002) (Figure 8B). 2μM SB-431542 can completely inhibit the activity of endogenous ALK5 receptors with little apparent non-specific effects. For example, it does not affect growth factors' mediated pathways, such as EGFR induced ERK/MAP kinases or stress induced JNK or p38 MAP kinases (Inman et al., 2002). Importantly, it does not cross-inhibit the BMP type-I receptors (ALK1, ALK2, ALK3 and ALK6), except at very high concentration of 10μM, it starts to exert relatively weak activity against ALK3 (Inman et al., 2002).

1.5.7 Dorsomorphin and LDN1931890, the two potent BMP receptors inhibitors used in this study

Dorsomorphin selectively inhibits the BMP type-I receptors ALK2, ALK3 and ALK6 and thus blocks BMP-mediated SMAD1/5/8 phosphorylation and their respectively downstream signals (Yu et al., 2008) (Figure 8B). It does not inhibit TGFβ type-I receptors (ALK4, ALK5 and ALK7). Dorsomorphin's action is mediated by blocking the constitutively active form of the BMP type-I receptor kinases (Yu et al., 2008). Conversely, it is unable to block SMAD-independent pathways (Yu et al., 2008). Dorsomorphin is structurally identical to compound C, a molecule previously shown to antagonize AMP-activated kinase (AMPK)

activity *in vitro* (Zhou et al., 2001; Yu et al., 2008). LDN-193189 is an optimized derivative of Dorsomorphin (Cuny et al., 2008; Yu et al., 2008b). It inhibits BMP-mediated phosphorylation of SMAD1/5/8 with an IC50 value that is much lower than that for Dorsomorphin (5nM versus 470nM) (Yu et al., 2008b). It also shows enhanced specificity for the BMP type-I receptors over TGF-β type I receptors and AMPK (Yu et al., 2008b).

1.6 Hepatocyte Nuclear Factor 4 – Alpha (HNF4α)

With an inspiration from the paper by Sirard et al., Genes Dev. 1998 "The tumour suppressor gene Smad4/Dpc4 is required for gastrulation and later for anterior development of the mouse embryo.", I directly established for the first time that the nuclear receptor HNF4α is downstream of the BMP-SMAD pathway, and that such pathway is selectively activated in a subset of pancreatic cancer cells. In this section, I am going to introduce what is known in the literature about this important nuclear receptor.

1.6.1 An overview of HNF4α

HNF4α is a highly conserved nuclear receptor that is expressed in almost all levels of animals, from sponge to humans (reviewed by Sladek 2011) (Figure 9A). It is classified as an 'orphan' receptor within the nuclear receptor superfamily and functions as a homodimer (Jiang et al., 1995). Like many other nuclear receptors, HNF4α is activated through a conformational change, which allows the release of co-repressors and binding of co-activators (reviewed by Gonzalez 2008). HNF4α activates the expression of a wide range of genes for metabolism, including those for glucose, fatty acid, cholesterol and xenobiotic and drug metabolism (Odom et al., 2004; Waxman et al., 2009). Expression of HNF4α can be driven by two promoters, and there are at least six splice variants, which are present in different cell types (reviewed by Sladek 2011).

1.6.2 HNF4α and SMAD4 during early embryogenesis

HNF4α is expressed during gastrulation of the mouse embryo. It is essential for the formation of visceral endoderm; as deletion of the *Dpc4* gene, which codes for SMAD4, causes growth retardation and absence of HNF4α in the mouse embryo (Sirard et al., 1998) (Figure 9B). Deletion of the *Alk2* gene, which codes for a BMP Type-I Receptor, causes decreased expression of HNF4α and failed gastrulation (Gu et al., 1999) (Figure 9B). On the

Figure 9

(A)

HNF4 alpha – degree of conservation of amino acids (a.a.) across species

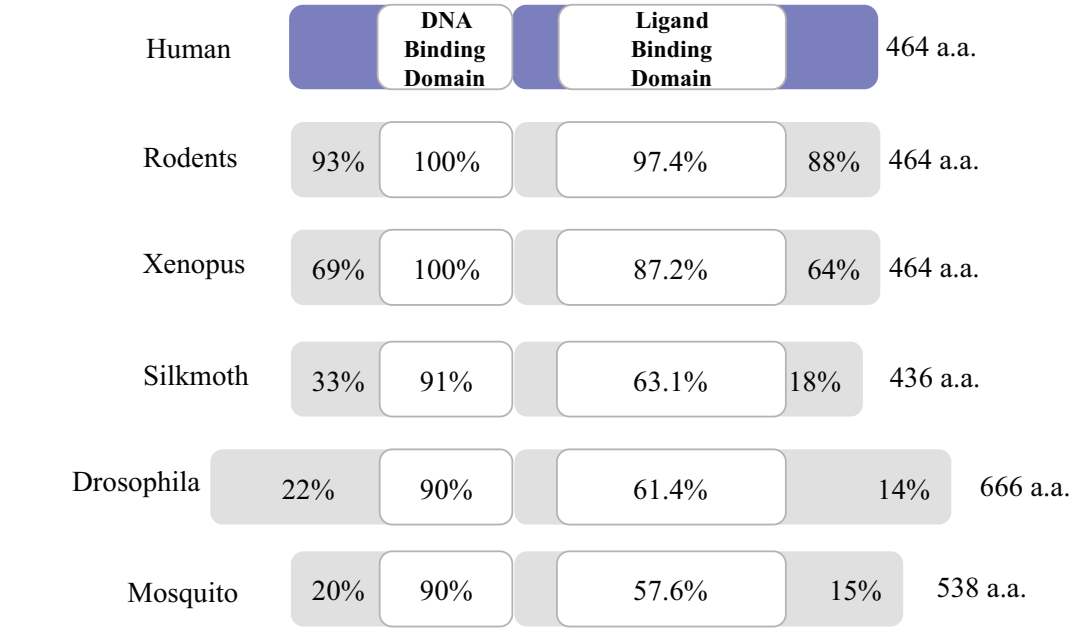

(B)

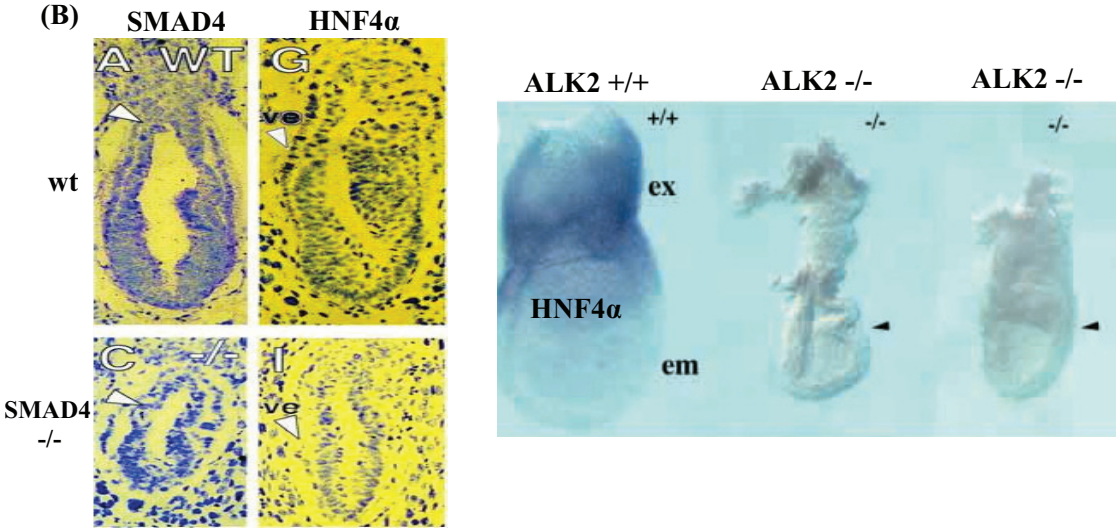

Figure 9(A) – The amino acid sequence of Hepatocyte Nuclear Factor 4-α (HNF4α) is highly conserved across species. **(B) –** Left, deletion of SMAD4 in the the mouse embryo disrupts gastrulation and results in absence of the endoderm marker HNF4α (Source: Sirard et al., 1998). Right, deletion of ALK2, a BMP Type-I receptor, also disrupts gastrulation of the mouse embryo, showing compromised HNF4α expression (Source : Gu et al., 1999)

other hand, data suggests that TGFβ down-regulates the expression of HNF4α, reportedly by inducing proteasome-dependent degradation; however, it is not clear whether or not SMAD4 is involved (Lucas et al., 2004).

1.6.3 Inactivation of HNF4α causes diabetes

In humans, HNF4α is mainly expressed in organs along the gastrointestinal tract, including liver, pancreas, small intestine, where they are all endoderm-derived tissue (with reference to mouse development); however, there is one exception – the kidneys, which are derived from the mesoderm (Sladek et al. 1990; Si-Tayeb 2010). In human hepatocytes and pancreatic islet cells, HNF4α regulates a large fraction of their transcriptomes by binding directly to as many as half of the actively transcribed genes, as shown by Chromatin Immunoprecipitation (CHIP) assays; this may well explain why HNF4α is essential to both development and proper function of the liver and pancreas (Odom et al., 2004).

Indeed, heterozygous mutations of HNF4α cause type-1 maturity-onset diabetes of the young (MODY1), a genetic disorder of the insulin-secreting pancreatic beta cells characterized by diabetes mellitus before 25 years of age with an autosomal dominant pattern of inheritance (Fajans et al., 2001). These MODY1 patients show normal insulin sensitivity, and both liver and kidney function, but have a defect in glucose-stimulated insulin secretion from the pancreatic β-cells (Gupta et al., 2005). Of interest, no homozygous mutations of the HNF4α gene have been found in humans. This is in agreement with the neonatal lethality found in mice with ubiquitous deletion of HNF4α (Chen et al., 1994), in which the mouse embryos failed to go through normal gastrulation; in which HNF4α is normally expressed specifically in the visceral endoderm (Duncan et al., 1994, 1997).

1.6.4 Ablation of HNF4α in mice

Mice with homozygous deletion of HNF4α in pancreatic β-cells (*Ins*-Cre; $Hnf4\alpha^{flox/flox}$) show impaired insulin secretion, resembling maturity-onset diabetes of the young (MODY). Unlike in humans, heterozygous deletion of HNF4α in mice does not result in diabetes (Gupta et al., 2005; Miura et al., 2006).

In the embryonic mouse liver, HNF4α is essential for the differentiation of hepatocytes and is engaged in hepatocyte-specific gene regulation related to the synthesis of apolipoproteins, acute phase reactive proteins, and many other secreted proteins (Mizutani et al., 2011). In the adult mouse liver, deletion of HNF4α causes severe deregulation of fatty acid metabolism, resulting in higher mortality (Hayhurst et al., 2001; Inoue et al., 2002, 2004, 2006). Furthermore, HNF4α is required for development of the mouse colon, as HNF4α deficiency in the developing colon results in absence of crypt formation (Garrison et al., 2006).

1.6.5 HNF4α in drug metabolism

HNF4α is also an important player in cellular response to xenobiotics. It directly participates in xenobiotics induced expression of Cytochrome P450 3A4 (CYP3A4), a well documented enzyme responsible for the biotransformation of many structurally divergent drugs in clinical use (Tirona et al., 2003). Conditional heterozygous deletion of HNF4α in the fetal mouse liver showed little expression of CYP3A, and reduced basal and inducible expression of CYP3A in the adult mouse liver (Tirona et al., 2003).

1.6.6 HNF4α and reactive oxygen species in cancer

Conflicting reports have put HNF4α in both tumour-promoting and tumour suppressing roles depending on the cellular context. Transient inhibition of HNF4α initiates hepatocellular transformation through a microRNA inflammatory feedback loop circuit in mouse (Hatziapostolou et al., 2011). However, HNF4α acts to protect intestinal cancer cells from the generation of reactive oxygen species (ROS) (Darsigny et al., 2010). Microarray analysis of gene expression profiles from mice lacking HNF4α in the intestinal epithelium identified novel functions of HNF4α in targeting oxidoreductase-related genes involved in the regulation of ROS levels.

1.7 The pancreas and mouse models of pancreatic cancer

1.7.1 Overview of the pancreas

The pancreas has both exocrine (regulation of protein and carbohydrate digestion) and endocrine (glucose homeostasis) compartments (Figure 10A, B). The exocrine pancreas,

Figure 10
(A)

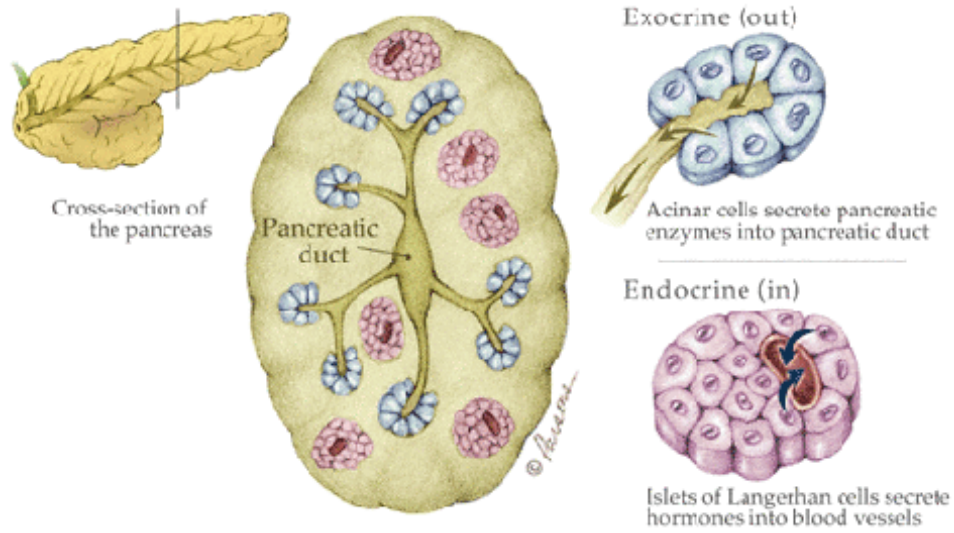

(B)

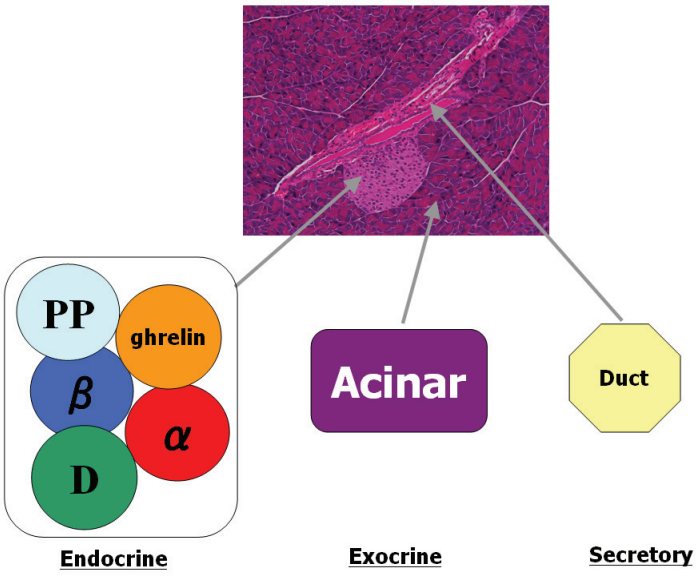

Figure 10 (A) - Distribution of the exocrine and endocrine glands in the pancreas - taken from the website of Johns Hopkins University Pancreatic Cancer Center: www.path.jhu.edu/pancreas/professionals/DuctLesions.php. **(B) –** An illustration of the known cell types present in the normal adult pancreas (a mouse pancreas in the H&E stained photograph). In the endocrine pancreas, alpha cells produce glucagon (15–20% of total islet cells), Beta cells produce insulin (65–80%), Delta cells produce somatostatin (3–10%), PP cells (gamma cells) produce pancreatic polypeptide (3–5%), and Epsilon cells produce ghrelin (<1%). In the exocrine pancreas, acinar cells produce digestive enzymes such as amylase, secret and deliver enzymes via the duct cells to duodenum (source: Elayat et al., 1995) .

which makes up over 95% of the pancreatic mass, is composed of a branching network of acinar and duct cells (reviewed by Murtaugh & Melton 2003 and Hezel et al., 2006). The acinar cells, which are organized in functional units along the duct network, synthesize and secrete zymogens, such as trypsin and amylase, into the ductal lumen in response to cues from the stomach and duodenum (reviewed by Hezel et al., 2006). These pancreatic ducts merge and feed into progressively larger structures, finally connecting to the common bile duct (reviewed by Murtaugh & Melton 2003). Within the acinar units, near the ducts, are centroacinar cells.

Endocrine cells are organized into globular clusters of Islets of Langerhan and are dispersed throughout the exocrine tissue. The islets make up only a small fraction of the total organ mass, about 1–2% (reviewed by Murtaugh & Melton 2003). Within the islets, the endocrine cell types are present in varying proportions: β-cells make up the majority (60–80%) and form a core around which the others are arranged. α-cells comprise 15–20% of the islet mass, and the remaining cells are of δ and Pancreatic Polypeptide (PP) type (reviewed by Murtaugh & Melton 2003). Rare cells expressing endocrine markers, such as insulin, can also be found associated with the acini and the ductal epithelium (Mills, 2007).

1.7.2 Lineage-specific promoters used in mouse models

Pancreas and liver progenitors develop from endoderm cells in the embryonic foregut (Zaret et al., 2008). Specifically, the pancreas derives from two patches of epithelial outgrowth that bud dorsally and ventrally from the gut epithelium, between the stomach and duodenum. This starts in the mouse at about embryonic day 9 (E9). Prior to and during budding of the pancreatic primordium, all progenitor cells express the homeodomain protein Pdx1, and these cells later give rise to all pancreatic cell types (Figure 11A), (Ohlsson et al. 1993, Gu et al. 2002), including pancreatic duct cells (Gu et al. 2002).

During the course of budding, *Pdx1* expression was at high levels in developing β-cells and at lower levels in undifferentiated precursors (Guz et al. 1995, Jensen et al. 2000a). Inactivation of the *Pdx1* gene in the pancreata results in growth arrest just after budding (Ahlgren et al. 1996, Offield et al. 1996), indicating that although Pdx1 expression has been initiated before budding, its functions are mainly in post-budding differentiation of the endocrine cells (Burlison et al., 2008). Thus, some other developmental transcription

Figure 11

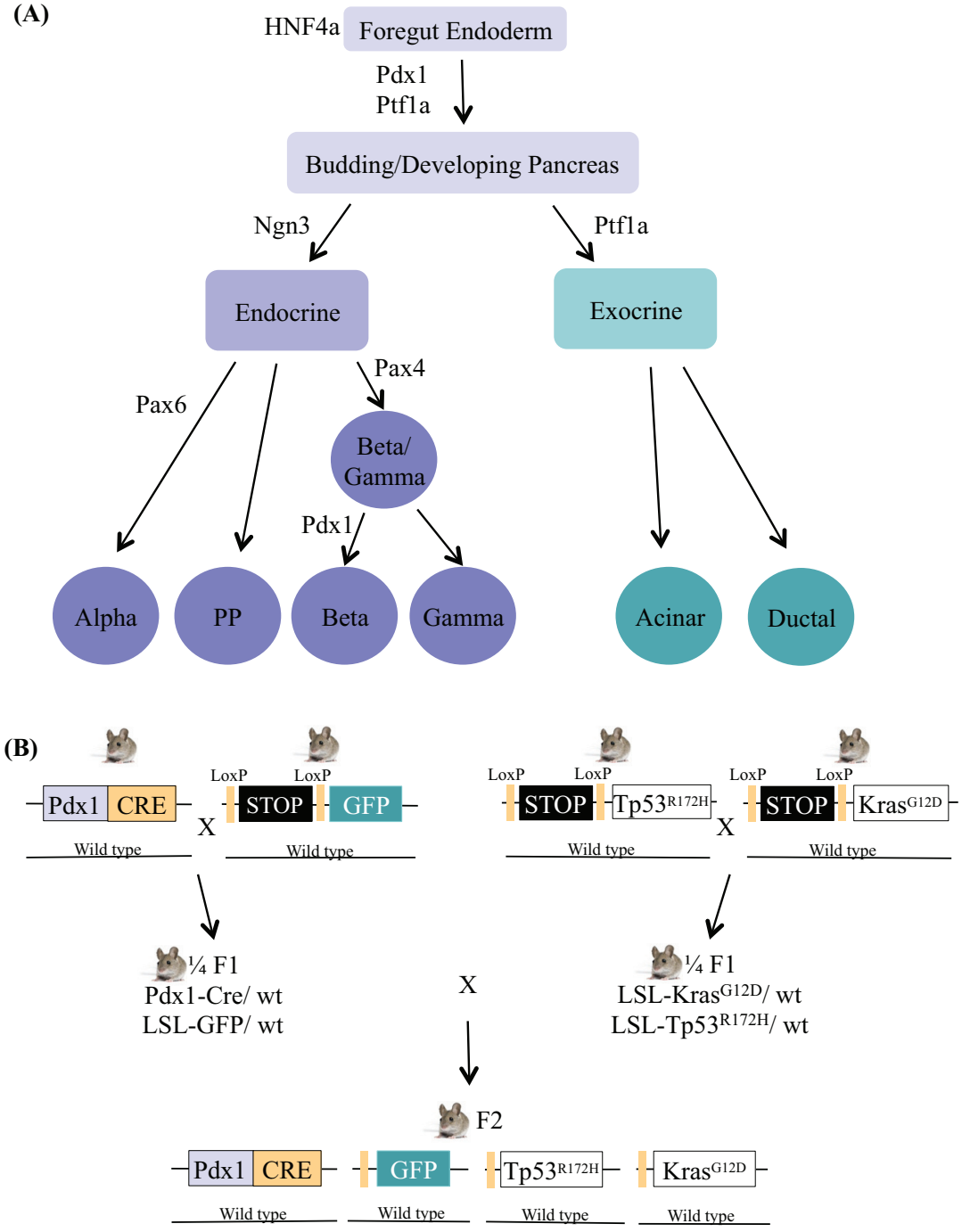

Figure 11 (A) - Lineage specification during pancreas development, showing *Ptf1a* and *Pdx1* are among the earliest genes expressed in the developing pancreatic duct, and Pdx1 is eventually also expressed in β-cells. (Hruban et al., 2006). **(B) -** Cross of strains to generate *Pdx1-Cre; LSL-Kras$^{G12D+/-}$; LSL-Tp53$^{R172H+/-}$,* with options to include a Green Fluorescent Protein reporter.

factors, but not Pdx1, are required for budding of the pancreatic epithelium (reviewed by Murtaugh & Melton 2003). Furthermore, Pdx1 is required for proliferation in the post-budding pancreatic epithelium; conditional suppression of the *Pdx1* gene, using tetracycline transactivator protein (tTA), perturbs islet and acinar differentiation (Holland et al. 2002). However, at later stages of development beyond E9.5, *Pdx1* is also expressed in the epithelium of the duodenum, the bile duct, and the posterior part of the stomach (Li et al., 1999, Offield et al. 1996, Miller et al., 1994, Guz et al., 1995; Jørgensen et al., 2007).

In the adult pancreas, Pdx1 was originally found to be a critical transcriptional inducer of insulin and somatostatin in adult islet cells (Ohlsson et al., 1991, 1993; Miller et al., 1994; Leonard et al., 1993; Peshavaria et al., 1994; reviewed by Jørgensen et al., 2007). Pdx1 expression is limited to β-cells in the Islet of Langerhans; β-cell-specific deletion of the *Pdx1* gene results in loss of insulin production and diabetes (Ahlgren et al. 1998). Heterozygous ablation of *Pdx1* in mice results in a MODY-like diabetic phenotype (Dutta et al. 1998).

Another pancreatic lineage promoter that has been widely used for pancreatic specific transgenic expression is *Ptf1a*. It is coexpressed with Pdx1 in both dorsal and ventral pre-budding pancreatic epithelia from E9.0 to E9.5 (Jørgensen et al., 2007). At E10.5, Ptf1a is restricted to the epithelium of the pancreatic primordia with sharp boundary with the duodenum (Jørgensen et al., 2007). Later at E12.5, Ptf1a expression segregates to the growing tips of the branching epithelium to eventually end up in the acinar cells (Jørgensen et al., 2007), in contrast, Pdx1 is also expressed in some extra-pancreatic tissues and eventually in mature β-cells. Like Pdx1, Ptf1a is dispensable for budding of the early pancreatic epithelium, but indispensable for post-budding differentiation of the exocrine-acinar lineage (Krapp et al. 1998; Kawaguchi et al., 2002; Burlison et al., 2008). Co-expression of Ptf1a and Pdx1 is required for pancreas development, as pancreas formation is restored in the offspring from crossing *Pdx1*-null mice with *Ptf1a-Pdx1* mice (expressing *Pdx1* under the control of the *Ptf1a* promoter) (Kawaguchi et al. 2002).

In the developing pancreatic primordium, *Ptf1a*-expressing cells contribute to almost all cell types of the dorsal and ventral pancreas (Kawaguchi et al. 2002). This has been shown by lineage tracing in mice using the $Ptf1a^{Cre/+}$ genotype coupled to a Cre-catalyzed activation of a *LacZ* reporter gene (Kawaguchi et al. 2002). Furthermore, *Ptf1a*-null mice fail to develop

the ventral pancreatic bud, and cells are instead integrated into the duodenum, resulting in absence of acinar cells (Krapp et al. 1998; Kawaguchi et al., 2002). While in the dorsal pancreas, outgrowth and branching are decreased comparing with the wild-type pancreatic buds (Kawaguchi et al., 2002). These lines of evidence suggest that *Ptf1a* is essential for specification and terminal differentiation of acinar cells and for suppression of an intestinal fate.

1.7.3 Lineage specificity of *Pdx1* and *Ptf1a*

In terms of specificity to the pancreas, both *Pdx1* and *Ptf1a genes* are not exclusive. Pdx1 is also expressed in cells that give rise to stomach and duodenum during embryogenesis (Gannon et al., 2000), while Ptf1a is also expressed in the cerebellum (Hoshino et al., 2005). In transgenic models, the *Pdx1*-Cre system occasionally develops extra-pancreas tumours (Aguirre et al. 2003; Hingorani et al. 2005), in contrast to *Ptf1a*-Cre which was reported to be free of extra-pancreas tumours, even in the cerebellum (Ijichi et al., 2006). Moreover, Cre-mediated recombination appears to be more homogeneous in the *Ptf1a*-Cre system than in the *Pdx1*-Cre system (Ijichi et al., 2006; Hingorani et al. 2003). Hence the *Ptf1a-Cre* system may have a small advantage in specificity over the *Pdx1*-Cre system. While the mouse model used for my experiment in this thesis were driven by *Pdx1*-Cre, with reference to Hingorani et al., 2003; 2005.

1.7.4 The *Pdx1*-Cre/ *LSL-Kras$^{G12D/+}$* / *LSL-Tp53$^{R172H/+}$* (KPC) mouse model

The so called KPC mouse model was originally developed by Tyler Jacks and David Tuveson's group, in which mouse pancreatic malignant neoplasia and cancer are efficiently generated by conditional expression of KRas^{G12D} and p53^{R172H}, driven by Cre-recombinase under control of the *Pdx1* promoter that covers all pancreatic lineage (Figure 11B). Once the LoxP-Stop-LoxP (*LSL*) sequence upstream of the knock-in mutant allele is removed by Cre-mediated recombination, KRas^{G12D} and p53^{R17H2} mutant proteins can continue to be expressed in all surviving progeny, even while Pdx1 has ceased expression in the mature acinar cells in the postnatal pancreas (reviewed Hruban et al., 2006) (Figure 12A). Importantly, expression of KRas^{G12D} and p53^{R17H2} do not visibly affect normal development of the pancreas. As shown by very young KPC mice of about 4 to 6 weeks old, most of the pancreatic parenchyma appears histologically normal, suggesting tumorigenesis is unlikely to have begun *in utero* or in the immediate postnatal period (Hingorani et al., 2005).

Figure 12

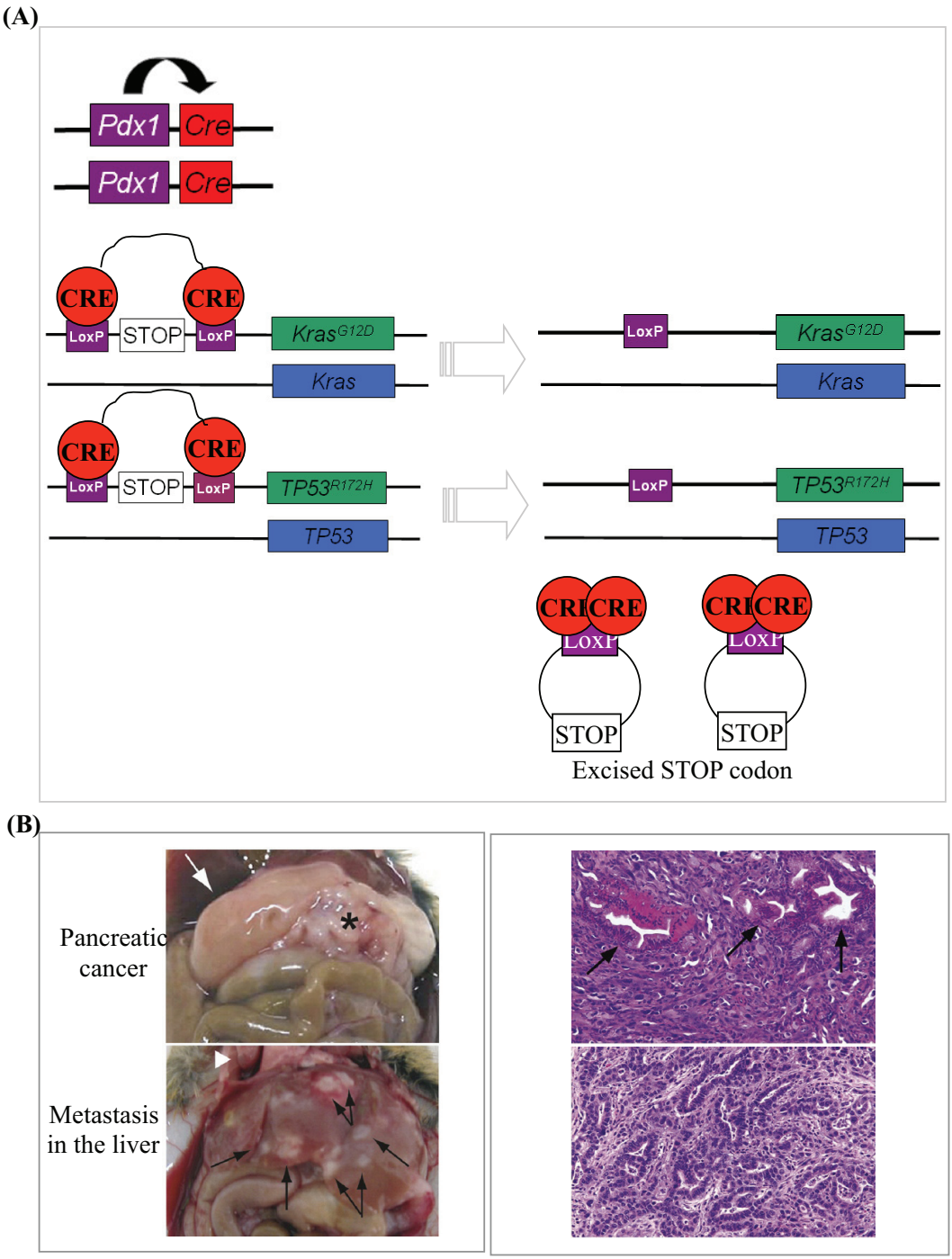

Figure 12 (A) - Mechanism of CRE-recombinase to target conditional expression of KRas^{G12D} and p53^{R172H} in all pancreatic lineage under the control of a pancreas-specific transcription factor, PDX1. **(B) -** An example of the appearance of mouse pancreatic cancer and liver metastasis (left) and the microscopic view of tumour sections by H&E staining (right); photographs from Hingorani et al., 2005.

Expression of $KRas^{G12D}$ alone is sufficient to induce PanIN lesions in about 12 months time, with only occasional incidences of tumour development (Hingorani et al., 2003); but when the mutant p53 is also expressed together with $KRas^{G12D}$ in the pancreas, these premalignant lesions are rapidly transformed into pancreatic ductal adenocarcinoma and metastasized to the liver and lung, at around 10-week old, and their median survival length is only 20 weeks (Hingorani et al., 2005) (Figure 12B). The mutant $p53^{R172H}$ (or loss of p53) acts to retain $KRas^{G12D}$-expressing cells in the pancreas by overcoming growth arrest or senescence (Morton et al., 2009), while the remaining wild-type *Tp53* allele is uniformly lost and genomic instability is acquired. Moreover, the mutant $p53^{R172H}$ can simultaneously inhibit the wild type counterpart (Kern et al., 1992). Since PanIN lesions are observed in a similar stage and degree in both the $Kras^{G12D/+}$/ $Tp53^{R172H/+}$ and $Kras^{G12D/+}$-alone mice, additional genetic alterations must have been acquired to promote neoplasia development.

The KPC mouse model closely recapitulates the human pancreatic cancer in many respects. The mice display symptoms that are highly reminiscent of clinical symptoms, including cachexia, abdominal distension, and obstruction of the biliary and small bowel (Hingorani et al., 2005). The pattern of *Erbb2/Her2* in mouse pancreatic tumour is variable even within a given animal, consistent with the heterogeneous nature of *Erbb2/Her2* expression observed in human pancreatic cancer (Day et al., 1996). Phospho-ERK/MAP kinase level is variable and appears to correlate with the pattern of *Erbb2/Her2* expression (Hingorani et al., 2005). Furthermore, mutant $p53^{R172H}$ is stabilized while the wild-type *Tp53* allele is lost in all primary and metastatic pancreatic tumour cell lines (Hingorani et al., 2005). This is in agreement with observations in human (Rozenblum et al., 1997; Scarpa et al., 1993), suggesting LOH is a requisite step in tumour progression (Hingorani et al., 2005). Furthermore, the distribution of metastases also resembles that of human pancreatic cancer, mostly encountered in the liver (80%), lung (50% to 60%), adrenal glands (20%), and peritoneum (20% to 30%) (reviewed by Lillemoe et al., 2000; Hingorani et al., 2005).

1.7.5 Roles of SMAD4 (*Dpc4*) and TGFβR2 during pancreatic carcinogenesis

The combination of $KRas^{G12D}$ and SMAD4 deficiency causes rapid development of tumours resembling IPMN lesions, and consequently a dramatic reduction in survival compared with $KRas^{G12D}$ alone (Bardeesy et al., 2006). All these mice, regardless of whether *Pdx1* or *Ptf1a* was used, presented with a palpable abdominal mass between ages 7 and 12 weeks, and

reached terminal morbidity between ages 8 and 24 weeks of age. Comparing age-matched Cre *LSL-Kras*$^{G12D/+}$ and Cre *LSL-Kras*$^{G12D/+}$/ *Dpc4*$^{lox/lox}$ pancreas at 2 weeks, there was no significant differences in tumour morphology, but the 4-week time point shows a SMAD4 deficiency that correlated with a significant increase in both the number and size of the lesions. These early lesions progress to extensive IPMN and advanced PanIN lesions by 8 weeks, while the age-matched *Ptf1a*-Cre/ *LSL-Kras*$^{G12D/+}$ counterparts had only focal low-grade PanINs. BrdU staining also revealed that PanINs and metaplastic ductal lesions in Cre *LSL-Kras*$^{G12D/+}$/ *Dpc4*$^{lox/lox}$ mice demonstrated increased proliferation relative to lesions in Cre *LSL-Kras*$^{G12/+}$/ *Dpc4*$^{+/+}$ mice and to controls, for both epithelial and stromal tissues.

The *Tgfbr2* gene is inactivated in less than 5% of human pancreatic cancers, and mostly in medullary carcinoma types, a rare variant of pancreatic cancer (Goggins et al. 1998). Similar to deletion of SMAD4, deletion of *Tgfbr2* in the context of KRas^{G12D} develop well-differentiated mouse pancreatic cancer with 100% penetrance and a median survival of about 15 weeks (Ijichi et al., 2006). In the absence of KRas^{G12D}, deficiency in TGFβR2 alone in the *Ptf1a*-expressing lineage did not affect pancreas development or cause tumour development (Ijichi et al., 2006), but ubiquitous deficiency of TGFβR2 is embryonic lethal (Oshima et al., 1996). Unlike *Pdx1*- or *Ptf1a*-Cre/ *LSL-Kras*$^{G12D/+}$/ *Dpc4*$^{lox/lox}$ mice, which develop locally advanced disease, the *Ptf1a*-Cre/ *LSL-Kras*$^{G12D/+}$/ *Tgfbr2*$^{flox/flox}$ tumours also displayed distant metastasis, local invasion, and peritoneal dissemination; the mice survived to a similar age to the *Pdx1*-Cre/ *LSL-Kras*$^{G12D/+}$/ *LSL-Tp53*$^{R172H/+}$ mice, which produces highly metastatic tumours (Ijichi et al., 2006).

The SMAD4-deficient mice show different histological phenotypes from that in human pancreatic cancer. Loss-of-SMAD4 has had a well-documented correlation with metastasis in human (discussed in the previous paragraph), but no metastases are found in aged *Pdx1*-Cre/ *Kras*$^{G12D/+}$/ *Dpc4*$^{lox/lox}$ mice up to 33 weeks. Furthermore, loss-of-SMAD4 is not typically found in association with IPMN in human pancreatic cancer (Furukawa et al., 2005; Iacobuzio-Donahue et al., 2000). However, mice bearing *Ptf1a*-Cre/ *LSL-Kras*$^{G12D/+}$, ablation of SMAD4, but not TGFβR2, develop IPMN (Ijichi et al., 2006). This suggests that mutations in just KRas and SMAD4 in mice are unable to resemble the human cancer, which is likely to involve additional genetic aberrations. For example, p16^{Ink4A} and p53 are known to be frequently mutated in human pancreatic cancer; while in the mouse models, both may

have remained wild-type (Kojima et al., 2007), let alone other potential non-conserved underlying pathways between human and mouse.

In addition, discrepancies in the phenotype between SMAD4-null and TGFβR2-null mice suggest a potential involvement of the BMP-SMAD1/5/8 route, which surprisingly, has not been studied much in pancreatic cancer to date – only a few in vitro reports using established cell lines can be found in the literature. This may have been due to lacking robust antibodies to distinguish different SMADs on immunohistochemistry. Nevertheless, BMPR1 and SMAD3 (of the TGFβ route) mutations have already been identified by high throughput sequencing in human pancreatic cancer samples (Jones et al., 2008). Hence, it would be of immediate interest for the research community to investigate the roles of the BMP-SMAD4 pathway during pancreatic carcinogenesis, such as via the use of the *Pdx*-Cre/*Ptf1a*-Cre system in mice, along with some improved SMAD antibodies that may now be available.

1.8 Thesis Aims

It is not clear whether human cancers originated from a single cell or from multiple cells, or from particular lineages of cells in an organ. However, in the mouse model used in this project, all pancreatic cells could express the mutant $KRas^{G12D}$ and mutant $p53^{R172H}$ under the control of *Pdx1*-Cre-mediated recombination. Considering the pancreas parenchyma already comprises different cells types, along with genomic instability acquired during cancer progression, heterogeneous tumour cells were likely to evolve simultaneously from different cell compartments in the pancreas. Moreover, histology of both human and mouse pancreatic cancer already demonstrate extensive heterogeneity of cells. Hence, I wished to identify some important differences in the properties between individual tumour cell types, and to find out what pathways and transcription factors were activated in the background of $Kras^{G12D}$ and $p53^{R172H}$.

In order to first find out if heterogeneous cell types exist in the primary culture of mouse pancreatic cancer cells, I conducted single-cell cloning, which has never been done with this mouse model in the literature. I identified at least seven cell sub-clones were present, in which they showed different morphologies under the light microscope, and each having a gene expression profile indicated by screenings with PCR and immunoblots. Among the pathways examined, I found that the canonical Wnt pathway and ERK phosphorylation were

more active in some of the cell-sub-clones that proliferated under anchorage independent conditions. As a minor project, I examined which pathway was playing a stronger role in supporting proliferation under anchorage independent conditions.

As my main project and of particular interest, the mouse pancreatic cancer cell sub-clones demonstrated differential phospho-SMADs downstream of the TGFβ/BMP receptors, which appeared to correlate with HNF4α expression in some of the cell sub-clones. Since SMAD4 is lost in 50% of the pancreatic cancer cases, such differential SMAD phosphorylation would be of high relevance to human pancreatic cancer. Moreover, HNF4α is well documented in the control of glucose metabolism, I therefore investigated a potential relationship between the TGFβ/BMP pathway, HNF4α expression, and influence of glucose concentration on the mouse pancreatic cancer cells.

2 MATERIALS & METHODS

2.1 Materials

2.1.1 Subcutaneous injection in mice

Supplier: Charles River, UK

CD1 nude mice

Supplier: Invitrogen, Paisley, UK

Hank's Buffered Salt Solution (HBSS)

Supplier: Beckman Coulter UK Ltd, Buckinghamshire, UK

21G needle and 1ml syringe

2.1.2 Cell culture medium & routine buffers

Supplier: Invitrogen, Paisley, UK

Foetal Bovine Serum

Dulbecco's Modified Eagle Medium (DMEM - high glucose)

Dulbecco's Modified Eagle Medium (DMEM - no glucose)

Minimum Essential Medium (MEM)

L-Glutamine

Non Essential Amino Acids

200mM L-Glutamine

MEM Vitamins (100x)

MEM Non-Essential Amino Acids (NEAA) (100x)

2.5% Trypsin solution

Supplier: Edinburgh Cancer Research Centre

Sterile PBS

Sterile PBS/1mM EDTA

2.1.3 Cell culture plastic ware

Supplier: TPP Helena Biosciences, Tyne & Wear, UK

FACS polypropylene tubes

Falcon tissue culture dishes (60mm, 90mm and 120mm)

Falcon tissue culture plates (6, 12, 24 and 96 well)

Cryotubes

Cell Scrapers

2.1.4 Cell culture chemicals

Supplier: Sigma Chemical Co, Poole, UK

Dimethyl Sulphoxide (DMSO)

Sodium Pyruvate

Calcium Chloride

Propidium Iodide (PI)

Bovine Serum Albumin (BSA) solution

Supplier: Qiagen, Crawley, UK

RNase A

Supplier: Sigma Chemical Co, Poole, UK

SB-431542

UO126

XAV939

IWR1

Puromycin

G418

Thymidine

Supplier: Selleck Chemicals, USA

PD184352

LDN-193189

Supplier: R&D systems, Abingdon, UK

Recombinant mouse BMP9

Supplier: Cell Signaling Technologies, Hertfordshire, UK

Recombinant mouse TGFβ1

Supplier: Millipore, Hampshire, UK

Polybrene (10mg polybrene per ml stock)

2.1.5 Immunofluorescence

Supplier: Thermo Fisher Scientific, Loughborough, UK

37% Formaldehyde Solution

Supplier: Invitrogen, Paisley, UK

Alexa Fluor® 488 Goat Anti-Mouse IgG (H+L)

Alexa Fluor® 488 Goat Anti-Rabbit IgG (H+L)

Alexa Fluor® 594 Goat Anti-Mouse IgG (H+L)

Alexa Fluor® 594 Goat Anti-Rabbit IgG (H+L)

Supplier: Thermo Fisher Scientific, Loughborough, UK

Microscope glass slides
Coverslips (19mm)

Supplier: Vector Laboratories Ltd, Peterborough, UK

Vectashield mounting medium

Vectashield mounting medium with DAPI

Supplier: Olympus UK Ltd, Hertfordshire, UK

Olympus FV1000 Confocal microscope

(Primary antibodies)

Supplier: Cell Signaling Technologies, Hertfordshire, UK

Anti phospho-Histone H3 rabbit Ab

Supplier: R&D systems, Abingdon, UK

Anti HNF4α mouse monoclonal Ab

Supplier: Transduction Laboratories, BD Biosciences, Oxford, UK

Anti E-cadherin monoclonal mouse Ab

Supplier: Abcam plc, Cambridge, UK

Anti Pdx1 mouse Ab

2.1.6 Immunohistochemistry

Supplier: Dako UK Ltd, Ely, UK

DAKO Envision kit ™ (mouse and rabbit)

Supplier: Olympus UK Ltd, Hertfordshire, UK

Olympus BX51 microscope

Supplier: Sigma Chemical Co, Poole, UK

Sodium citrate

Haematoxylin

Xylene

Ethanol

Supplier: Vector Labs, UK

Immedge pen

Supplier: Thermo Fisher Scientific, Loughborough, UK

DPX mounting reagent

Supplier: Leica Microsystems, Milton Keynes, UK

Glass slides and coverslips

(Primary antibodies)

Supplier: R&D systems, Abingdon, UK

Anti-HNF4α mouse monoclonal Ab (used 1 in 500)

Supplier: Santa Cruz Biotechnology Inc, USA

Anti-SMAD4 mouse monoclonal Ab clone B8 (used 1 in 100)

2.1.7 Protein extraction & western blotting

Supplier: PERBIO, Glasgow, UK

Micro BCA ™ protein assay kit

Supplier: Beckman Coulter UK Ltd, Buckinghamshire, UK

Beckman DU® 650 spectrophotometer

Supplier: GE Healthcare, Little Chalfont, UK

Full range molecular weight rainbow ™ marker

Supplier: Genetic Research Instrumentation, Dunmow, UK

Atto protein electrophoresis apparatus

Supplier: Jencons, Leighton Buzzard, UK

Wet blotting apparatus

Supplier: Severn Biotech Ltd, Kidderminster, UK

Design-a-gel 30% acrylamide, Bis-Tris (37: 5: 1)

Supplier: Schleicher and Schuell, London, UK

Nitrocellulose membrane

Supplier: Whatman, Maidstone, UK

3mm filter paper

Supplier: Cell Signaling Technologies, Hertfordshire, UK

Anti-mouse/horseradish peroxidase conjugate

Anti-rabbit/horseradish peroxidase conjugate

Supplier: Millipore, UK

Re-blot Plus Strong antibody stripping solution

Supplier: Sigma Chemical Co, Poole, UK

Ammonium persulphate (APS)

Bovine serum albumin (BSA)

TEMED

Tween 20

0.1% (v/v) aprotinin

Bovine serum albumin (BSA)

2mM phenylmethylsulphonyl fluoride (PMSF) TEMED

Sodium fluoride (NF)

Sodium orthovanadate (Na3VO4)

Sodium chloride (NaCl)

Sodium pyrophosphate (Na4P2O7)

Sodium dodecyl sulphate (SDS)

Magnesium chloride (MgCl2) EGTA

Sodium deoxycholate

Triton X-100

NP40

Leupeptin

2-mercaptoethanol

Glycerol

Bromophenol blue

Glycine

Ethanol

Methanol

Tween 20

Supplier: Tesco, UK

Marvel skimmed milk powder

Supplier: Sigma Chemical Co, Poole, UK

Mouse IgG (whole molecule)

Anti-mouse IgG-Agarose

(Primary antibodies)

Supplier: Santa Cruz Biotechnology Inc, USA

Anti-SMAD4 mouse monoclonal Ab clone B8

Supplier: Cell signalling Technologies, Hertfordshire, UK

Anti-FAK rabbit Ab

Supplier: R&D systems, Abingdon, UK

Anti-HNF4α mouse Ab

Supplier: Merck, UK

Anti-p53 (PA240) mouse monoclonal Ab

Anti-p53 (PA421) mouse monoclonal Ab (a gift from Ted Hupp lab)

Supplier: Cell signalling Technologies, Hertfordshire, UK

Anti Axin1 rabbit Ab

Anti ERK rabbit Ab

Anti MEK mouse Ab

Anti FAK rabbit Ab

Anti Src rabbit Ab

Anti phospho-MEK1/2 (Ser217/221) rabbit Ab

Anti phospho-ERK-S42/S44 rabbit Ab

Anti phospho-FAK-Y397 rabbit Ab

Anti SMAD1 rabbit Ab

Anti phospho-SMAD1/5/8 rabbit Ab

Anti phospho-SMAD2 rabbit Ab

Anti phospho-Src-Y416 rabbit Ab

Anti γ-tubulin mouse Ab

Anti Wnt5A rabbit Ab

Anti ZO2 rabbit Ab

Anti Phospho β-catenin (Ser33/37/Thr41) Ab

Supplier: Sigma Chemical Co, Poole, UK

Anti β-actin mouse Ab

Anti Vimentin mouse Ab

Anti Actin mouse Ab

Supplier: Transduction Laboratories, BD Biosciences, Oxford, UK

Anti E-cadherin mouse Ab

Anti N-cadherin mouse Ab

Anti β-catenin muose Ab

Anti ILK mouse Ab

Anti $p27^{KIP1}$ mouse Ab

Supplier: Darling lab, University of Louisville, USA

Anti ZEB1 goat Ab

Supplier: Epitomics Inc, USA

Anti phosphoSMAD3 (SMAD1/2/3) rabbit Ab

Supplier: Fujifilm, Bedford, UK

X-ray films

Supplier: Agfa, UK

X-ray film developer

2.1.8 DNA/RNA preparations

Supplier: Sigma Chemical Co, Poole, UK

Agarose (electrophoresis grade)

Ethidium bromide

Supplier: Bioline, UK

DNA Hyperladder

Supplier: Sigma Chemical Co, Poole, UK

Mission PLKO non-targeting shRNA control plasmid

Supplier: Open Biosystems, Thermo Scientific, Abgene Ltd., Epsom, UK

PLKO lentiviral shRNA sets (individual shRNA used in this thesis)

Dpc4

TRCN0000025881 (s41)

TRCN0000025885 (s42)

Smad1

TRCN0000025876 (s11)

TRCN0000025884 (s12)

TRCN0000025933 (s13)

TRCN0000025963 (s14)

Hnf4α

TRCN0000026149 (sα1)

TRCN0000026158 (sα2)

TRCN0000026216 (sα3)

Ctnnb1

TRCN0000012688

Supplier: Beaton Institute, Glasgow, UK (gift)

pCMV-HIV1

pCMV-VSVG

Supplier: Ambion, UK

DNase turbo kit

Supplier: Qiagen, Crawley, UK

miRNeasy mini RNA extraction

QIAquick Gel purification Kit

QIAprep Spin Miniprep Kit

QIAprep Plasmid Maxi Kit

Supplier: Invitrogen, Paisley, UK

Superscript First-Strand cDNA synthesis kit

2.1.9 Polymerase chain reactions

Supplier: Bio-Rad, Hertfordshire, UK

DNA Engine ® thermal cycler

DNA Engine ® thermal gradient cycler

Supplier: Qiagen, Crawley, UK

TopTaq Master Mix Kit

Supplier: Bioline, UK

Quantitative PCR sensimix Kit (one step)

Supplier: Qiagen, Crawley, UK

Corbett Robocycler

Rotorgene tubes and caps

Supplier: Agilent, Berkshire, UK

PFU Ultra Mastermix

Supplier: Invitrogen, Paisley, UK

(Mouse genes, designed by MIT Primer3, http://bioinfo.ut.ee/primer3-0.4.0/)

Axin2

5' GCTCCAGAAGATCACAAAGAGC 3'

3' AGCTTTGAGCCTTCAGCATC 5'

Lgr5

5' GAGTCAACCCAAGCCTTAGTATCC 3'

3' CATGGGACAAATGCAACTGAAG 5'

cMyc

5' TGAAGAAGAGCAAGAAGATGAG 3'

3' CTGGATAGTCCTTCCTTGTG 5'

Cxcr4

5' CGGCTGCACCTGTCAGTGGCTGACCTCCTCTTT 3'

3' CATAGACTGCCTTTTCAGCCAGCAGTTTCCTTGGC 5'

***Cdh1* (E-cadherin)**

5’ GCACTGGCCGGCCAAGGACAGCCTTCTTTTCG 3’

3’ GGTGGTGCCCCATGGACTTCAGCGTCACTTTG 5’

Hnf4α

5’ CCTCACCTGATGCAAGAACA 3’

3’ TGGCAGGAGCTTGTAGGATT 5’

Gata6

5’ ATGCTTGCGGGCTCTATATGAA 3’

3’ AGGTGGTCGCTTGTGTAGAAGG 5’

Pdx1

5’ GAAATCCACCAAAGCTCACG 3’

3’ TTCAACATCACTGCCAGCTC 5’

2.1.10 SRB cell proliferation assay

Supplier: Sigma Chemical Co, Poole, UK

Sulforhodamine B

Trichloroacetic acid

Supplier: Thermo Fisher Scientific, Loughborough, UK

Glacial acetic acid

Supplier: TPP Helena Biosciences, Tyne & Wear, UK

96-well plates

Supplier: Biohit, UK

BP800 microplate photometer

Supplier: Gilson, Bedfordshire, UK

Multichannel Pipette P200

2.1.11 Soft agar assay

Supplier: R&D systems, Abingdon, UK

2.8% Methylcellulose in MEM

Supplier: Invitrogen, Paisley, UK

Minimal Essential Medium (MEM) power

Supplier: Sigma Chemical Co, Poole, UK

Ultrapure agarose (low melting point - 65.5°C)

2.1.12 Stock solutions and buffers

RIPA buffer for protein lysis

50mM Tris/HCl, pH 7.4

150mM Sodium Chloride

Triton X-100

1% Sodium Deoxycholate

1% NP40

5mM EGTA

100μM Sodium Orthovanadate

1mM PMSF

10µg/ml Aprotinin

100mM Sodium Fluoride

10µg/ml Leupeptin Hemisulfate

10mM Tetra-Sodium Pyrophosphate

DNA electrophoresis running buffer (TBE) 10X

890mM Tris-borate

890mM boric acid

20mM EDTA

Acrylamide gel (8.5%)

11.3ml 30% Acrylamide Bis-Tris (37: 5: 1)

15ml Tris pH 8.8

13.7ml H_2O

400µl 10% SDS

375µl 10% APS

20µl TEMED

Acrylamide gel (15%)

20ml 30% Acrylamide Bis-Tris (37: 5: 1)

15ml Tris pH 8.8

10ml H_2O

400µl 10% SDS

375µl 10% APS

20µl TEMED

Stacker Acrylamide gel

3.2ml 30% Acrylamide, Bis-Tris (37: 5: 1)

2.5ml Tris pH 6.8

14ml H_2O

200µl 10% SDS

200µl 10% APS

20µl TEMED

Protein sample buffer – 5x

800µl 2-mercaptoethanol

1.3ml Tris pH 6.8

2ml glycerol

5ml 10% SDS

1.3ml H2O

Bromophenol blue

Tank buffer - 10x

0.05M Tris

0.05M glycine

0.1% SDS

Transfer buffer

50mM Tris

40mM glycine

0.04% SDS

20% methanol

Membrane Wash buffer

0.2% Tween 20 in Phosphate Base Solution

Electrochemiluminescence (ECL) solution A (500 ml)

20ml 1M Tris pH 8.5

1 vial of Luminol

1 vial of pCoumaric Acid

Electrochemiluminescence (ECL) solution B (500 ml)

20ml 1M Tris pH 8.5

128µl of 30% NaOH

Fix solution (SRB assay)

25% trichloroacetic acid (TCA) solution in distilled water.

Wash solution (SRB assay)

1% glacial acetic acid in distilled water.

SRB staining solution

0.4% Sulforohodamine B (SRB) solution in 1% acetic acid.

SRB solubilising solution

10mM Tris base pH 10.5 in distilled water with pH adjusted using 1M sodium Hydroxide.

Fix and permeabilisation buffer (Immunofluorescence)

1ml formaldehyde 1ml

100mM EGTA 4ml

250mM Pipes 10ml

1M MgCl2 20l

Triton X-100 3.7ml H2O

Wash buffer (Immunofluorescence)

100ml PBS

100µl Triton X-100

Block buffer (Immunofluorescence)

100ml PBS

100µl Triton X-100

2g BSA

Antibodies	Supplier	Clone/Catalog	Westen	IF	IHC
Anti-SMAD4 mouse monoclonal Ab	Santa Cruz	B8	1 in 2000	1 in 500	1 in 100
Anti phospho(S10)-Histone H3 rabbit Ab	Cell Signaling	3377	n/a	1 in 500	n/a
Anti HNF4α mouse monoclonal Ab	R&D systems	H1415	1 in 1000	1 in 1000	1 in 500
Anti SMAD1 rabbit Ab	Cell Signaling	9743	1 in 1000	n/a	n/a
Anti phospho-SMAD2 rabbit Ab	Cell Signaling	(138D4) 3108	1 in 500	n/a	n/a
Anti phospho-SMAD1/5/8 rabbit Ab	Cell Signaling	9511	1 in 1000	n/a	n/a
Anti phospho-SMAD3 (SMAD1/2/3) rabbit Ab	Epitomics	EP823Y	1 in 1000	n/a	n/a
Anti $p27^{KIP1}$ mouse Ab	BD	G173-524	1 in 500	n/a	n/a
Anti Pdx1 mouse Ab	Abcam	ab47267	n/a	1 in 500	n/a
Anti-p53 (PA240) mouse monoclonal Ab	Abcam	ab26	1 in 1000	n/a	n/a
Anti-p53 (PA421) mouse monoclonal Ab	EMD Millipore	MABE283	1 in 1000	n/a	n/a
Anti ERK rabbit Ab	Cell Signaling	4370	1 in 1000	n/a	n/a
Anti MEK mouse Ab	Cell Signaling	L38C12/4694	1 in 1000	n/a	n/a
Anti phospho-MEK1/2 (Ser217/221) rabbit Ab	Cell Signaling	9121	1 in 1000	n/a	n/a
Anti phospho-ERK-S42/S44 rabbit Ab	Cell Signaling	9101	1 in 1000	n/a	n/a
Anti Src rabbit Ab	Cell Signaling	2109	1 in 1000	n/a	n/a
Anti phospho-Src-Y416 rabbit Ab	Cell Signaling	2101	1 in 1000	n/a	n/a
Anti FAK rabbit Ab	Cell Signaling	3285	1 in 1000	n/a	n/a
Anti phospho-FAK-Y397 rabbit Ab	Cell Signaling	3283	1 in 1000	n/a	n/a

Anti E-cadherin mouse Ab	BD	610182	1 in 1000	1 in 200	n/a
Anti N-cadherin mouse Ab	BD	610921	1 in 1000	n/a	n/a
Anti β-catenin muose Ab	BD	610154	1 in 1000	n/a	n/a
Anti ILK mouse Ab	BD	611803	1 in 1000	n/a	n/a
Anti ZO2 rabbit Ab	Cell Signaling	2847	1 in 1000	n/a	n/a
Anti Vimentin mouse Ab	Sigma Aldrich	VIM13.2	1 in 5000	n/a	n/a
Anti ZEB1 goat Ab	DS Darling, Louisville KY	n/a	1 in 5000	n/a	n/a
Anti Wnt5A rabbit Ab	Cell Signaling	2392	1 in 1000	n/a	n/a
Anti Phospho β-catenin (Ser33/37/Thr41) Ab	Cell Signaling	9561	1 in 500	n/a	n/a
Anti Axin1 rabbit Ab	Cell Signaling	C76H11/2087	1 in 1000	n/a	n/a
Anti γ-tubulin mouse Ab	Cell Signaling	2144	1 in 2000	n/aå	n/a
Anti Actin mouse Ab	Sigma Aldrich	A4700	1 in 2000	n/a	n/a

2.2 Methods

2.2.1 Cell culture

Human Primary mouse pancreatic cancer cells were originally derived by Jennifer Morton at the Beatson Institute for Cancer Research (Glasgow, Scotland), from tumour pieces of mouse number 83320, with genotype *Pdx1*-Cre/ $Kras^{G12D/+}$/ $Tp53^{R172H/+}$. Mouse pancreatic cancer cells were maintained in Dulbecco's Modified Eagle Medium (Gibco, Invitrogen) supplemented with 10% Fetal Bovine Serum (Invitrogen) and 2mM L-Glutamine (Gibco, Invitrogen). Single cell clones were isolated by distributing 30 cells in a 96-well plate and resulting colonies were transferred to T25 flasks until 80% confluent. Cells were detached by 0.25% Trypsin, 1.3mM EDTA, PBS, and re-suspend in DMEM/ 10%FBS/ 2mM L-Glutamine. Cells were then split to a T75 flask at 1 in 15 dilution. The remaining cells were centrifuged at 1500rpm for 4 min, resuspended in ice cold FBS with 10% DMSO and stored as backup stocks in the liquid nitrogen tank. Cells were regularly maintained by splitting 1 in 15 for every 3 days. Cells were not kept for more than 15 passages; then a new vial cells at their earliest passage was taken out from the liquid nitrogen and recovered in the tissue culture. As for established human cancer cell lines, A549, HepG2, Caco, HT29 and SW480

were originally from American Type Culture Collection (ATCC); they were cultured in the medium as described above.

2.2.2 Immunoblotting

Cells were washed twice in ice cold PBS and then lysed in ice cold RIPA buffer (50mM Tris, pH7.4, 150mM NaCl, 5mM EGTA, 0.1% SDS, 1% NP40, 1% sodium deoxycholate) with inhibitors: 1mM phenylmethylsulfonyl fluoride (PMSF), 10µg/ml aprotinin, 10µg/ml leupeptin, 100µM sodium vanadate, 500µM sodium fluoride, and 10mM Tetra-sodium pyrophosphate. Cells were washed twice in ice-cold PBS and scraped from the plate on ice by a sterile plastic cell scraper. Crude lysate was clarified by spinning at maximum speed for 15 min at 4°C in bench top Eppendorf centrifuge. Protein concentration was measured by Micro BCA protein assay kit (Thermo Scientific), light absorbance of protein-BCA complexes (purple) was then measured with a cuvette-based spectrophotometer (Biorad) at a wavelength of 562nm. Protein samples at a final concentration of 1µg/µl were denatured with addition of 5x sample buffer by heating at 95°C for 5 min. Samples were kept on ice in all steps before heat-denaturation.

Denatured samples were run on SDS acrylamide gels, transferred to nitrocellulose membrane in transfer buffer, and blocked with 5% Bovine Serum Albumin (BSA) or skimmed milk, in either PBS or TBS containing 0.1% Tween. Primary antibodies used have been listed in the 'Materials' section. Secondary antibodies anti-rabbit HRP and anti-mouse HRP were purchased from Cell Signaling Technologies. Membranes were stripped by incubating on the shaker for 10 min at room temperature, in 1X Re-blot Plus Strong solution (Millipore), then re-blocked for 45 min in 5% BSA (or milk) in PBS (or TBS) with 0.1% Tween. HRP-bounded protein-bands on membranes were amplified by Enhanced chemiluminescence (ECL), followed by exposure on x-ray films (Fujifilm) in the dark room and visualised through a film developer (Agfa AC002). Quantification of intensity of protein bands were done by using ImageJ software (National Institute of Health, Bethesda, USA), relative to the corresponding loading control (Actin or Tubulin).

2.2.3 Immunofluorescence

Glass coverslips had been auto-claved before seeding cells. Each coverslip was seeded with 0.5 x 10^5 cells, in a 12-well plate. After 2 days in the incubator, cells were washed once with TBS and immediately fixed for 10 min in 3.7% Formaldehyde, 10mM EGTA pH8, 25mM Pipes pH6.8, 0.1mM $MgCl_2$, 0.002% Triton X100. Fixation buffer was removed and coverslips were washed twice with wash buffer (TBS, 0.1% Triton X100), followed by 1 hr in blocking buffer (TBS, 2% Bovine Serum Albumin, 0.1% Triton X100). Fixed cells were then incubated overnight with primary antibody diluted in blocking buffer. The next day, coverslips were washed three times in wash buffer and incubated with secondary fluorescent antibodies (Invitrogen) and/or Rhodamine-Phalloidin (Sigma Aldrich) for 45 min at room temperature. Coverslips were washed three times with wash buffer, drained excess buffer, and mounted onto glass slides (Fisher Scientific) with Vectrashield mounting reagent with DAPI (Vector Labs). Photographs of 'stained cells' in the glass slides were taken via a Olympus Confocal Microscope FV1000. Images were processed by FV1000 Viewer (complementary software provided by Olympus) and Photoshop CS3 (Adobe).

2.2.4 RNA extraction and RT-PCR

On Day0, 0.5 x 10^6 cells were plated on 10cm dish. Cells at growth phase (50-70% confluence) on Day 2 were lysed to extract total RNA by RNeasy Mini Kit (Qiagen) according to manufacturer's protocol. Genomic DNA was removed by using DNase turbo kit (Ambion) according to manufacturer's protocol. RNA concentration was measured using Nanodrop (Thermo Scientific). For Reverse Transcriptase reaction (non quantitative), 1µg of RNA of each sample was converted to cDNA by SuperScript First Strand Reverse Transcriptase kit (Invitrogen) according to manufacturer's protocol. PCR was conducted by using Abgene PCR Ready Mix (Thermo scientific) with 20ng cDNA running on Biorad PCR machine; product was analyzed by 1.5% agarose gel electrophoresis in TBE. All primers were designed using PRIMER-3 website (MIT, MA, USA) and purchased from Invitrogen. Sequencing was conducted by the MRC Human Genetics Unit, University of Edinburgh.

2.2.5 Quantitative RT-PCR

0.5 x 10^6 cells were plated on 10cm dish on Day 0. Cells at growth phase (50-70% confluence) on Day 2 were lysed to extract total RNA by RNeasy Mini Kit (Qiagen) according to manufacturer's protocol. Genomic DNA was removed by using DNase turbo

kit (Ambion) according to manufacturer's protocol. RNA concentration was measured using Nanodrop (Thermo Scientific). For quantitative RT-PCR, a reaction standard curve was generated by using 50ng, 5ng, 0.5ng and 0.05ng total RNA of the cell line that most robustly expresses the gene of interest. The control (also known as the housekeeping gene) used for all reactions was 18s rRNA. RNA samples to be measured were loaded at 20ng per reaction. Standard curve reactions were done in duplicates, and sample reactions were done in triplicates, running in a Rotorgene Robocycler (Corbett Research, Qiagen). Quantification of transcript abundance of samples was done by using Rotorgene 6000 software (Qiagen).

2.2.6 Soft agar assay

In a six-well plate for each well, a base agarose layer (0.9% agarose by weight) was prepared by mixing 1ml of 2x concentration of MEM (with 20% FBS, 2x concentration for each of non essential amino acid, vitamins, sodium pyruvate, and L-glutamine, diluted from 100x Invitrogen stock) and 1ml 1.8% low melting-point agarose that had been dissolved in dH_2O (autoclaveed). Such 2x concentration of MEM was prepared by dissolving twice the amount of MEM powder (Invitrogen) needed for 1x MEM. The base layer was left to set at room temperature. The top layer was 1.4% methylcellulose in MEM (with 10% FBS, 1x concentration of each of non essential amino acid, vitamins, sodium pyruvate, and L-glutamine, diluted from 100x Invitrogen stock), which was made up from a stock of 2.8% methyl cellulose in MEM.

Cells were added to the 1.4% methylcellulose MEM to a density of 10,000 cells per ml; 2ml of such cell-methylcellulose suspension was placed on top of the base agarose layer in each well. Cells were then left overnight in the incubator to allow suspended cells to settle on top of the agarose layer (Day0). On Day1 and Day7, photographs of suspended cells were captured by Qimaging Retiga Exi CCD camera attached to Leica Dmil LED inverted routine microscope. Photographs were processed by ImageJ (National Institute of Health, Bethesda, MD, USA), by measuring arbitrary particle area of single cells or colonies. Quantification of colony sizes and plotting of graphs were done by using Microsoft Excel.

2.2.7 Treatment with inhibitors

In soft agar assay, tankyrase inhibitors (XAV939 and IWR1) and MEK inhibitors (UO126 and PD184352) were used. Each inhibitor was dissolved in DMSO as stock (10mM), and diluted into both the bottom agar layer and the top methylcellulose layer, before mixing the suspended cells into the methylcellulose layer. Both XAV939 and IWR was added (and well mixed by pipetting up and down) to a final concentration of 5μM in the medium of both the agar and the methylcellulose layers, while PD184352 was used at final a concentration of 0.25μM. UO126 was used at a final concentration of 1μM. In immunoblot analysis, cells were seeded on 6cm plates at 2.5 x 10^6 cells with DMEM/ 10% FBS/ 2mM L-Glutamine. On Day1, respective inhibitors or DMSO (as the vehicle) was added to the medium and well-mixed, to a final concentration as the same as in soft agar assay. Cells were then left in the incubator overnight. On Day2, protein of cells was harvested and analysed by immunoblots as described in 2.2.2.

2.2.8 Sulforhodamine B (SRB) colorimetric assay

Cells were plated on wells of a 96-well plate on Day0; they were then fixed and SRB-stained on required dates to measure any changes in total protein content. Fixation was done by adding 50μl of 25% Trichloracetic acid solution (ice cold) into each well, originally containing 200μl culture medium. Plates were chilled in the cold room for 1 hour. Wells were then washed 10 times with dH_2O, and dried in an 50°C oven. Staining of protein content in the well was by adding 50μl 0.4% SRB solution in 1% acetic acid into each well, incubated at room temperature for 30 min. Wells were then washed four times with 1% glacial acetic acid in dH_2O, and dried in a 50°C incubator. SRB-stained protein was resuspended in 150μl 10 mM Tris solution (pH 10.5) by leaving on shaker for 1 hr at room temperature. Protein content was measured by absorbance at 540nM, using BP800 microplate photometer (Biohit). Data analysis was done using Microsoft Excel.

2.2.9 Immunohistochemistry

Fresh mouse tissues were fixed by formalin overnight, which were then processed (dehydration, clearing and embedding in paraffin block) by the histology service department of the Breakthrough Research Centre (Western General Hospital, Edinburgh). Paraffin blocks of human pancreatic cancer tissues were obtained from Experimental Cancer Medicine Centre (ECMC, reference code TR163). Paraffin blocks of tissue were sectioned

to 5-micron thick and mounted on slides (positively charged on the surface) by the Breakthrough Research Centre. Slides containing tissue section were dewaxed by immersing in xylene for 5min, twice, and rehydrated for 5min in 99%, 99%, 80% and 50% ethanol, chronologically. Slides were then boiled in a pressure cooker containing antigen retrieval buffer (10mM Sodium Citrate pH6.0) for 10 min, and left to cool down at room temperature for 20min. After washing with dH_2O, slides were washed twice with TBS-0.025% Triton x100, followed by drawing around the tissue with Immedge pen (Vector Science) to form a water repellent barrier. Tissues were then blocked with DAKO total protein block for 2hr. Upon draining away the block solution, tissues were immersed in primary antibody of the appropriate concentration (listed in the Materials section) in DAKO antibody diluent, overnight.

The next morning, tissues were washed twice with TBS-0.025% Triton x100 for 5min, followed by adding DAKO peroxidase block for 15min, and then wash once with TBS for another 5min. Tissues were then immersed in DAKO Envision labelled Polymer (secondary antibody and HRP conjugated to a Dextran molecule) for 1hr, plus two washes with TBS for 5min each, then added DAB chromogen for peroxidise reaction for 10min. After a quick rinse in water, tissues were counter-stained with Haematoxylin for 5 min to stain nuclei blue, and then washed in water for another 5min. Upon dehydration with ascending % of ethanol (50%, 80%, 99%, 99%), and eventually xylene, tissues were mounted to coverslips with Di-n-butyl Phthalate in Xylene (DPX) and air-dried. Slides were processed using an Olympus BX51 microscope system and its adjunct software.

2.2.10 DNA preparation

Each glycerol stock of bacteria (E-coli) carrying individual PLKO-shRNA plasmids (Thermo Scientific) was gently streaked on ampicillin (50mg/ml) selection plates and incubated at 37°C. The next day, a single colony was picked by an autoclaved pipette tip, inoculated into 250ml of L-broth medium containing ampicillin (50mg/ml), and incubated overnight at 37°C on a rotating shaker. The next day, cells were spun down by centrifugation at 500g, supernatant was discarded and the pellet was lysed to extract DNA plasmid using Qiagen's Plasmid Maxi Kit. DNA was eventually dissolved in dH2O, and the concentration was measured by Nanodrop (Thermo Scientific). In addition, both plasmids of

pcDNA3.HIV1 and pcDNA3.VSV-G were prepared from glycerol using the same Maxi Kit of Qiagen, according to the protocol recommended by the manufacturer.

2.2.11 Transfection of HEK293FT cells and lentiviral infection of shRNA

HEK293FT cells were used as host cells to produce virus. They were maintained in DMEM with 10% FBS and G418 at 100mg/ml. On Day0, 1 x 10^6 HEK293FT cells were plated on 10cm culture plate. The next day, HEK293FT cells were transfected with 10μg PLKO shRNA plasmid, 6.5μg pcDNA3.HIV1, and 3.0μg pcDNA3.VSV-G, using calcium chloride dissolved in Hepes Buffered Saline at pH6.9, at a final volume of 1ml, in the category-2 tissue culture facility. On Day-2, transfection medium on HEK293FT was replaced by fresh DMEM with 20% FBS, as higher serum level enhances production of virus by the transfected HEK293FT cells. Concurrently, at 0.25 x 10^6 murine pancreatic cancer cells (the target cells) were plated on 10cm plates.

Conditioned medium was prepared on Day 3, by passing the HEK293FT medium through a 0.45μm filter, supplemented with the same volume of fresh DMEM-10% FBS and 5μg/ml polybrene. Mouse pancreatic cancer cells were incubated in this conditioned medium overnight, and this step of conditioned medium was repeated on Day-4. On Day-5, the conditioned medium on mouse pancreatic cancer cells was replaced by fresh DMEM with 10% FBS, followed by antibiotics selection using 5μg/ml puromycin in DMEM with 10%FBS on Day-6. Infected mouse pancreatic tumour cells were passaged at 1 in 5 and further selected for 6 days with 5μg/ml puromycin. Before moving the infected mouse pancreatic cancer cells out of the category-2 tissue culture, infected mouse pancreatic cells were ensured not themselves producing lentivirus, by treating a dish of uninfected cells with conditioned medium of the infected cells, followed by addition of 5μg/ml puromycin which was supposed to kill all the uninfected cells.

2.2.12 Cell cycle blockage with thymidine or with Gemcitabine

On Day0, cells were seeded on 6cm plates at 2.5 x 10^6 cells with DMEM/ 10% FBS/ 2mM L-Glutamine. On Day1, cells were washed once with sterile PBS, and then replaced with 1mM glucose DMEM/ 10% FBS, with the addition of thymidine (2μM), or Gemcitabine

(100nM or 500nM), or just PBS (the vehicle). On Day2, protein of cells was harvested and analysed by immunoblots as described in 2.2.2.

2.2.13 Treatment with recombinant mouse TGFβ1 and BMP9

On Day0, Cells were seeded on a 6-well plate at 0.1 x 10^6 cells with DMEM/ 10% FBS/ 2mM L-Glutamine. On Day1, photographs of cells were taken using a phase contrast microscope (Leica) connected to a Qimaging Retiga EXi camera. Cells were then washed twice with PBS, and replaced with serum free DMEM at 1mM or 25mM glucose, plus recombinant mouse BMP9 or recombinant mouse TGFβ1 to a final concentration of 2.5ng/ml; whereas BSA was added to the well of carrier control. Photographs of cells were then taken on Day2. Both recombinant mouse BMP9 and recombinant mouse TGFβ1 were reconstituted in a stock solution of 10 μg/mL in sterile 4mM HCl containing 0.1% BSA.

2.2.14 Immunoprecipitation

Cells at 80% confluence were lysed in ice cold RIPA buffer with protease and phosphatase inhibitors as described previously in western blot. Lysate was cleared by spinning at full speed by a bench top eppendorf centrifuge. Protein concentration was measured by MicroBCA assay (Thermo Scientific). 20μg of each sample protein lysates was retained to load to reflect the total protein input. 1μg of β-catenin antibody was added to 1000μg protein for immunoprecipitation; after overnight incubation with antibody in the cold room, 25μl of 50% slurry of protein-G conjugated agarose was added to each sample, and further incubated in the cold room for 45 min. The control sample was added with IgG-conjugated agarose. Agarose was then spun down and washed for three times with ice cold RIPA buffer with inhibitors. 20μl of 5x sample buffer was added to the Pelleted agarose and boiled at 98°C, followed by SDS-PAGE and western blot for phospho-β-catenin and total β-catenin.

2.2.15 Subcutaneous injection

Cells at about 60-70% confluence were trypsinized, spun down at 1400rpm in a universal tube and washed once with PBS. Cell number was counted by a haemocytometer. 5 x 10^4 cells in 100μl HBSS were injected into both sides of a nude mouse in a sterile hood; three mice (6 injections) were used for each cell sub-clone, in the animal facility, by Ms Morwenna Muir, in the Western General Hospital. Two perpendicular diameters of each

tumour were measured by a caliper twice a week for 28 days. Measurements were recorded, analysed and plotted against time (days) using Microsoft Excel.

3. RESULTS

3.1 Characterization of heterogeneity of mouse pancreatic cancer cells

3.1.1 Isolation of heterogeneous cell types from primary culture

I started my project with a flask of primary culture of mouse pancreatic cancer cells, which had been derived from an excised portion of a primary pancreatic tumour of a *Pdx1*-Cre/ *LSL-Kras*$^{G12D/+}$/ *LSL-Tp53*$^{R172H/+}$ mouse (number 83320), by Dr Jennifer Morton at the Beatson Institute, Glasgow. Such mouse lived for around 11 weeks, with locally advanced pancreatic cancer and ascites, but with no metastasis at that time. The mouse's genotype had been confirmed by routine PCR at the Beatson Institute, before the derived-cells were brought over to the Edinburgh Cancer Research Centre.

Under the light microscope, these primary mouse pancreatic cells exhibited mixed morphologies; some cells appeared epithelial and grew in flat clusters, while some others appeared spindly and grew on top of each other (data not shown). In order to examine whether these primary cells comprised heterogeneous cell populations, I conducted 'separation' of distinct cell morphologies, using a method of single-cell cloning, by dilution and distribution of 30 single cells into a 96-well plate. Upon picking and expanding colonies in larger culture flasks, in around 3 weeks, I identified at least 7 types of cells which differed in morphology and growth properties on tissue culture dishes. In total, 14 colonies had been picked, and based on morphological characteristics, those 14 were eventually narrowed down to 7 distinct clones for further characterization (Figure 13). I named each of them with a single letter. Cell sub-clone E had an epithelial morphology with well defined cell-cell junctions. Cell sub-clones V and H were of another morphological type, as both appeared to be elongated, but sub-clone H was more spindle-like with sharper ends, whereas sub-clone V was relatively flatter with rounder edges. Cell sub-clones N and T were close in appearance and look mesenchymal with less well-defined cell junctions, but sub-clone T had more filopodia-like protrusions than sub-clone N. Cell sub-clone K was even flatter and spread-out, with low contrast under the light microscope, while sub-clone M was cobble-stone-like, with clear cell-cell junctions, and it grew in clusters. These seven cell sub-clones were stable in culture, as their morphology had not changed for at least 15 passages, the time point at

Figure 13

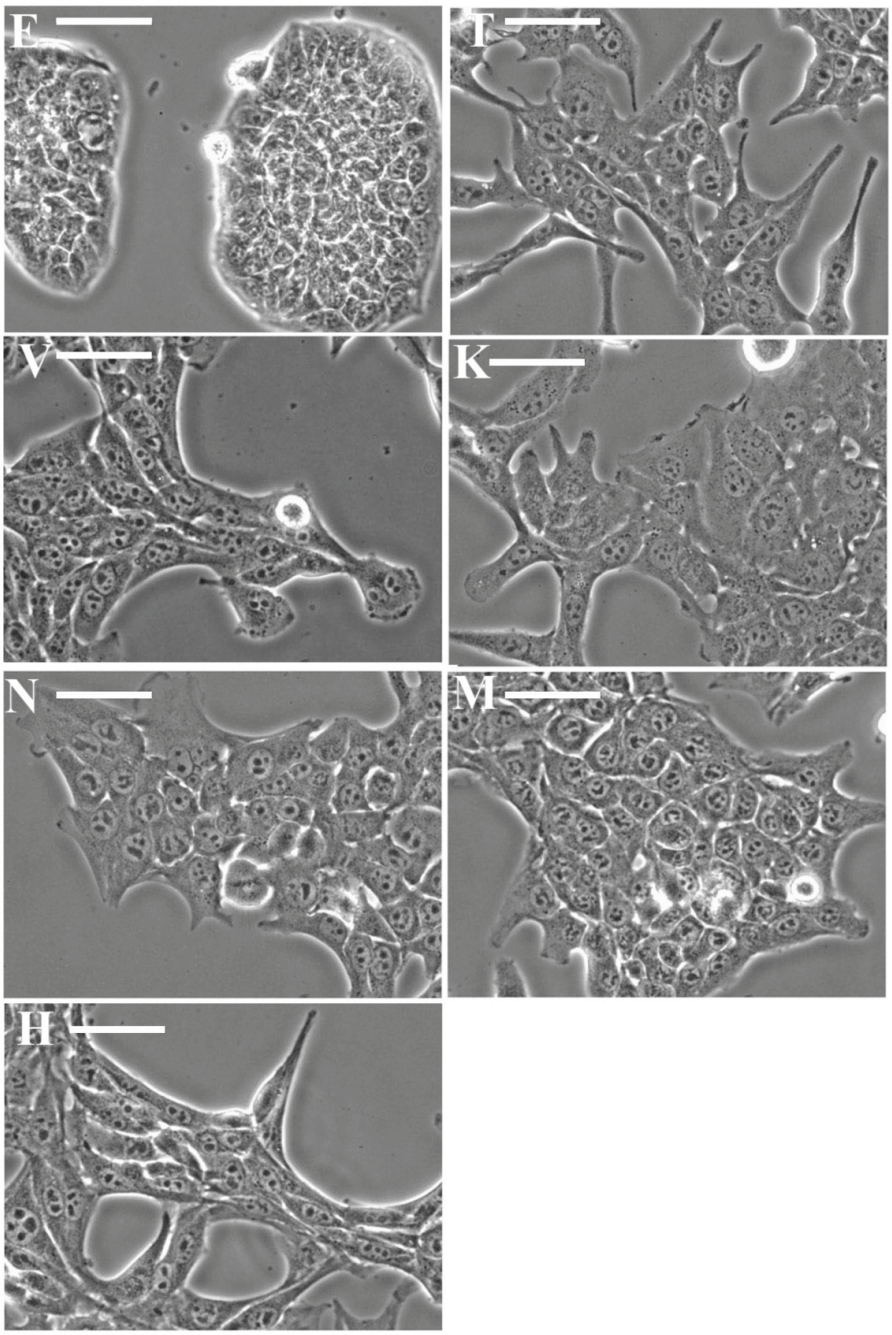

Figure 13 - Morphology of the seven mouse pancreatic cancer cell sub-clones derived from primary culture of pancreatic cancer from mouse 83320. **Condition**: 50 x 10^4 cells were seeded onto a 6 cm dish on Day0 in normal DMEM, 10% serum; on Day1, photographs were taken under the light microscope using the standard 40x objective (scale bar = 50μm).

which I replaced the flask with an early passage from the liquid nitrogen. Moreover, immunoblots generally appeared consistent between early and later passages. Yet I could not eliminate the possibility that when these sub-clones were growing in the original mixture of primary cells, some or all of them would induce plasticity through interactions between multiple cell types. However, they were stable upon isolation, which provided a basis for studying heterogeneity of tumour cells within a pancreatic cancer.

3.1.2 Confirmation of pancreatic cell identity

I first ensured that the seven cell sub-clones were of the *Pdx1*-expressing pancreatic lineage, but not of some other cell types, such as fibroblast, that might have come along with tumour cells into culture. I conducted reverse transcriptase-PCR and amplified the *Pdx1* gene transcript (mRNA) (Figure 14B), confirming the transcription activity of *Pdx1*. I also used confocal microscopy to detect immunofluorescence-labelled PDX1 protein, along with a negative control, M15 mouse kidney fibroblasts, which showed minimal staining (Figure 14A). In addition, the PDX1 protein was detected by immunofluorescence in Panc1 cells, but not Miapaca2 cells, both of which are established human pancreatic cancer cell lines (Figure 14C). This was in agreement with a recent report showing by immunohistochemistry that PDX1 was expressed in some but not all human pancreatic cancer sections (Park et al., 2010). Sequencing of PCR-amplified cDNA confirmed that all 7 mouse pancreatic cancer cell sub-clones expressed mutant $Kras^{G12D}$ and $p53^{R172H}$, indicating successful recombination by CRE-recombinase (one example is shown in Figure 15A, which was of cell sub-clone E). Both mutants appeared to be dominantly expressed in these cells, as no fluorescence signal of the wild-type nucleotide had been detected in the sequencing chromatograms. Possibly, the remaining wild type allele had been eliminated due to selective pressure to lose heterozygosity during cancer progression.

3.1.3 Evidence for heterogeneity among the sub-clones

Since these 7 mouse pancreatic cancer sub-clones showed distinctive morphology, I hypothesised that they had different genetic profiles and protein expressions. To address this, I conducted pathway screens by immunoblots and PCR.

Figure 14

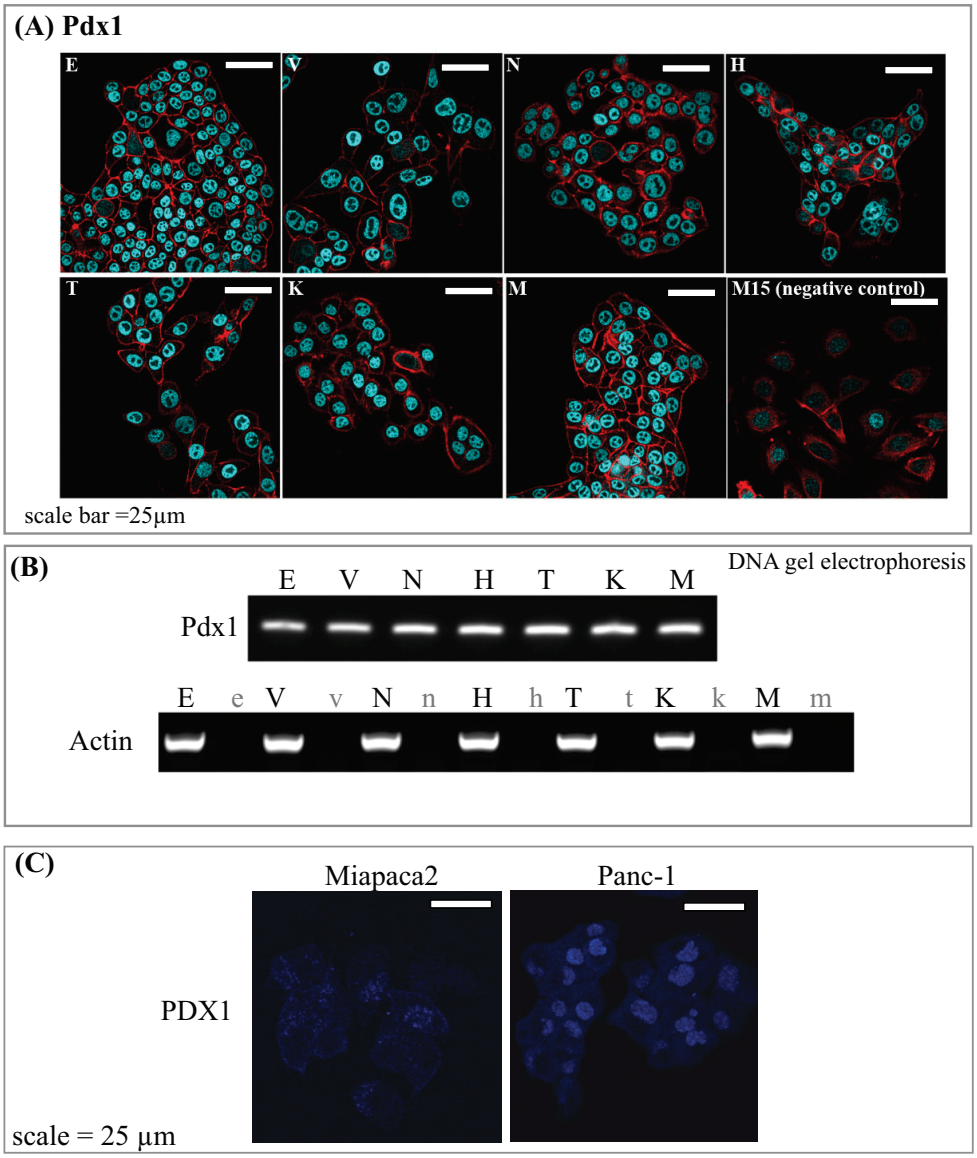

Figure 14 (A) - Immunofluorescence staining of Pdx1 protein in the nucleus of all seven sub-clones, compared with the the negative control, M15 mouse embryonic kidney fibroblast. **(B) -** Reverse Transcriptase PCR confirms that Pdx1 gene is expressed in all seven cell sub-clones; PCR of the actin cDNA was used as a arbitrary loading control; and the empty lanes labeled with a lower case letter are the corresponding RNA-only negative controls, to show that the genes amplified were essentially from cDNA, and not from contaminated genomic DNA **(C) -** Pdx1 is expressed in human pancreatic cell line, Panc1, but not in Miapaca2.

Figure 15

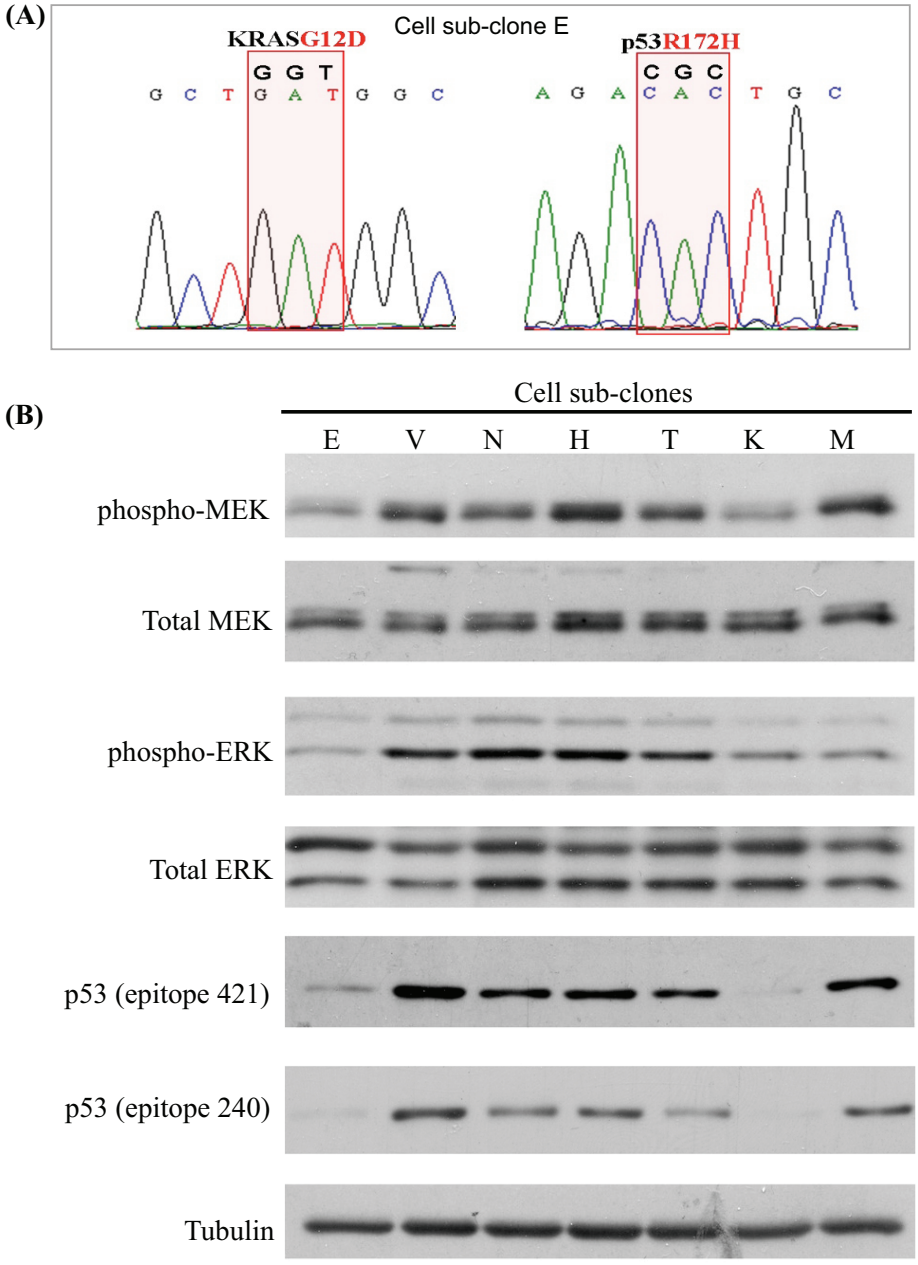

Figure 15 (A) – Showing sub-clone E as an example, sequencing of the amplified cDNA confirmed that all seven sub-clones express $KRas^{G12D}$ and mutant $p53^{R172H}$. **(B)** – Western blot shows activated MEK-ERK pathway, suggesting upstream activity of the constitutively activated $KRas^{G12D}$; mutant p53 levels varied among the cell sub-clones. **Condition:** 50 x 10^4 cells were seeded onto a 6 cm dish on Day0 in normal DMEM, 10% serum; cells were harvested for protein on Day2; 20µg protein was loaded into each lane.

I first examined the ERK pathway, which is downstream of mutant $KRas^{G12D}$, and levels of mutant $p53^{R172H}$ (Figure 15B), as both mutants were the basis of the mouse model. Western blot revealed that both MEK1/2 and ERK1/2 were phosphorylated and thus activated in all 7 cell sub-clones, indicating the activity of the upstream mutant $KRas^{G12D}$. As for p53 levels, I used two antibodies, PAb240 (epitope at a.a. 207-212) and PAb421 (epitope at a.a. 363-372), so as to minimize the risk of one epitope being shielded by post-translational modifications, of which p53 is well-known to have numerous types (reviewed by Bode & Dong 2004). Among the 7 cell sub-clones, only E and K did not show stabilized p53 on western blot, suggesting that they might have lower transcription levels or faster turnover rates of mutant p53 than the other cell sub-clones. In the *Pdx1*-Cre/ *LSL-Kras*$^{G12D+/-}$ mice (without mutant p53), it has been known that most of the $KRas^{G12D}$-expressing cells would be lost over time due to growth arrest and senescence; only a minority of them could overcome this senescence barrier to form premalignant lesions (Morton et al., 2009). Therefore, cell sub-clones E and K might be two examples of such cell types that were not so reliant on mutant $p53^{R172H}$ to survive.

In addition, I also examined the possibility that these cells were different with respect to epithelial-to-mesenchymal states, because they showed distinctive morphology under the phase contrast microscope. I performed western blotting to examine some common junctional proteins, namely E-cadherin, β-catenin and N-cadherin for adheren junctions, as well as a major tight-junction protein, ZO2 (Figure 16A). E-cadherin levels varied among the seven sub-clones, while β-catenin levels were relatively similar, and N-cadherin level was the highest in cell sub-clone K, which along with M, expressed little E-cadherin. ZO2-levels did not vary much among the sub-clones, indicating that these cells probably had similar levels of ZO-2-dependent tight junctional complexes. Under the confocal microscope, immunofluorescence staining of E-cadherin showed that only cell sub-clones E and V still possessed some E-cadherin visibly localized to cell-cell junctions, while the other five sub-clones showed mostly cytoplasmic E-cadherin (Figure 17).

I then asked whether such difference in E-cadherin levels was attributed to different levels of transcriptional repression by classical 'Epithelial-Mesenchymal Transition' (EMT) mediators that had been reported in human pancreatic cancer (Hotz et al., 2007). In particular, I looked at protein levels of ZEB1, which is a transcriptional repressor of the E-cadherin promoter, and also an antagonist of a family of 'anti-stemness' microRNAs in pancreatic cancer cells

Figure 16

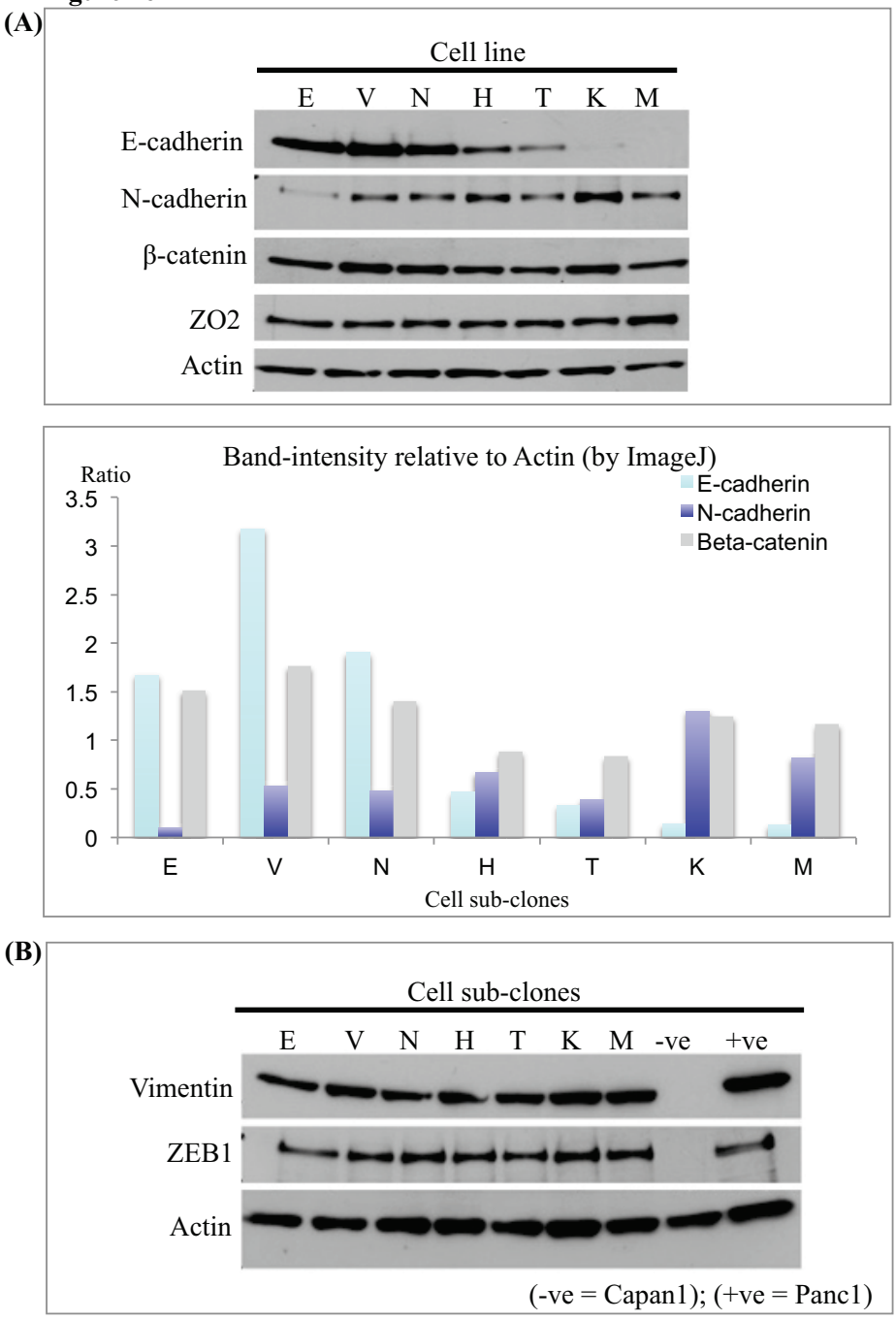

Figure 16 (A, upper panel) – Immunoblot analysis of some classical pro-epithelial cell-cell junction proteins in the seven cell sub-clones; 20µg protein was loaded into each lane. **(A, lower panel) –** Quantification of band intensities of the epithelial markers relative to Actin, using ImageJ. **(B) -** Immunoblot analysis of some classical "mesenchymal markers", along with Capan1 cell-lysate as the negative control, and Panc1 cell-lysate as the positive control. **Condition:** 50 x 10^4 cells were seeded onto a 6cm dish on Day0 in normal DMEM, 10% serum; cells were harvested for protein on Day2; 20µg protein was loaded into each lane.

Figure 17
Scale bar = 25 μm

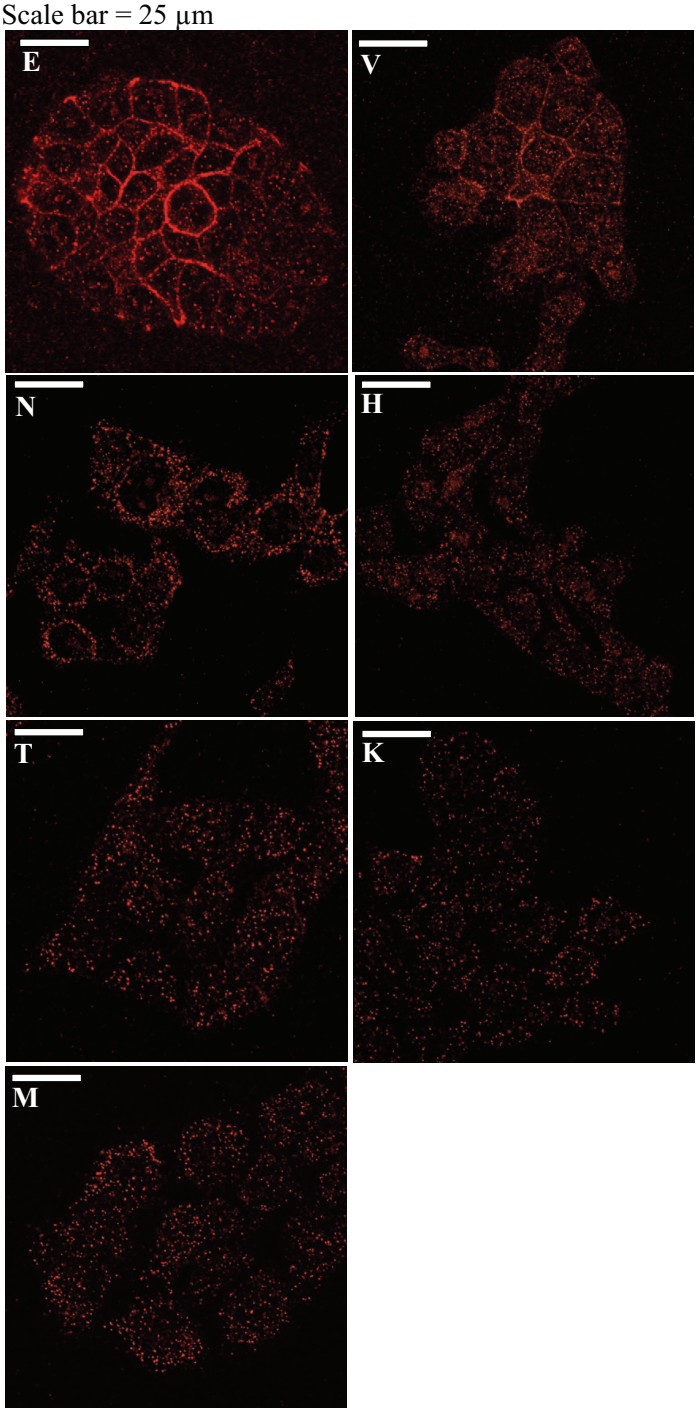

Figure 17 - Immunofluorescent staining of E-cadherin in the seven sub-clones; please note that it was only based on one focal plane, a better indication of E-cadherin localization should have been a photo of stacked focal layers taken from top to bottom of the cells on the coverslip. **Condition:** on Day0, 1 x 10^4 cells were seeded on each coverslip in a 12-well plate, in 10% serum DMEM; cells were fixed on Day2, at about 50% confluency.

(Aigner et al., 2007; Spaderna et al., 2008; Wellner et al., 2009). However, all seven cell sub-clones expressed similar amounts of ZEB1 (Figure 16B), implying that ZEB1 was unlikely repressing E-cadherin in these mouse pancreatic cancer cells.

I also examined whether or not these cell sub-clones differed in expressions of proteins associated with focal adhesions and 'mesenchymalness', as activation of these proteins is often believed to be implicated in acquired invasive capacity, for example, after EMT. Vimentin, which is often used as a marker of mesenchymal cells or cells that have undergone EMT in developmental biology and in some putative "cancer stem cell" studies, was expressed by all seven cell sub-clones (Figure 16B). This suggests that either the sub-clones were all putative mesenchymal cells, or Vimentin has not been a universal mesenchymal-marker as previously thought, at least for this mouse model of pancreatic cancer. As for focal adhesion proteins, phospho-Focal Adhesion Kinase (FAK) levels appeared to be the lowest in sub-clones E and V, which had the highest E-cadherin levels, whereas sub-clones K and M showed the highest levels of phospho-FAK (Figure 18). This roughly paralleled decrease of E-cadherin levels among the seven sub-clones, suggesting an overall correlation between increase in FAK activity and decrease in E-cadherin levels. In addition, sub-clones V and H showed higher phospho-Src family kinase levels. This was consistent with the observation that they were morphologically closer, compared with the other cell sub-clones. More similarities and differences between sub-clones V and H will be discussed in following paragraphs.

I also investigated whether the cell sub-clones differed in certain signalling pathways or key transcription factors that had been implicated in pancreatic cancer or in pancreas development. Of interest, the TGFβ/BMP pathway and the canonical Wnt pathway were active only in some of the cell sub-clones, and they respectively became the major and the minor studies in my project. Other lines of evidence for heterogeneity among the sub-clones included detection of the mRNA transcript of CXCR4 (a chemokine receptor), GATA6 (a developmental transcription factor), WNT5A (a well established ligand of non-canonical Wnt pathway) and HNF4α (an orphan nuclear receptor, discussed in Introduction), in distinct subsets of cells (Figure 19). CXCR4 was exclusively expressed in sub-clone V, while the ligand CXCL12/SDF1 was also expressed in sub-clones V, T, K and M (Figure 19A). CXCR4-mediated signalling has been reported to play a central role during metastasis, including in pancreatic cancer (Heeschen et al., 2007). This suggests the presence of an

Figure 18

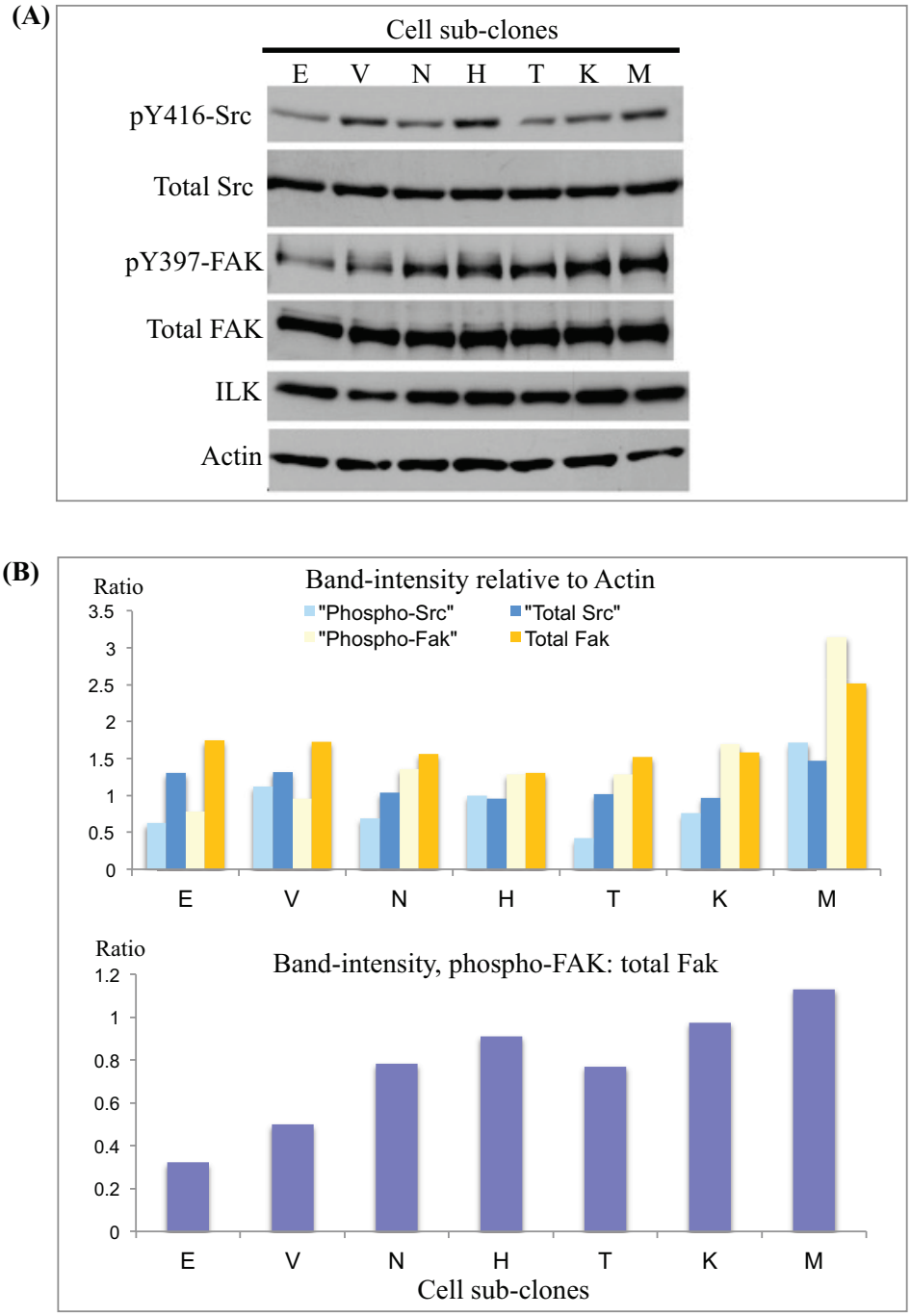

Figure 18 (upper panel) – Immunoblot analysis of proteins involved in focal adhesion. **(lower panel)** – Quantification of the respective band intensities of the focal adhesion proteins, relative to actin levels, using ImageJ. **Condition:** 50 x 10^4 cells were seeded onto a 6 cm dish on Day0 in normal DMEM, 10% serum; cells were harvested for protein on Day2.

Figure 19

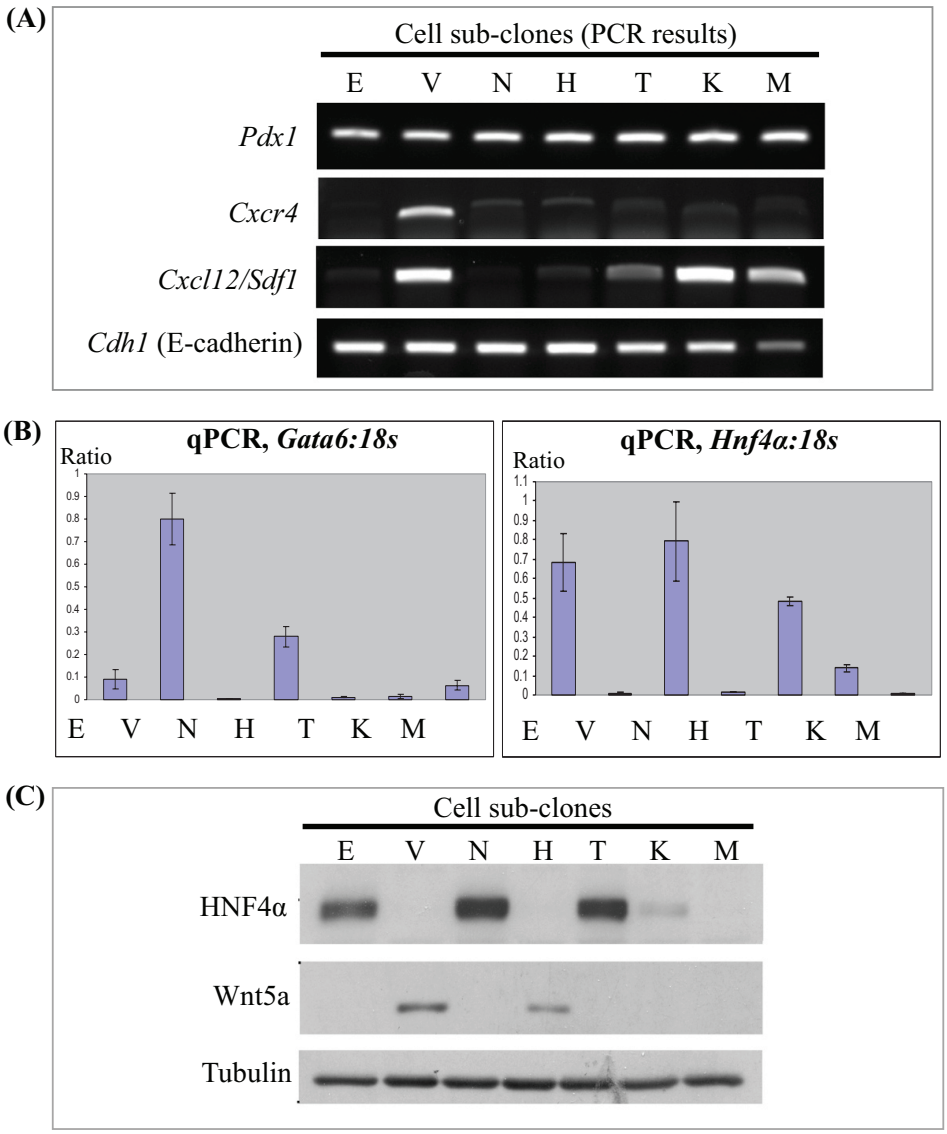

Figure 19 (A) – Representative results from RTPCR screens for marker gene expressions in the seven cell sub-clones of mouse pancreatic cancer. **(B) –** Quantitative PCR analysis of *Gata6* and *Hnf4α;* error bar = standard deviation of the mean. **(C) –** Representative results from immunoblot screens for heterogeneous protein expressions in the seven cell sub-clones. **Condition:** 50 x 10^4 cells were seeded onto a 6cm dish on Day0 in normal DMEM, 10% serum; cells were harvested for protein/RNA on Day2.

autoloop in sub-clone V, while sub-clones T, K and M could present the ligand to sub-clone V, as these cell types co-existed in the original tumour. However, I was unable to detect the CXCR4 protein, no matter by flow cytometry or by western blotting; verification of this result requires the future use of a positive control.

Multiple studies have shown that the *Gata6* gene is amplified in a subset of pancreatic cancer cells in human (discussed in Introduction), and among the seven cell sub-clones, *Gata6* was transcribed only in V and H (Figure 19B), the two sub-clones that shared a spindly morphology. Of interest, Wnt5a was also expressed exclusively in sub-clones V and H, with H having proportionally lower levels of *Gata6* transcription and WNT5A protein than V, indicating a potential correlation between GATA6, Wnt5a and higher levels of phospho-Src family kinases in these two cell sub-clones.

In addition, HNF4α, a nuclear receptor that is crucial to gene regulation of glucose metabolism in hepatic and pancreatic cells, was expressed only in sub-clones E, N and T (Figure 19B, C). In Chapter 3.4, I am going to establish a novel connection between HNF4α and the BMP-SMADs pathway. To sum up, screenings by immunoblots and by qRTPCR confirmed that the seven mouse pancreatic cancer sub-clones were heterogeneous not only in their morphology, but also in their respective signalling drivers.

3.1.4 Differential rates of 2D- and anchorage independent proliferation

On polystyrene culture dish in DMEM with 10% FBS, the fastest-proliferating sub-clone (T) was about 2 times the rate of the slowest proliferating sub-clone (V), and the other sub-clones lay in between. This was measured by SRB assay, which was based on measuring protein content per well in a 96-well plate over 5 days (Figure 20A). When serum was reduced to only 0.5% in DMEM, all seven cell sub-clones proliferated very slowly (SRB-stained protein content merely doubled over 5 days), with negligible differences between each sub-clone (data not shown). However, when they were subjected to anchorage-independent conditions in DMEM-methylcellulose suspension with 10% FBS, some of their intrinsic difference in "strength" of transformation was unveiled. In this soft-agar/methylcellulose assay, the average area of cell spheres on Day1 was used as the baseline (denominator) to that measured on Day7, using the 'arbitrary particle area measurement' function in ImageJ (National Institute of Health). Interestingly, sub-clones V,

Figure 20

(A)

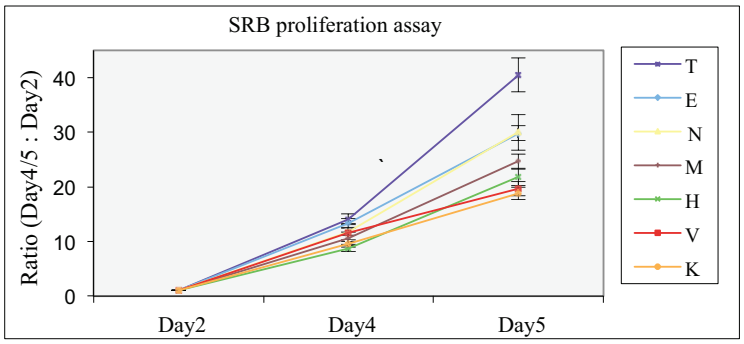

(B)

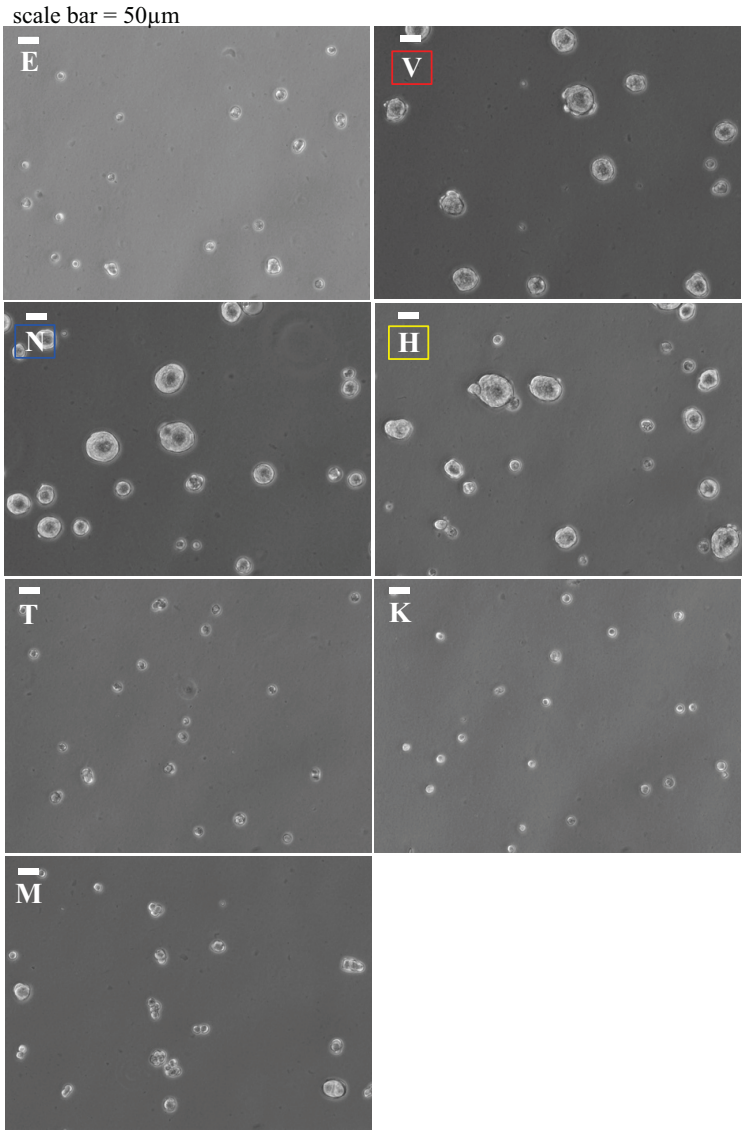

Figure 20 (A) - SRB proliferation assay shows the differences in proliferation speed among the sub-clones, in which the fastest (T) and slowest (K) proliferating cells does not exceed one fold. **Condition:** 500 cells were seeded on each well of 96-well plates on Day0, identical plates were then fixed with Trichloroacetic acid on Day2, Day4 and Day5. **(B)** In soft agar assay, sub-clones V, N and H stand out of the other sub-clones in their strength of colony formation. **Condition:** On Day0, single cell suspensions each containing 2 x 10^4 cells of respective sub-clone were respectively mixed with methylcellulose on top of a soft agar layer, both layers contain nutrients equivalent to 10% serum, normal DMEM; photographs were taken on Day1 and Day7; the photographs shown above are of Day7.

N and H stood out of the others with around 3 to 4 times increase in average particle area over 7 days; while the other sub-clones had only around 1 to 2 times increase in average particle area (Figure 21B, 22).

However, it is important to understand the limitations in this assay. In particular, analysis of photographs by ImageJ software reflected only the area of one side facing the camera, but not the back-side of the spheres. Hence if cells proliferate toward the "unexposed side", it was impossible to measure using 2D photographs. In addition, not all single cells on Day0 could start to divide and eventually proliferate into larger spheres till Day7. Hence the analysis had a number of assumptions, including survival of the suspending cells; changes in sphere size were based on proliferation, and that individual cell size did not change throughout the incubation period.

3.1.5 Growth of subcutaneous xenograft tumour in CD1 nude mice

Anchorage independent proliferation *in vitro* is often believed to reflect a cancer cell line's potential to form tumours *in vivo* (Cifone & Fidler 1980; Mani et al., 2008). Since sub-clones V, N and H showed stronger anchorage independent proliferation than the others, it would be important to examine if they actually bear any advantage during *in vivo* growth. In order to compare the sub-clones *in vivo*, all seven of them, along with the original primary mixture (designated as X), were injected into the subcutaneous layer of nude mice. Tumour growth (in terms of increase in two perpendicular diameters of the tumour) was measured by a caliper twice a week (Figure 22A). In the growth curve of tumours over 28 days, growth rates of sub-clones V and H were always ahead of the rest after Day10, whereas sub-clones E, N, T and the original primary mixture (X) grew at similar rate with about a 5-day lag behind V and H to reach the same tumour size. Sub-clone K displayed about another 5-day lag behind E, N, T and X, and sub-clone M was the slowest with around a 18-day lag behind sub-clones V and H to reach the same tumour size. Hence, no direct relationship was observed between anchorage independent proliferation and subcutaneous tumour growth among these mouse pancreatic cancer cells. Despite that, sub-clones V, N and H did grow relatively well in the subcutaneous layer of immunocompromised mice.

Figure 21

(A)

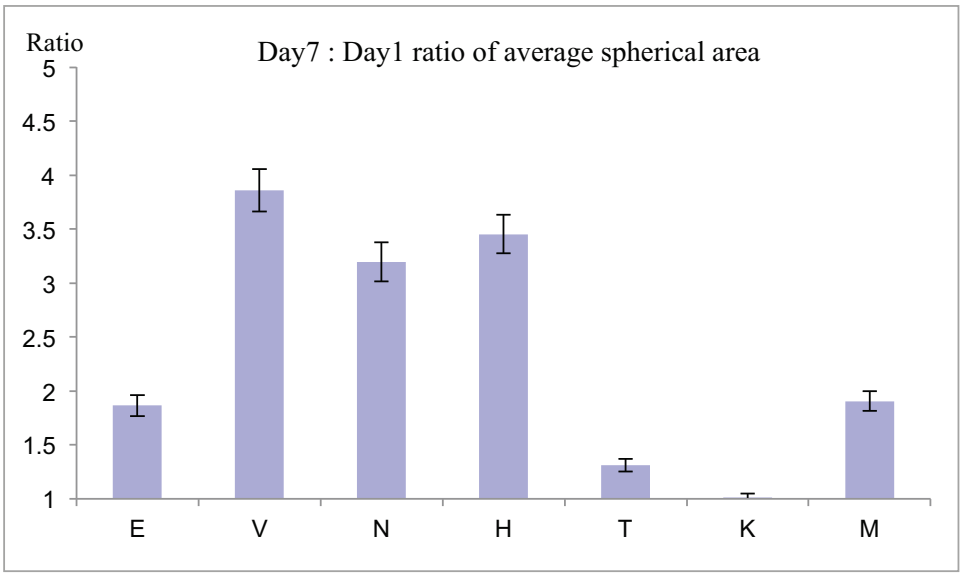

(B)

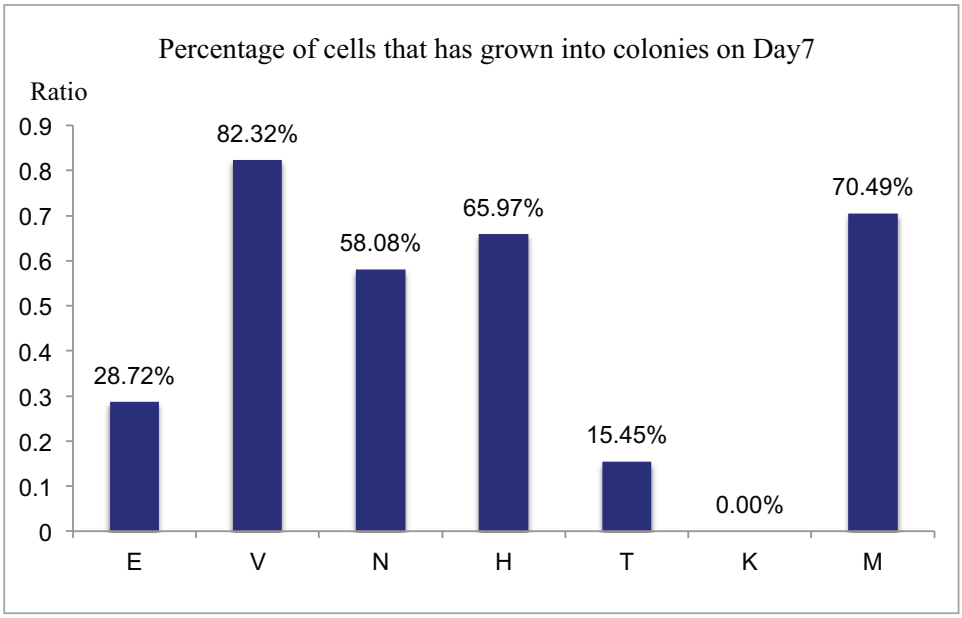

Figure 21 A representative set of data of anchorage independent proliferation of the seven sub-clones. **(A)** – Ratio of average 2D-size of cell spheres (measured by ImageJ arbitrary particle area) on Day7 versus that on Day1; error bars represent standard error with sample size (colony counts) > 150 **(B)** - Percentage of cells that had grown into colonies on Day7; a colony was defined by the size being equal to or more than double over 7 days, i.e. proliferated. **Condition:** On Day0, single cell suspensions containing 2 x 10^4 cells of each sub-clone were mixed with methylcellulose on top of a soft agar layer, both layers contain nutrients equivalent to 10% serum, normal DMEM; photographs were taken on Day1 and Day7, and analyzed by ImageJ using "arbitrary particle area".

Figure 22

(A)

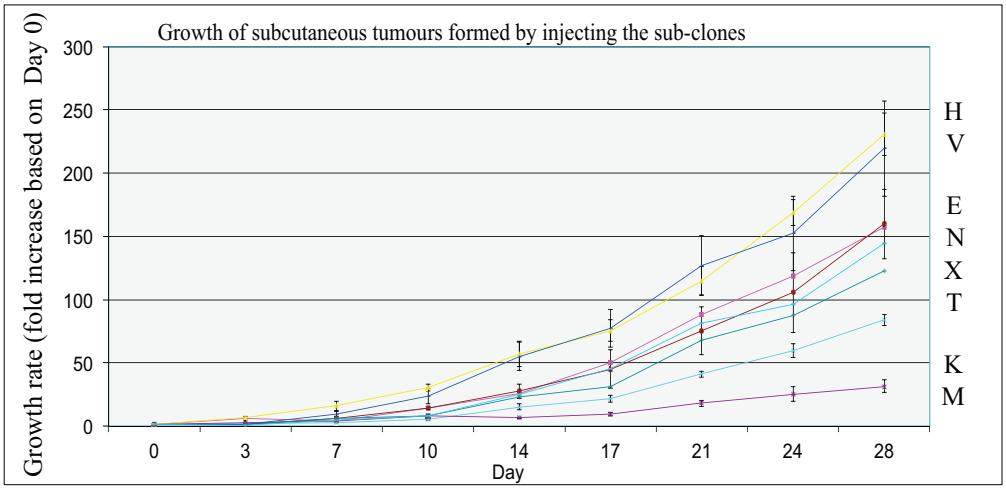

error bar = standard deviation of the mean of 6 measurements of tumour diameters

(B)

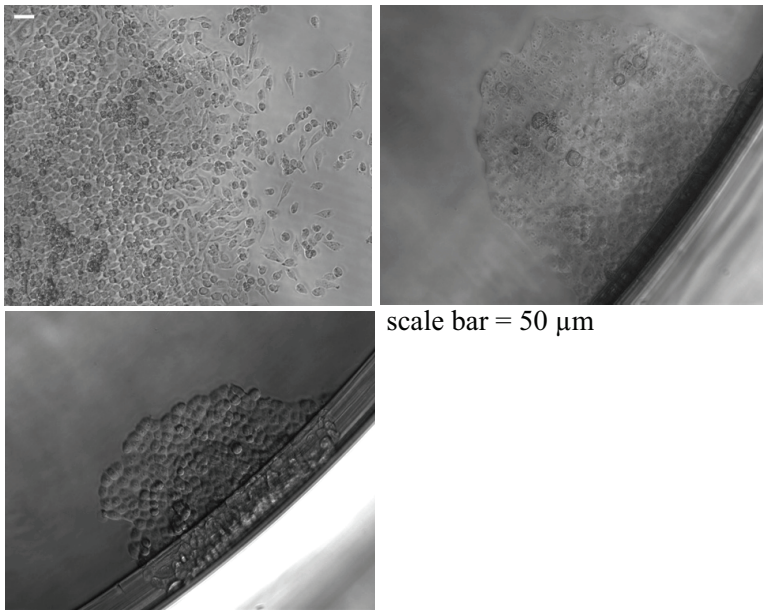

Figure 22 (A) – Subcutaneous growth rate of tumours formed with each pancreatic cancer cell sub-clone, alongside the original primary cells (PDX-X, mixed population) in nude mice over a 28 day period. **Condition:** Three mice were injected with one kind of the sub-clones (5 x 10^4 cells), both sides, 6 injections in total; a pair of perpendicular diameters were measured by a caliper twice a week. Growth rate was calculated by dividing average diameters of the six tumours at a time point, by the average diameters on Day1 as the basis. **(B)** – Three seemingly heterogeneous human pancreatic cancer cell sub-clones (in terms of morphology) isolated from primary cell culture, which was originally derived by Mark Duxbury (currently a consultant surgeon at Glasgow Royal Infirmary) with an excised piece of cancer tissue from a patient; photographs were taken using a 4x objective.

3.1.6 Isolation of heterogeneous sub-clones from another mouse and from patient tumour tissues

If heterogeneous cell types were isolated from only one mouse pancreatic tumour, it would have been questionable of being an exception in the transgenic strain. Nevertheless, I did identify four heterogeneous cell types with primary culture derived from another mouse pancreatic tumour (mouse number 82739, data not shown). Since the seven sub-clones from mouse 83320 offered higher potential of genetic variations, I did not further characterize that series of four sub-clones from mouse 82739. Moreover, multiple genomics studies with patient samples have supported the existence of heterogeneous clonal populations in the human cancer (discussed in Introduction). Therefore, the next essential task would be to see if I could isolate, in tissue culture, heterogeneous pancreatic cancer cells from patients.

As a complementary investigation, I obtained primary human pancreatic cancer cells of two patients, which were originally derived by Mr Mark Duxbury, a Hepatobiliary consultant surgeon in the Royal Infirmary of Edinburgh. By the same 96-well method to separate and to sub-clone mouse pancreatic cancer cells, at least 3 human pancreatic cancer cell types have been isolated (Figure 22B). Due to time-limit, I only conducted one preliminary western blot analysis on these human cancer cell sub-clones. In brief, they proliferated at different rates, particularly, one of them grew at a rate of three times faster than the others, and they expressed different levels of E-cadherin (data not shown), but without showing heterogeneity in phospho-SMADs status, p53 levels, and they did not express HNF4α. I conclude that heterogeneous pancreatic cancer cells can also be found in some human tumours. However, this would require much more work to characterize them and establish how similar or different they are to the mouse tumour heterogeneity I have identified in my work.

3.1.7 Summary

I identified heterogeneous cell sub-clones from primary cell culture of a mouse pancreatic tumour, in the sense that each of them has a unique genetic profile. No two of them were the same, albeit with the limited analysis I performed. Their cell junctional protein levels did not agree with the classical hypothesis of epithelial-mesenchymal transition, as they all expressed similar levels of ‘mesenchymal markers’, such as Vimentin, and ZEB1, while at the same time, they also expressed different levels of E-cadherin. Hence they could not

simply be classified into either epithelial or mesenchymal cell types. Conversely, these sub-clones seem to agree with the hypothesis of clonal evolution in human pancreatic cancer cells (Yachida et al., 2010), as already discussed in the Introduction. Notably, they showed differing phospho-SMAD status (which are downstream of the BMP/TGFβ receptor), and distinct upregulation of canonical Wnt target genes. Hence I focused on investigating the BMP/TGFβ pathway, the canonical Wnt pathway, and their possible biological relevance to pancreatic caner progression.

If resources were available during the course of my project, more efficient methods of characterization of the cell sub-clones could have been used, such as DNA microarray and proteomics. DNA microarray can simultaneously screen thousands of gene expressions with the cDNA library of the sub-clones, down to pico mole scale; while proteomics systems provide simplified and automated solutions to simultaneously detect multiple proteins by pre-defined antibodies. Both methods could offer informative preliminary screenings for activities of any "signature pathways" in the sub-clones.

A summary table of for Chapter 3.1:

		Proliferation		
Sub-clones	Morphology	on agar	on plastic	in nude mice (subcutaneous)
E	compact	modereate	fast	2
V	spiky/ ellipse	best	slow	1 (fastest)
N	spiky	best	fast	2
H	spiky, overlapping	best	slow	1 (fastest)
T	spiky	moderate	fastest	2
K	flat	weak	slowest	3
M	cubical	weak	slow	4

Molecular Markers

Sub-clones	p53	HNF4α	Gata6	Wnt5a	CXCR4/SDF1	pSrc	pFAK
E	lower	higher	nil	nil	nil	lower	lower
V	higher	nil	highest	highest	Both	higher	lower
N	higher	higher	nil	nil	nil	lower	lower
H	higher	nil	high	high	nil	higher	lower
T	higher	higher	nil	nil	SDF1	lower	higher
K	lower	lower	nil	nil	SDF1	lower	higher
M	higher	nil	nil	nil	SDF1	lower	higher

3.2 The MEK-ERK pathway correlated with anchorage independent proliferation, but not 2-dimensional proliferation on plastic culture plates.

3.2.1 Phospho-ERK1/2 levels correlated with anchorage independent proliferation

The ERK pathway correlated with stronger anchorage independent proliferation of cell sub-clones V, N and H, as they have higher phosphorylation levels of ERK1 and ERK2 (Figure 16B). Although sub-clone T also showed comparable phospho-ERK levels, T is not as competent as V, N and H to grow in soft agar, which may be attributed to other factors that affect functions of phosphorylated ERK in cells, such as localization of ERK in different cellular compartments. Moreover, there have been reports linking the ERK pathway to anchorage independent proliferation, including in some breast cancer cell lines bearing mutant KRas (Fukazawa & Uehara et al., 2000).

To examine this hypothesis in the mouse pancreatic cancer sub-clones described here, I used two potent MEK inhibitors, U0126 and PD184352 (a more specific, second generation MEK inhibitor), which prevents MEK1/2 from phosphorylating ERK1/2. For PD184352, 0.25μM was sufficient to decrease phospho-ERK levels by more than 50%, and at 1μM, virtually all detectable phospho-ERK levels are lost on western blot (Figure 23). Accordingly, when 0.25μM of PD184352 was added to V, N and H growing in soft agar assay, the average colony size of all three sub-clones decreased, particularly in sub-clones V and H, which were most sensitive to PD184352 with about 67% decrease, whereas N is less sensitive to MEK inhibition, showing a decrease in average colony size of about 35% (Figure 24). U0126, a less specific inhibitor for MEK, also resulted in the same degree of inhibition on anchorage independent proliferation of sub-clones V, N, and H, but required a higher concentration than that of PD184352 (data not shown).

Figure 23

(A)

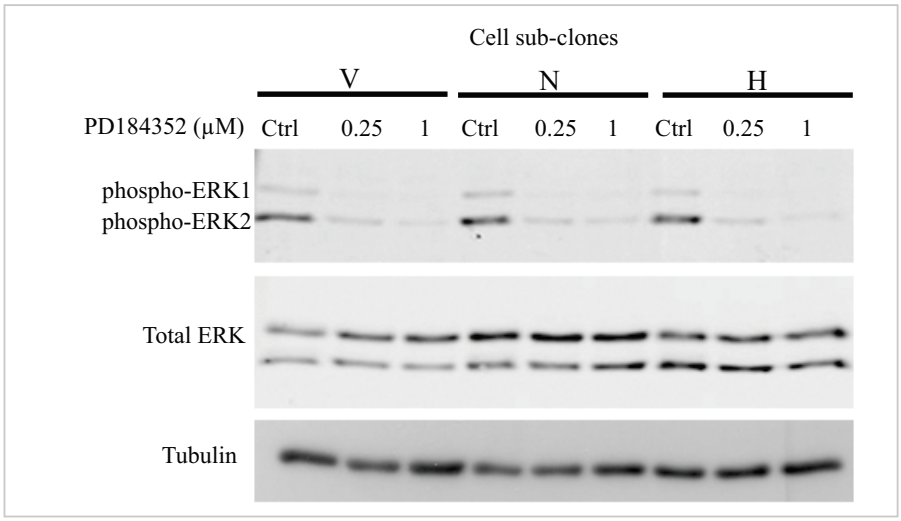

(B)

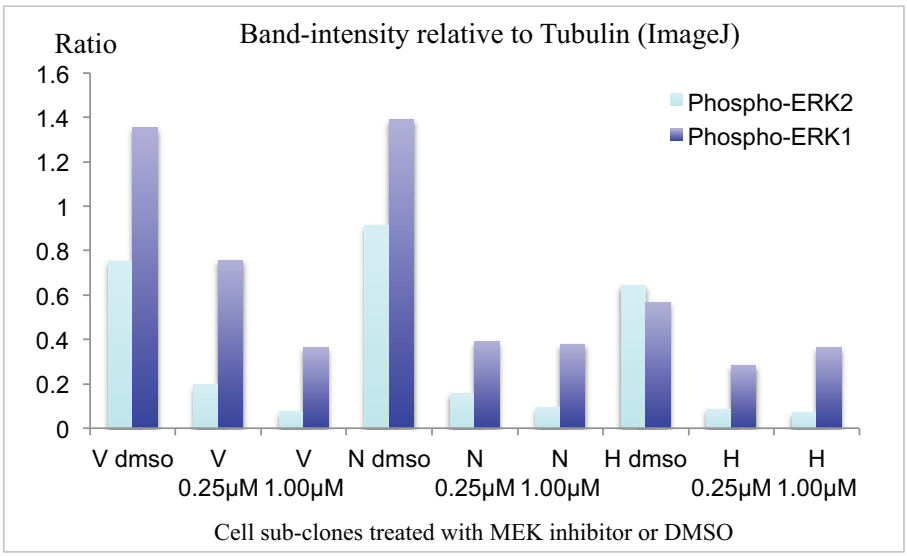

Figure 23 (A) – Immunoblot analysis of the effect by the MEK inhibitor PD184352 on ERK1/2 phosphorylation in the three "anchorage independent sub-clones", V, N and H. **Condition:** Cells were seeded on Day0 in DMEM with 10% serum, then on Day1, replaced with fresh 10%-serum medium, plus PD184352 or DMSO as shown above, and incubated for 16 hr before harvesting protein. **(B)** - Quantification of band intensity of phospho-ERK2 and phospho-ERK1, relative to tubulin, as shown in **(A)** using ImageJ.

Figure 24

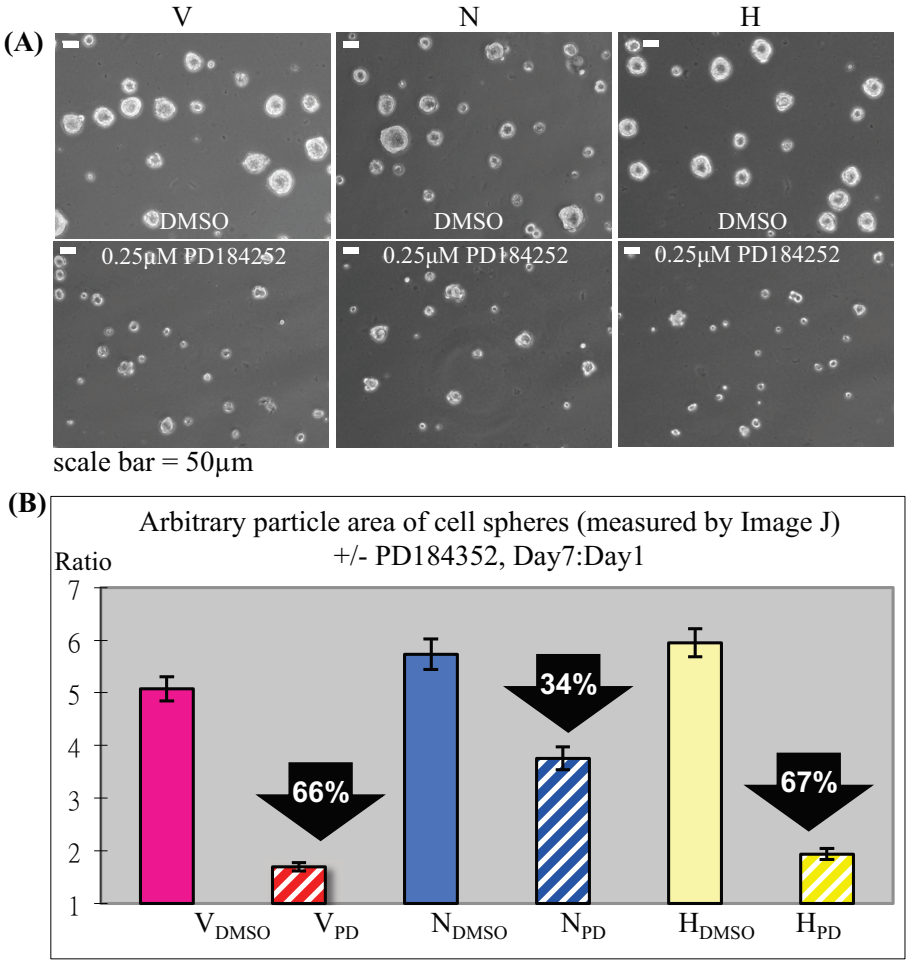

Figure 24 (A) – Anchorage Independent proliferation of sub-clones V, N and H, in the presence of a relatively new and specific MEK inhibitor, PD184352, or with DMSO as the control. **Condition:** On Day0, single cell suspensions each containing 2 x 10^4 cells of respective sub-clone were respectively mixed with methylcellulose on top of a soft agar layer, both layers contain nutrients equivalent to 10% serum, normal DMEM, plus 0.25μM PD184352 or DMSO; photographs were taken on Day1 and Day7; the photographs shown above are of Day7. **(B)** Quantification of average 2D-size of colonies in ratio of Day7: Day1 (by ImageJ); slashed bars represent samples treated with PD184352. (error bar = standard error with cell spheres counted (n) > 150)

3.3 The canonical Wnt pathway

3.3.1 Axin2 and Lgr5 as two readouts of the canonical Wnt pathway

Since sub-clones V and H were more dependent on the ERK pathway than sub-clone N in anchorage independent proliferation, it implied that additional drivers were used by sub-clone N to proliferate under anchorage independent conditions. One of the pathways I examined was the canonical Wnt pathway. First, quantitative PCRs screens of Wnt target genes revealed that sub-clone N had the highest transcription levels of *Axin2* and *Lgr5*, followed by sub-clone V, which had around half the level, while other sub-clones show comparatively low transcription levels of *Axin2* and *Lgr5* (Figure 25). For example, cell sub-clone H expressed more or less the same levels of *Axin2* and *Lgr5* as sub-clone T, which did not grow as well as sub-clone H on soft agar, suggesting that sub-clone H was unlikely to rely on the canonical Wnt pathway to form colonies in soft agar.

There was no correlation between cells' 2D proliferation rate on plastic culture plates and transcription levels of *Axin2* and *Lgr5*. Furthermore, comparisons of transcription levels of *Axin2* between the sub-clones were in agreement with that of *Lgr5*, implying that both genes were effective readouts of the canonical Wnt pathway in these mouse pancreatic cancer cells. In contrast, other Wnt target genes that had been tested, such as *Tcf7* and *cMyc*, did not show a consistent trend of transcription levels across the seven cell sub-clones. Moreover, *Myc* is overexpressed in many cancer cells bearing $KRas^{G12D}$, because Myc is a also a downstream transcription target of ERK (Sears et al., 2000), hence it was not a specific Wnt taget. While *Sox9* showed a relatively better-matched trend of transcription levels with *Axin2* and *Lgr5*, its levels were higher in K and M In addition, both *Axin2* and *Lgr5* reporter mice, but not that of *Myc* or *Sox9*, are available from the Jackson laboratory and well documented for use in specifically visualising canonical Wnt activity *in vivo* (commented by Roel Nusse, the Wnt homepage, Stanford University). Therefore, transcription levels of *Axin2* and *Lgr5* were adopted as the Wnt-readouts in this study.

LGR5 is a G-protein coupled receptor that is present in adult stem cells in the colon and the skin (reviewed by Haegebarth & Clevers 2009), as well as in a subset of colorectal cancer cells. It has been used as a crypt stem cell marker. It has recently been identified as a receptor of the R-spondin family ligands (de Lau et al., 2011). Hence, for future

Figure 25

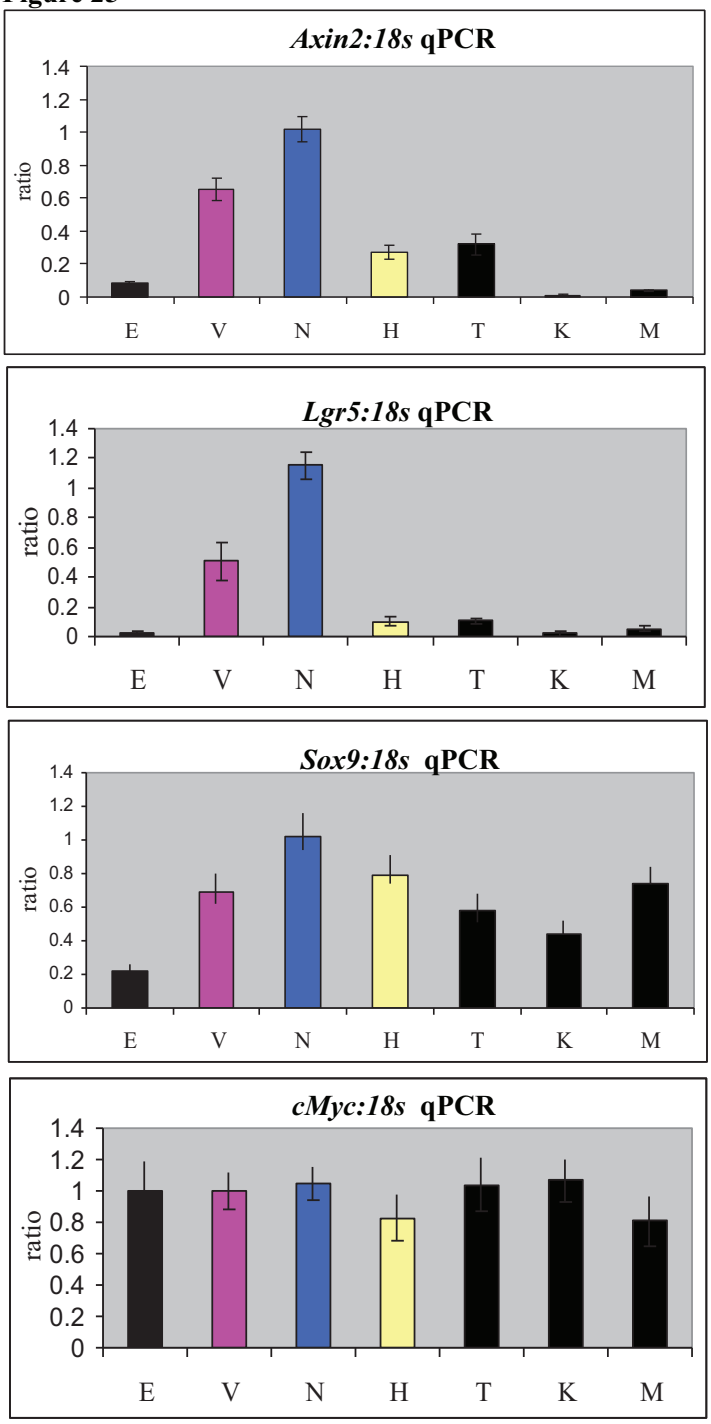

Figure 25 - Quantitative PCR of analysis of some well documented Wnt target genes, (relative to the *18s* gene), showing that *Axin2*, *Lgr5* and *Sox9* are expressed in a similar trend among the seven cell sub-clones, but not c-Myc. Notably, V and N show elevated levels of Wnt target-gene transcriptions (error bar = standard deviation of the mean of 3 samples). **Condition:** 50 x 10^4 cells were seeded onto a 6 cm dish on Day0 in normal DMEM, 10% serum; cells were harvested for RNA on Day2.

experiments, it would be of interest to find out by knockdown experiments if the canonical Wnt pathway promotes growth via activation of Lgr5-mediated signals in cancer cells.

3.3.2 Tankyrase inhibitors suppress anchorage independent growth

In order to examine that transcription levels of *Axin2* and *Lgr5* are genuinely reflecting the activity of the canonical Wnt pathway in promoting anchorage independent proliferation in these mouse pancreatic cancer cells, I used two chemically unrelated tankyrase inhibitors, XAV939 and IWR (their background information has been discussed in Introduction), I found that both drugs have consistent effects on all three sub-clones V, N and H. Tankyrase binds and promotes Axin ubiquitination (Huang et al., 2009), hence inhibiting tankyrase is expected to stabilize Axin and in turn promote degradation of free β-catenin by the Axin1-GSK3β-APC complex, thus suppressing the canonical Wnt transcription programmes (Chen et al., 2009; Huang et al., 2009).

Incubation with 5μM of XAV939 for 16 hours resulted in substantial increase in Axin1 protein levels in all three sub-clones of V, N and H (Figure 26), in which two of them had high Wnt pathway activity. At the same time, quantitative PCR indicated a decrease in transcription levels of *Axin2* and *Lgr5*, without affecting transcription levels of Axin1 (Figure 27). This implies that transcription of *Axin2* and *Lgr5* are indeed responsive to stabilization of the Axin1 protein and decreased in activity of canonical Wnt signalling. In soft agar assays, 5μM of XAV939 decreased average colony size of both N and V down to 50% of the corresponding DMSO control, whereas H only showed a more modest decrease (around 11%) (Figure 28). Consistently, use of 5μM IWR1 also resulted in the same degree of inhibition (data not shown).

3.3.3 knockdown of β-catenin suppressed anchorage independent proliferation in cell sub-clone N.

Since β-catenin acts as the "central messenger" in the canonical Wnt pathway, I examined whether depletion of β-catenin would affect anchorage independent proliferation of the three cell sub-clones V, N and H. Knockdown of β-catenin by viral shRNA (Figure 29B) resulted in decrease in anchorage independent proliferation of sub-clone N, but not sub-clones V and H (Figure 30A). Consistent with the knockdown, transcription levels of both *Axin2* and *Lgr5*

Figure 26

(A)

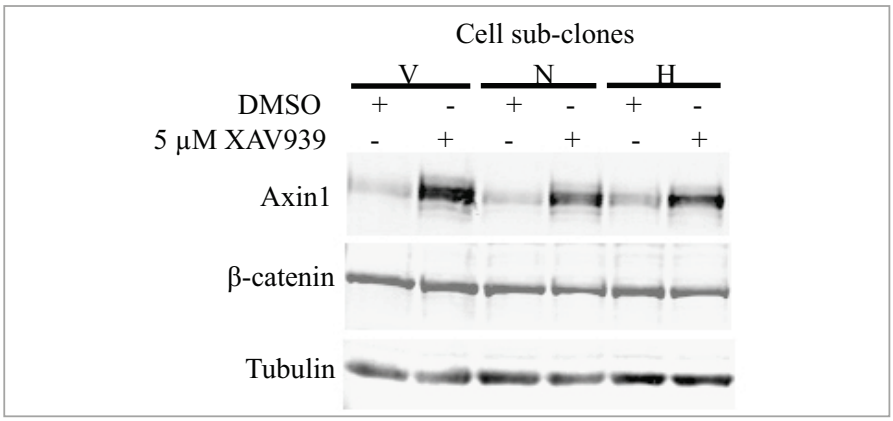

(B)

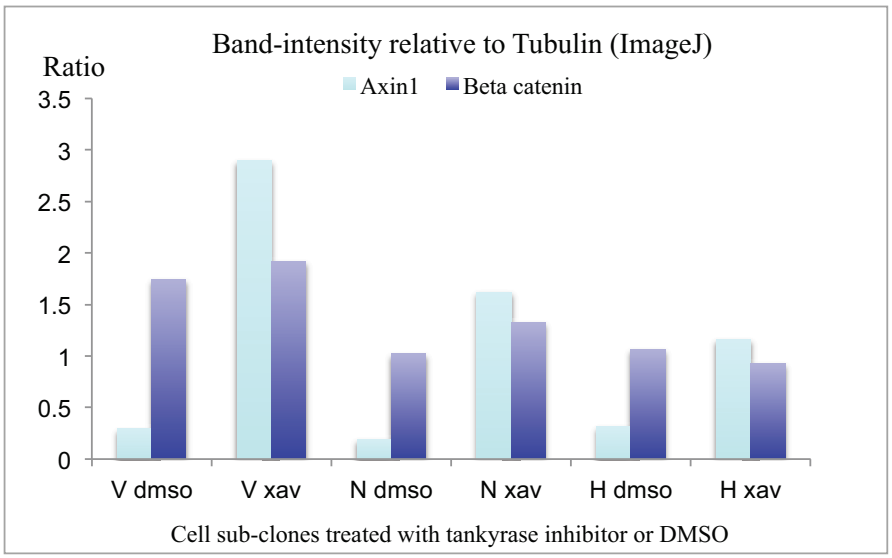

Figure 26 (A) – Immunoblot analysis of the effect by the tankyrase inhibitor XAV939 on Axin1 levels in the three "anchorage independent sub-clones", V, N and H. **(B)** - Quantification of band intensity of Axin1 and β-catenin, relative to tubulin, as shown in (A) using ImageJ. **Condition:** Cells were seeded on Day0 in DMEM with 10% serum, then on Day1, replaced with fresh 10%-serum medium, plus XAV939 or DMSO as shown above, and incubated for 16 hr before harvesting protein.

Figure 27

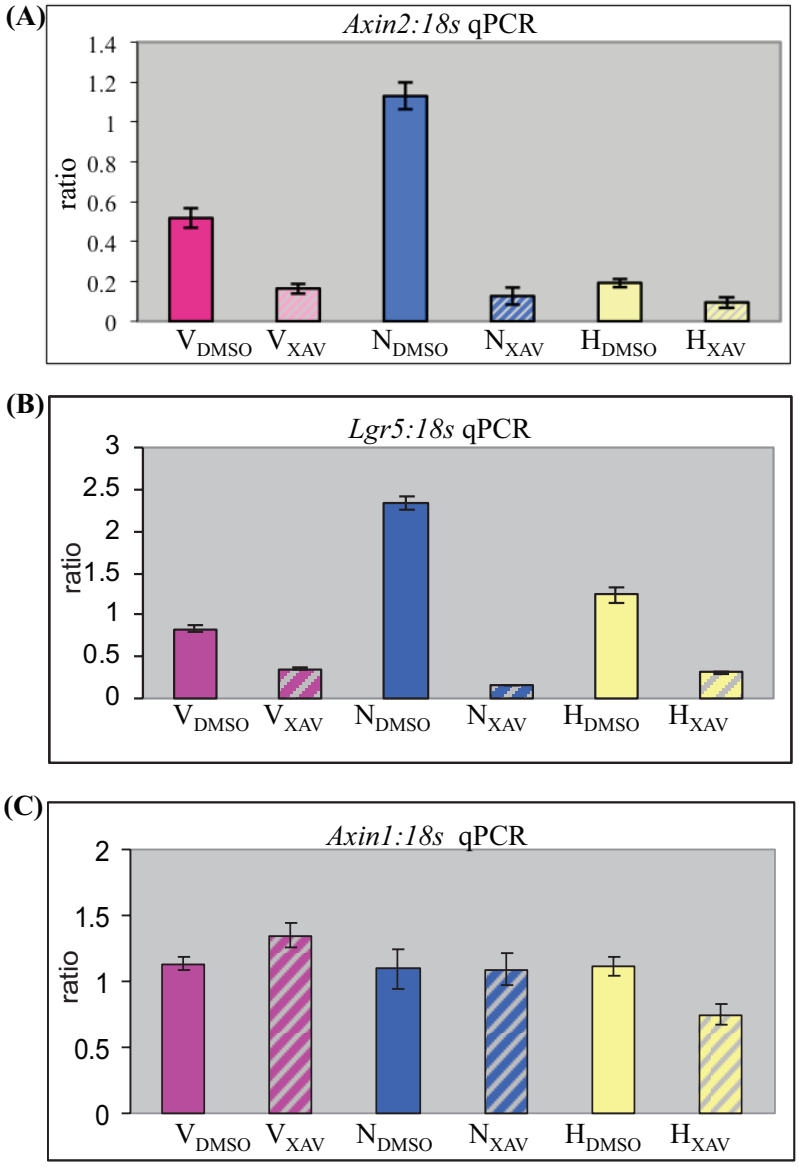

Figure 27 - Quantitative PCR analysis of *Axin1*, *Axin2* and *Lgr5* transcriptions in response to XAV939 treatment in the anchorage independent sub-clones V, N and H, (relative to *18s* transcription). **Condition:** 50 x 10^4 cells were seeded onto a 6cm dish on Day0 in normal DMEM, 10% serum; cells were harvested for RNA on Day2.

Figure 28

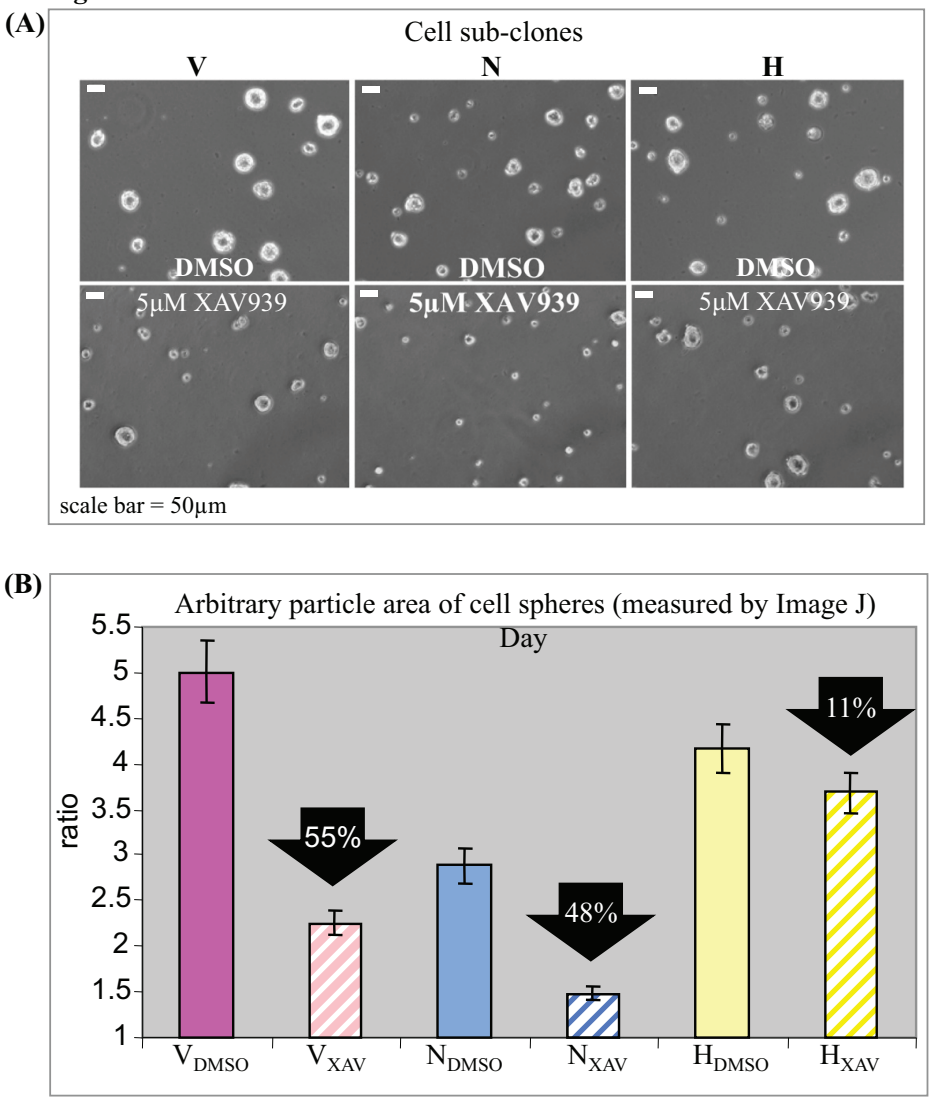

Figure 28 (A) Tankyrase inhibitor suppresses anchorage independent proliferation on soft-agar of sub-clones V and N (about 50% down), but only 11% down in sub-clone H, suggesting V and N are relatively (to sub-clone H) more sensitive to down-regulation of the canonical Wnt activity. **Condition:** On Day0, single cell suspensions each containing 2 x 10^4 cells of respective sub-clone were respectively mixed with methylcellulose on top of a soft agar layer, both layers contain nutrients equivalent to 10% serum, normal DMEM, plus 5μM XAV939 or DMSO; photographs were taken on Day1 and on Day7; the photographs shown above are of Day7. **(B)** Quantification of colony size by Image J, using ratio of arbitrary particle area of Day7: Day1 (Error bar = standard error, with cell sphere counts > 150).

were downregulated in all V, N and H (Figure 30B, C). This indicates that N was more dependent on the canonical Wnt pathway in anchorage independent proliferation than the other sub-clones.

Furthermore, immunoprecipitation and immunoblots revealed that sub-clone V had less β-catenin phosphorylation by Glycogen Synthase Kinase 3 beta (GSK3β) than sub-clones N and H. These phospho-β-catenin were known to be targeted for ubiquitination and proteasomal degradation (Liu et al., 2002). This implies that sub-clone V might have a higher amount of active β-catenin than sub-clones N and H, perhaps due to lower rate of β-catenin degradation (Figure 29A). Hence, if only a small amount of β-catenin was needed to transduce sufficient Wnt signals to the nucleus, sub-clone V might still retain sufficient active β-catenin to support anchorage independent proliferation. Nevertheless, I could not rule out another possibility that suppression of anchorage independent proliferation was attributed to depletion of cell-cell adhesion required during colony formation, rather than the canonical Wnt pathway itself.

3.3.4 Summary

Three out of the seven murine pancreatic cancer cell sub-clones, V, N and H, demonstrated stronger anchorage independent proliferation than the others. Their extra-strength in anchorage independent proliferation was driven by both the MEK-ERK pathway and the canonical Wnt pathway, in which activation of the canonical Wnt pathway could be measured by transcription levels of two downstream target genes, *Axin2* and *Lgr5*. In addition, MEK inhibitors suppressed anchorage independent proliferation more effectively in cell sub-clones V and H than sub-clone N. Conversely, Wnt inhibition by tankyrase inhibitors, suppressed anchorage independent proliferation in sub-clones V and N more effectively than in H. However, both the MEK-ERK pathway and the canonical Wnt pathway were dispensable for 2-dimensional proliferation of tumour cells on plastic culture dishes.

Thus, analysing anchorage independent proliferation revealed heterogeneous dependency on the MEK-ERK and the canonical Wnt pathway in a subset of cell types from a genetically-induced mouse pancreatic tumour. Due to limited time of my studentship, and the fact that the BMP-SMAD4 pathway was highly relevant to human pancreatic cancer, I chose to

concentrate on this, and I did not further study anchorage independent proliferation of sub-clone N.

A summary table for Chapter 3.2 and 3.3, regarding anchorage independent proliferation:

Sub-clones	dependency on the canonical Wnt	dependency on MEK/ERK
V	high	high
N	highest	lower
H	lower	highest

Figure 29

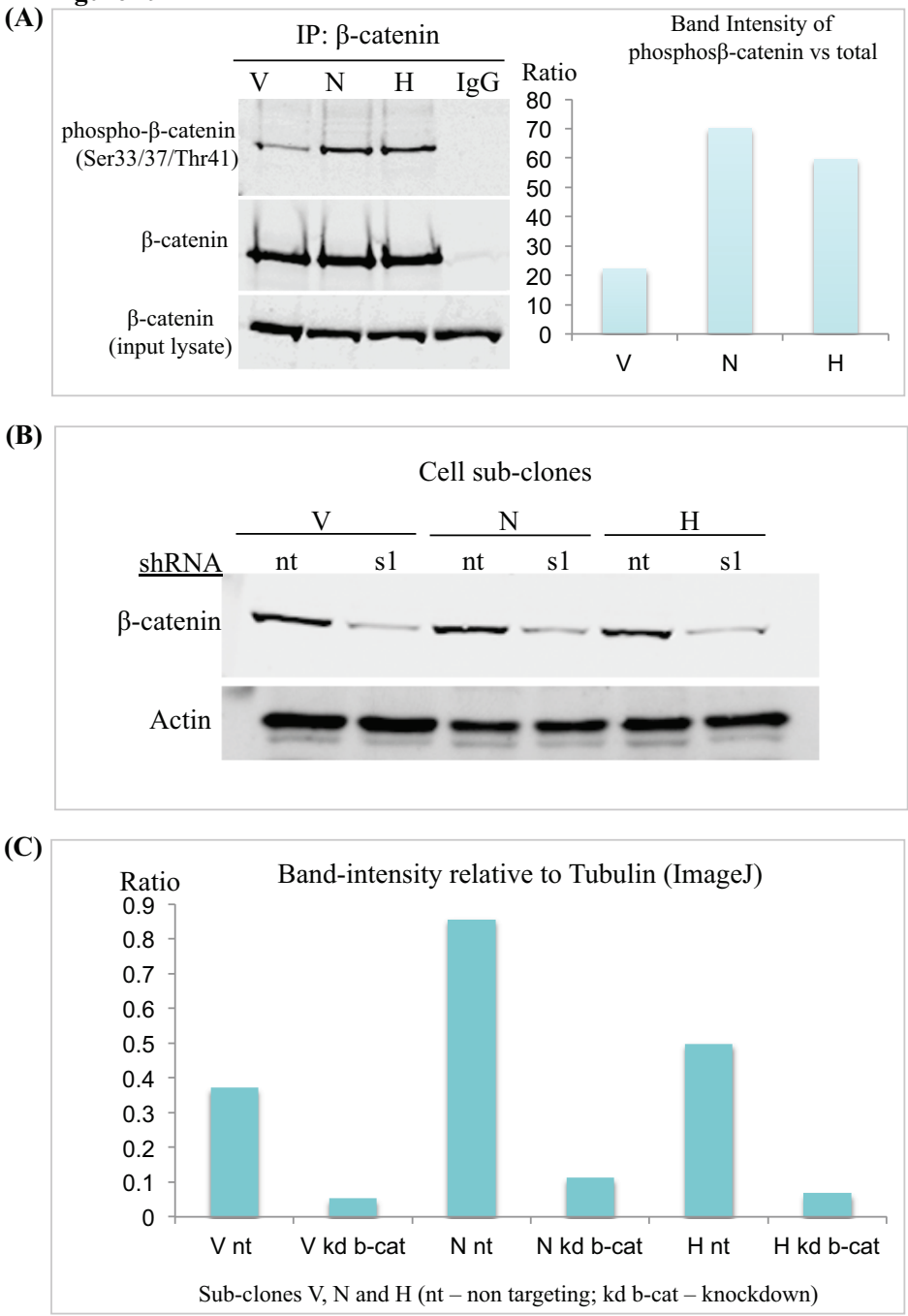

Figure 29 (A) - Left, immunoprecipitation of β-catenin from 1mg protein lysate of each of sub-clones V, N and H; right - quantification of phospho-β-catenin relative to total β-catenin levels, using ImageJ. **(B)** Immunoblot of β-catenin knockdown (kd b-cat) in sub-clones V, N and H, compared with the non-targeting controls (nt). **(C)** – Quantification of immunoblot of the β-catenin knockdown and the non-targeting control of sub-clones V, N and H, relative to Actin, using Image J. **Condition:** 50 x 10^4 cells were seeded onto a 6cm dish on Day0 in normal DMEM, 10% serum; cells were harvested for protein on Day2.

Figure 30

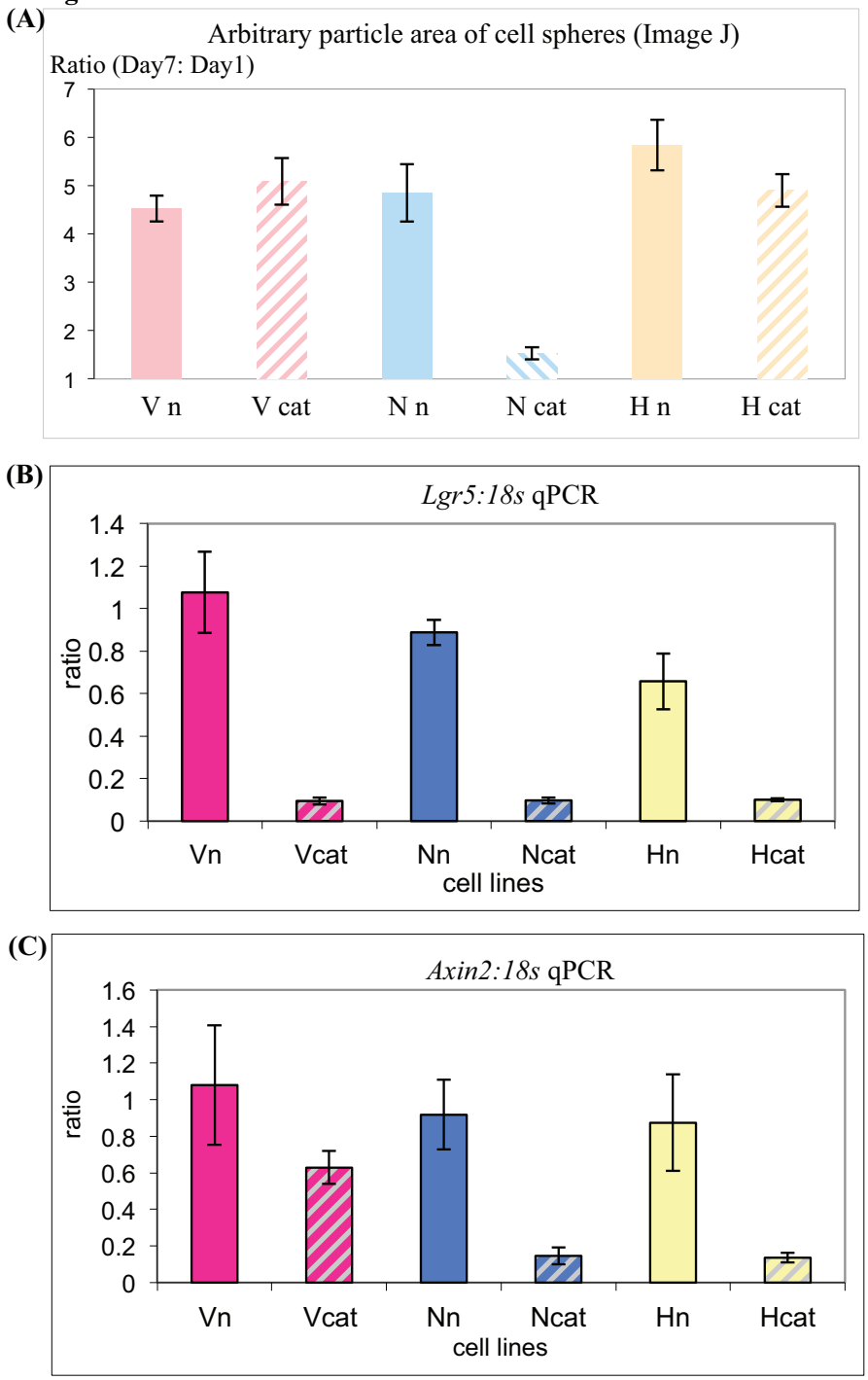

Figure 30 (A) - Quantification of colony size by Image J; Vn refers to sub-clone V infected with non-targeting shRNA, "Vcat" refers to cells infected with shRNA targeting β-catenin, and vice versa for sub-clones N, and H (Error bar = standard error with counts > 150). **(B)** and **(C)** – qRTPCR analysis of transcription levels of two Wnt target genes, *Axin2* and *Lgr5*, in sub-clones V, N and H, upon knocking down β-catenin. **Condition:** 50 x 10^4 cells were seeded onto a 6cm dish on Day0 in normal DMEM, 10% serum; cells were harvested for RNA on Day2.

3.4 The-SMAD4-HNF4α pathway and metabolic stress in pancreatic cancer cells

3.4.1 Heterogeneous R-SMADS phosphorylation and HNF4α expression

SMAD4 is one of the most common aberrations in pancreatic cancer; the *Dpc4* gene, which encodes SMAD4, is lost in ductal tumours of around 50% of patients (Hruban et al., 2006). Western blot analysis showed that all seven cell sub-clones expressed SMAD4 at similar levels, suggesting that $Kras^{G12D}$ and $p53^{R172H}$ did not necessarily cause loss of the *Dpc4* gene during tumorigenesis of Pdx1 positive cells (Figure 31). Furthermore, immunofluorescence showed that SMAD4 accumulates in the nucleus of all seven sub-clones with seemingly uniform intensity of staining (Figure 31C). However, it is well documented that SMAD4 mediates at least two closely related pathways initiated by the BMP/TGFβ superfamily of ligands.

To examine whether or not the seven murine pancreatic cancer cells possessed heterogeneous signalling in the BMP/TGFβ-SMADs pathway upstream of SMAD4, I used antibodies against phospho-SMAD1/2/3, phospho-SMAD1/5/8 and phospho-SMAD2 for western blotting (Figure 31B). I temporarily assumed a classical definition that BMP triggers SMAD1/5/8 phosphorylation, while TGFβ triggers SMAD2/3 phosphorylation, although cross BMP/TGFβ phosphorylation of SMADs had also been reported (Irwin et al., 2008; Wrighton et al., 2009). Of interest, the BMP-responsive phospho-SMAD1/5/8 was detected only in cell sub-clones E, N, T, K and M, whereas the TGFβ-responsive phospho-SMAD2 was detected only in sub-clones V, H and K, and phosho-SMAD3 in only sub-clones V and H. Hence, these mouse pancreatic cancer cells demonstrated heterogeneity in having either phospho-SMAD1/5/8 or phospho-SMAD2/3, except for sub-clone K, which had both BMP- and TGFβ-mediated SMAD phosphorylation.

As discussed in an earlier 'Result' section (3.1), screening for heterogeneous gene expressions revealed that only cell sub-clones E, N and T, and very weakly for sub-clone K, expressed HNF4α, an orphan nuclear receptor (and also a transcription factor) that is critical in embryonic development and glucose metabolism in the adults pancreatic cells. A correlation has thus emerged between HNF4α expression and SMAD1/5/8 phosphorylation, as cell sub-clones V and H, which had phospho-SMAD2/3 but not phospho-SMAD1/5/8, did

Figure 31

(A)

Phospho-SMAD antibodies	**Specificity**
Cell Signaling 9511	SMAD1 (60kDa), SMAD5 (60kDa), SMAD8 (52kDa)
Cell Signaling 3108 (138D4)	SMAD2 (60kDa)
Epitomics EP823Y	SMAD1 (60kDa), SMAD2 (60kDa), SMAD3 (52kDa)

(B)

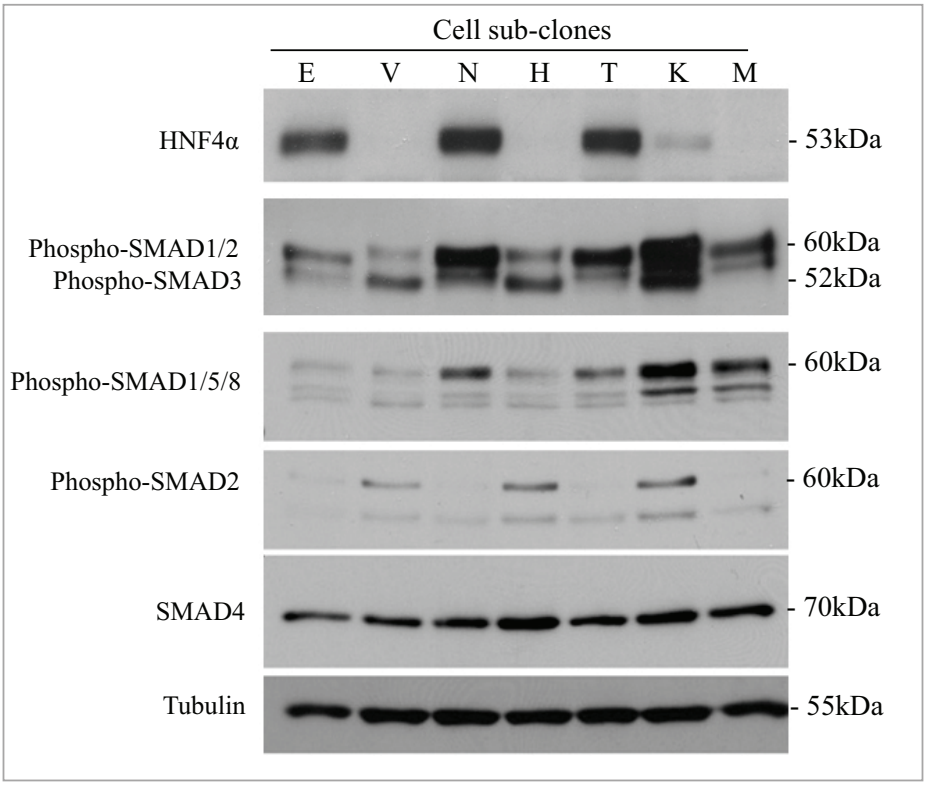

(C)

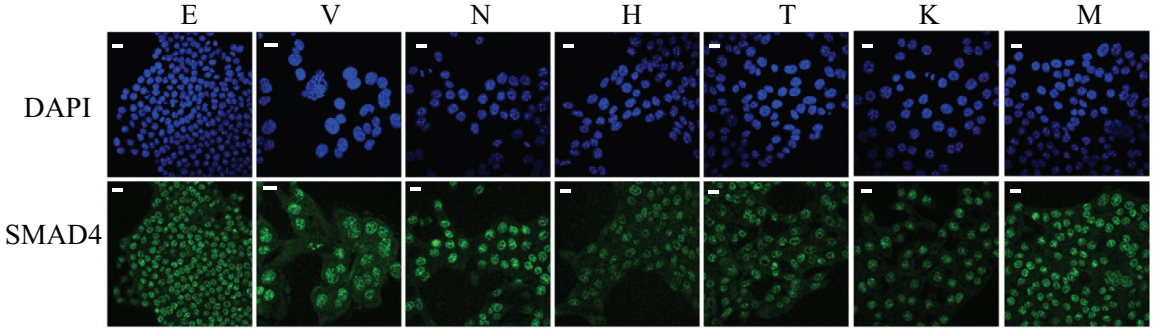

Figure 31 – (A) A list of SMAD antibodies used in the immunoblot in (B), and their respective specificity to different SMADs. **(B)** Immunoblot analysis of phospho-SMAD status and expression of HNF4α, in the seven mouse pancreatic cancer cell sub-clones. **Condition:** 50 x 10^4 cells were seeded onto a 6cm dish on Day0 in normal DMEM, 10% serum; cells were harvested for protein on Day2. **(C)** Immunofluorescent staining of SMAD4 and DAPI in the nuclei of the seven cell sub-clones. **Condition:** cells were seeded on coverslips on Day0 in 10% serum normal DMEM; then on Day2, cells were fixed for confocal microscopy.

not express HNF4α. While cell sub-clone K, which showed both phospho-SMAD1/5/8 and phospho-SMAD2/3, expressed little HNF4α. Such a low level of HNF4α in sub-clone K might have been an outcome of counteractions between the BMP-SMADs and the TGFβ-SMADs pathways (this will be further discussed in a later section). Furthermore, sub-clone M did not express HNF4α despite having phospho-SMAD1/5/8. This indicates that phospho-SMAD1/5/8 might be required but not sufficient to induce HNF4α expression.

To sum up with these observations, I made a hypothesis that HNF4α was downstream of the BMP-SMADs pathway in some of these heterogeneous mouse pancreatic cancer cell sub-clones. Importantly, my hypothesis was also supported by two reports in the literature that ablation of SMAD4 or the BMP type-1 Receptor 1A (BMPR1A) in the mouse embryo caused absence of HNF4α expression in the primitive endoderm and failed gastrulation (Sirard et al., 1998; Gu et al., 1999, discussed in Introduction 1.6.2). In view of this, it would be of interest to investigate why (biological meaning) and how (signalling) such mouse embryonic pathway was reactivated in this mouse model of pancreatic cancer, and whether HNF4α was similarly expressed in a subset of cells in human pancreatic cancer samples.

3.4.2 HNF4α was directly downstream of SMAD1/SMAD4

In cell sub-clones E, N and T, knockdown of SMAD4 simultaneously suppressed HNF4α expression by a close percentage, but not in the controls which had been infected by a non-targeting viral shRNA instead (Figure 32). Quantitative RT-PCR showed that transcription of the *Hnf4α* gene decreased upon knocking down SMAD4 in cell sub-clone N, compared with the "control-N" which had been infected with non-targeting shRNA. Hence both transcription and expression of HNF4α required SMAD4. This was in agreement with a previous observation in the *Dpc4*$^{-/-}$ mouse embryo, in which SMAD4-deficiency caused absence of HNF4α expression in the primitive endoderm (Sirard et al., 1998).

SMAD4 is so-called a co-SMAD that binds different TGFβ/BMP responsive R-SMADs and mediates their nuclear translocation. Two of the HNF4α-negative cell sub-clones (V and H) showed phosphorylation of SMAD2 and SMAD3 instead of SMAD1. Moreover, a previous study has shown that ubiquitous genetic deletion of BMPR1A in the mouse embryo results in absence of HNF4α expression and failed gastrulation, therefore, it is likely that the BMP

Figure 32

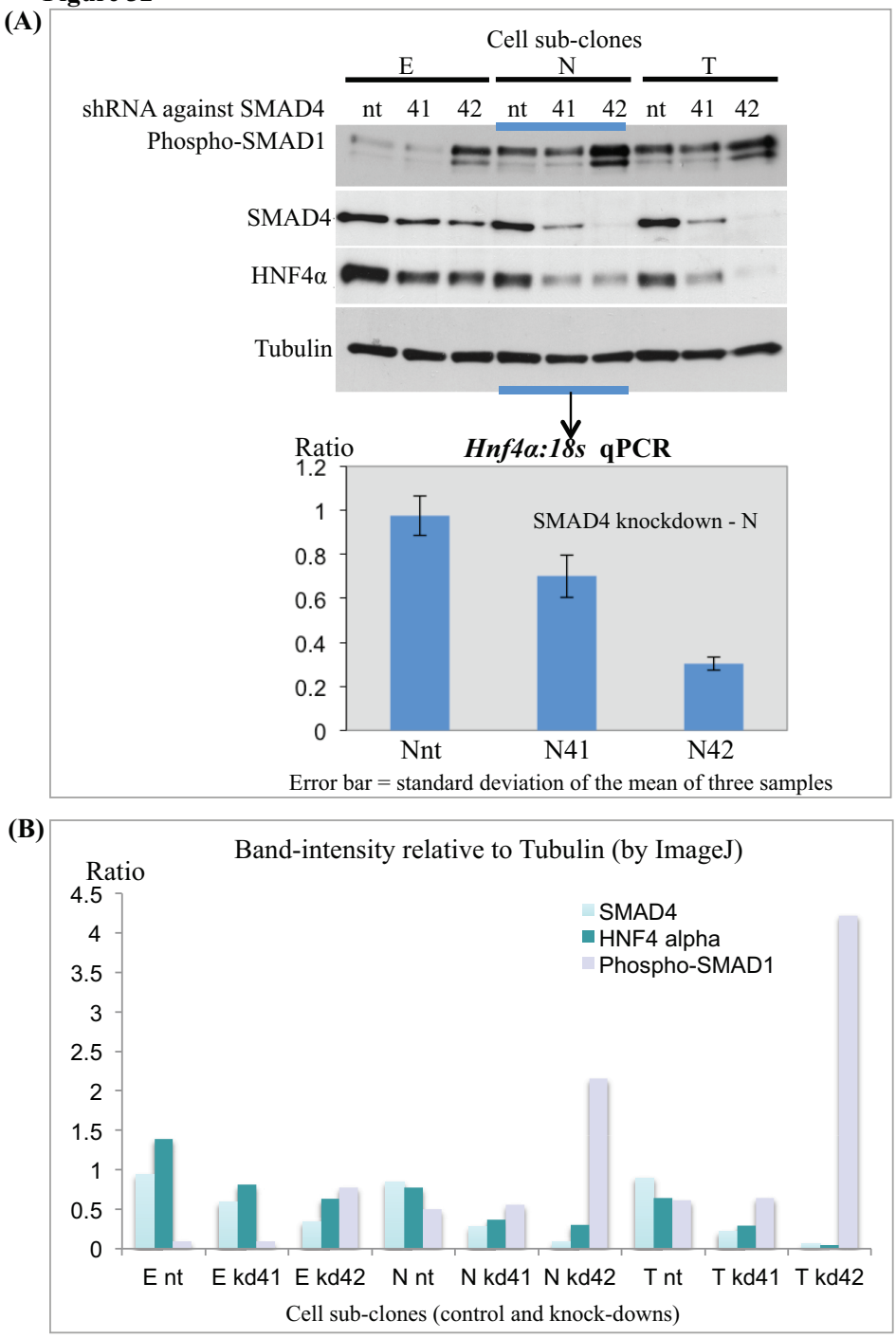

Figure 32 (A) –Top: Immunoblot analysis of HNF4α-expressing sub-clones E, N and T, infected with non-targeting shRNA (N nt, the control) and with SMAD4 knockdown shRNA (Nkd41, Nkd42). Bottom: qRTPCR analysis of *Hnf4α* transcription upon knocking down SMAD4 in sub-clone N. **(B)** – Quantification of the immunoblot in (A), relative to Tubulin levels, using ImageJ. **Condition:** 50 x 10^4 cells were seeded onto a 6cm dish on Day0 in normal DMEM, 10% serum; cells were harvested for protein on Day2.

receptors, SMAD1, SMAD4 and HNF4α are linked in the same pathway. To test this hypothesis, I knocked down SMAD1 in cell sub-clone N using viral shRNAs. Consistent with knocking down SMAD4, knocking down SMAD1 compromised HNF4α expression, suggesting that HNF4α was downstream of the classical SMAD1/SMAD4 pathway in these mouse pancreatic cancer cells (Figure 33).

From here, I postulate with findings in the literature that either the TGFβ family receptors or the BMP family receptors were upstream of SMAD1 phosphorylation. As a quick test for this postulation, I used two specific chemical inhibitors, Dorsomophin (Yu et al., 2008) and SB431542 (Inman et al., 2002), respectively against the BMP- and TGFβ- type-1 receptors. Dorsomophin suppressed phosphorylation of SMAD1 and inhibited HNF4α expression without affecting total SMAD4 levels (Figure 34A), whereas SB431542 did not affect SMAD1 phosphorylation and HNF4α expression. SB431542 is potent inhibitor of the TGFβ type-1 receptors (ALK4, 5 and 7) and it potently suppressed phosphorylation of SMAD2 and SMAD3 in these mouse pancreatic cancer cells (Figure, 34B). Hence treatment with Dorsomophin provided the first line of evidence showing that HNF4α expression was upregulated by SMAD1/SMAD4 downstream of the BMP receptors.

3.4.3 Glucose was required for the BMP-HNF4α pathway

The next questions were how these different mouse pancreatic cancer cells activated the BMPR-SMAD1-SMAD4-HNF4α pathway, i.e., was it autocrine or paracrine, and how to silence such pathway for further analysis. In addition, since HNF4α is known to regulate a broad range of genes related to glucose metabolism in human pancreatic cells (Odom et al., 2004), I also asked whether or not extracellular glucose concentration could affect the activity of the SMAD1/SMAD4-HNF4α pathway. Both questions could be simultaneously answered by removing serum from the medium, while at the same time lowering glucose concentration from the 25mM present in standard growth medium (DMEM) to concentrations that are more physiologically relevant. In human blood, 1mM glucose is regarded as hypoglycaemia while 4-5mM is the minimum of the normal concentration range (Cryer 2001, in Goodman et al., section 7 of Handbook of Physiology).

Using cell sub-clone N as the paradigm, immunoblots showed that serum was dispensable for SMAD1 phosphorylation and HNF4α expression, but glucose was required, as both

Figure 33

(A)

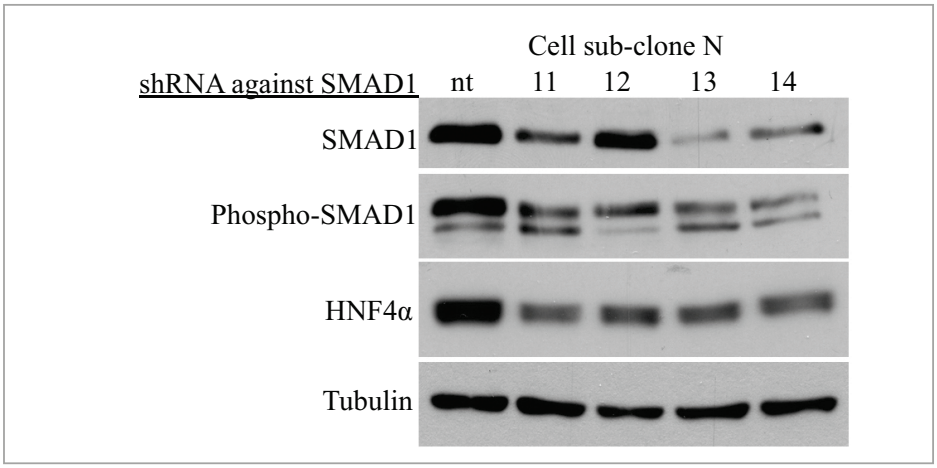

(B)

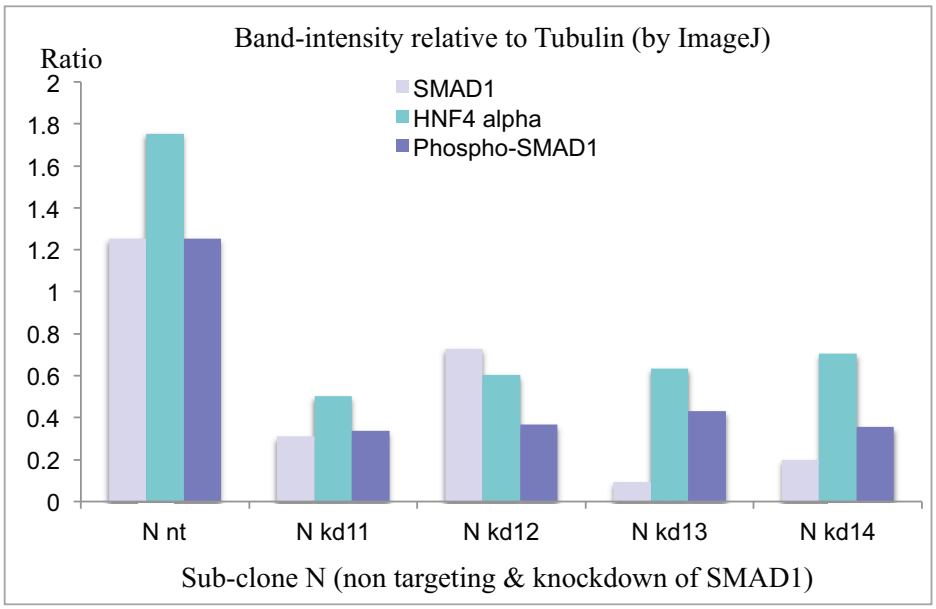

Figure 33 (A) – Immunoblot analysis of sub-clone N infected with non-targeting shRNA (nt, the control) and five individual SMAD1 knockdown shRNAs (11, 12, 13, and 14). **(B)** – Quantification of the immunoblot in (A), relative to Tubulin levels, using ImageJ. **Condition:** 50 x 10^4 cells were seeded onto a 6cm dish on Day0 in normal DMEM, 10% serum; cells were harvested for protein on Day2.

Figure 34

(A)

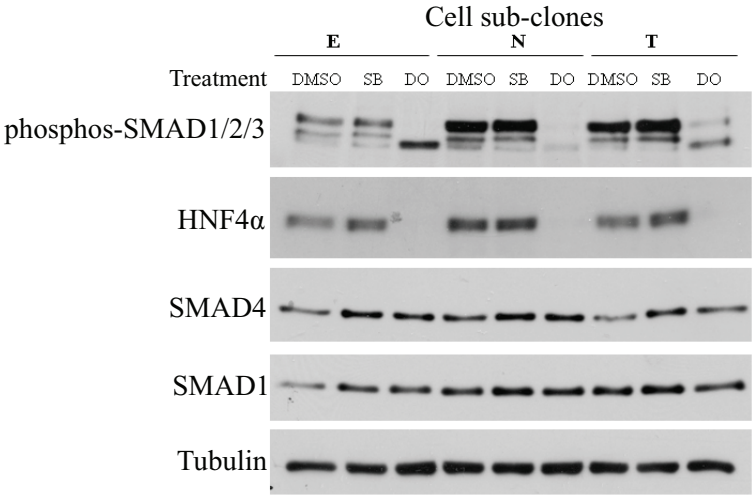

(B)

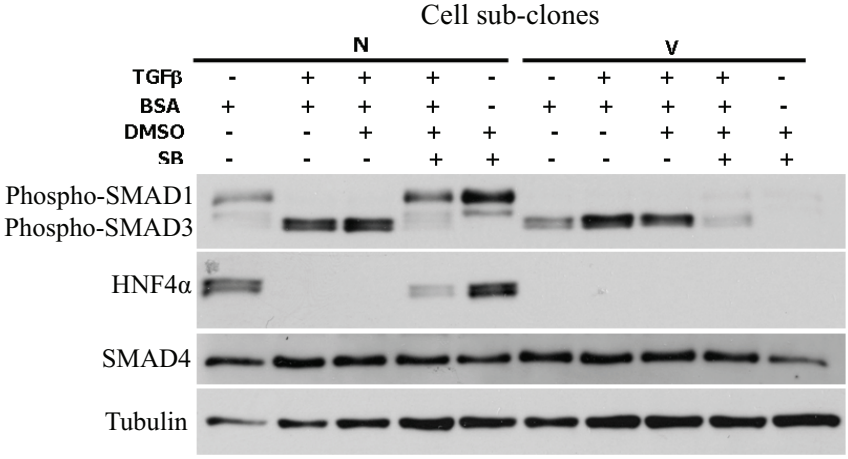

Figure 34 (A) - Immunoblot analysis of changes in HNF4α levels, in response to 5μM Dorsomorphin (DO), the BMPR1 inhibitor, and SB431542 (SB), the TGFβR1 inhibitor, of sub-clones E, N and T. **Condition:** Cells were seeded on Day0 in normal DMEM with 10% serum, then on Day1, replaced with fresh serum medium, plus respective inhibitors or DMSO as shown above, and incubated for 16 hr before harvesting protein.

(B) - Immunoblot analysis of the changes in phospho-SMADs status of sub-clones V and N, in response to 10ng/ml TGFβ and in the presence or absence of the TGFβR1 inhibitor, SB431542 (SB). **Condition:** Cells were seeded on Day0 in DMEM with 10% serum, then on Day1, washed twice with PBS and replaced with fresh 1mM glucose DMEM, without serum, plus SB, and control treatments as shown above, and incubated for 16 hr before harvesting protein.

phospho-SMAD1 and HNF4α diminished in the absence of glucose (Figure 35). Although 10% serum stimulated rapid phosphorylation of SMAD1 in the absence of glucose (neglecting the trace amount of diluted glucose from the 10% serum), HNF4α expression was not upregulated. Hence, SMAD1 phosphorylation was required but not sufficient to induce HNF4α expression.

Next, increasing glucose concentration to 0.1mM simultaneously increased phospho-SMAD1 and HNF4α levels. At 1mM glucose, levels of both phospho-SMAD1 and HNF4α appeared to have reached their maximum, as an increase in glucose concentration up to 25mM even decreased HNF4α and phospho-SMAD1 levels. Therefore, 1mM glucose in the medium was the minimum or the threshold concentration for sub-clone N to maintain a "maximal intrinsic activity" of the SMAD1/SMAD4-HNF4α pathway, under serum starvation. In contrast, pyruvate, another source of energy commonly used in culture medium, was unable to induce phosphorylation of SMAD1 or HNF4α expression.

Since HNF4α levels appeared to be higher when cells were serum starved than with serum (comparing with the standard DMEM at 25mM glucose), I asked whether or not the pathway correlated with synchronization of cells at the G0 phase of the cell cycle. I therefore probed for a G0 phase (quiescence) marker, $p27^{KIP1}$ (Georgia et al., 2006; Besson et al., 2006; Oesterle et al., 2011), which also marks metabolic stress (Liang et al., 2007; Björklund et al., 2010), and found that it was indeed upregulated upon serum starvation in a manner proportional to that of HNF4α levels. More interestingly, $p27^{KIP1}$ levels also correlated with both glucose concentration and HNF4α levels, in which $p27^{KIP1}$ reached the highest level at a minimum of 1mM glucose.

To sum up with the new information discussed above, intrinsic SMAD1 phosphorylation and HNF4α expression of the cells under serum starvation required at least 1mM glucose. Also, HNF4α was more abundant when cells were blocked at the G0 phase by metabolic stress under serum starvation, which was marked by expression of $p27^{KIP1}$. In the presence of serum, SMAD1 phosphorylation was required but not sufficient to induce downstream expression of HNF4α. Glucose was essential to activate the pathway in both serum starved cells and proliferating cells.

Figure 35

(A)

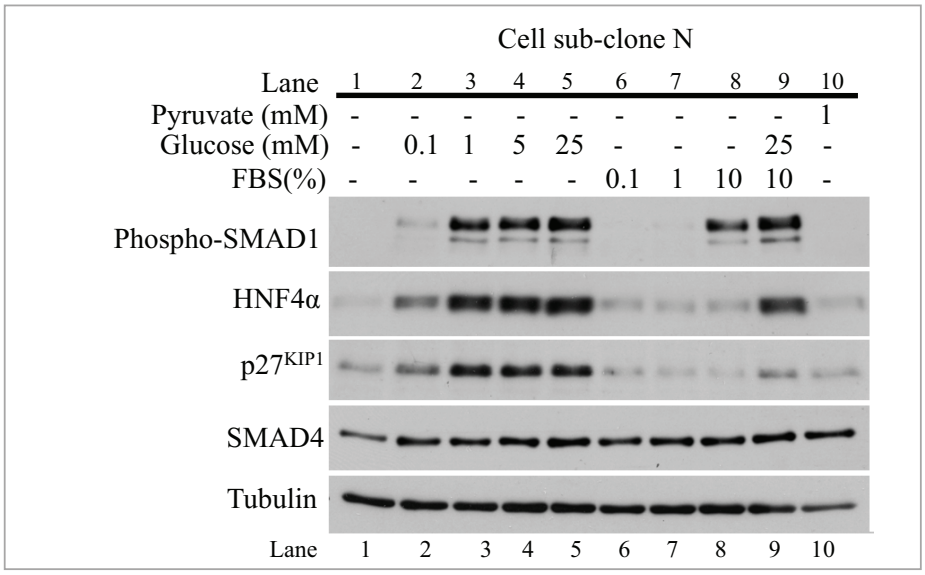

(B)

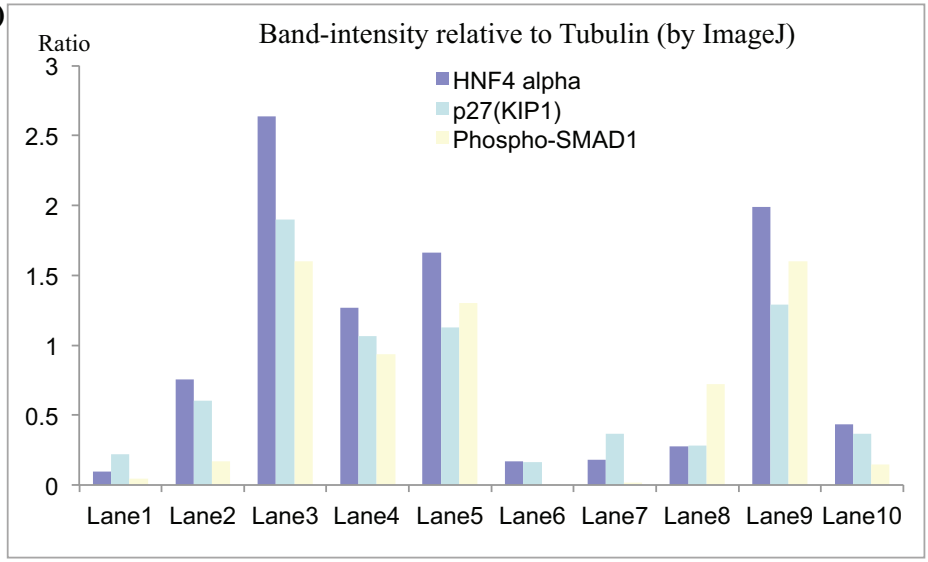

Figure 35 (A) – Immunoblot analysis of changes in HNF4α levels in cell sub-clone N, under different concentrations of glucose and serum. **Condition:** Cells were seeded on Day0 in normal DMEM with 10% serum (50 x 10^4 cells onto a 6 cm plate), then on Day1, washed twice with PBS and replaced with the medium as shown above, and incubated for 16 hr before harvesting for protein. **(B)** – Quantification of the immunoblot in (A) relative to Tubulin levels, using ImageJ.

3.4.4 Recombinant BMP9 induced HNF4α expression

In order to confirm that the SMAD1/SMAD4-HNF4α pathway could be activated by the BMP-family ligands, I treated the mouse pancreatic cell sub-clones with recombinant mouse BMP9 (Figure 36). The basis for picking BMP9 among about ten other variants of BMP family ligands was its involvement in glucose metabolism (Chen et al., 2003; Caperuto et al., 2008), and in phosphorylation of SMAD1/5/8 via BMP type-I receptors (David et al., 2007; Herrera et al., 2009).

Using cell sub-clone N as the paradigm, 16 hour treatment with excess (10ng/ml) BMP9 in 0.1mM glucose of serum-free medium increased phospho-SMAD1 and HNF4α expression up to a level similar to that when the cells were in 1mM glucose and treated only with BSA (the carrier protein of BMP9 in the stock solution). This suggests that excess exogenous BMP9 and probably also some other BMP ligands could induce SMAD1 phosphorylation and HNF4α expression, even when glucose concentration was lower than the 1mM required by the cells to intrinsically activate the pathway. Such requirement of 1mM glucose was likely to be upstream of the production and secretion of BMP ligands by the cells, if this was the true mechanism used by the cells to self-initiate the pathway in the presence of sufficient glucose. Alternatively, glucose could have been upstream of some other parallel pathways which by-passed the normal ligand-receptor interaction to induce SMAD1 phosphorylation and HNF4α expression.

Furthermore, in serum-medium at 0.1mM glucose, recombinant BMP9 induced only a modest increase in HNF4α expression. This consistently showed that the overall HNF4α levels were suppressed when cells were progressing through the cell cycle (in the presence of serum), comparing with that when cells were under metabolic stress in the absence of serum. To sum up, BMP9 was identified to be an upstream ligand of the SMAD1/SMAD4-HNF4α pathway. HNF4α expression was more effectively induced by recombinant BMP9 in the absence of serum than in the presence of serum. In the next section, I am going to discuss the differences in the efficacy of HNF4α expression between serum starved cells and proliferating cells.

Figure 36

(A)

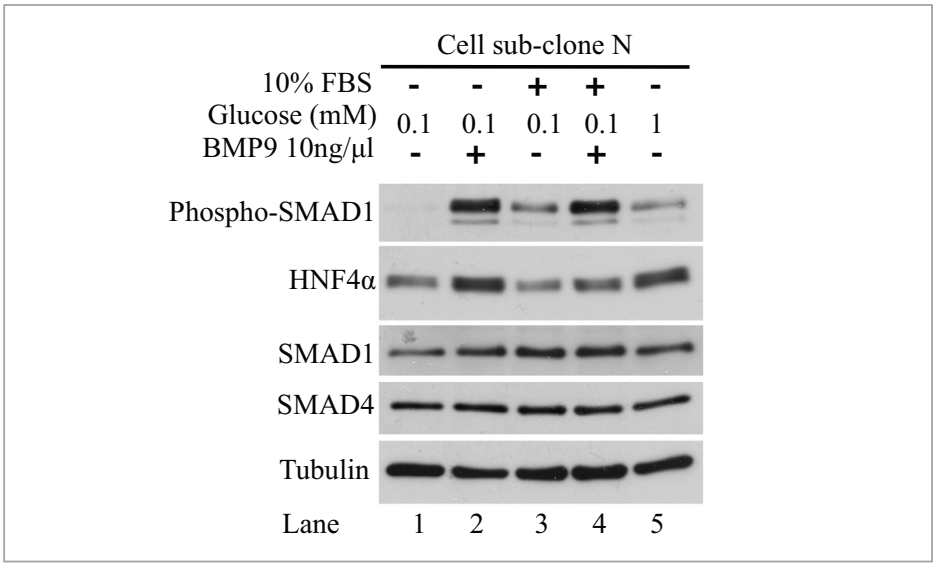

(B)

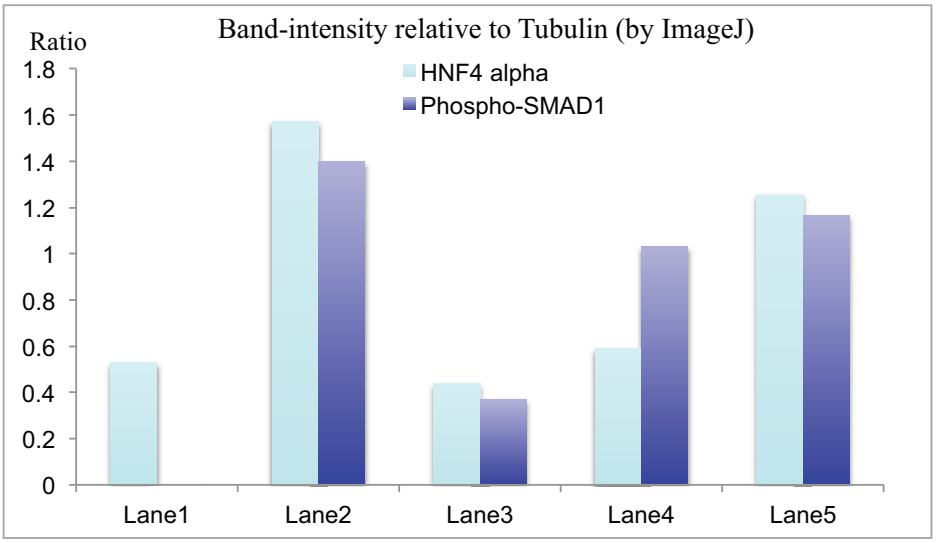

Figure 36 (A) – Immunoblot analysis of changes in HNF4α levels in cell sub-clone N, under different concentrations of glucose and serum. **Condition:** Cells were seeded on Day0 in normal DMEM with 10% serum (50×10^4 cells onto a 6 cm plate), then on Day1, washed twice with PBS and replaced with the medium with treatments as shown above, and incubated for 16 hr before harvest. **(B)** – Quantification of the immunoblot in (A) relative to Tubulin levels, using ImageJ.

3.4.5 Recombinant TGFβ suppressed HNF4α expression

Like cell sub-clone N, treatment with recombinant BMP9 also caused SMAD1 phosphorylation and upregulated HNF4α expression in sub-clones E and T. In contrast, recombinant TGFβ1 induced SMAD3 phosphorylation, but not SMAD1 or SMAD2, and diminished HNF4α levels in all three sub-clones E, N and T (Figure 37A). This suggests that BMP and TGFβ pathways were counteracting each other in these mouse pancreatic cancer cells (Figure 37). This was also consistent with the observation that cell sub-clones V and H, which did not express HNF4α, had intrinsic SMAD3 phosphorylation (Figure 37B).

To check whether phospho-SMAD3 was preventing expression of HNF4α in cell sub-clones V and H, they were treated with recombinant mouse BMP9. BMP9 effectively stimulated SMAD1/2 phosphorylation in sub-clones V and H, but no induction of HNF4α was detected. This suggests that additional factors were preventing or required for HNF4α expression in these two cell sub-clones (Figure 37C).

One of the potential antagonistic factors against HNF4α expression in sub-clones V and H might be phospho-SMAD2, which appeared to have an inverse correlation with HNF4α expression among the seven cell sub-clones (Figure 31). As mentioned in the previous paragraph, in sub-clones V and H, BMP9 induced SMAD1/2 phosphorylation, and recombinant mouse TGFβ1 induced SMAD3 phosphorylation, but not SMAD2 (Figure 37C); while in the presence of serum in normal DMEM, both SMAD2 and SMAD3 were phosphorylated (Figure 31). This suggests that ligands other than TGFβ1 in the serum could have induced SMAD2 phosphorylation. Moreover, the cell sub-clone K, which weakly expressed HNF4α, had both intrinsic phospho-SMAD1/5/8 and phospho-SMAD2, but not SMAD3. If sub-clone K's weak HNF4α expression was attributed to a net balance of BMP- and TGFβ-mediated phospho-SMADs activity, then SMAD2, as a well document TGFβ-SMAD, could have been a counteracting factor against BMP-mediated HNF4α expression.

Nevertheless, since SMAD1 and SMAD2 are of the same molecular weight, they are indistinguishable on the immunoblots when using the phospho-SMAD1/2/3 antibody. The anti-phospho-SMAD2 initially used in Figure 32 should have been able to address whether SMAD2 was phosphorylated in response to BMP9 in sub-clones V and H. However, it was in short supply and I was facing a time limit of my project. Furthermore, although cell sub-

Figure 37

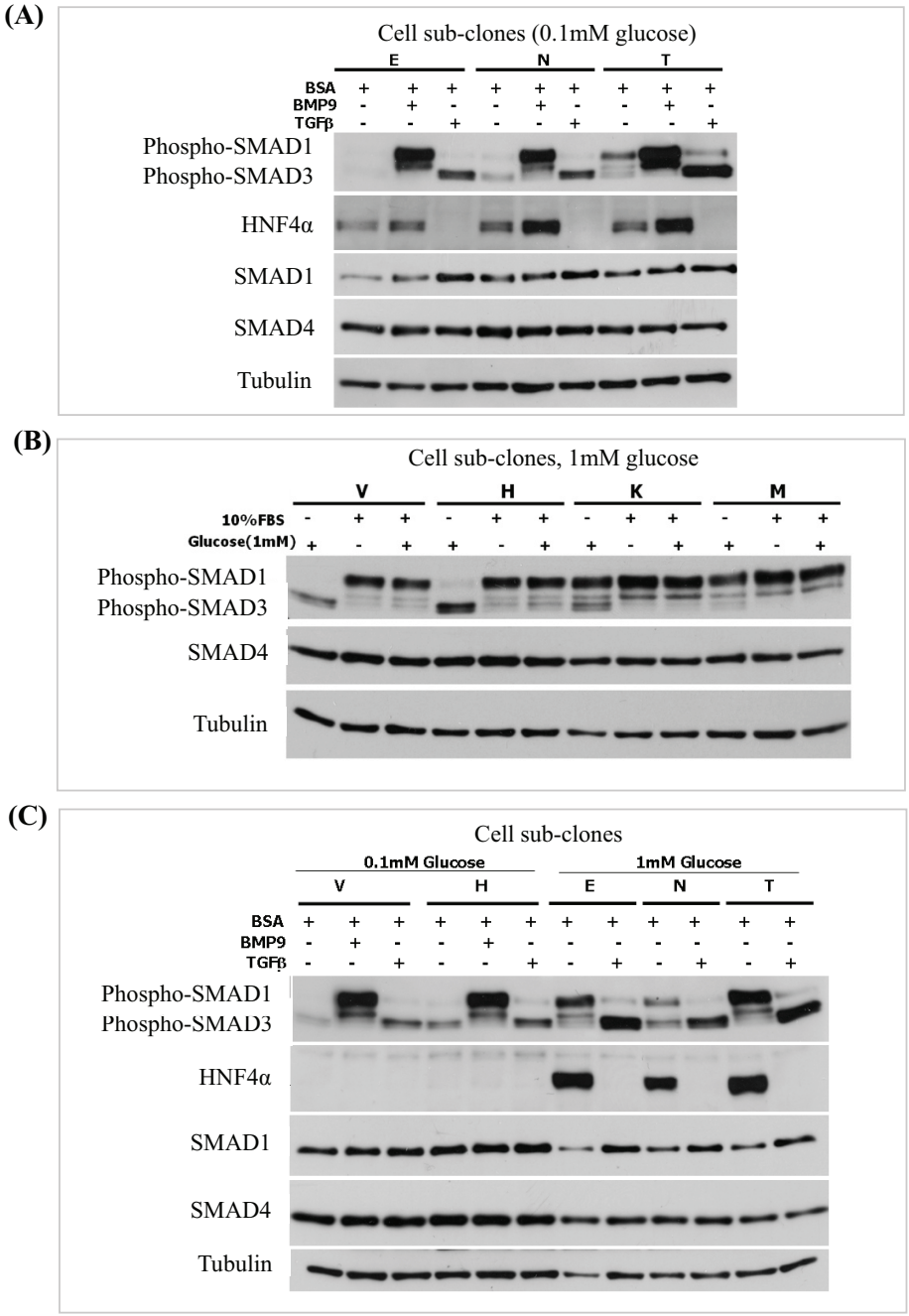

Figure 37 (A) – Immunoblot analysis; treatment with 10ng/ml recombinant mouse BMP9 or TGFβ, sub-clones E, N and T, under 0.1mM glucose, which kept intrinsic phosphorylation of SMADs minimal. **(B)** – Immunoblot analysis of serum starved sub-clones V, H, K and N, showing intrinsic phospho-SMADs as compared with that in the presence of serum, at 1mM glucose. **(C)** – Immunoblot analysis; treatment of recombinant BMP9 on sub-clones V and H, and side by side, treatment with recombinant TGFβ on sub-clones E, N and T. **Condition:** Cells were seeded on Day0 in normal DMEM with 10% serum, then on Day1, washed twice with PBS, and replaced with 1mM glucose DMEM serum free medium, plus the treatments as shown above, and incubated for 16 hr before harvest.

clone M possessed intrinsic phosphorylation of SMAD1, it did not express HNF4α. This strengthens the idea that additional factors were required for HNF4α expression.

3.4.6 HNF4α was transiently expressed and stabilized at its peak level during cell cycle progression

In order to examine the intrinsic phospho-SMADs status of all seven heterogeneous mouse pancreatic cancer cell sub-clones, I put them under 1mM glucose and compared by immunoblotting with protein samples of cells in the presence and absence of 10% serum. Consistent with cell sub-clone N, the other two HNF4α-expressing sub-clones E and T, also had constitutive pathway activity in 1mM glucose of serum-free medium. However, in the presence of serum (which means the cells were proliferating), HNF4α expression was suppressed (Figure 38).

This implies at least two non-mutually-exclusive possibilities that may explain the relationship between the presence of serum and HNF4α expression. First, the SMAD1/SMAD4-HNF4α pathway may be active only in certain phases of the cell cycle, such as at the G0 phase. In this case, when cells were proliferating and transitioning in cell cycle, the time opportunity for the SMAD1/SMAD4-HNF4α pathway throughput would be smaller than when cells were serum starved, leading to lower HNF4α levels on immunoblots, which represented an average level of all phases in the cell cycle. Second, the SMAD1/SMAD4-HNF4α pathway may have been upregulated by metabolic stress during serum starvation; when cell are proliferating in the serum, stress was relatively minimal, and therefore lowering HNF4α levels. Alternatively, serum may contain factors that suppress HNF4α expression, despite promoting SMAD1 phosphorylation.

I first examined the possibility that HNF4α expression was upregulated only in a limited period in the cell cycle, as this had been suggested by several studies in the literature (Verdeguer et al., 2010; Takagi et al., 2010; Bonzo et al., 2012). Notably, Verdeguer et al., 2010 demonstrated by a time lapse video that ectopic HNF4α-GFP was expressed in the nucleus before and just after mitosis, using an immortalized mouse kidney cell line. I therefore conducted immunofluorescence to co-stain HNF4α and phospho-histoneH3, a marker for mitotic nuclei (Figure 39), so as to examine whether or not these mouse

Figure 38

(A)

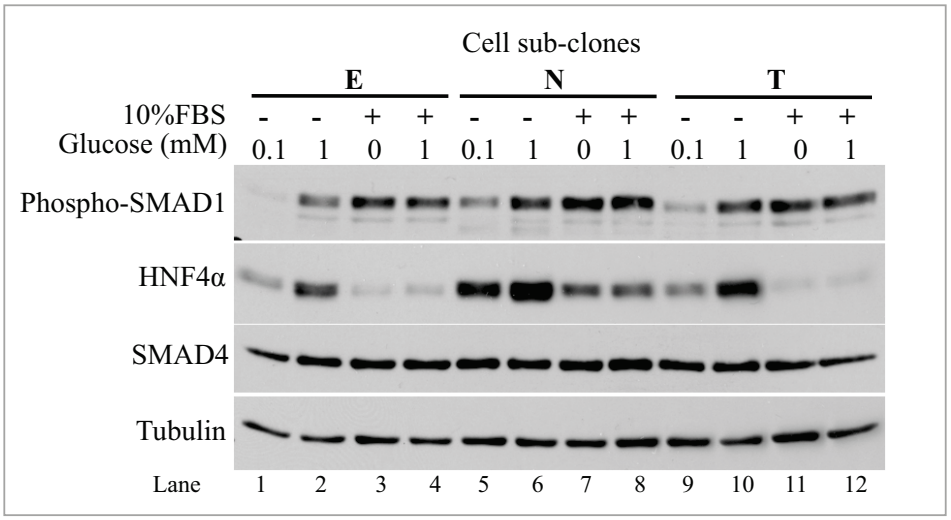

(B)

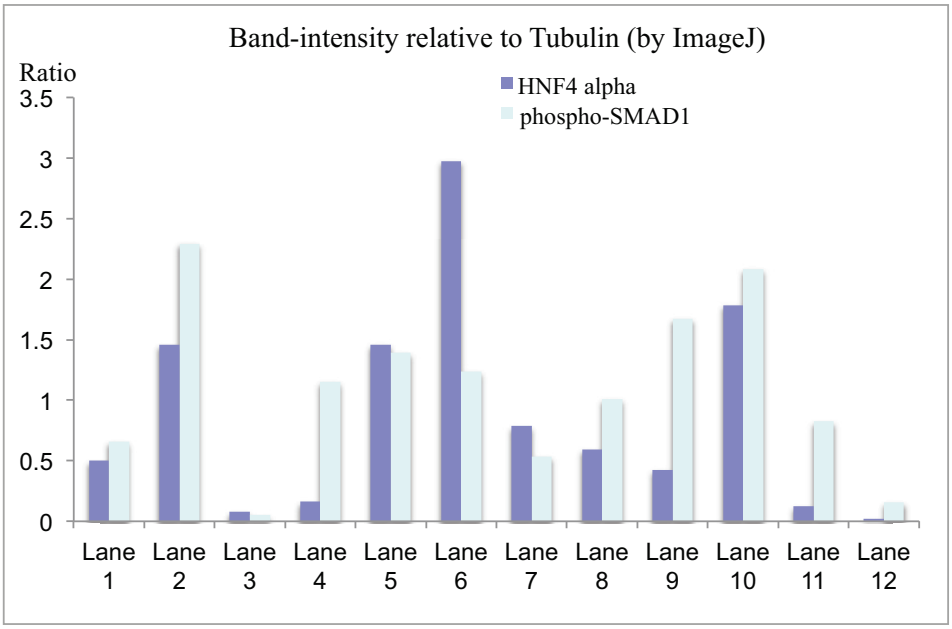

Figure 38 (A) – Immunoblot analysis of HNF4α expressions in sub-clones E, N and T, in DMEM containing 0.1mM glucose, 1mM glucose, and 1mM glucose plus 10% serum. **Condition:** Cells were seeded on Day0 in normal DMEM with 10% serum, then on Day1, washed twice with PBS, and replaced with modified DMEM with different glucose concentrations as shown above, and incubated for 16 hr before harvest. **(B)** – Quantification of HNF4α and phospho-SMAD1 levels in the immunoblot in (A), relative to Tubulin levels, using ImageJ.

pancreatic cancer cells expressed endogenous HNF4α in the same manner as in Verdeguer et al., 2008.

Using cell sub-clone N as the paradigm, in serum-medium at 1mM glucose (i.e. proliferating cells), HNF4α was strongly stained in 9.5% of the nuclei, while another 11.3% showed a moderate-to-weak HNF4α staining, and the rest were essentially negative. Importantly, HNF4α staining did not co-localize with that of phospho-histoneH3, indicating that HNF4α was not expressed during mitosis. Moreover, among the HNF4α-positive nuclei, almost half of them (0.095/0.113 = 0.4) showed distinctively strong HNF4α staining. This suggests that HNF4α expression may have started going up when the cells enter a particular stage in the cell cycle. Upon reaching a maximum level, HNF4α expression started to decrease as the cells transit to another phase of the cell cycle.

I then looked at staining of serum starved cells in 1mM glucose. Consistent with immunoblot analysis described in previous sections, an overall increase in HNF4α staining relative to that of proliferating cells was observed, with 17% of the nuclei showing intense HNF4α staining, 40% showing moderate-to-weak staining, and the rest were essentially negative. Nevertheless, in the absence of both glucose and serum, with camera exposure settings unchanged, there were still 12% of the nuclei showing intense HNF4α staining, while only 8% of the nuclei remained to show moderate-or-weak HNF4α staining. This suggests that the glucose-dependent SMAD4-HNF4α pathway promoted an overall increase in HNF4α-positive nuclei, however, such pathway did not have a strong correlation with the nuclei showing high-HNF4α staining. Rather, those high-HNF4α nuclei were most likely attributed to a glucose-independent pathway that induced transient and rapid HNF4α expression or stabilization, or both. In addition, the intensity of nuclear SMAD4 staining did not have a correlation with the "high-and-low" levels of nuclear HNF4α staining, as SMAD4 was uniformly stained in all nuclei when cells were in 1mM glucose, the same as shown in Figure 31C. This suggests that as long as SMAD4 is present at a basal level, HNF4α can be expressed and additional pathways must have stepped in to regulate the turnover of HNF4α across different stages of cell cycle progression.

To sum up, HNF4α expression appeared to start at a particular time point in the cell cycle; it progressively increased to a peak level, then gradually decreased to nil. Such fluctuation

was mainly attributed to the glucose-dependent SMAD1/SMAD4 pathway upstream. At the peak level of HNF4α expression, an unknown glucose-independent pathway "stepped-in" to rapidly and transiently stabilize HNF4α or to strengthen HNF4α expression. This was evident by an observation that the percentage of high-HNF4α nuclei changed very little in response to glucose deprivation or serum starvation, comparing with changes in the percentage of other nuclei showing moderate-to-weak HNF4α staining.

3.4.7 HNF4α can be expressed in mitotic stress under serum starvation and during cell proliferation at 25mM glucose in standard DMEM

HNF4α was not expressed during the mitotic phase of proliferating cells. However, when sub-clone N was serum starved, 3% of the nuclei appeared to have "trapped" in the M phase, and among them, 51.4% showed co-staining of HNF4α (moderate-to-weak intensity only) and phospho-histone-H3. This suggests that the SMAD4-HNF4α pathway could be conditionally activated even during the mitotic phase, when cells experience stress of serum starvation.

Similarly, co-staining of HNF4α (weak and moderate intensity only) and phospho-histone-H3 was also observed in proliferating cell sub-clone N in serum-medium at 25mM glucose (data not shown). In proliferating cells in 10% serum, massive activation of HNF4α under normal DMEM (with artificially high 25mM glucose) compared with that in 1 or 5 mM Glucose DMEM (Figure 40) may have been due to excessive oxidative stress arising from rapid metabolism of glucose during proliferation. If time was sufficient, It would be informative to also conduct immunofluorescence of cells under 25mM glucose DMEM with 10% serum, and see whether such increase in HNF4α was attributed to an increase in overall "moderate-to-weak" nuclear HNF4α staining, or to those "high-HNF4α nuclei". As shown in Figure 39, increase in "moderate-to-weak" HNF4α expression was due to metabolic stress when cells are deprived of serum (suppressed metabolism, quiescent G0 state as marked by expression of p27 on western in Figure 35), and such stress response required at least 1mM glucose. However, the cause of those "high-HNF4α nuclei" is unclear. It would be tempting to investigate whether we would see an increase in "high-HNF4α nuclei" of proliferating sub-clone N under 25mM glucose DMEM, relative to 1mM glucose. If so, this would suggest that HNF4α is stabilized in response to rapid

Figure 39

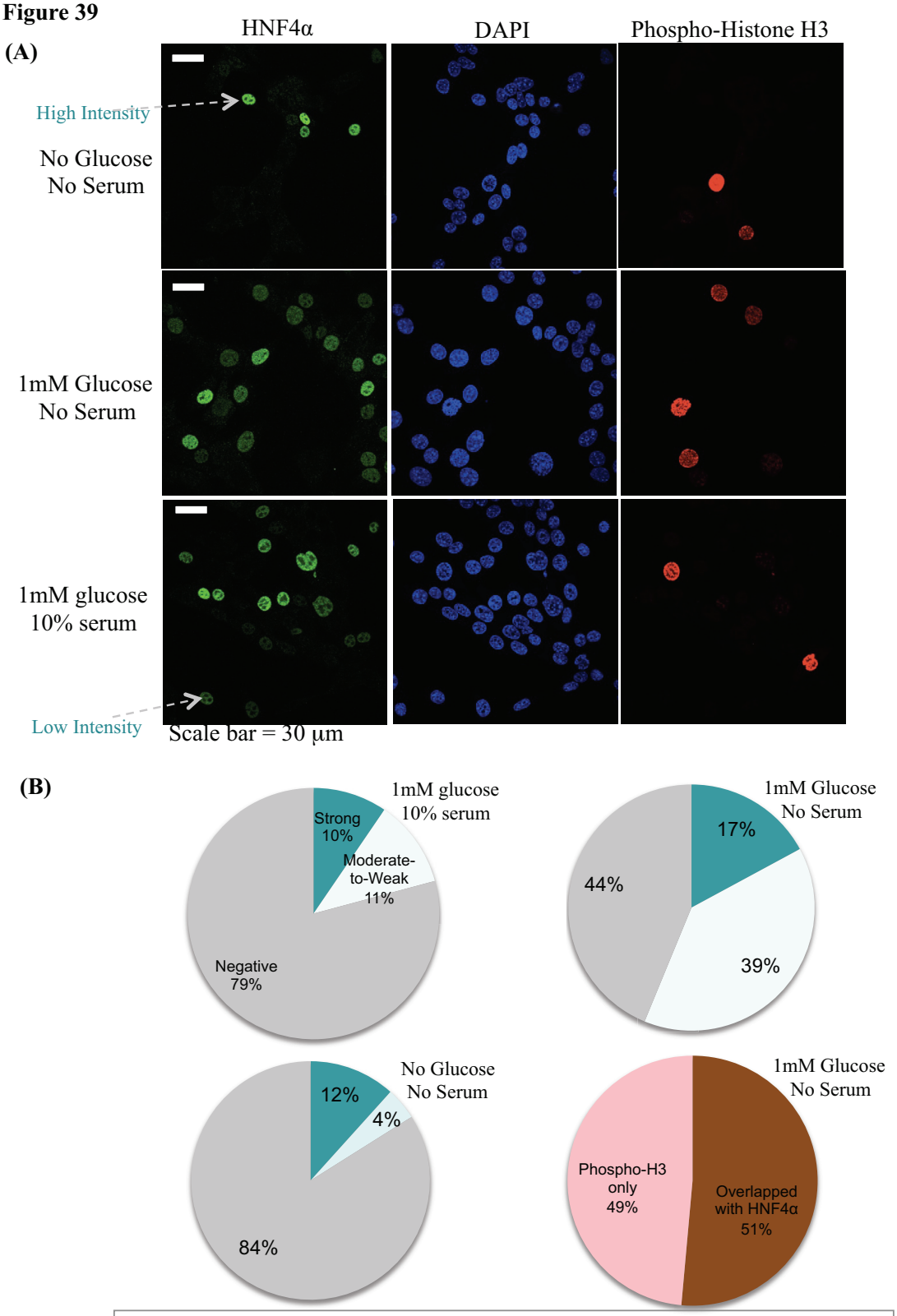

Figure 39 (A) - Co-immunofluorescence of HNF4α and Phospho-histone H3, of cell sub-clone N under starvation of serum or glucose or both. **Condition:** cells were seeded on coverslips on Day0 in 10% serum normal DMEM; then on Day1, being washed twice with PBS, and replaced with serum free medium conditions as shown above, and on Day2 being fixed for confocal microscopy. **(B)** – Percentage of cells that showed high nuclear HNF4α staining, moderate-to-weak HNF4α staining, and no HNF4α staining, for each condition tested. Over 200 cells were counted and analyzed for each sample condition.

Figure 40

(A)

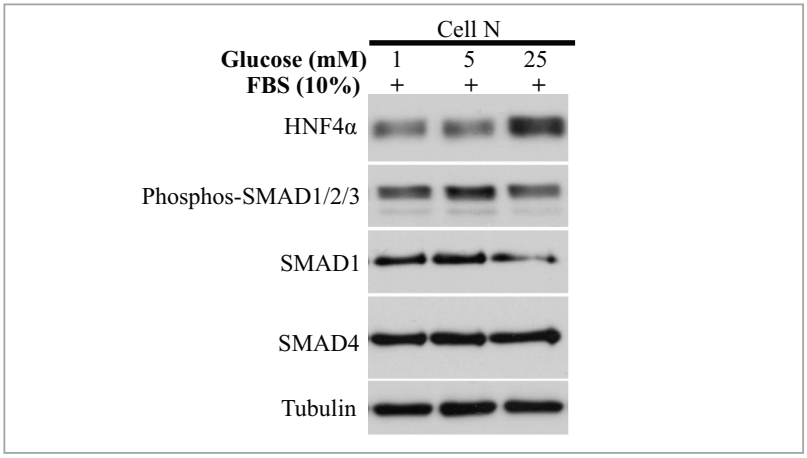

(B)

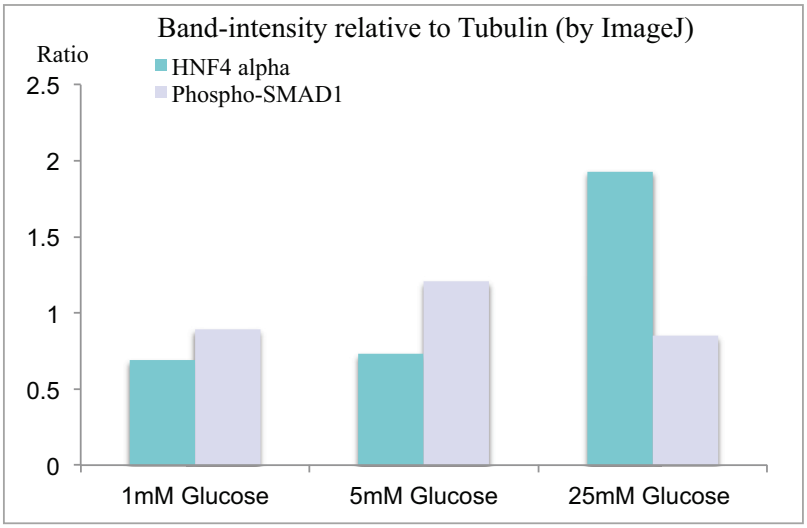

Figure 40 (A) – immunoblot analysis of HNF4α expression in cell sub-clone N, at 1mM, 5mM, and 25mM glucose medium, in the presence of 10% serum. **Condition:** Cells were seeded on Day0 in normal DMEM with 10% serum, then on Day1, washed twice with PBS, and replaced with 10% serum, DMEM with glucose concentration respectively at 1mM, 5mM, and 25mM (normal DMEM concentration), and incubated for 16 hr before harvest. **(B)** Quantification of the immunoblot in (A), relative to Tubulin levels, using ImageJ.

glucose metabolism, potentially involving oxidative stress from the citric acid cycle, at a particular time point in the cell cycle.

Nevertheless, since 25mM glucose wasmuch higher than the physiological range of glucose concentration, it would be of little relevance to conduct further investigation at this glucose concentration.

3.4.8 Replicative stress induced by thymidine or Gemcitabine block cell cycle progression and upregulated HNF4α expression

Since blockage of cell cycle progression at the G0 phase by serum starvation upregulated HNF4α expression, I more specifically asked whether replicative stress was one of the stress factors for activating the SMAD4-HNF4α pathway. I found that treatment with excess thymidine (in 1mM glucose with 10% serum) upregulated HNF4α expression in sub-clone cell N (infected with a non-targeting shRNA), and proportionally less so in the SMAD4 knocked-downs of sub-clone N (Figure 41). This shows that when DNA replication was blocked by thymidine, HNF4α expression was also induced by SMAD4. Although I was unable to find an usable antibody for a marker of the G1-S phase, decreased $p27^{KIP}$ levels indicated departure from the G0 phase of the cells.

Next, I tested if cells could also respond to Gemcitabine by inducing HNF4α expression. As discussed in section 1.1.7 of Introduction, Gemcitabine is the first ever therapy for the treatment of pancreatic cancer. It is a nucleoside analogue in which the hydrogen atoms on the 2' carbon of deoxycytidine are replaced by fluorine atoms, thereby substituting for normal cytidine during DNA replication (reviewed by Rivera et al 2009). Hence DNA-replication is attenuated at the G1-S phase by the insertion of a faulty nucleoside (Gemcitabine), and eventually induced apoptosis.

Similar to the thymidine-block experiment, HNF4α expression increased in response to incubation with 100nM Gemcitabine (Figure 42), the minimum amount to kill these mouse pancreatic cancer cells in 5 days in vitro, as determined by SRB assay (Figure 43). Conversely, at 500nM Gemcitabine, induction of HNF4α expression was less robust than at 100nM, probably due to accelerated cytotoxic effects over the 16 hr incubation period.

Figure 41

(A)

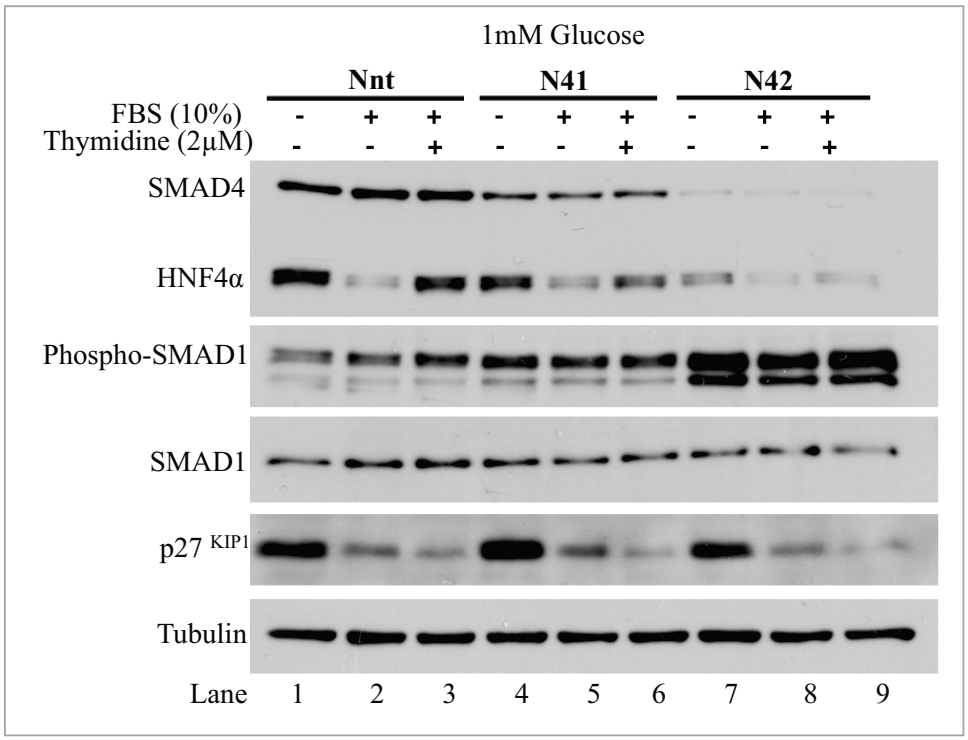

(B)

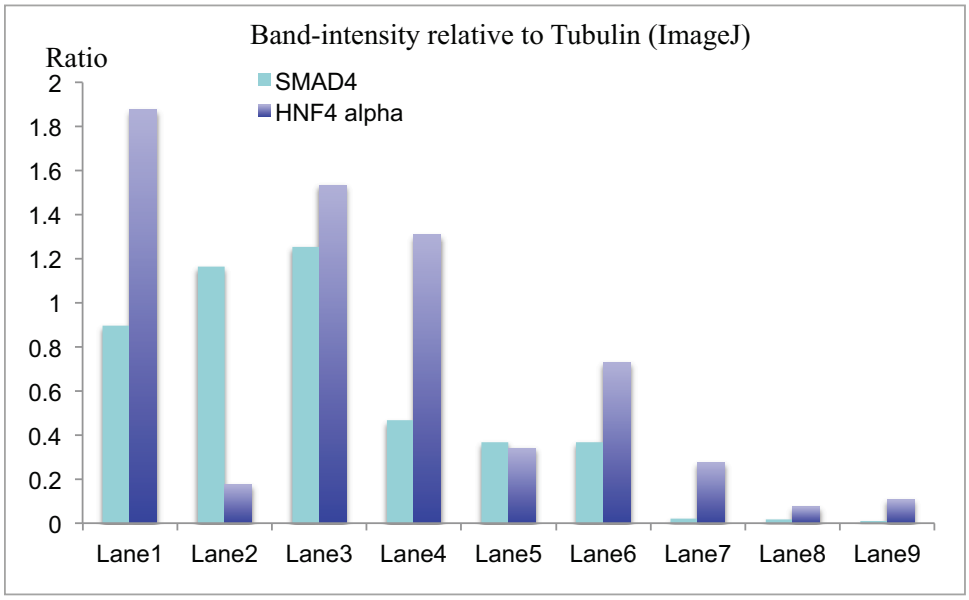

Figure 41 (A) – Immunoblot analysis of changes in HNF4α levels in response to thymidine block at 1mM glucose, in cell sub-clone N infected by non-targeting shRNA (Nnt) and that infected by SMAD4-knockdown shRNAs (N41, N42). **Condition:** Cells were seeded on Day0 in normal DMEM with 10% serum, then on Day1, washed twice with PBS, and replaced with 1mM glucose DMEM serum free medium, plus the treatments as shown above, and incubated for 16 hr before harvest. **(B)** – Quantification of the immunoblot in (A), relative to Actin levels, using ImageJ.

Figure 42

(A)

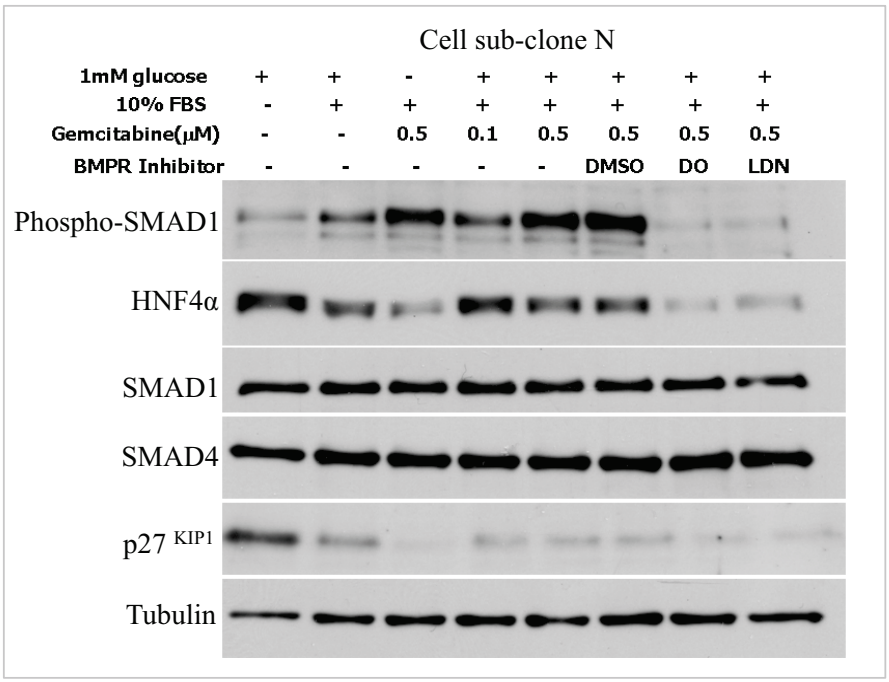

(B)

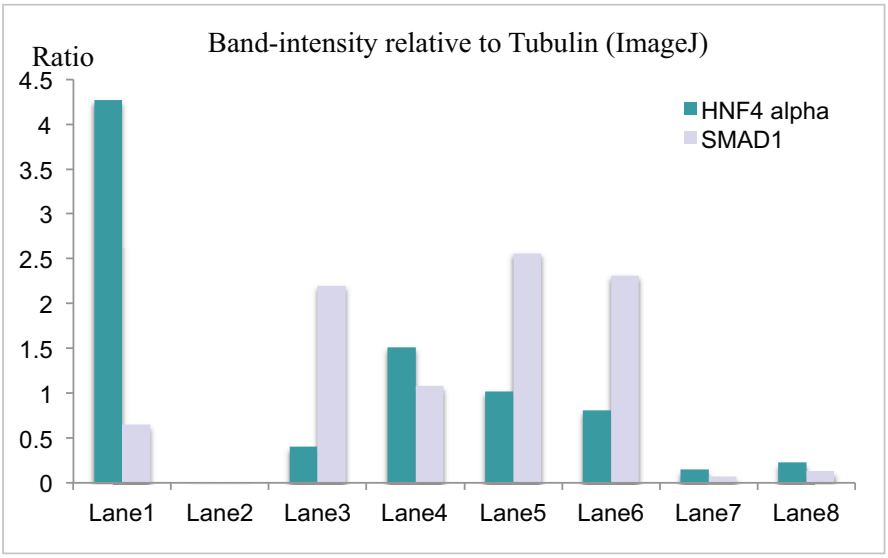

Figure 42 (A) - Immunoblot analysis of changes in HNF4α levels in response to 100nM and 500nM Gemcitabine, and in the presence or absence of BMP receptor-inhibitors. **Condition:** Cells were seeded on Day0 in normal DMEM with 10% serum, then on Day1, washed twice with PBS and replaced with 1mM glucose DMEM serum free medium, plus the treatments as shown above, and incubated for 16 hr before harvest. **(B) –** Quantification of the immunoblot in (A), relative to Tubulin levels, using ImageJ.

Figure 43

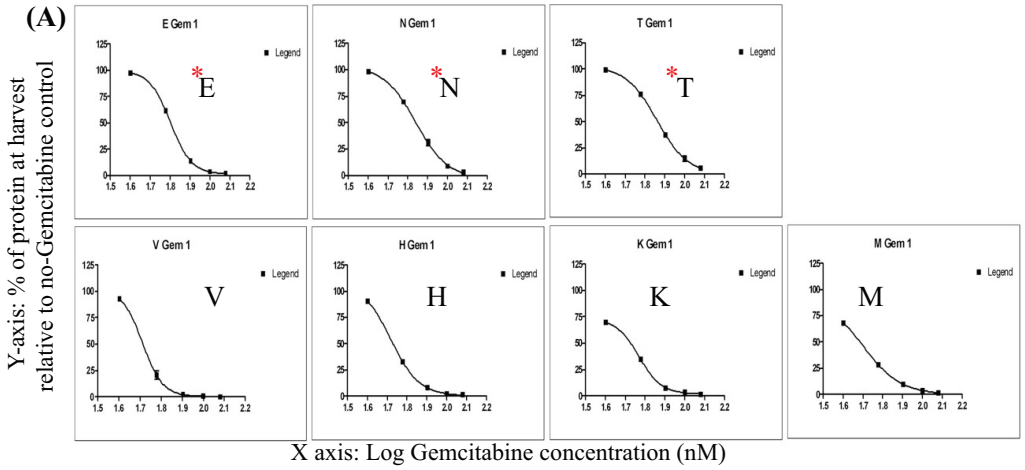

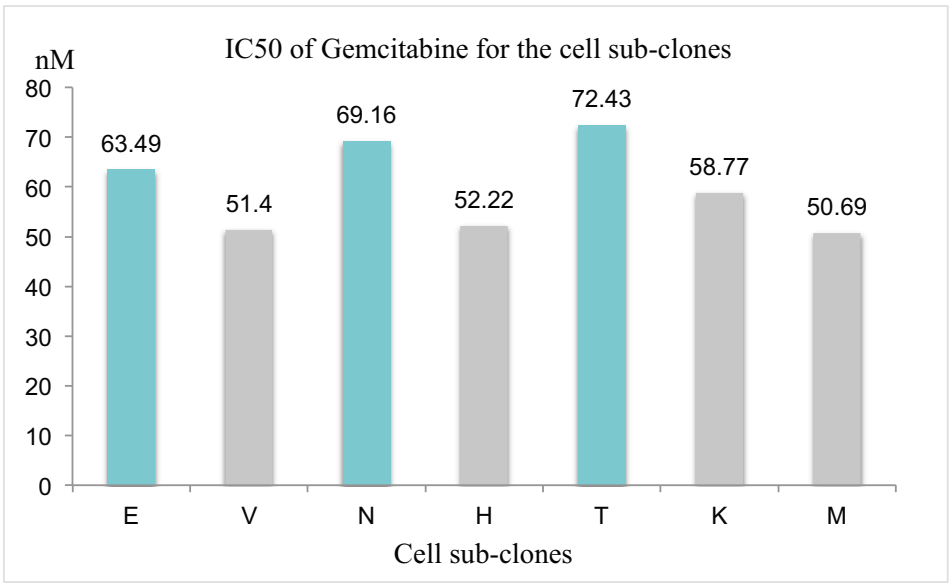

Figure 43 (A) – The "kill curve" by Gemcitabine of each of the seven cell sub-clones, measured by SRB assay, over a 5-day incubation period with a range of Gemcitabine concentration at 10, 20, 40, 80, or 100nM. **(B)** – Showing the seven sub-clones' IC50, the concentration of Gemcitabine needed to reduce cell population to half of that of the control, which was treated with only PBS. IC50 calculation was performed by using Prism software; please note that sub-clones K and M were sensitive to Gemcitabine even at 10nM, so the IC50 value of them were not accurate.

Hence, a titration experiment will be required to determine an optimal concentration (between 100nM to 500nM) of Gemcitabine that would cause maximal induction of HNF4α expression in these mouse pancreatic cancer cells over 16 hr incubation. Furthermore, Gemcitabine-induced HNF4α expression could be suppressed by both Dorsomorphin and LDN193189, and this was also true in thymidine blocked sub-clone N (data not shown), suggesting that HNF4α was upregulated downstream of the BMP pathway while under replicative stress.

I also compared the sensitivity to Gemcitabine of all seven mouse pancreatic cancer cell sub-clones, using SRB assay. Notably, in standard DMEM at 25mM glucose with 10% serum, the three HNF4α-expressing cell sub-clones E, N and T, had a moderately higher IC50 of Gemcitabine than the other cell sub-clones, suggesting that the BMP-SMAD1/SMAD4-HNF4α pathway might have offered survival advantage in coping with cell cycle blockage and apoptosis caused by Gemcitabine. Owing to time limit within the scope of the project, I was unable to further investigate into this potential relationship. Especially, I would need to optimise a condition for cells to proliferate in serum medium at 1mM glucose for a long enough period of time, in order to observe cytotoxic effects induced by Gemcitabine.

To sum up with the new information described above, the BMP-SMAD1/SMAD4-HNF4α pathway can be activated by replicative stress caused by Gemcitabine or excess thymidine, which blocked DNA replication at the G1-S phase. However, HNF4α levels during "thymidine- or Gemcitabine-block" of cells were essentially lower than that when cells were serum starved. This may be because serum starvation induced both metabolic and replicative stress to the cells, while thymidine block induced replicative stress only.

In addition, HNF4α could also be upregulated in proliferating cells by high glucose concentration (25mM), and this implies a potential role of oxidative stress in HNF4α expression. However, since 25mM glucose is much higher than the physiological concentration range of 1-to-5 mM, other methods should be used to induce oxidative stress in proliferating cells in serum-medium at 1mM glucose (this will be discussed in the Discussion).

3.4.9 HNF4α is overexpressed in early PanIN lesions

Consistent with what is published in the literature, HNF4α is widely expressed in the normal pancreas in mouse. Immunohistochemical staining of murine pancreatic tumour sections, from which the heterogeneous cell sub-clones were derived, revealed that HNF4α was overexpressed in epithelial tumour cells, but not in stromal cells (Figure 44). In some less well-differentiated tumour regions, cells having positive nuclear HNF4α staining co-existed with cells not having nuclear HNF4α staining in a woven-like pattern, indicating possible dissociation and invasion of tumour cells into the surrounding stroma (Figure 44E). Results from staining HNF4α in sections of *Pdx1*-Cre/ $Kras^{G12D/+}$ mice indicated that HNF4α was already overexpressed in early PanIN lesions induced by mutant KRas. Five out of five pancreatic tumours from *Pdx1*-Cre/ $Kras^{G12D/+}$ mice show readily detectable HNF4α staining, and nuclear staining of SMAD4 was also observed in all corresponding lesions (Figure 45). Mutant p53 was not required for upregulation of HNF4α, as knockdown of mutant p53 in cell sub-clone N did not obviously affect HNF4α levels.

Likewise, HNF4α was overexpressed in epithelial neoplasia and tumours in human pancreatic caner sections, but not in stromal cells, in 8 out of 8 cases examined (Figure 46). Unlike in the mouse model with both mutant KRas and mutant p53, HNF4α staining was not observed in any of the less well-differentiated regions in human pancreatic cancer sections. This may be due to the fact that transgenic mice are homogenously bearing the $p53^{R172H}$ mutant, which is known to have caused properties associated with invasion and metastasis. However, in human pancreatic cancer, there are a lot more variations among patients; p53 may have been lost, or mutated, but not necessarily at codon-175.

Unsurprisingly, staining of SMAD4 in consecutive sections of human pancreatic cancers revealed more diverged genetic differences between human cancers and the Pdx1 mouse model. Around 50% cases demonstrated the co-presence of both SMAD4 and HNF4α in epithelial tumour cells (Figure 46), while the 50% cases had lost SMAD4, despite HNF4α being expressed (Figure 47). In one case, SMAD4 was present in only some forms of the HNF4α-positive tumours or lesions, indicating that overexpression of HNF4α in human pancreatic cancer may be subjected to different upstream regulations. This idea may be further supported by the fact that two human colorectal cancer cell lines, HT-29 and SW480, expressed HNF4α even though SMAD4 is lost. In addition, Dorsomorphin only partly

Figure 44

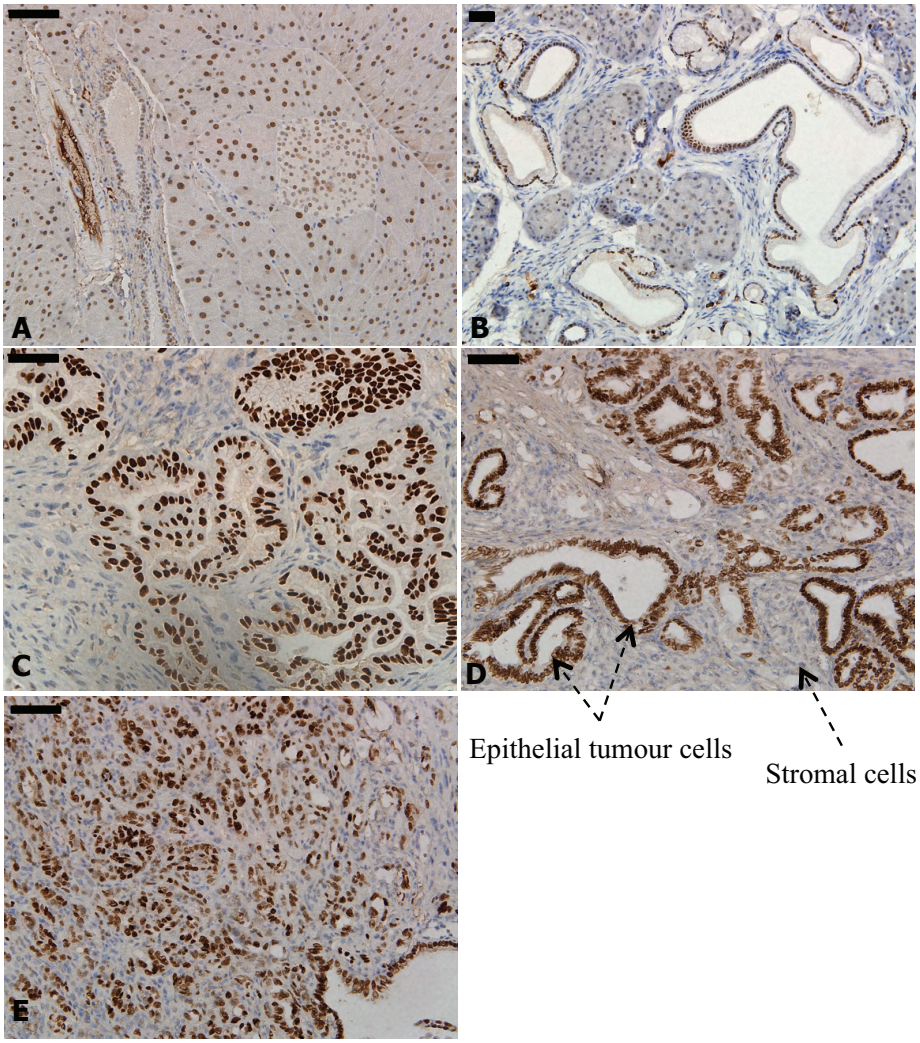

Scale bar = 50 μm

* D and E are sections of the tumour (*Pdx1*-Cre; *LSL-Kras*^{G12D}*; LSL-Tp53*^{R172H}) from the mouse where the seven sub-clones were derived.

Figure 44 - Immunohistochemistry of HNF4α on mouse pancreatic sections, photographs were taken using the 20x objective lens, except for (B) which was taken using the 10x objective lens. **(A)** - Normal pancreas of a 12-week old adult mouse. **(B) -** Low grade PanINs observed in a *Pdx1*-Cre; *LSL-Kras*^{G12D} mouse. **(C)** - High grade PanINs / tumours (*Pdx1*-Cre; *LSL-Kras*^{G12D}) **(D)**- Tumours (*Pdx1*-Cre; *LSL-Kras*^{G12D}*; LSL-Tp53*^{R172H}). **(E)** Poorly differentiated regions in the tumour (*Pdx1*-Cre; *LSL-Kras*^{G12D}*; LSL-Tp53*^{R172H}) .

Figure 45

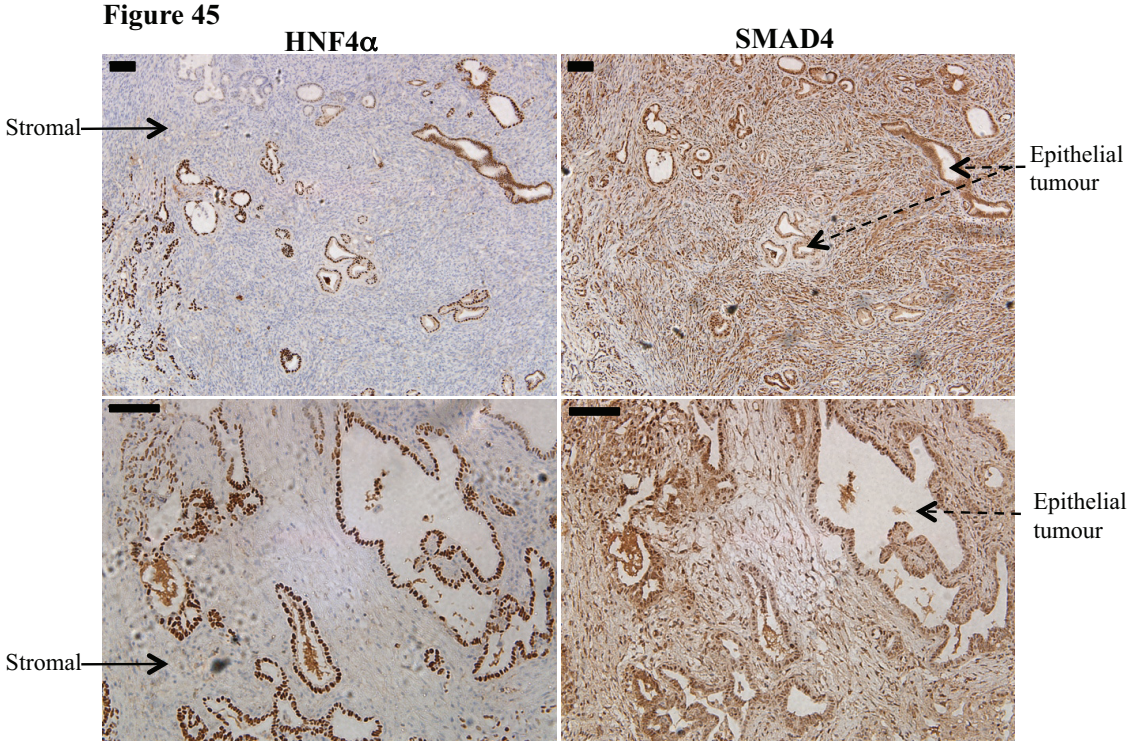

Scale bar = 50 μm

Figure 45 - Immunohistochemistry of SMAD4 and HNF4α on consecutive paraffin sections of mouse pancreatic cancer. Co-localization was found in 5 out of 5 *Pdx1*-Cre*; LSL-Kras*^{G12D} mice. The pair of photographs on the top row were taken using the 10x objective lens, while the pair at the bottom were taken using the 20x objective.

Figure 46

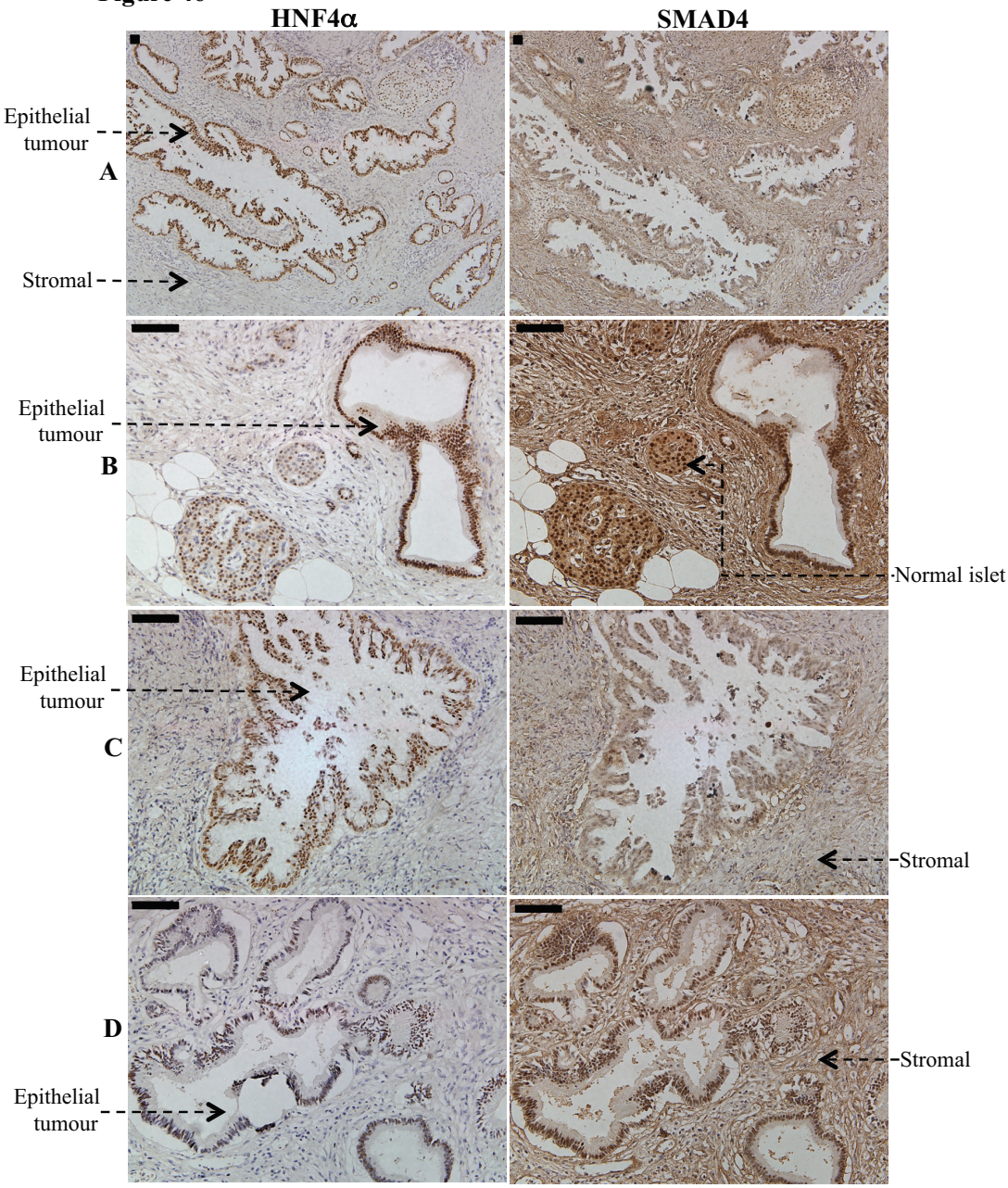

Scale bar = 50 µm

Figure 46 - Immunohistochemistry of SMAD4 and HNF4α on consecutive sections of human pancreatic adenocarcinoma (4 of the 8 cases that show co-localization of SMAD4 and HNF4α). **(A)**: UB05-11932-1E **(B)** UB04-17103-1d **(C)** UB05-11932-1E `**(D)** UB05-18166-1O. Photographs were taken using the 20x objective lens, except for (A) which was taken using the 4x objective lens.

Figure 47

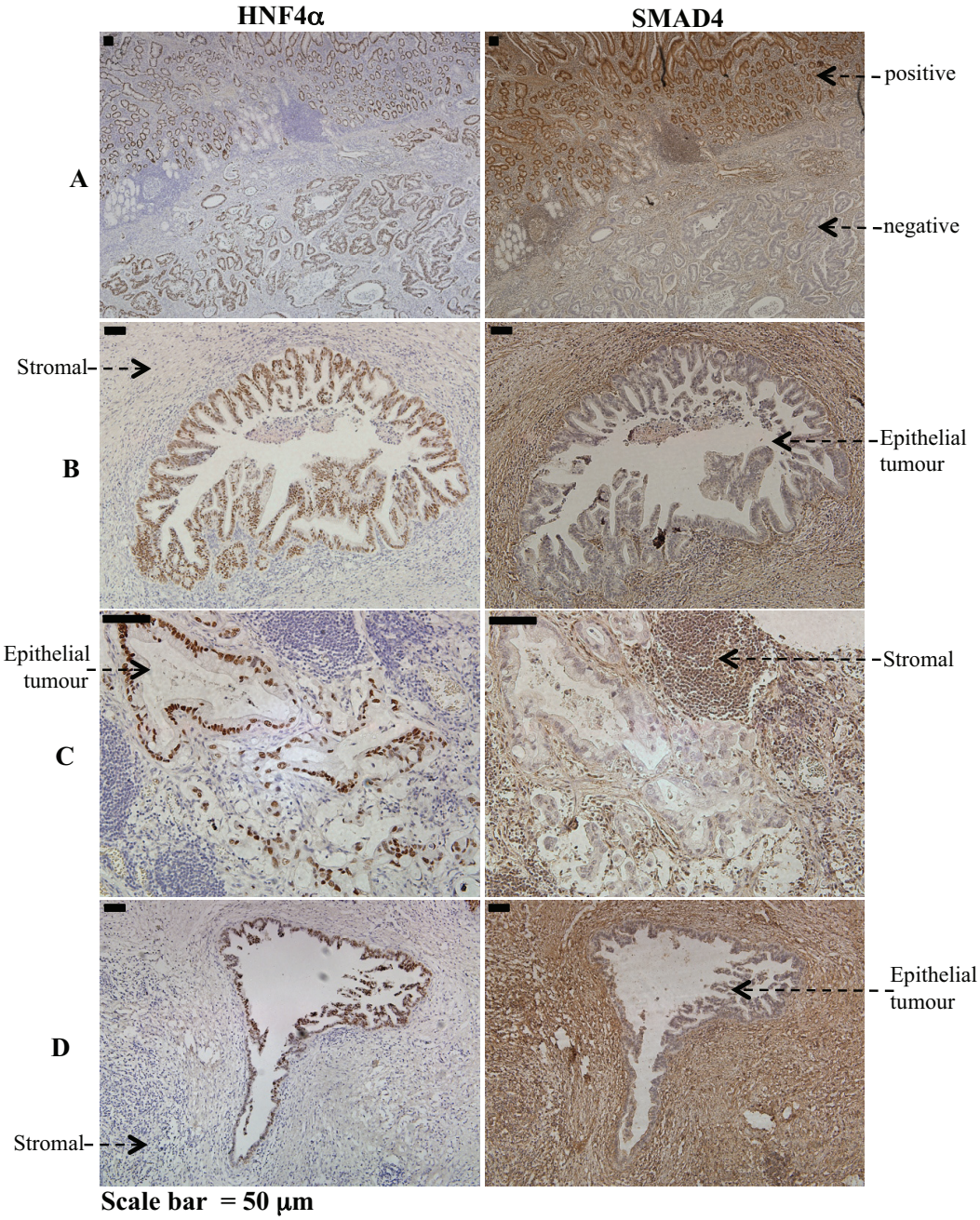

Figure 47, Immunohistochemistry of SMAD4 and HNF4α on consecutive sections of human pancreatic adenocarcinoma (another 4 of the 8 cases that show positive HNF4α but negative SMAD4 staining). ECMC patient sample number **(A):** UB06-1467-1J **(B):** UB05-21131 **(C):** UB05-21131-1P, **(D):** UB05-18166-1O. Photographs (A) were taken using the 4x objective lens; (B) and (D) were taken using the 10x objective lens; (C) was taken using the 20x objective lens.

suppressed HNF4α expression in three other SMAD4-intact cell lines tested (A549, lung carcinoma; HepG2, hepatocarcinoma; Caco2, colorectal cancer) (Figure 48). This was in contrast to the mouse pancreatic cancer cell sub-clones, which showed near complete absence of HNF4α upon Dorsomorphin treatment (Figure 34A).

To sum up, overexpression of HNF4α was an early event during the formation of pancreatic lesions as a consequence of $KRas^{G12D}$ mutation. HNF4α continued to be irregularly expressed in epithelial cells throughout the progression from early PanINs to higher grade PanINs, and eventually to pancreatic adenocarcinomas. HNF4α was also overexpressed in human pancreatic cancer, but in contrast to the mouse model, SMAD4 was not necessarily present, indicating that in human pancreatic cancer, there are likely additional regulatory levels of HNF4α expression, as well as more complicated genetic aberrations during carcinogenesis. This is further supported by the observation that, in a series of human cancer cell lines endogenously expressing HNF4α, Dorsomorphin downregulated HNF4α only in some of the these cell lines, whereas Dorsomorphin can downregulate HNF4α levels in all three E, N and T murine pancreatic sub-clones.

3.4.10 HNF4α was dispensable for proliferation in standard DMEM with serum

In order to find out the biological function of HNF4α and the BMP pathway in these mouse pancreatic tumour cells, HNF4α was stably knocked down by three individual viral shRNAs (Figure 49). Comparing with the non-targeting shRNA controls, all three HNF4α-positive cell sub-clones E, N and T, upon knockdown of HNF4α, did not show obvious changes in proliferation rate in complete medium (Figure 49). Owing to limited time towards the end of my studentship, I could not further investigate whether or not HNF4α played a role in cell proliferation of sub-clones E, N and T under more physiologically relevant glucose conditions, such as 1mM and 5mM.

3.4.11 HNF4α expressing cells appear more tolerant to stress under low glucose condition

Because of the roles of HNF4α in controlling glucose metabolism, I asked whether or not HNF4α-positive tumour cells were more resistant to hypoglycaemic conditions in the absence of exogenous serum growth factors. Of interest, cell sub-clone N could maintain a

Figure 48

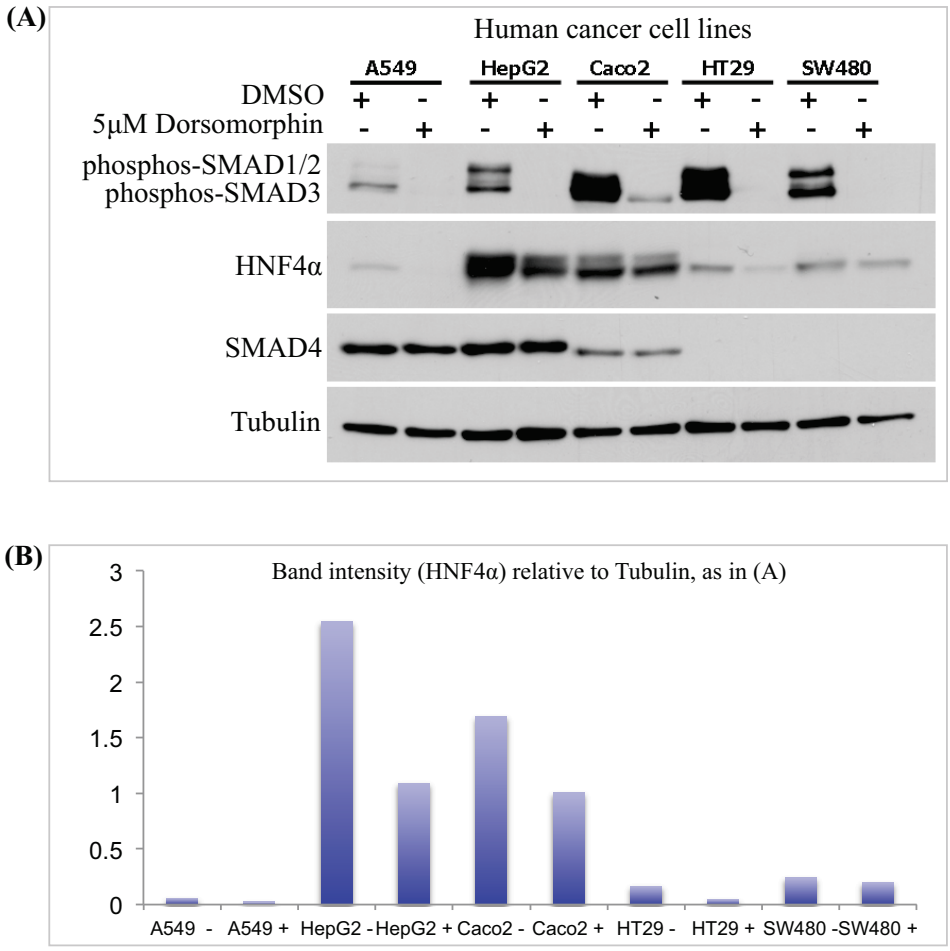

Figure 48 (A) – Immunoblot analysis of changes in HNF4α levels, in response to 5μM Dorsomorphin, of five established human cancer cell lines that express HNF4α, respectively, A549 (lung cancer), HepG2 (hepatocarcinoma), Caco2, HT29, and SW480 (colorectal cancer). **Condition:** Cells were seeded on Day0 in normal DMEM with 10% serum, then on Day1, replaced with the same but fresh serum medium with 5μM Dorsomorphin or DMSO, and incubated for 16 hr before harvest **(B)** – Quantification of the immunoblot in (A), relative to Tubulin levels, using ImageJ.

Figure 49

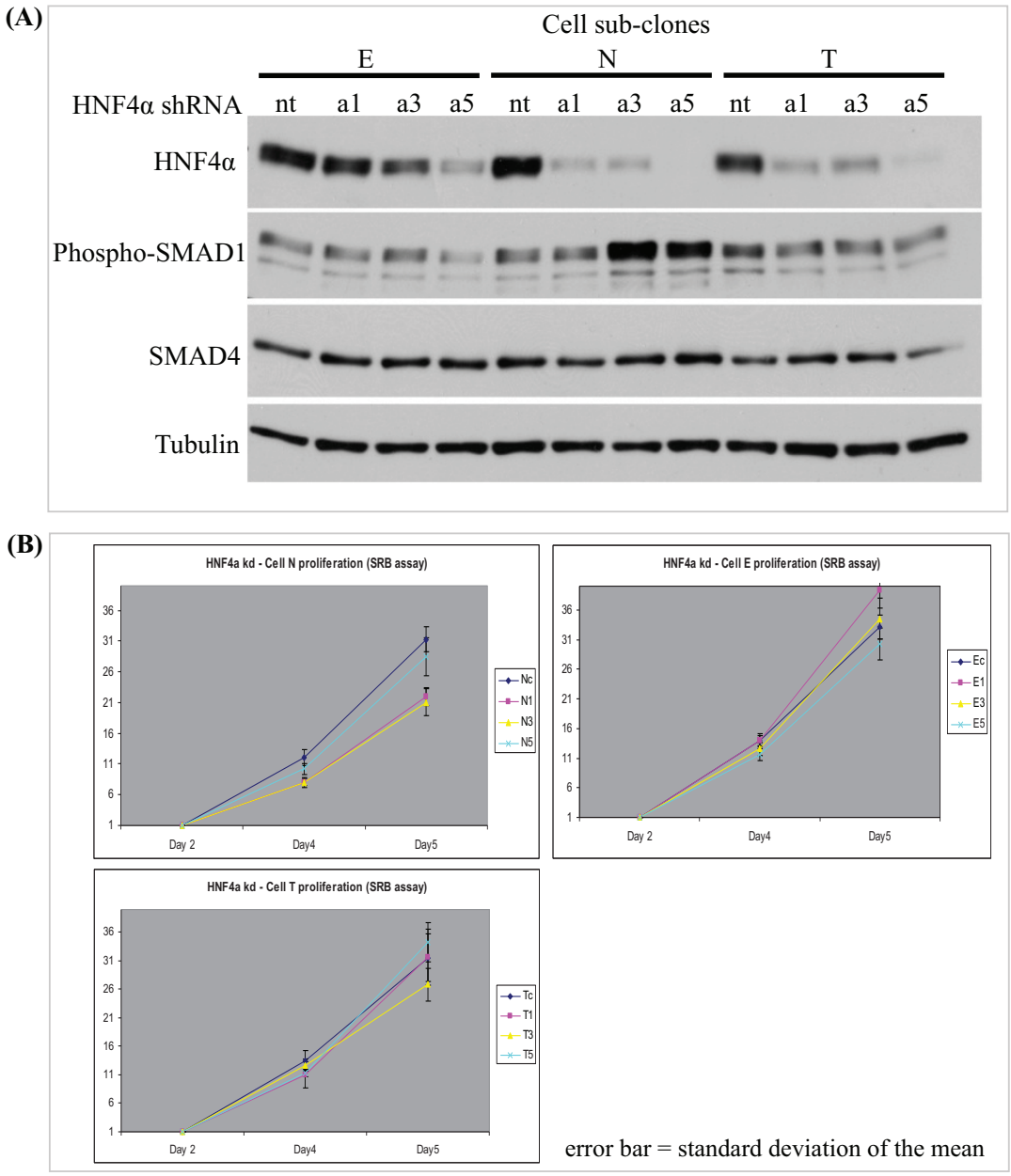

Figure 49 (A) – Immunoblot analysis of knocking-down HNF4α in sub-clones E, N and T, using three individual viral shRNAs (a1, a3, a5), along with the control cells infected with non-targeting shRNA (nt). **(B) –** SRB proliferation assay of the HNF4α-knocked-down sub-clones, over 5 days in normal DMEM with 10% serum. **Condition:** on Day0, 500 cells were seeded onto each well of a 96-well plate, repeated for 6 wells per knockdown/control, and setting up three identically seeded plates for harvesting protein (fixing cells for SRB staining) on Day2, Day4 and Day5.

"healthy", unstressed morphology for at least 2 days in 1mM glucose containing DMEM, showing little difference from that in 25mM glucose DMEM; except that the cell density became higher in 25mM glucose (Figure 50). This suggested that higher glucose concentration resulted in more cell proliferation over two days.

In contrast, cell sub-clones V and H did not appear to be able to tolerate a low 1mM glucose concentration, as they displayed a "stressed" morphology, and many detached from the displayed culture dish (Figure 51, 52). However, V and H remained typical in morphology and confluency in 25mM glucose, suggesting that glucose was more likely the determinant of viability. Hence the HNF4α-positive cell sub-clone N was more tolerant to low glucose conditions than HNF4α-negative cell subclones, such as V and H. Recombinant BMP9 neither relieved the "stress" morphology of V and H nor induced any changes in the morphology of N, suggesting that although BMP9 could trigger phospho-SMAD1/5/8 responses in V and H, this was insufficient to provide support for their survival under hypoglycaemic conditions.

To test whether or not HNF4α conferred sub-clone cell N with its ability to survive under low glucose conditions, I treated the cells with recombinant mouse TGFβ1, which I previously showed that it inhibited phosphorylation of SMAD1/5 and HNF4α expression (back in Figure 37C). Cell sub-clones E, N and T responded to recombinant mouse TGFβ1 with an apparently "stressed" morphology (Figure 53). In contrast, V and H, in which there was intrinsic phosphorylation of SMAD2 and SMAD3, only showed modest morphological changes in response to recombinant mouse TGFβ1 (Figure 54). As a control, I added SB-431542, a TGFβ type-1 receptor inhibitor, and this relieved the "stress" morphology induced by recombinant mouse TGFβ1 on cell sub-clones E, N and T, and the inhibitor did restore phosphorylation of SMAD1 and HNF4α as shown on immunoblots (Figure 53). As for the two phospho-SMAD1 expressing but HNF4α-low or negative cell sub-clones, K and M, they appeared stressed and more spindly-like (Figure 55), but not as severely as that was observed in cell sub-clones E, N and T.

To sum up, the BMP-SMAD1/SMAD4-HNF4α pathway appeared to be important for cell sub-clones E, N and T to survive and proliferate (with usual morphology) under low glucose

Figure 50

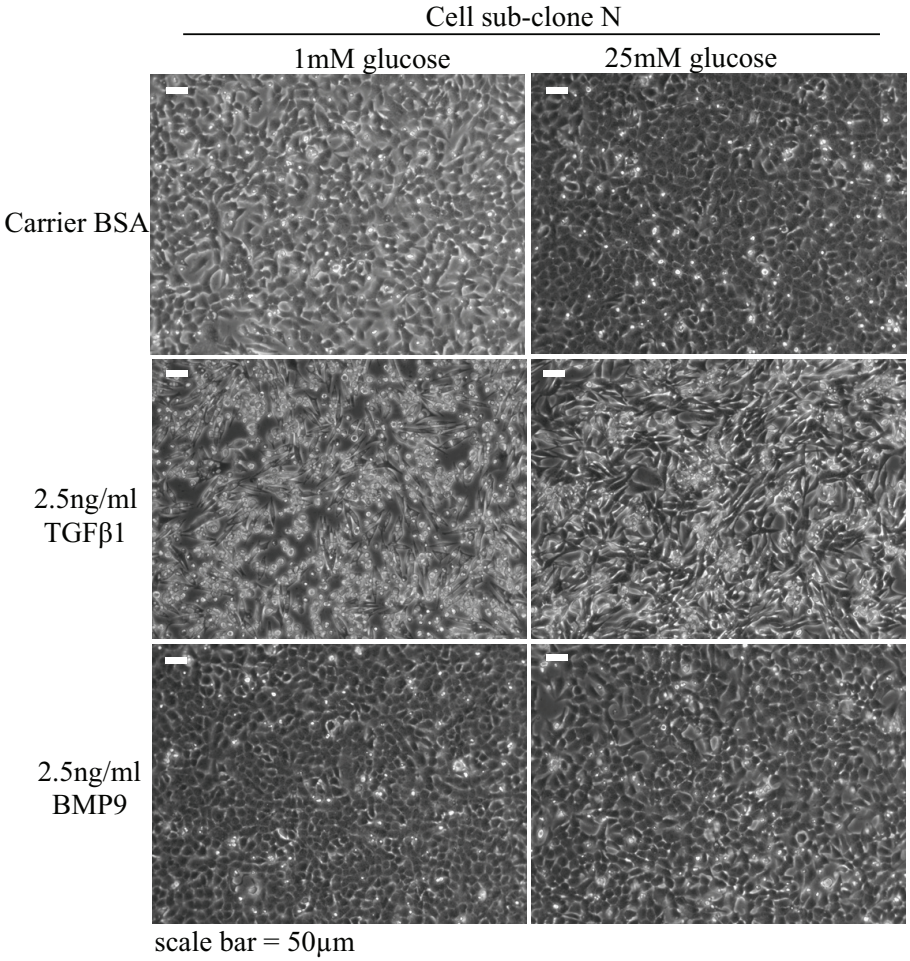

Figure 50 - Phase contrast photographs (taken with a 10x objective lens) showing the morphologies of sub-clone N upon treatment with recombinant mouse BMP9 or with recombinant mouse TGFβ1 for 48 hr. **Condition:** cells were seeded in normal DMEM with 10% serum on Day0; then on Day1, cells were washed with PBS twice and replaced with normal DMEM or 1mM glucose-DMEM, serum free, plus respective treatments as shown above. Photographs were taken on Day3.

Figure 51

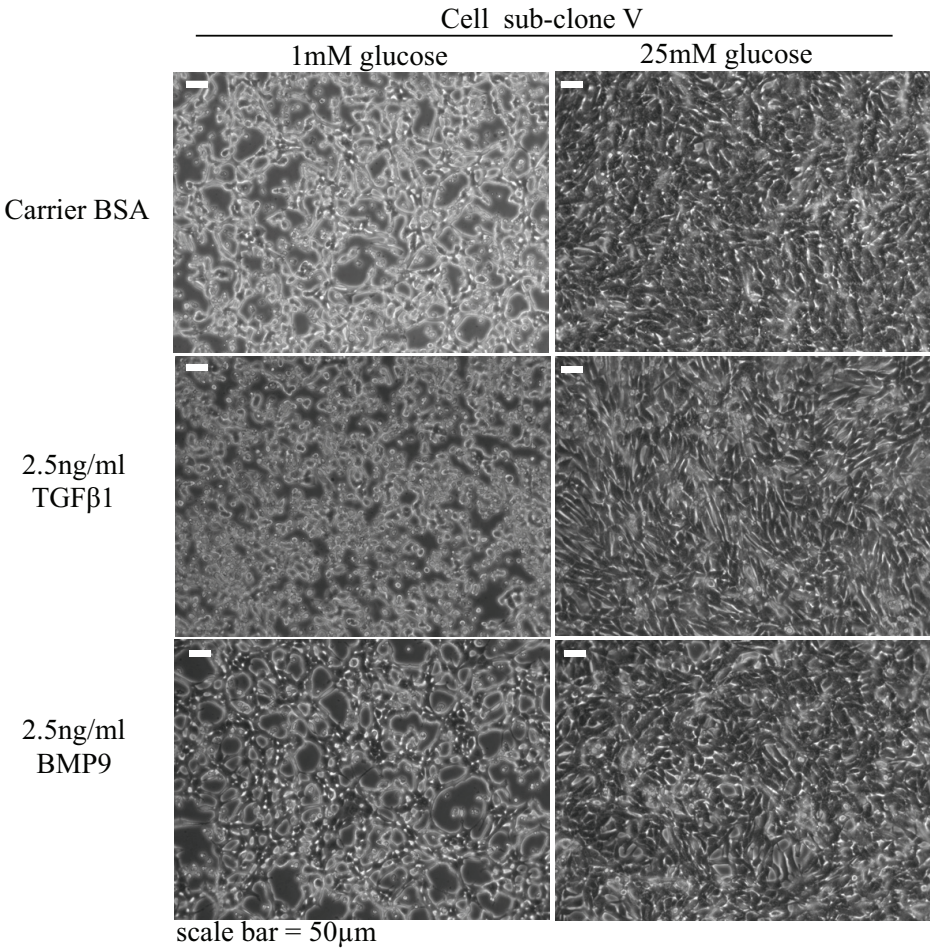

Figure 51 - Phase contrast photographs (taken with a 10x objective lens) showing the morphologies of sub-clone V upon treatment with recombinant mouse BMP9 or with recombinant mouse TGFβ1 for 48 hrs. **Condition:** cells were seeded in normal DMEM with 10% serum on Day0; then on Day1, cells were washed with PBS twice and replaced with normal DMEM or 1mM glucose-DMEM, serum free, plus respective treatments as shown above. Photographs were taken on Day3.

Figure 52

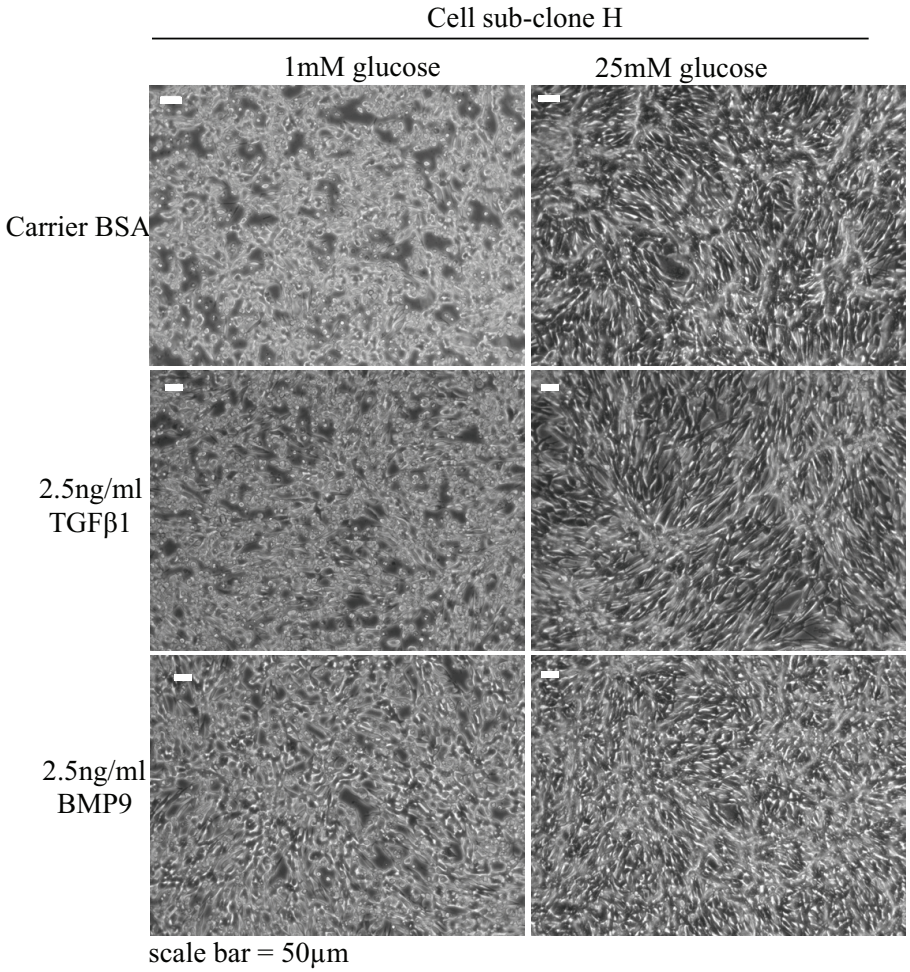

Figure 52 - Phase contrast photographs (taken with a 10x objective lens) showing the morphologies of sub-clone H upon treatment with recombinant mouse BMP9 or with recombinant mouse TGFβ1 for 48 hrs. **Condition:** cells were seeded in normal DMEM with 10% serum on Day0; then on Day1, cells were washed with PBS twice and replaced with normal DMEM or 1mM glucose-DMEM, serum free, plus respective treatments as shown above. Photographs were taken on Day3.

Figure 53

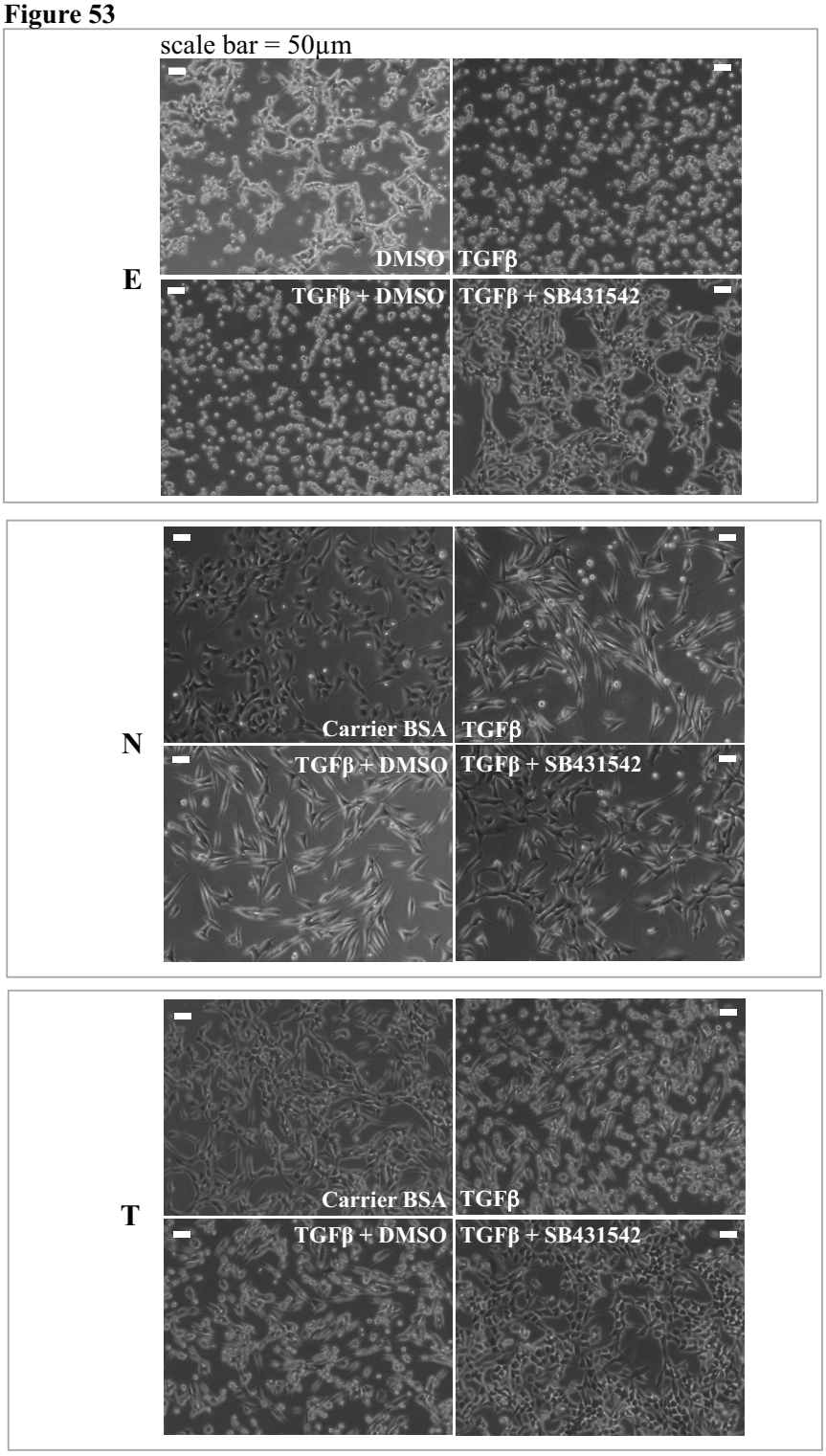

Figure 53 -Phase contrast photographs (taken with a 10x objective lens) showing the morphologies of sub-clones E, N and T incubated in 1mM Glucose DMEM, serum free. **Condition:** cells were seeded in normal DMEM with 10% serum on Day0; then on Day1, cells were washed with PBS twice and replaced with 1mM glucose-DMEM, serum free, plus respective treatments (2.5ng/ml mouse recombinant TGFβ, 5µM SB431542). Photographs were taken on Day3.

Figure 54

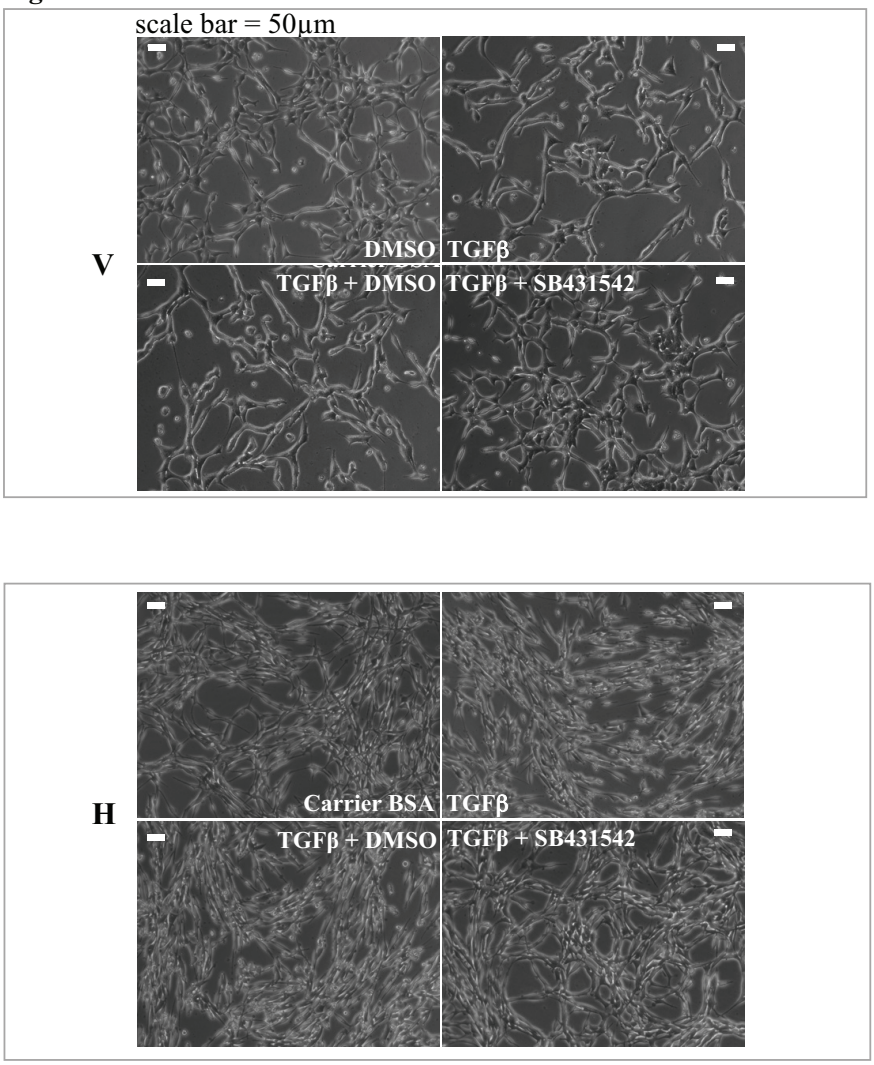

Figure 54 - Phase contrast photographs (taken with a 10x objective lens) showing the morphologies of sub-clones V and H incubated in 1mM Glucose DMEM, serum free. **Condition:** cells were seeded in normal DMEM with 10% serum on Day0; then on Day1, cells were washed with PBS twice and replaced with 1mM glucose-DMEM, serum free, plus respective treatments as shown above (2.5 ng/ml mouse recombinant TGFβ, 5µM SB431542). Photographs were taken on Day3.

Figure 55

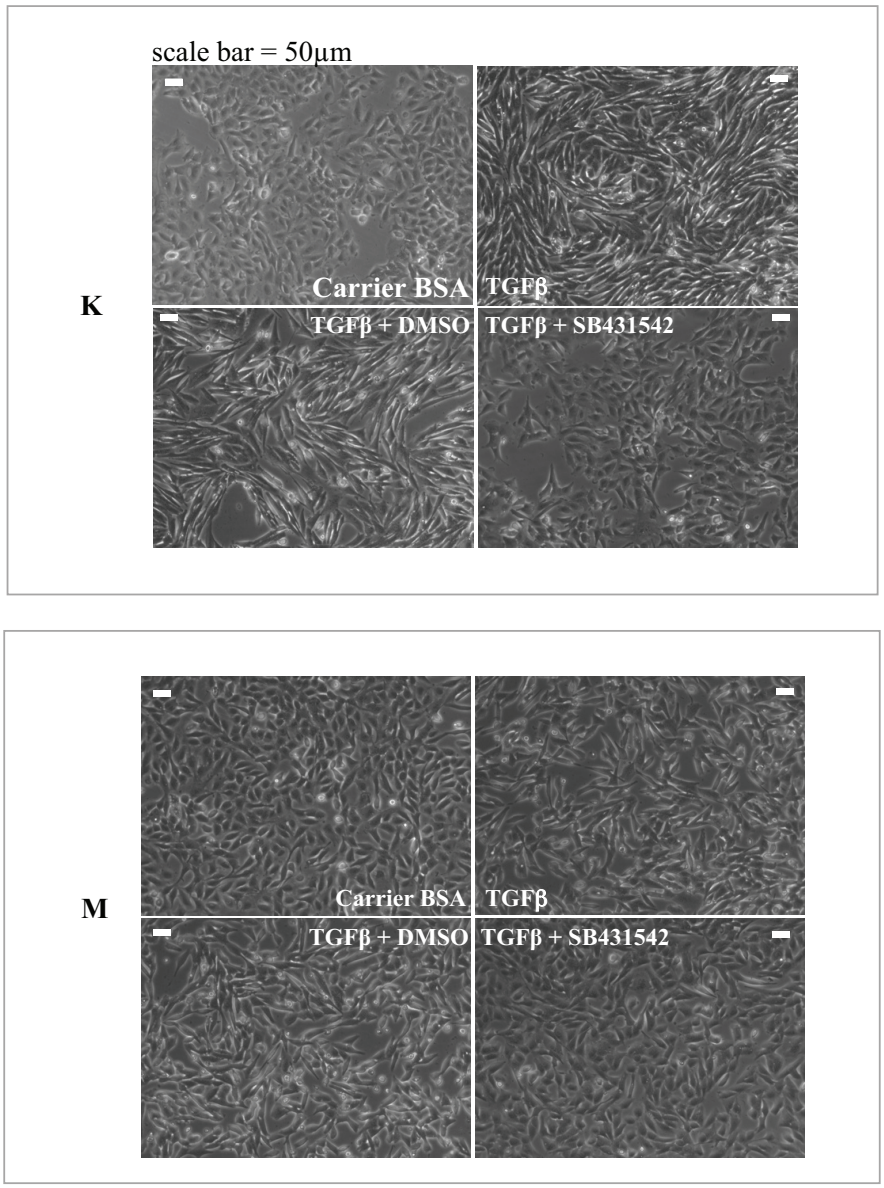

Figure 55 – Phase contrast photographs (taken with a 10x objective lens) showing the morphologies of sub-clones K and M incubated in 1mM Glucose DMEM, serum free. **Condition:** cells were seeded in normal DMEM with 10% serum on Day0; then on Day1, cells were washed with PBS twice and replaced with 1mM glucose-DMEM, serum free, plus respective treatments as shown above (2.5 ng/ml mouse recombinant TGFβ, 5µM SB431542). Photographs were taken on Day3.

and serum-deprived conditions, implying that HNF4α may play a role in survival or maintenance of a subset of pancreatic tumour cells.

3.4.12 Summary of the novel SMAD4-HNF4α pathway

HNF4α was expressed at a basal level in many cells of the normal pancreas, but was overexpressed in a subset of neoplastic cells as early as in PanIN lesions during tumorigenesis induced by mutant $KRas^{G12D}$ alone or by the presence of both mutant $KRas^{G12D}$ and mutant $p53^{R172H}$. HNF4α expression in cultured mouse pancreatic cancer cells was directly downstream of the BMP pathway, as knockdown of SMAD4 or SMAD1 in mouse pancreatic cancer cells shows correspondingly decreased HNF4α levels. Notably, this pathway has been indirectly indicated by two previous studies using knockout mouse embryos (Sirard et al., 1998; Gu et al., 1999, discussed in Introduction 1.6.2).

This SMAD4-HNF4α pathway was cell autonomous and required the presence of at least 1mM glucose (at the point of cell seeding). In proliferating cells, HNF4α appeared to be progressively increased to a peak level, then gradually decreased to nil within a particular time frame in the cell cycle. Once HNF4α reached its peak level in the nucleus, an unknown, glucose-independent pathway rapidly and transiently stabilized HNF4α, before HNF4α levels went downhill. On the other hand, in cells being blocked from cell cycle progression, the SMAD4-HNF4α pathway could be upregulated as long as stress persists, including metabolic stress under serum starvation, which was marked by expression of $p27^{KIP1}$, and replicative stress, which resulted from blockage of DNA replication by thymidine or by Gemcitabine.

Treatment with recombinant BMP9 induced HNF4α expression, while recombinant TGFβ1 inhibited HNF4α and induced SMAD3 phosphorylation. This suggests that BMP-and TGFβ-mediated pathways played a counteracting role in controlling expression of HNF4α. Loss of HNF4α expression upon TGFβ1 treatment causes an apparently stressed-phenotype in cell sub-clones E, N and T under serum starvation, but not in control conditions. Along with HNF4α's well documented roles in mediating glucose metabolism, these data suggest that HNF4α may promote the survival of cell sub-clones E, N and T when glucose is low and growth factors are scarce in the hypoxic intra-tumour environment of pancreatic adenocarcinoma.

When the BMP pathway was inhibited by Dorsomorphin (which suppresses ALK2, 3, 6) in sub-clone E, phospho-SMAD3 levels increased sharply (Figure 34A). This suggests that activated BMPR1 (ALK2, 3, 6) may have an inhibitory effect on TGF β R1 (ALK4, 5, 7)'s serine/threonine kinase activity, which was relieved upon inhibition by Dorsomorphin. Alternatively, activation of the BMP pathway may have suppressed the expression of TGF β receptor kinases that phosphorylate SMAD3. In contrast, sub-clones N and T did not appear to share a similar mechanism of flipping between phospho-SMAD1 and phospho-SMAD3.

In fact, under 1mM glucose DMEM with 10% serum, all seven sub-clones showed strong phosphorylation of the BMP-SMADs (1/5/8), but not TGF β -SMADs (2/3), as shown in Figure 37B and 38. Only under artificially high 25mM glucose DMEM with 10% serum, could we see phosphorylation of TGF β -SMADs (2/3), as in Figure 31. These suggest that when mouse pancreatic cancer cells were under 1mM glucose DMEM, and exposed to both TGF β and BMP ligands in serum, the BMP pathway was preferentially activated. When glucose was high at 25mM, phosphorylation of TGF β -SMADs (2/3) started increase in sub-clones V and H (Figure 31), which were their intrinsic "preferred pathway" in the absence of serum (Figure 37B). So there are a pair of competitive mechanisms in which glucose boost the cells' intrinsic pathway, in a glucose concentration-dependent manner; while growth factors in serum tend to divert the cells to activate the BMP pathway.

4 DISCUSSION

4.1 On clonal heterogeneity and origin of cancer cells

As a supplement to Introduction Chapter 1.8, nevertheless, it is important to note that isolation of the cell sub-clones does not indicate whether they were of monoclonal or polyclonal origin, or transformed through clonal evolution; they could have evolved during primary culture *in vitro*, too. Since most if not all normal pancreatic cells are subjected to express $Kras^{G12D}$ and $p53^{R172H}$ under *Pdx1*-CRE, pancreatic cancers in this mouse model are more likely to be of polyclonal origin. This also formed the basis of my project trying to identify heterogeneous cancer cell populations, and their molecular markers and properties.

With the use of the Estrogen Receptor (ER)/Tamoxifen system, as well as fluorescent proteins, perhaps in the future more lineage genes will be examined for the types of pancreatic cells that are susceptible to transformation by mutant $Kras^{G12D}$. For example, somatostatin, glucagon, pancreatic polypeptide, and gherlin, which mark their corresponding pancreatic cell types, as shown in Figure 10. If time was sufficient during the course of my project, karyotyping of chromosomes may also reveal more of the similarities and differences between the sub-clones, and if any of them retain some markers of their lineage origin. This may answer, for example, whether sub-clones E, N and T were evolved from the same particular normal pancreatic compartment, and sub-clones V and H from another.

4.2 Common features among subgroups of heterogeneous cell sub-clones

HNF4α was expressed only in cell sub-clones E, N and T, which had intrinsic phospho-SMAD1. In contrast, two of the HNF4α-negative cell sub-clones V and H, had intrinsic phospho-SMAD2 and phospho-SMAD3. Such diversity implied two groups of cells respectively sharing common features, possibly evolved from two different 'lineages' in the normal pancreas during tumorigenesis driven by $Kras^{G12D}$ and $p53^{R172H}$.

In particular, both V and H transcribed the *Gata6* gene (detected by QRT-PCR) and the WNT5A protein. GATA6 expression has been reported to suppress HNF4α expression in the developing mouse embryo (Morrisey et al., 1998). Interestingly, cell sub-clone K had both BMP- and TGFβ-mediated phospho-SMADs and it weakly expressed HNF4α.

Although cell sub-clone M had intrinsic phospho-SMAD1, it did not express HNF4α, suggesting that additional pathways, genetic or epigenetic factors were required for the *Hnf4α* gene transcription. This strengthens the idea that cell sub-clones E, N and T share more common genetic characteristics with one another.

In view of this, it would be of interest to examine whether cell sub-clones E, N, and T, or the other subgroup of V and H, share common chromosome alterations. It would also be of interest if time allowed me to conduct immunohistochemistry with phospho-Smad2 and Phospho-Smad1/5/8 antibodies, and to see how these two cell types are distributed in the normal pancreas and in the original tumour sections. Because these would visualise in which pancreatic compartments or neoplastic lesions are the two groups of cells located, and hence the populations of cells that are susceptible to $Kras^{G12D}$-induced transformation.

4.3 The BMP-HNF4α pathway and low glucose conditions

The HNF4α-positive cell sub-clones, E, N and T, could survive and proliferate in 1mM-glucose-containing serum-free medium for at least for 2 days, whereas sub-clones V and H appeared to become 'stressed' on Day1 and completely detached from the culture dish bottom on Day2. This indicates sub-clones V and H were less tolerant to stress under low glucose/serum starved conditions.

Moreover, only 1mM glucose (at the point of cell seeding) was sufficient to fully activate the SMAD4-HNF4α pathway, which may be equivalent to hypoglycaemia in human tissues (assuming a similar definition in mouse). This further suggests that HNF4α may be playing a pro-survival, stress-responsive role to buffer against "stress". Considering the fact that TGFβ1 is inhibitory to the BMP-HNF4α pathway, overexpression of TGFβ1 in the tumour may gradually select against these HNF4α-positive cells as clonal evolution progresses through the late stage tumour. This would be consistent with the observation that HNF4α-positive cells are less often found in late stage, poorly differentiated human pancreatic tumour sections. Reports in the literature have generally suggested that HNF4α more often acts as a tumour suppressor. However, it could be that its presence may support survival of a subset of cancer cells that are under environmental stress to proliferate.

4.4 HNF4α may be regulated by multiple pathways in vivo

As discussed in Introduction, HNF4α is well documented as a direct cause of maturity onset diabetes of the young. However, it is not known whether HNF4α expression in normal pancreatic cells is also regulated by the BMP-SMAD4 pathway. In a mouse model, deletion of BMPR1A restricted to the insulin-expressing cells does not affect pancreas development, but it does perturb glucose homeostasis by decreased expressions of genes related to insulin secretion and metabolism (Goulley et al., 2007). On the other hand, deletion of SMAD4 in the mouse pancreas (using *Ptf1a*-Cre) does not affect glucose tolerance, serum lipase or amylase levels in 10-week old mice (Bardeesy et al., 2006). If both observations are assumed to be on a compatible basis, it would mean that HNF4α expression may be regulated by BMP-mediated non-SMAD-dependent pathways in normal pancreatic cells. Alternatively, compensatory pathways may have been activated downstream of the BMP receptors in response to ablation of the SMAD4-HNF4α pathway.

However, the most direct way to know whether HNF4α is downstream of SMAD4 in normal pancreatic cells, and in which cellular compartments *in vivo*, is to stain pancreas sections of SMAD4-null mice. I have been seeking paraffin sections of *Pdx*/*Ptf1a*-Cre; $Dpc4^{flox/flox}$ pancreas, but so far without success. Specifically, requests have been sent to Nabeel Bardeesy (Massachusetts General Hospital) - declined, Christopher Klug (University of Alabama at Birmingham) - materials no longer available, and Chu Xia Deng (National Institute of Health) – no reply.

4.5 Potential roles of HNF4α in Warburg effect

Most differentiated normal cells metabolize glucose to carbon dioxide by oxidation of glycolytic pyruvate in the mitochondrial tricarboxylic acid (TCA) cycle. This reaction produces NADH [nicotinamide adenine dinucleotide (NAD^+), reduced], which then fuels oxidative phosphorylation to maximize ATP production, with minimal production of lactate (reviewed by Vander Heiden et al., 2009). Otto Warburg found that unlike most normal tissues, cancer cells tend to “ferment” glucose into lactate (glycolysis), even in the presence of sufficient oxygen to support mitochondrial oxidative phosphorylation (diagram in Figure 56A). For example, lung tumours arising in the airways exhibit aerobic glycolysis even though these tumour cells are exposed to oxygen during tumorigenesis (Christofk et al., 2008; Nolop et al., 1987; reviewed by Vander Heiden et al., 2009).

Figure 56

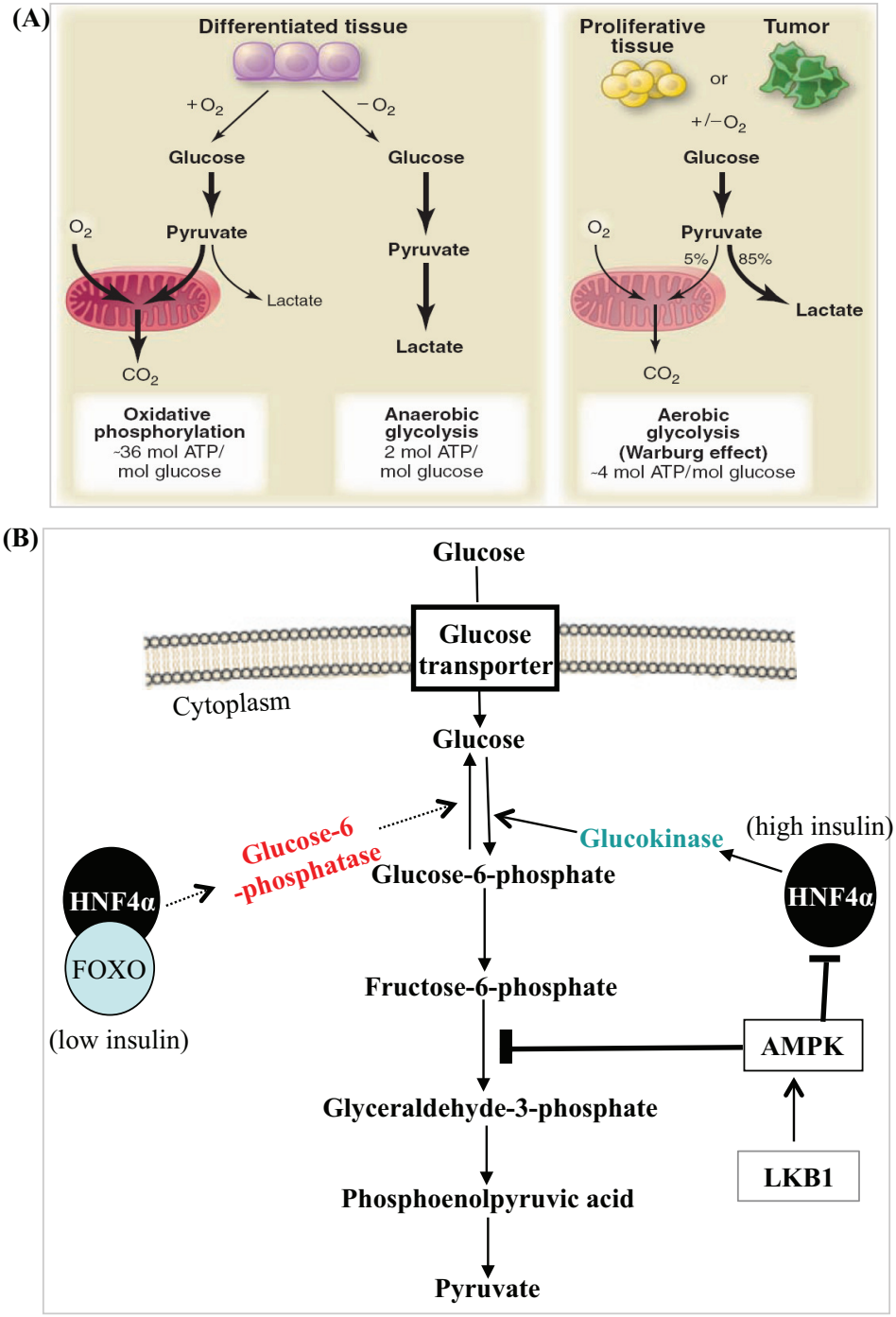

Figure 56 (A) - An illustration of Warburg's effect in tumour cells as compared with normal metabolism in differentiated cells, taken from Vander Heiden et al., 2009. **(B) -** Illustration of the known roles of HNF4α, this far, in the glucose metabolic pathway.

This 'aerobic glycolysis' of glucose to lactate generates only 2 ATPs per molecule of glucose, whereas oxidative phosphorylation generates up to 36 ATPs upon complete oxidation of one glucose molecule (Lehninger et al., 1993; reviewed by Vander Heiden et al., 2009). Hence aerobic glycolysis is in fact much less efficient in generating ATP than oxidative phosphorylation, and the reasons or advantages for such a change in glucose metabolism remain uncertain. Importantly, mitochondrial functions in many cancer cells are not impaired (Weinhouse et al., 1976; Fantin et al., 2006; Moreno-Sanchez et al., 2007; reviewed by Vander Heiden et al., 2009).

HNF4α is potentially linked to the Warburg effect because it can regulate the transcription of genes involved in glucose entry and glycolysis in vitro and in vivo (Stoffel et al., 1997), particularly, the glycolytic enzymes glyceraldehyde-3-phosphate dehydrogenase (GAPDH), and pyruvate kinase (Stoffel et al., 1997). GAPDH acts in one of the multi-step chemical reactions to convert glyceraldehyde-3-phosphate to Phosphoenolpyruvic acid (PEP), which is then converted to pyruvate. Pyruvate kinase is the key enzyme that dictates whether pyruvate is to undergo fermentation to lactate or to enter the mitochondrial oxidative phosphorylation, in which cancer cells often favour the former path.

4.6 HNF4α and its role in glucose metabolism

HNF4α has well documented roles in the metabolic control of gene expression when insulin is low (Yoon et al., 2001; Rhee et al., 2003). When fasting (low insulin), HNF4α induces gene expressions that promote gluconeogenesis (generation of glucose from non-carbohydrate carbon substrates such as lactate, glycerol, and glucogenic amino acids), such as phosphoenol pyruvate carboxykinase (PEPCK) and glucose-6-phosphatase (reviewed by Gonzalez 2008). This requires the presence of an HNF4α-coactivator, namely PPARγ-coactivator-1-α (PGC-1α), which is upregulated by a cyclic-AMP cascade initially induced by glucagon. In the absence of PGC-1α, HNF4α-induced expression of PEPCK and Glucose-6-Phosphatase is greatly decreased (reviewed by Gonzalez 2008). PGC-1α also regulates other metabolic transcription factors, such as FOXO1 (reviewed by Gonzalez 2008).

Another study shows that in the absence of insulin, HNF4α synergizes with FOXO1 in activating transcription of the gene encoding Glucose-6-phosphatase, while FOXO1

conversely represses HNF4α from inducing transcription of the Glucokinase gene (Hirota et al., 2003, 2008; Ganjam et al., 2009). Both of these HNF4α-dependent events are abrogated by treating cells with insulin, which stimulates translocation of FOXO1 to the cytosol (Hirota et al., 2008; Ganjam et al., 2009; reviewed by Barthel et al., 2005), and instead allow HNF4α to potentiate transcription of the Glucokinase/Hexokinase gene (Hirota et al., 2008; Ganjam et al., 2009). Hence the reciprocal action of FOXO1 and HNF4α appeared to be an important determinant of the metabolic shift toward glycolysis, or the reverse process, gluconeogenesis (Figure 56B).

Relating this published literature back to my mouse pancreatic cancer cell sub-clones, in 1mM glucose (at the point of seeding cells) without serum, and therefore in a situation similar to fasting and low insulin, HNF4α and its co-activator, such as FOXO1, may induce increased expression of Glucose-6-phosphatase, which would facilitate gluconeogenesis to produce glucose from non-carbohydrate carbon sources, particularly as the need for energy is lower in the absence of serum mitogens. However, the cells need to survive in this low glucose environment as long as possible, and there will be selection for survival. Hence, HNF4α-mediated gluconeogenesis may offer an advantage for these HNF4α-expressing cell sub-clones (E, N and T) to survive.

However, in the presence of serum, which contains insulin, FOXO1 would be inactivated and excluded from the nucleus, meaning that HNF4α induces transcription of Glucokinase, which phosphorylates glucose to glucose-6-phosphate and glycolysis. Consumption of glucose by proliferating tumour cells will lower the glucose concentration in medium down to below 1mM glucose, the threshold for effective HNF4α expression, and this may explain the overall decrease in HNF4α levels in cycling cells.

Furthermore, substitution of 1mM glucose with 1mM pyruvate did not cause an increase in HNF4α levels, suggesting that upregulation of HNF4α in response to serum starvation was independent of pyruvate and its downstream metabolism. Hence, HNF4α was apparently linked to the series of metabolic reactions, that begin with uptake of glucose by its transporters to the generation of phosphoenolpyruvate (the precursor of pyruvate). Perhaps once there is excess pyruvate, the need for glucose uptake and the immediate metabolism of

glucose to produce pyruvate, is no longer required, and thus high levels of HNF4α would no longer be required.

4.7 HNF4α overexpression suggests inactivation of the LKB-AMPK pathway

When malignant cells exhibit a shift from oxidative phosphorylation to 'aerobic glycolysis', ATP to AMP ratios declined, and accumulation of AMP activates AMP-activated protein kinase (AMPK), which in turn acts to shift the metabolic pathway back to oxidative phosphorylation (reviewed by Vander Heiden et al., 2009). This causes opposition to abnormal proliferation signals resulting from oncogene expression (reviewed by Vander Heiden et al., 2009; reviewed by Cairns et al., 2011). Activation of AMPK requires the upstream kinase Liver Kinase B1 (LKB1), which is encoded by the gene *Stk11* (Lizcano et al., 2004). LKB1 is a well-documented tumour suppressor, and it is frequently mutated in sporadic cases of non-small-cell lung cancer and cervical carcinoma (Ji et al., 2007; Wingo et al., 2009; reviewed by Cairns et al., 2011). Somatic mutation of LKB1 is found in patients with Peutz–Jeghers syndrome, in which they develop benign gastrointestinal and oral cancer lesions and an increased risk of developing a broad range of malignancies (Jenne et al., 1998; reviewed by Cairns et al., 2011).

AMPK has been shown to negatively regulate HNF4α (Leclerc et al., 2001; Hong et al., 2003); hence it would be of interest to elucidate the relationship between LKB1-AMPK, HNF4α and cancer cell metabolism. Importantly, heterozygous deficiency of LKB1 does lower phospho-AMPK levels and accelerate mouse pancreatic tumorigenesis in a mutant $KRas^{G12D}$ background (Morton et al., 2010). In isolated islet cells from mice with widespread homozygous deletion of the AMPKα2 subunit, glucose stimulated insulin secretion is not affected (Viollet et al., 2003). This possibly indicates that absence of AMPK in normal cells does not necessarily lead to deregulated HNF4α activity, as HNF4α can be regulated by a densely overlapping network of other HNFs and transcriptional co-factors (Odom et al., 2004). Hence, the regulation and role of HNF4α is complex, and requires further investigation.

4.8 Drawbacks in subcutaneous or orthotopic injection experiments

Tumours formed by injection of mouse pancreatic cancer cells to the subcutaneous layer or back to the pancreas did not resemble the original tumour's microenvironment. Importantly, no HNF4α staining was detected on sections of subcutaneous tumours of cell sub-clones E, N and T. This is also true for tumour sections from orthotopic injection, in which HNF4α is stained only in the remaining normal pancreatic cells surrounded by injected tumour cells. Hence injections of cultured cells back to the mouse do not seem to be of value to study this BMP-SMAD1/SMAD4-HNF4α pathway, and this probably reflects how limited is this approach trying to study native signalling pathways of cancer using xenograft tumours. Particularly, from what is published in the literature, xenograft has never been able to reproduce the full scope of heterogeneity or pathology in the original tumour, which argues strongly against the hypothesis that a few cancer stem cells eventually contribute to all cancer cell types in a tumour (reviewed by Visvader et al., 2008). This is not surprising at all, considering how long it generally takes for tumours to evolve in their environment and acquire additional mutations, and to overcome internal selective pressure.

4.9 Targeting ERK, and probably also Wnt, are not enough

Despite the fact that inhibiting MEK could suppress anchorage independent proliferation of the seven mouse pancreatic tumour cell sub-clones, their proliferation on 2D-plastic culture dish was unaffected. Consistently, David Tuveson's group found that knocking down mutant $KRas^{G12D}$ in primary cells derived from the same mouse model only affects anchorage independent proliferation, but not 2D proliferation on tissue culture dishes (unpublished observation, reported during the 50th BACR conference in Edinburgh 2010), suggesting that cell adhesion is sufficient to provide signals for tumour cells to proliferate in a $KRas^{G12D}$-independent manner. Furthermore, in a multicentre phase-II study, the MEK inhibitor PD184352 (CI-1040), which was used in my study, had been found well tolerated in patients, but demonstrated little antitumor activity in pancreatic cancer patients (Rinehart et al., 2004). However, such study could not rule out the possibility that delivery of PD184352 to the tumour was not sufficiently efficient, as pancreatic adenocarcinomas commonly bare poor vasculature (Olive et al., 2009).

Likewise, inhibition of the canonical Wnt pathway only partially suppressed anchorage independent proliferation in cell sub-clones V and N, but not 2-dimensional proliferation.

Considering only two out of the seven murine pancreatic cancer cell sub-clones were sensitive to Wnt-inhibition under anchorage independent condition, targeting Wnt alone would probably be ineffective in suppressing the overall tumour growth attributed to a combination of cell sub-clones that are addicted to distinct, although possibly overlapping, cancer driver pathways.

4.10 Notes on results presentation

All experiments shown in this thesis are representative experiments that have been repeated at least once, and among them, experiments related to the initial characterization of the cell sub-clones and to the SMAD4-HNF4α pathway have been repeated at least twice.

However, and ideally, data should have been collected and presented using an average of data from at least three independent experiments. For example, in analysis of cell-sphere sizes in anchorage independent proliferation, the correct way to present data is to take the mean of the average sphere area from three independent soft-agar assays, and present this with an error bar showing the standard deviation of the three independent averages of colony area. For western blot analysis, ideally, quantification of band intensity using ImageJ should have been based on the average of three independent blots.

5. FUTURE PERSPECTIVES

5.1 Deletion of HNF4α in the Pdx1 lineage

The most straightforward way to understand the role of HNF4α in pancreatic carcinogenesis is to knockout HNF4α in the pancreas using the *Pdx1*-Cre system. Direct homozygous deletion of HNF4α in the mouse pancreatic β-cells (insulin positive cells) did not cause developmental defects but a diabetic phenotype (Gupta et al., 2005; Miura et al., 2006), but it is still not known whether deletion of HNF4α in the whole pancreas will cause developmental defects. It will be necessary to generate a test strain of mice with the genotype *Pdx1*-Cre/ *Hnf4α*$^{flox/flox}$. More precisely, use of the genotype of *Pdx1*-CreER/ *LSL-Kras*$^{G12D/+}$/ *Hnf4α*$^{flox/flox}$, with or without *LSL-Tp53*^{R172H}, in which Cre recombinase is activated only when the animal is treated with Tamoxifen, will provide controls over the timing of transgenic expressions, by controlling the time and space where gene deletion occurs. This would avoid any acquired artefacts during developmental stages. Tamoxifen is an antagonist of the estrogen receptor which is metabolised into compounds that bind the estrogen receptor (ER) but without activating it (Indra et al., 1999). Alternatively, since heterozygous deficiency in HNF4α did not cause diabetes in mice, it may be worth testing whether decreased HNF4α expression will have an effect on the formation of Kras^{G12D}-induced PanIN lesions.

5.2 Investigation into the glucose metabolic pathways that may involve HNF4α in pancreatic cancer

Assuming that the HNF4α-positive cell sub-clones E, N and T have a different glucose metabolic status from the rest of the cell sub-clones, an immediate experiment of interest will be to check the transcription levels of important metabolic enzymes that are known to be direct targets of HNF4α, such as glucose-6-phosphatase and Glucokinase. This may also provide insight on how glucose metabolism is coupled to secretion of BMP ligands and initiate an 'autoloop' pathway. As discussed earlier in Introduction, HNF4α is closely integrated into the metabolic pathway of AMPK, which is known to suppress HNF4α expression (Figure 56B). Chemical agonists of AMPK, such as Metformin and the chemically related Phenformin (reviewed by Vander Heiden et al., 2009) can be used to see if HNF4α is suppressed, and to simultaneously determine whether the BMP-SMAD1/SMAD4 pathway is affected. Furthermore, a straightforward way to understand

how the BMP-SMAD4 is coupled to the AMPK pathway via HNF4α in the pancreas, and in pancreatic cancer, is to stain for HNF4α, phospho-SMAD1/5/8 and phospho-SMAD2 on tissue sections of *Pdx1*-Cre; $Lkb1^{flox/flox}$, *and Pdx1*-Cre; *LSL-*$Kras^{G12D}$; $Lkb1^{flox/flox}$ (Morton et al., 2010). Loss of LKB1 in the pancreas is sufficient to initiate cancer progression, and heterozygous deletion of Lkb1 accelerates $KRas^{G12D}$-induced pancreatic cancer progression (Morton et al., 2010). Since LKB1 is long known to be an upstream activator of AMPK, loss of LKB would mean decreased AMPK activity, and in turn allowing increased HNF4α expression. If we could understand the methods those "tougher" cancer cells use to survive in idle under nutrients-scarce conditions, we may be able to clear them up early before they "wake up" and acquire metastatic potential.

5.3 Further refinement of *in-vitro* experimental conditions needed in order to accurately study pancreatic caner cell metabolism.

One drawback of using standard DMEM in tissue culture is its high glucose concentration (25mM). It was supposed to maximise the energy provided to cells so as to maximise survival or proliferation, however, the accuracy to study cellular pathways and gene expressions under such unrealistically high glucose concentration is questionable. If time were sufficient within the scope of my studentship, I would examine the cell sub-clones' proliferation rate or survival using DMEM with glucose concentration at 1mM (hypoglycaemia-equivalent) and at 5mM (normal level equivalent), in the presence of 10% serum. In this case, the medium may have to be refreshed daily in order to avoid over-depletion of glucose in the medium. I would also put the cells under hypoxic conditions in an nitrogen-adjusted incubator, due to the fact that pancreatic cancer is known to be poorly vascularized, and therefore the cancer cells within a tumour are likely to experience both low glucose and low oxygen supply.

5.4 Which HNF4α promoter of the two is a BMP-SMAD target?

As discussed earlier, there are multiple splice variants of HNF4α that can be transcribed by two independent promoters. A report has shown that most cell types in the pancreas, no matter whether human or mouse, express a basal level of HNF4α, which in some of the cell types are mediated by promoter-1 and while in some others by promoter-2 (Jiang et al., 2003). The antibody that I have been using recognizes all variants of HNF4α, therefore, use of antibodies that specifically recognize variants by either promoter-1 or promoter-2 (if

available) will be more informative on how HNF4α is overexpressed during pancreatic carcinogenesis in a mutant $KRas^{G12D}$ background. This may also reveal which cellular compartments and which cell type in the pancreas may have given rise to cancer cell sub-clones E, N and T. Alternatively, performing PCRs with oligonucleotides targeting promoter-specific regions of the HNF4α transcript will be complementary to check which of the two HNF4α promoters were active in cell sub-clones E, N and T. It is not clear whether these splice variants possessed different functions or are redundant; most studies in the literature have so far been based on the two longest variants (including my study). Hence, if normal pancreatic cells express different variants of HNF4α, or using a different promoter from that downstream of SMAD4 ("the embryonic promoter"). Moreover, overexpression of HNF4α was an early event as observed in immunohistochemistry in my study, we may be able to distinguish early neoplastic cells from normal pancreatic cells right at the tipping point of PanIN evolution.

5.5 Roles of the BMP-SMAD1/5 pathway in pancreatic carcinogenesis

Although BMP induces expression of HNF4α via SMAD1/5 and SMAD4, HNF4α is unlikely to be the only downstream target. Previous mouse models have provided details on the roles of the TGFβ type-2 receptor and SMAD4 during carcinogenesis driven by mutant $KRas^{G12D}$, however, the BMP pathway, which classically signals through SMAD1/5/8 and SMAD4, has not been specifically studied. Deletion of SMAD4 only abolishes R-SMAD-dependent pathways, and this may have shifted the activity to non-SMAD-dependent pathways. Conversely, deletion of SMAD1/5/8 may shift the BMP pathway to the SMAD2/3 pathway or other non-SMAD-dependent pathways, and vice versa. It is known that deletion of the BMP type-2 receptor in insulin-positive cells leads to diabetic mice in the $KRas^{G12D}$ background, hence it will also provide information on whether deregulated insulin secretion and glucose metabolism can accelerate pancreatic carcinogenesis induced by $KRas^{G12D}$. In addition, it would also be informative to stain sections of normal pancreas and pancreatic cancer, for phospho-SMAD1/5/8 and phosphos-SMAD2/3, and to compare whether activities of these two classes of SMADs have a distinctive pattern in different pancreatic compartments.

5.6 Do the SMADs regulate HNF4α expression via binding to its promoter(s) ?

If ablation of HNF4α in the adult pancreas has an effect on pancreatic cancer progression in mice, it would then be important understand the details in how HNF4α expression is

regulated by the SMADs, for example, whether the SMADs directly bind to the promoter(s) of HNF4α. To do so, chromatin immunoprecipitation (ChIP) can be performed, which involves cross-linking DNA to protein in cell lysates using formaldehyde, sonication to shear DNA into fragments of less than 1000 base pairs, purification with anti-SMADs-linked beads, and uncoupling DNA from protein using proteinase K. DNA is eventually purified and used to run quantitative PCR with oligos designed to prime for mouse HNF4α sequences and HNF4α promoter sequences, respectively.

For cell sub-clone N as an example, setup of ChIP samples would be as follows:

Glucose	Condition (DMEM)	Treatment
1mM	Serum free	BSA alone
1mM	Serum free	BSA, TGFβ
1mM	Serum free	BSA, BMP9

ChIP with SMAD4 antibody could be used to check whether SMAD4 binds HNF4α's promoter(s) sequences, and whether such binding is suppressed by treatment with TGFβ, or enhanced by treatment with BMP9. Then, use of SMAD1, SMAD2, and SMAD3 antibodies, respectively, can unveil which additional R-SMAD plays a dominant role in binding to HNF4α's DNA or promoter(s) sequences in BMP- or TGFβ-stimulated conditions. SMADs-DNA binding can be quantified by running qPCR with samples immunoprecipitated with the same SMAD antibody under the three different conditions. Quantitative PCR can indicate relative SMAD-DNA binding activity under different conditions.

Potential SMAD-binding sites in the promoters(s) of HNF4α could be first predicted by aligning the HNF4α promoter(s) against classical SMAD-binding sequences. If such a potential binding site is confirmed by PCR with DNA from ChIP, a reporter plasmid containing GFP or luciferase downstream of the identified SMAD-binding sequences can be used to monitor the kinetics of such binding in live cells through time-lapse imaging techniques.

ChIP often needs time for optimization of conditions, a potentially quicker method to "pre-check" DNA-protein binding is to use Electrophoretic mobility shift assay (EMSA), in which the presence of protein-DNA complexes is reflected by an up-shift of bands on a SDS-PAGE, comparing with the control band using DNA or RNA alone. The gel can also be transferred onto nitrocellulose membrane to probe for the protein of interest by immunoblotting, such as SMAD4 in this case. However, it only addresses whether the SMADs have the affinity to bind a DNA sequence in the running buffer, but not whether such binding actually takes place in the cells.

7. CONCLUSIONS

My PhD project provided evidence to establish for the first time:

- Cancer (malignant tumour) cells in this *Pdx1*-Cre mouse model are highly heterogeneous, and this may also apply to many other mouse cancer models that are driven by a pan-organ-specific promoter. We cannot simply study primary tumour cells as if they were homogeneous.

- A connection between the BMP/TGFβ-SMAD4 pathway and glucose metabolism, which acts as a stress response in mouse pancreatic cancer cells. Although both SMAD4 and HNF4α appeared to be tumour suppressors during early tumourigenesis, as suggested by some studies in the literature, this pathway may in turn provide survival advantage to some of the cancer cells in a poorly vascularized intra-tumour environment.

- A developmental pathway (SMAD4-HNF4α) that appeared to have been "reactivated" during $KRas^{G12D}$ induced-transformation. This implies potential similarities in signalling between gastrulation of the mouse embryo and PanIN formation in $Kras^{G12D}$-expressing compartments, considering the well-documented importance of wild-type KRas during embryonic development.

- HNF4α IHC can be used to mark epithelial pancreatic cancer cells on tumour sections, in both mouse and human pancreatic cancer tissues.

8 REFERENCES

Aberle H, Bauer A, Stappert J, Kispert A, Kemler R. 1997. Beta-catenin is a target for the ubiquitin-proteasome pathway. EMBO J. 16:3797–804

Ahlgren U, Jonsson J, Edlund H. 1996. The morphogenesis of the pancreatic mesenchyme is uncoupled from that of the pancreatic epithelium in IPF1/PDX1–deficient mice. Development 122:1409–16

Ahlgren U, Jonsson J, Jonsson L, Simu K, Edlund H. 1998. Beta-cell-specific inactivation of the mouse Ipf1/Pdx1 gene results in loss of the beta-cell phenotype and maturity onset diabetes. Genes Dev. 12:1763–68

Aigner K, Dampier B, Descovich L, Mikula M, Sultan A, Schreiber M, Mikulits W, Brabletz T, Strand D, Obrist P, Sommergruber W, Schweifer N, Wernitznig A, Beug H, Foisner R, Eger A. The transcription factor ZEB1 (deltaEF1) promotes tumour cell dedifferentiation by repressing master regulators of epithelial polarity. Oncogene. 2007 Oct 25;26(49):6979-88.

Amit S, Hatzubai A, Birman Y, Andersen JS, Ben-Shushan E, Mann M, Ben-Neriah Y, Alkalay I. Axin-mediated CKI phosphorylation of beta-catenin at Ser 45: a molecular switch for the Wnt pathway.

Genes Dev. 2002 May 1;16(9):1066-76.Andrea Haegebarth and Hans Clevers Wnt Signaling, Lgr5, and Stem Cells in the Intestine and Skin. Am J Pathol. 2009 March; 174(3): 715–721.

Anna Mizutani, Daizo Koinuma, Shuichi Tsutsumi, Naoko Kamimura, Masato Morikawa, Hiroshi I. Suzuki, Takeshi Imamura, Kohei Miyazono, Hiroyuki Aburatani Cell Type-specific Target Selection by Combinatorial Binding of Smad2/3 Proteins and Hepatocyte Nuclear Factor 4α in HepG2 Cells/ J Biol Chem. 2011 August 26; 286(34): 29848–29860.

Arnold SJ, Maretto S, Islam A, Bikoff EK, Robertson EJ. Dose-dependent Smad1, Smad5 and Smad8 signaling in the early mouse embryo. Dev Biol. 2006 Aug 1;296(1):104-18.

Ashcroft GS, Yang X, Glick AB, Weinstein M, Letterio JL, Mizel DE, Anzano M, Greenwell-Wild T, Wahl SM, Deng C, Roberts AB. Mice lacking Smad3 show accelerated wound healing and an impaired local inflammatory response. Nat Cell Biol. 1999 Sep;1(5):260-6.

Ashcroft GS, Yang X, Glick AB, Weinstein M, Letterio JL, Mizel DE, Anzano M, Greenwell-Wild T, Wahl SM, Deng C, Roberts AB. Mice lacking Smad3 show accelerated wound healing and an impaired local inflammatory response. Nat Cell Biol. 1999 Sep;1(5):260-6.

Ashton-Rickardt PG, Dunlop MG, Nakamura Y, Morris RG, Purdie CA, Steel CM, Evans HJ, Bird CC, Wyllie AH. High frequency of APC loss in sporadic colorectal carcinoma due to breaks clustered in 5q21-22. Oncogene. 1989 Oct;4(10):1169-74.

Bailey JM, Singh PK, Hollingsworth MA. Cancer metastasis facilitated by developmental pathways: Sonic hedgehog, Notch, and bone morphogenic proteins. J Cell Biochem. 2007 Nov 1;102(4):829-39.

Balmain A, Ramsden M, Bowden GT, Smith J. Activation of the mouse cellular Harvey-ras gene in chemically induced benign skin papillomas. Nature. 1984 Feb 16-22;307(5952):658-60.

Bardeesy N, Cheng KH, Berger JH, Chu GC, Pahler J, Olson P, Hezel AF, Horner J, Lauwers GY, Hanahan D, DePinho RA. Smad4 is dispensable for normal pancreas development yet critical in progression and tumor biology of pancreas cancer. Genes Dev. 2006 Nov 15;20(22):3130-46.

Behrens J, Jerchow BA, Würtele M, Grimm J, Asbrand C, Wirtz R, Kühl M, Wedlich D, Birchmeier W. Functional interaction of an axin homolog, conductin, with beta-catenin, APC, and GSK3beta. Science. 1998 Apr 24;280(5363):596-9.

Barthel A, Schmoll D, Unterman TG. FoxO proteins in insulin action and metabolism. Trends Endocrinol Metab. 2005 May-Jun;16(4):183-9.

Besson A, Gurian-West M, Chen X, Kelly-Spratt KS, Kemp CJ, Roberts JM. A pathway in quiescent cells that controls p27Kip1 stability, subcellular localization, and tumor suppression. Genes Dev. 2006 Jan 1;20(1):47-64

Bivona TG, Quatela SE, Bodemann BO, Ahearn IM, Soskis MJ, Mor A, Miura J, Wiener HH, Wright L, Saba SG, Yim D, Fein A, Pérez de Castro I, Li C, Thompson CB, Cox AD, Philips MR. PKC regulates a farnesyl-electrostatic switch on K-Ras that promotes its association with Bcl-XL on mitochondria and induces apoptosis. Mol Cell. 2006 Feb 17;21(4):481-93.

Björklund MA, Vaahtomeri K, Peltonen K, Viollet B, Mäkelä TP, Band AM, Laiho M. Non-CDK-bound p27 (p27(NCDK)) is a marker for cell stress and is regulated through the Akt/PKB and AMPK-kinase pathways. Exp Cell Res. 2010 Mar 10;316(5):762-74. doi: 10.1016/j.yexcr.2009.12.014.

Bode, AM; Dong, ZG; Post-translational modification of p53 in tumorigenesis. NATURE REVIEWS CANCER Volume: 4 Issue: 10 Pages: 793-805 DOI:10.1038/nrc1455 Published: Oct 2004 Blanpain C, Fuchs E. Epidermal stem cells of the skin. Annu Rev Cell Dev Biol. 2006; 22:339-73. Cancer Res. 2007 Sep 1;67(17):8149-55.

Boj SF, Parrizas M, Maestro MA, Ferrer J. 2001. A transcription factor regulatory circuit in differentiated pancreatic cells. Proc. Natl. Acad. Sci. USA 98:14481–86

Bonzo JA, Ferry CH, Matsubara T, Kim JH, Gonzalez FJ. Suppression of hepatocyte proliferation by hepatocyte nuclear factor 4α in adult mice. J Biol Chem. 2012 Mar 2;287(10):7345-56. doi: 10.1074/jbc.M111.334599.

Brembeck FH, Schreiber FS, Deramaudt TB, Craig L, Rhoades B, Swain G, Grippo P, Stoffers DA, Silberg DG, Rustgi AK. The mutant K-ras oncogene causes pancreatic periductal lymphocytic infiltration and gastric mucous neck cell hyperplasia in transgenic mice. Cancer Res. 2003 May 1;63(9):2005-9.

Brosh R, Rotter V. When mutants gain new powers: news from the mutant p53 field. Nat Rev Cancer. 2009 Oct;9(10):701-13.

Burlison JS, Long Q, Fujitani Y, Wright CV, Magnuson MA. Pdx-1 and Ptf1a concurrently determine fate specification of pancreatic multipotent progenitor cells. Dev Biol. 2008 Apr 1;316(1):74-86.

Calhoun ES, Jones JB, Ashfaq R, Adsay V, Baker SJ, Valentine V, Hempen PM, Hilgers W, Yeo CJ, Hruban RH, Kern SE. BRAF and FBXW7 (CDC4, FBW7, AGO, SEL10) mutations in distinct subsets of pancreatic cancer: potential therapeutic targets. Am J Pathol. 2003 Oct;163(4):1255-60.

Calva-Cerqueira D, Chinnathambi S, Pechman B, Bair J, Larsen-Haidle J, Howe JR. The rate of germline mutations and large deletions of SMAD4 and BMPR1A in juvenile polyposis. Clin Genet. 2009 Jan;75(1):79-85.

Campbell PJ, Yachida S, Mudie LJ, Stephens PJ, Pleasance ED, Stebbings LA, Morsberger LA, Latimer C, McLaren S, Lin ML, McBride DJ, Varela I, Nik-Zainal SA, Leroy C, Jia M, Menzies A, Butler AP, Teague JW, Griffin CA, Burton J, Swerdlow H, Quail MA, Stratton MR, Iacobuzio-Donahue C, Futreal PA. The patterns and dynamics of genomic instability in metastatic pancreatic cancer. Nature. 2010 Oct 28;467(7319):1109-13.

Caperuto LC, Anhê GF, Cambiaghi TD, Akamine EH, do Carmo Buonfiglio D, Cipolla-Neto J, Curi R, Bordin S. Modulation of bone morphogenetic protein-9 expression and processing by insulin, glucose, and glucocorticoids: possible candidate for hepatic insulin-sensitizing substance. Endocrinology. 2008 Dec;149(12):6326-35.

Chan IT, Kutok JL, Williams IR, Cohen S, Kelly L, Shigematsu H, Johnson L, Akashi K, Tuveson DA, Jacks T, Gilliland DG. Conditional expression of oncogenic K ras from its endogenous promoter induces a myeloproliferative disease. J. Clin. Invest. 113, 528–538 (2004).

Chari ST, Leibson CL, Rabe KG, Timmons LJ, Ransom J, de Andrade M, Petersen GM. Pancreatic cancer-associated diabetes mellitus: prevalence and temporal association with diagnosis of cancer. Gastroenterology 2008; 134: 95–101.

Chen B, Dodge ME, Tang W, Lu J, Ma Z, Fan CW, Wei S, Hao W, Kilgore J, Williams NS, Roth MG, Amatruda JF, Chen C, Lum L. Small molecule-mediated disruption of Wnt-dependent signaling in tissue regeneration and cancer. Nat Chem Biol. 2009 Feb;5(2):100-7.

Chen C, Grzegorzewski KJ, Barash S, Zhao Q, Schneider H, Wang Q, Singh M, Pukac L, Bell AC, Duan R, Coleman T, Duttaroy A, Cheng S, Hirsch J, Zhang L, Lazard Y, Fischer C, Barber MC, Ma ZD, Zhang YQ, Reavey P, Zhong L, Teng B, Sanyal I, Ruben SM, Blondel O, Birse CE. An integrated functional genomics screening program reveals a role for BMP-9 in glucose homeostasis. Nat Biotechnol. 2003 Mar;21(3):294-301.

Chen, W. S., Manova, K., Weinstein, D. C., Duncan, S. A., Plump, A. S., Prezioso, V. R., Bachvarova, R. F. and Darnell, J. E., Jr. (1994). Disruption of the HNF-4 gene, expressed in visceral endoderm, leads to cell death in embryonic ectoderm and impaired gastrulation of mouse embryos. Genes Dev. 8, 2466-2477.

Cheng JQ, Ruggeri B, Klein WM, Sonoda G, Altomare DA, Watson DK, Testa JR. 1996. Amplification of AKT2 in human pancreatic cells and inhibition of AKT2 expression and tumorigenicity by antisense RNA. Proc. Natl. Acad. Sci. USA 93:3636–41

Chia, IV; Costantini, F Mouse axin and Axin2/conductin proteins are functionally equivalent in vivo. Molecular and Cellular Biology Volume: 25 Issue: 11 Pages: 4371-4376 Jun 2005

Chiaradonna F, Sacco E, Manzoni R, Giorgio M, Vanoni M, Alberghina L. Ras-dependent carbon metabolism and transformation in mouse fibroblasts. Oncogene. 2006 Aug 31;25(39):5391-404.

Chiu VK, Bivona T, Hach A, Sajous JB, Silletti J, Wiener H, Johnson RL 2nd, Cox AD, Philips MR. Ras signalling on the endoplasmic reticulum and the Golgi. Nature Cell Biol. 4, 343–350 (2002)

Cho, Y., Gorina, S., Jeffrey, P. D. & Pavletich, N. P. Crystal structure of a p53 tumor suppressor–DNA complex: understanding tumorigenic mutations. Science 265, 346–355 (1994).

Choi J, Park SY, Costantini F, Jho EH, Joo CK. Adenomatous polyposis coli is down-regulated by the ubiquitin-proteasome pathway in a process facilitated by Axin. J Biol Chem. 2004 Nov 19;279(47):49188-98.

Christofk HR, Vander Heiden MG, Harris MH, Ramanathan A, Gerszten RE, Wei R, Fleming MD, Schreiber SL, Cantley LC. The M2 splice isoform of pyruvate kinase is important for cancer metabolism and tumour growth. Nature. 2008 Mar 13;452(7184):230-3. doi: 10.1038/nature06734.

Cifone MA, Fidler IJ. Correlation of patterns of anchorage-independent growth with in vivo behavior of cells from a murine fibrosarcoma. Proc Natl Acad Sci U S A. 1980 Feb;77(2):1039-43.

Constam DB, Robertson EJ. Regulation of bone morphogenetic protein activity by pro domains and proprotein convertases. J Cell Biol 1999; 144:139–149.

Cryer, Philip E. (2001). "Hypoglycemia". In Jefferson L, Cherrington A, Goodman H, eds. for the American Physiological Society. Handbook of Physiology; Section 7, The Endocrine System.. II. The endocrine pancreas and regulation of metabolism.. New York: Oxford University Press. pp. 1057–1092.

Cuny GD, Yu PB, Laha JK, Xing X, Liu JF, Lai CS, Deng DY, Sachidanandan C, Bloch KD, Peterson RT. Structure-activity relationship study of bone morphogenetic protein (BMP) signaling inhibitors. Bioorg Med Chem Lett. 2008 Aug 1;18(15):4388-92

Daly, A. C., Randall, R. A. & Hill, C. S. Transforming growth factor β–induced Smad1/5 phosphorylation in epithelial cells is mediated by novel receptor complexes and is essential for anchorageindependent growth. Mol. Cell. Biol. 28, 6889–6902 (2008).

Darsigny, M., Babeu, J.P., Seidman, E.G., Gendron, F.P., Levy, E., Carrier, J., Perreault, N., and Boudreau, F. (2010). Hepatocyte nuclear factor-4alpha promotes gut neoplasia in mice and protects against the production of reactive oxygen species. Cancer Res. 70, 9423–9433.

D'Adda di Fagagna F. 2008. Living on a break: Cellular senescence as a DNA-damage response. Nat Rev Cancer 8: 512–522.

David L, Mallet C, Mazerbourg S, Feige JJ, Bailly S Blood. 2007 Mar 1; 109(5):1953-61. Identification of BMP9 and BMP10 as functional activators of the orphan activin receptor-like kinase 1 (ALK1) in endothelial cells.

Day JD, Digiuseppe JA, Yeo C, Lai-Goldman M, Anderson SM, Goodman SN, Kern SE, Hruban RH. Hruban Immunohistochemical evaluation of HER-2/neu expression in pancreatic adenocarcinoma and pancreatic intraepithelial neoplasm. Hum. Pathol., 27 (1996), pp. 119–124

de Lau W, Barker N, Low TY, Koo BK, Li VS, Teunissen H, Kujala P, Haegebarth A, Peters PJ, van de Wetering M, Stange DE, van Es JE, Guardavaccaro D, Schasfoort RB, Mohri Y, Nishimori K, Mohammed S, Heck AJ, Clevers H. Lgr5 homologues associate with Wnt receptors and mediate R-spondin signalling. Nature. 2011 Jul 4;476(7360):293-7. doi: 10.1038/nature10337.

DeNicola GM, Tuveson DA. RAS in cellular transformation and senescence. Eur J Cancer. 2009 Sep;45 Suppl 1:211-6.

Derynck, R. & Zhang, Y. E. Smad-dependent and Smad-independent pathways in TGF-β family signalling. Nature 425, 577–584 (2003).

Descargues, P., Sil, A.K., Sano, Y., Korchynskyi, O., Han, G., Owens, P., Wang, X.J., and Karin, M. (2008). IKKalpha is a critical coregulator of a Smad4-independent TGFbeta-Smad2/3 signaling pathway that controls keratinocyte differentiation. Proc. Natl. Acad. Sci. USA 105, 2487–2492.

Donehower LA, Lozano G. 20 years studying p53 functions in genetically engineered mice. Nat Rev Cancer. 2009 Nov;9(11):831-41.

Dor Y., Brown J., Martinez O.I.,Melton D.A. (2004) Adult pancreatic β-cells are formed by self-duplication rather than stem-cell differentiation. Nature 429:41–46.

Dubois CM, Laprise MH, Blanchette F, Gentry LE, Leduc R. Processing of transforming growth factor beta 1 precursor by human furin convertase. J Biol Chem 1995; 270:10618–10624.

Duncan, S. A., Manova, K., Chen, W. S., Hoodless, P., Weinstein, D. C., Bachvarova, R. F. and Darnell, J. E., Jr. (1994). Expression of transcription factor HNF-4 in the extraembryonic

endoderm, gut, and nephrogenic tissue of the developing mouse embryo: HNF-4 is a marker for primary endoderm in the implanting blastocyst. Proc. Natl. Acad. Sci. USA 91, 7598-7602.

Duncan, S. A., Nagy, A. and Chan, W. (1997). Murine gastrulation requires HNF-4 regulated gene expression in the visceral endoderm: tetraploid rescue of Hnf-4(-/-) embryos. Development 124, 279-287.

Dutta S, Bonner-Weir S, Montminy M, Wright C. 1998. Regulatory factor linked to late-onset diabetes? Nature 392:560

Eberle M.A., Pfutzer R., Pogue-Geile K.L., Bronner M.P., Crispin D., Kimmey M.B., Duerr R.H., Kruglyak L., Whitcomb D.C., Brentnall T.A (2002) A new susceptibility locus for autosomal dominant pancreatic cancer maps to chromosome 4q32-34. Am. J. Hum. Genet. 70:1044–1048.

Elayat AA, el-Naggar MM, Tahir M (1995). "An immunocytochemical and morphometric study of the rat pancreatic islets". Journal of Anatomy. 186. (Pt 3) (Pt 3): 629–37.

Esteban LM, Vicario-Abejón C, Fernández-Salguero P, Fernández-Medarde A, Swaminathan N, Yienger K, Lopez E, Malumbres M, McKay R, Ward JM, Pellicer A, Santos E. Targeted genomic disruption of H-ras and N-ras, individually or in combination, reveals the dispensability of both loci for mouse growth and development. Mol Cell Biol. 2001 Mar;21(5):1444-52.

Fajans SS, Bell GI, Polonsky KS.Molecular mechanisms and clinical pathophysiology of maturity-onset diabetes of the young.N Engl J Med. 2001 Sep 27;345(13):971-80.

Feng XH, Derynck R (Review) Specificity and versatility in tgf-beta signaling through Smads. Annu Rev Cell Dev Biol. 2005; 21():659-93.

Feng Z, Hu W, de Stanchina E, Teresky AK, Jin S, Lowe S, Levine AJ. The regulation of AMPK beta1, TSC2, and PTEN expression by p53: stress, cell and tissue specificity, and the role of these gene products in modulating the IGF-1–AKT–mTOR pathways. Cancer Res. 67, 3043–3053 (2007).

Fink SP, Mikkola D, Willson JK, Markowitz S. TGF-β-induced nuclear localization of Smad2 and Smad3 in Smad4 null cancer cell lines. Oncogene 2003; 22: 1317–23.

Fishman EK, Topazian MD, Takahashi N, Lee JH, Tamm EP, Vikram R, Syngal S, Saltzman JR, Mortele KJ, Farrell JJ, Margolis D, Zhang Z, Petersen GM, Hruban RH, Goggins MG. Screening for familial pancreatic neoplasia: a prospective, multicenter blinded study of EUS, CT, and Secretin-MRCP. Presented at Digestive Disease Week DDW 2010; New Orleans, LA, USA; May 1–5, 2010. Abstract 415g.

Freed-Pastor WA, Prives C. Mutant p53: one name, many proteins. Genes Dev. 2012 Jun 15;26(12):1268-86. doi: 10.1101/gad.190678.112.

Friedl W, Uhlhaas S, Schulmann K, Stolte M, Loff S, Back W, Mangold E, Stern M, Knaebel HP, Sutter C, Weber RG, Pistorius S, Burger B, Propping P. Juvenile polyposis: massive gastric polyposis is more common in MADH4 carriers than in BMPR1A mutation carriers. Hum Genet. 2002; 111:108-11.

Furukawa T, Fujisaki R, Yoshida Y, Kanai N, Sunamura M, Abe T, Takeda K, Matsuno S, Horii A. Distinct progression pathways involving the dysfunction of DUSP6/MKP-3 in pancreatic intraepithelial neoplasia and intraductal papillary-mucinous neoplasms of the pancreas. Mod Pathol 2005; 18: 1034–42.

Ganjam GK, Dimova EY, Unterman TG, Kietzmann T. FoxO1 and HNF-4 are involved in regulation of hepatic glucokinase gene expression by resveratrol. J Biol Chem. 2009 Nov 6;284(45):30783-97

Gannon M, Herrera PL, Wright CV. Mosaic Cre-mediated recombination in pancreas using the pdx-1 enhancer/promoter. Genesis 2000; 26: 143–4.

Garrison WD, Battle MA, Yang C, Kaestner KH, Sladek FM, Duncan SA. Hepatocyte nuclear factor 4alpha is essential for embryonic development of the mouse colon. Gastroenterology. 2006 Apr;130(4):1207-20.

Georgia S, Bhushan A. Regulates the transition of beta-cells from quiescence to proliferation. Diabetes. 2006 Nov;55(11):2950-6. p27

Gidekel Friedlander SY, Chu GC, Snyder EL, Girnius N, Dibelius G, Crowley D, Vasile E, DePinho RA, Jacks T. Context-dependent transformation of adult pancreatic cells by oncogenic K-Ras. Cancer Cell. 2009 Nov 6;16(5):379-89.

Gittes GK. Developmental biology of the pancreas: a comprehensive review. Dev Biol. 2009 Feb 1;326(1):4-35. Epub 2008 Oct 31.

Goggins M, Schutte M, Lu J, Moskaluk CA, Weinstein CL, Petersen GM, Yeo CJ, Jackson CE, Lynch HT, Hruban RH, Kern SE. Germline BRCA2 gene mutations in patients with apparently sporadic pancreatic carcinomas. Cancer Res. 1996 56:5360–64

Gonzalez FJ. Regulation of hepatocyte nuclear factor 4 alpha-mediated transcription. Drug Metab Pharmacokinet. 2008;23(1):2-7. Review.

Gorgoulis VG, Vassiliou LV, Karakaidos P, Zacharatos P, Kotsinas A, Liloglou T, Venere M, Ditullio RA Jr, Kastrinakis NG, Levy B, Kletsas D, Yoneta A, Herlyn M, Kittas C, Halazonetis TD. Activation of the DNA damage checkpoint and genomic instability in human precancerous lesions. Nature 2005 434, 907–913.

Goulley J, Dahl U, Baeza N, Mishina Y, Edlund H. BMP4-BMPR1A signaling in beta cells is required for and augments glucose-stimulated insulin secretion Cell. Metab., 5 (2007), pp. 207–219

Goumans MJ, Valdimarsdottir G, Itoh S, Lebrin F, Larsson J, Mummery C, Karlsson S, ten Dijke P. Activin receptor‐like kinase (ALK)1 is an antagonistic mediator of lateral TGFβ/ALK5 signaling. Mol. Cell 2003 12, 817–828.

Granot D, Snyder M. Glucose induces cAMP-independent growth-related changes in stationary-phase cells of Saccharomyces cerevisiae. Proc Natl Acad Sci U S A. 1991 Jul 1;88(13):5724-8.

Gray AM, Mason AJ. Requirement for activin A and transforming growth factor--beta 1 pro-regions in homodimer assembly. Science 1990; 247:1328–1330.

Groden J, Thliveris A, Samowitz W, Carlson M, Gelbert L, Albertsen H, Joslyn G, Stevens J, Spirio L, Robertson M, Sargeant L, Krapcho K, Wolff E, Burt R, Hughes JP, Warrington J, McPherson J, Wasmuth J, Paslier DL, Abderrahim H, Cohen D, Leppert M, White R. Identification and characterization of the familial adenomatous polyposis coli gene. Cell 66, 589–600 (1991).

Gu Z, Reynolds EM, Song J, Lei H, Feijen A, Yu L, He W, MacLaughlin DT, van den Eijnden-van Raaij J, Donahoe PK, Li E. The type I serine/threonine kinase receptor ActRIA (ALK2) is required for gastrulation of the mouse embryo. Development. 1999 Jun;126(11):2551-61.

Gu G, Dubauskaite J, Melton DA. 2002. Direct evidence for the pancreatic lineage: NGN3+ cells are islet progenitors and are distinct from duct progenitors. Development 129:2447–57

Guasch G, Schober M, Pasolli HA, Conn EB, Polak L, Fuchs E. Loss of TGFbeta signaling destabilizes homeostasis and promotes squamous cell carcinomas in stratified epithelia. Cancer Cell. 2007 Oct;12(4):313-27.

Guasch G, Schober M, Pasolli HA, Conn EB, Polak L, Fuchs E. Loss of TGFbeta signaling destabilizes homeostasis and promotes squamous cell carcinomas in stratified epithelia. Cancer Cell 2007;

Guerra C, Schuhmacher AJ, Cañamero M, Grippo PJ, Verdaguer L, Pérez-Gallego L, Dubus P, Sandgren EP, Barbacid M. Chronic pancreatitis is essential for induction of pancreatic ductal adenocarcinoma by K-Ras oncogenes in adult mice. Cancer Cell. 2007 Mar;11(3):291-302.

Guerra C, Mijimolle N, Dhawahir A, Dubus P, Barradas M, Serrano M, Campuzano V, Barbacid M. Tumor induction by an endogenous K-ras oncogene is highly dependent on cellular context. Cancer Cell. 2003 Aug;4(2):111-20.

Gupta S, Ramjaun AR, Haiko P, Wang Y, Warne PH, Nicke B, Nye E, Stamp G, Alitalo K, Downward J. Binding of ras to phosphoinositide 3-kinase p110alpha is required for ras-driven tumorigenesis in mice. Cell. 2007 Jun 1;129(5):957-68.

Gupta, R. K., Vatamaniuk, M. Z., Lee, C. S., Flaschen, R. C., Fulmer, J. T., Matschinsky, F. M., Duncan, S. A. and Kaestner, K. H.: The MODY1 gene HNF-4alpha regulates selected genes involved in insulin secretion. J Clin Invest, 115: 1006–1015 (2005).

Guz Y, Montminy MR, Stein R, Leonard J, Gamer LW, Wright CV, Teitelman G. Expression of murine STF-1, a putative insulin gene transcription factor, in beta cells of pancreas, duodenal epithelium and pancreatic exocrine and endocrine progenitors during ontogeny. Development. 1995 Jan;121(1):11-8.

Haeno H, Gonen M, Davis MB, Herman JM, Iacobuzio-Donahue CA, Michor F. Computational modeling of pancreatic cancer reveals kinetics of metastasis suggesting optimum treatment strategies. Cell. 2012 Jan 20;148(1-2):362-75. doi: 10.1016/j.cell.2011.11.060.

Haegebarth Andrea; Clevers Hans. Wnt Signaling, Lgr5, and Stem Cells in the Intestine and Skin American Journal Of Pathology, Volume: 174 Issue: 3 Pages: 715-721

Hahn SA, Schutte M, Hoque AT, Moskaluk CA, da Costa LT, Rozenblum E, Weinstein CL, Fischer A, Yeo CJ, Hruban RH, Kern SE. DPC4, a candidate tumor suppressor gene at human chromosome 18q21.1. Science. 1996;271:350–353.

Hart MJ, de los Santos R, Albert IN, Rubinfeld B, Polakis P. 1998. Downregulation of beta-catenin by human Axin and its association with the APC tumor suppressor, beta-catenin and GSK3 beta. Curr. Biol. 8:573–81

Hayhurst, G. P., Lee, Y. H., Lambert, G.,Ward, J. M. and Gonzalez, F. J.: Hepatocyte nuclear factor 4alpha (nuclear receptor 2A1) is essential for maintenance of hepatic gene expression and lipid homeostasis. Mol Cell Biol, 21: 1393–1403 (2001).

He TC, Sparks AB, Rago C, Hermeking H, Zawel L, da Costa LT, Morin PJ, Vogelstein B, Kinzler KW. Identification of c-MYC as a target of the APC pathway. Science. 1998 Sep 4;281(5382):1509-12.

He, W., Dorn, D.C., Erdjument-Bromage, H., Tempst, P., Moore, M.A., and Massagué, J. (2006). Hematopoiesis controlled by distinct TIF1gamma and Smad4 branches of the TGFbeta pathway. Cell 125, 929–941.

Heider, T. R., Lyman, S., Schoonhoven, R. & Behrns, K. E. Ski promotes tumor growth through abrogation of transforming growth factor-β signaling in pancreatic cancer. Ann. Surg. 246, 61–68 (2007).

Heiser PW, Lau J, Taketo MM, Herrera PL, Hebrok M. Stabilization of beta-catenin impacts pancreas growth. Development. 2006 May;133(10):2023-32. Epub 2006 Apr 12.

Heldin, C. H., Miyazono, K. & ten Dijke, P. TGF−β signalling from cell membrane to nucleus through SMAD proteins. Nature 390, 465–471 (1997).

Herrera B, van Dinther M, Ten Dijke P, Inman GJ. Autocrine bone morphogenetic protein-9 signals through activin receptor-like kinase-2/Smad1/Smad4 to promote ovarian cancer cell proliferation. Cancer Res. 2009 Dec 15;69(24):9254-62.

Hidalgo, Manuel, Pancreatic cancer; 362;17 nejm.org april 29, 2010

Hingorani SR, Petricoin EF, Maitra A, Rajapakse V, King C, Jacobetz MA, Ross S, Conrads TP, Veenstra TD, Hitt BA, Kawaguchi Y, Johann D, Liotta LA, Crawford HC, Putt ME, Jacks T, Wright CV, Hruban RH, Lowy AM, Tuveson DA. Preinvasive and invasive ductal pancreatic cancer and its early detection in the mouse. Cancer Cell. 2003 Dec;4(6):437-50.

Hiroaki Ikushima1 & Kohei Miyazono TGFβ signalling: a complex web in cancer progression. Nature Reviews Cancer 10, 415-424 (June 2010) | doi:10.1038/nrc2853

Hirota K, Sakamaki J, Ishida J, Shimamoto Y, Nishihara S, Kodama N, Ohta K, Yamamoto M, Tanimoto K, Fukamizu A. A combination of HNF-4 and Foxo1 is required for reciprocal transcriptional regulation of glucokinase and glucose-6-phosphatase genes in response to fasting and feeding. J Biol Chem. 2008 Nov 21;283(47):32432-41.

Hirota K., Daitoku H., Matsuzaki H., Araya N., Yamagata K., Asada S., Sugaya T., Fukamizu A. (2003) J. Biol. Chem. 278, 13056–13060

Holland AM, Hale MA, Kagami H, Hammer RE, MacDonald RJ. 2002. Experimental control of pancreatic development and maintenance. Proc. Natl. Acad. Sci. USA 99:12236–41

Hong YH, Varanasi US, Yang W, Leff T. AMP-activated protein kinase regulates HNF4alpha transcriptional activity by inhibiting dimer formation and decreasing protein stability. J Biol Chem. 2003 Jul 25;278(30):27495-501.

Hoshino M, Nakamura S, Mori K, Kawauchi T, Terao M, Nishimura YV, Fukuda A, Fuse T, Matsuo N, Sone M, Watanabe M, Bito H, Terashima T, Wright CV, Kawaguchi Y, Nakao K, Nabeshima Y. Ptf1a, a bHLH transcriptional gene, defines GABAergic neuronal fates in cerebellum. Neuron. 2005 Jul 21;47(2):201-13.

Hotz B, Arndt M, Dullat S, Bhargava S, Buhr HJ, Hotz HG. Epithelial to mesenchymal transition: expression of the regulators snail, slug, and twist in pancreatic cancer. Clin Cancer Res. 2007 Aug 15;13(16):4769-76.

Howe JR, Roth S, Ringold JC, Summers RW, Järvinen HJ, Sistonen P, Tomlinson IP, Houlston RS, Bevan S, Mitros FA, Stone EM, Aaltonen LA. Mutations in the SMAD4/DPC4 gene in juvenile polyposis. Science. 1998 May 15;280(5366):1086-8

Howe JR, Shellnut J, Wagner B, Ringold JC, Sayed MG, Ahmed AF, Lynch PM, Amos CI, Sistonen P, Aaltonen LA. Common deletion of SMAD4 in juvenile polyposis is a mutational hotspot. Am J Hum Genet. 2002 May;70(5):1357-62. Epub 2002 Mar 27.

Hruban RH, Adsay NV, Albores-Saavedra J, Anver MR, Biankin AV, Boivin GP, Furth EE, Furukawa T, Klein A, Klimstra DS, Kloppel G, Lauwers GY, Longnecker DS, Luttges J, Maitra A, Offerhaus GJ, Pérez-Gallego L, Redston M, Tuveson DA. Pathology of genetically engineered mouse models of pancreatic exocrine cancer: consensus report and recommendations. Cancer Res. 2006 Jan 1;66(1):95-106.

Hruban RH, Goggins M, Parsons J, Kern SE. Progression model for pancreatic cancer. Clin Cancer Res 2000; 6: 2969–72.

Hruban RH, Klimstra DS, Pitman MB. 2006. Tumors of the Pancreas. Washington, DC: Armed Forces Inst. Pathol.

Hruban RH, Maitra A, Goggins M. Update on pancreatic intraepithelial neoplasia. Int J Clin Exp Pathol 2008; 1: 306–16.

Huang SM, Mishina YM, Liu S, Cheung A, Stegmeier F, Michaud GA, Charlat O, Wiellette E, Zhang Y, Wiessner S, Hild M, Shi X, Wilson CJ, Mickanin C, Myer V, Fazal A, Tomlinson R, Serluca F, Shao W, Cheng H, Shultz M, Rau C, Schirle M, Schlegl J, Ghidelli S, Fawell S, Lu C, Curtis D, Kirschner MW, Lengauer C, Finan PM, Tallarico JA, Bouwmeester T, Porter JA, Bauer A, Cong F. Tankyrase inhibition stabilizes axin and antagonizes Wnt signalling. Nature. 2009 Oct 1;461(7264):614-20.

Iacobuzio-Donahue CA, Klimstra DS, Adsay NV, Wilentz RE, Argani P, Sohn TA, Yeo CJ, Cameron JL, Kern SE, Hruban RH. Dpc-4 protein is expressed in virtually all human intraductal papillary mucinous neoplasms of the pancreas: comparison with conventional ductal adenocarcinomas. Am J Pathol. 2000 Sep;157(3):755-61.

Iacobuzio-Donahue CA, Fu B, Yachida S, Luo M, Abe H, Henderson CM, Vilardell F, Wang Z, Keller JW, Banerjee P, Herman JM, Cameron JL, Yeo CJ, Halushka MK, Eshleman JR, Raben M, Klein AP, Hruban RH, Hidalgo M, Laheru D. DPC4 gene status of the primary carcinoma correlates with patterns of failure in patients with pancreatic cancer. J Clin Oncol. 2009 Apr 10;27(11):1806-13. doi: 10.1200/JCO.2008.17.7188.

Ijichi H, Chytil A, Gorska AE, Aakre ME, Fujitani Y, Fujitani S, Wright CV, Moses HL. Aggressive pancreatic ductal adenocarcinoma in mice caused by pancreas-specific blockade of transforming growth factor-beta signaling in cooperation with active Kras expression. Genes Dev. 2006 Nov 15;20(22):3147-60.

Indra A.K., Warot, X., Brocard, J., Bornert, J.M., Xiao, J.H., Chambon, P., and Metzger, D. 1999. Temporally-controlled site-specific mutagenesis in the basal layer of the epidermis: Comparison of the recombinase activity of the tamoxifen-inducible Cre-ER(T) and Cre-ER(T2) recombinases. Nucleic Acids Res. 27: 4324-4327.

Inman GJ, Nicolás FJ, Callahan JF, Harling JD, Gaster LM, Reith AD, Laping NJ, Hill CS. SB-431542 is a potent and specific inhibitor of transforming growth factor-beta superfamily type I activin receptor-like kinase (ALK) receptors ALK4, ALK5, and ALK7. Mol Pharmacol. 2002 Jul;62(1):65-74.

Inoue, Y., Hayhurst, G. P., Inoue, J., Mori, M. and Gonzalez, F. J.: Defective ureagenesis in mice carrying a liver-specific disruption of hepatocyte nuclear factor 4alpha (HNF4alpha). HNF4alpha regulates ornithine transcarbamylase in vivo. J Biol Chem, 277: 25257–25265 (2002).

Inoue, Y., Peters, L. L., Yim, S. H., Inoue, J. and Gonzalez, F. J.: Role of hepatocyte nuclear factor 4alpha in control of blood coagulation factor gene expression. J Mol Med, 84: 334–344 (2006).

Inoue, Y., Yu, A. M., Inoue, J. and Gonzalez, F. J.: Hepatocyte nuclear factor 4alpha is a central regulator of bile acid conjugation. J Biol Chem, 279: 2480–2489 (2004).

Inoue, Y., Yu, A. M., Yim, S. H., Ma, X., Krausz, K. W., Inoue, J., Xiang, C. C., Brownstein, M. J., Eggertsen, G., Bjorkhem, I. and Gonzalez, F. J.: Regulation of bile acid biosynthesis by hepatocyte nuclear factor 4alpha. J Lipid Res, 47: 215–227 (2006).

Iynedjian PB, Gjinovci A, Renold AE. Stimulation by insulin of glucokinase gene transcription in liver of diabetic rats. J Biol Chem. 1988 Jan 15;263(2):740-4.

Iynedjian PB, Jotterand D, Nouspikel T, Asfari M, Pilot PR. Transcriptional induction of glucokinase gene by insulin in cultured liver cells and its repression by the glucagon-cAMP system. J Biol Chem. 1989 Dec 25;264(36):21824-9.

Iynedjian PB, Pilot PR, Nouspikel T, Milburn JL, Quaade C, Hughes S, Ucla C, Newgard CB. Differential expression and regulation of the glucokinase gene in liver and islets of Langerhans. Proc Natl Acad Sci U S A. 1989 Oct;86(20):7838-42.

Jackson EL, Willis N, Mercer K, Bronson RT, Crowley D, Montoya R, Jacks T, Tuveson DA. Analysis of lung tumor initiation and progression using conditional expression of oncogenic K-ras. Genes Dev. 2001 Dec 15;15(24):3243-8.

Jaffee, E.M., Hruban, R.H., Canto, M., and Kern, S.E. (2002). Focus on pancreas cancer. Cancer Cell 2, 25–28.

Jenne DE, Reimann H, Nezu J, Friedel W, Loff S, Jeschke R, Müller O, Back W, Zimmer M. Peutz-Jeghers syndrome is caused by mutations in a novel serine threonine kinase. Nat Genet. 1998 Jan;18(1):38-43.

Jensen J, Heller RS, Funder-Nielsen T, Pedersen EE, Lindsell C, Weinmaster G, Madsen OD, Serup P. Independent development of pancreatic alpha- and beta-cells from neurogenin3-expressing precursors: a role for the notch pathway in repression of premature differentiation. Diabetes. 2000 Feb;49(2):163-76.

Jho EH, Zhang T, Domon C, Joo CK, Freund JN, Costantini F. Wnt/beta-catenin/Tcf signaling induces the transcription of Axin2, a negative regulator of the signaling pathway. Mol Cell Biol. 2002 Feb;22(4):1172-83.

Ji H, Ramsey MR, Hayes DN, Fan C, McNamara K, Kozlowski P, Torrice C, Wu MC, Shimamura T, Perera SA, Liang MC, Cai D, Naumov GN, Bao L, Contreras CM, Li D, Chen L, Krishnamurthy J, Koivunen J, Chirieac LR, Padera RF, Bronson RT, Lindeman NI, Christiani DC, Lin X, Shapiro GI, Jänne PA, Johnson BE, Meyerson M, Kwiatkowski DJ, Castrillon DH, Bardeesy N, Sharpless NE, Wong KK. LKB1 modulates lung cancer differentiation and metastasis. Nature. 2007 Aug 16;448(7155):807-10. Epub 2007 Aug 5.

Jiang G, Nepomuceno L, Hopkins K, Sladek FM. Exclusive homodimerization of the orphan receptor hepatocyte nuclear factor 4 defines a new subclass of nuclear receptors. Mol Cell Biol. 1995 Sep;15(9):5131-43.

Jimeno A, Hidalgo M. Molecular biomarkers: their increasing role in the diagnosis, characterization, and therapy guidance in pancreatic cancer. Mol Cancer Ther. 2006 Apr;5(4):787-96.

Morris JP 4th, Wang SC, Hebrok M. KRAS, Hedgehog, Wnt and the twisted developmental biology of pancreatic ductal adenocarcinoma.Nat Rev Cancer. 2010 Oct;10(10):683-95. doi: 10.1038/nrc2899.

Johnson L, Greenbaum D, Cichowski K, Mercer K, Murphy E, Schmitt E, Bronson RT, Umanoff H, Edelmann W, Kucherlapati R, Jacks T. K-ras is an essential gene in the mouse with partial functional overlap with N-ras. Genes Dev. 1997 Oct 1;11(19):2468-81.

Johnson L, Mercer K, Greenbaum D, Bronson RT, Crowley D, Tuveson DA, Jacks T. Somatic activation of the K-ras oncogene causes early onset lung cancer in mice. Nature. 2001 Apr 26;410(6832):1111-6.

Jones S, Chen WD, Parmigiani G, Diehl F, Beerenwinkel N, Antal T, Traulsen A, Nowak MA, Siegel C, Velculescu VE, Kinzler KW, Vogelstein B, Willis J, Markowitz SD. Comparative lesion sequencing provides insights into tumor evolution. Proc Natl Acad Sci U S A. 2008 Mar 18;105(11):4283-8. doi: 10.1073/pnas.0712345105. Epub 2008 Mar 12.

Jones S, Zhang X, Parsons DW, Lin JC, Leary RJ, Angenendt P, Mankoo P, Carter H, Kamiyama H, Jimeno A, Hong SM, Fu B, Lin MT, Calhoun ES, Kamiyama M, Walter K, Nikolskaya T, Nikolsky Y, Hartigan J, Smith DR, Hidalgo M, Leach SD, Klein AP, Jaffee EM, Goggins M, Maitra A, Iacobuzio-Donahue C, Eshleman JR, Kern SE, Hruban RH, Karchin R, Papadopoulos N, Parmigiani G, Vogelstein B, Velculescu VE, Kinzler KW. Core signaling pathways in human pancreatic cancers revealed by global genomic analyses. Science. 2008 Sep 26;321(5897):1801-6. doi: 10.1126/science.1164368. Epub 2008 Sep 4.

Jornvall H, Blokzijl A, ten Dijke P, Ibanez CF (2001) The orphan receptor serine/threonine kinase ALK7 signals arrest of proliferation and morphological differentiation in a neuronal cell line. J Biol Chem 276:5140–5146.

Julian Downward, Targeting RAS signalling pathways in cancer therapy. Nature Reviews Cancer 3, 11-22 (January 2003)

Jungermann K, Kietzmann T. Zonation of parenchymal and nonparenchymal metabolism in liver. Annu Rev Nutr. 1996;16:179-203. Review.

Nolop KB, Rhodes CG, Brudin LH, Beaney RP, Krausz T, Jones T, Hughes JM. Glucose utilization in vivo by human pulmonary neoplasms. Cancer. 1987 Dec 1;60(11):2682-9.

Kang Y, He W, Tulley S, Gupta GP, Serganova I, Chen CR, Manova-Todorova K, Blasberg R, Gerald WL, Massagué J. Breast cancer bone metastasis mediated by the Smad tumor suppressor pathway. Proc Natl Acad Sci U S A. 2005 Sep 27;102(39):13909-14. Epub 2005 Sep 19. Erratum in: Proc Natl Acad Sci U S A. 2006 May 30;103(22):8570.

Kawaguchi Y, Cooper B, Gannon M, Ray M, MacDonald RJ, Wright CV. The role of the transcriptional regulator Ptf1a in converting intestinal to pancreatic progenitors. Nat Genet. 2002 Sep;32(1):128-34.

Kern, S. E., Pietenpol, J. A., Thiagalingam, S., Seymour, A., Kinzler, K. W. and Vogelstein, B. (1992) Oncogenic forms of p53 inhibit p53-regulated gene expression. Science 256, 827-830

Khalaf WF, White H, Wenning MJ, Orazi A, Kapur R, Ingram DA. K-Ras is essential for normal fetal liver erythropoiesis. Blood. 2005 May 1;105(9):3538-41. Epub 2005 Jan 11.

Khatri, S., Yepiskoposyan, H., Gallo, C. A., Tandon, P. & Plas, D. R. FOXO3a regulates glycolysis via transcriptional control of tumor suppressor TSC1. J. Biol. Chem. 285, 15960–15965 (2010).

Kim, W. Y. & Sharpless, N. E. The regulation of INK4/ARF in cancer and aging. Cell 127, 265–275 (2006).

Kishida S, Yamamoto H, Ikeda S, Kishida M, Sakamoto I, Koyama S, Kikuchi A.. Axin, a negative regulator of the wnt signaling pathway, directly interacts with adenomatous polyposis coli and regulates the stabilization of beta-catenin. 1998 J. Biol. Chem. 273:10823–26

Klaus A, Birchmeier W. Wnt signalling and its impact on development and cancer. Nat Rev Cancer. 2008 May;8(5):387-98. doi: 10.1038/nrc2389.

Klimstra D.S., Longnecker D.S. (1994) K-ras mutations in pancreatic ductal proliferative lesions. Am. J. Pathol. 145:1547–1550.

Koera K, Nakamura K, Nakao K, Miyoshi J, Toyoshima K, Hatta T, Otani H, Aiba A, Katsuki M. K-ras is essential for the development of the mouse embryo. Oncogene 15, 1151–1159 (1997).

Korinek V, Barker N, Moerer P, van Donselaar E, Huls G, Peters PJ, Clevers H. Depletion of epithelial stem-cell compartments in the small intestine of mice lacking Tcf-4. Nat Genet. 1998 Aug;19(4):379-83.

Korinek V, Barker N, Morin PJ, van Wichen D, de Weger R, Kinzler KW, Vogelstein B, Clevers H. Constitutive transcriptional activation by a beta-catenin-Tcf complex in APC−/− colon carcinoma. Science. 1997;275:1784–1787

Krapp A, Knöfler M, Ledermann B, Bürki K, Berney C, Zoerkler N, Hagenbüchle O, Wellauer PK. The bHLH protein PTF1-p48 is essential for the formation of the exocrine and the correct spatial organization of the endocrine pancreas. 1998 Genes Dev. 12:3752–63

Kuilman T, Michaloglou C, Mooi WJ, Peeper DS. The essence of senescence. Genes Dev. 2010 Nov 15;24(22):2463-79. doi: 10.1101/gad.1971610.

Lehninger L, Nelson DL , Cox MM, Principles of Biochemistry (Worth, New York, ed. 2, 1993).

Lammi L, Arte S, Somer M, Jarvinen H, Lahermo P, Thesleff I, Pirinen S, Nieminen P. (2004) Mutations in AXIN2 cause familial tooth agenesis and predispose to colorectal cancer. Am J Hum Genet 74:1043–1050.

Lammi L, Arte S, Somer M, Jarvinen H, Lahermo P, Thesleff I, Pirinen S, Nieminen P. Gain of function of a p53 hot spot mutation in a mouse model of Li-Fraumeni syndrome. Cell 119, 861–872 (2004).

Lassus, P., Ferlin, M., Piette, J. & Hibner, U. Anti-apoptotic activity of low levels of wild type p53. EMBO J. 15, 4566–4573 (1996).

Latres E, Chiaur DS, Pagano M. 1999. The human F box protein beta-Trcp associates with the Cul1/Skp1 complex and regulates the stability of beta-catenin. Oncogene 18:849–54

Leach SD. Mouse models of pancreatic cancer: the fur is finally flying! Cancer Cell. 2004 Jan;5(1):7-11.

Leclerc I, Lenzner C, Gourdon L, Vaulont S, Kahn A, Viollet B. Hepatocyte nuclear factor-4alpha involved in type 1 maturity-onset diabetes of the young is a novel target of AMP-activated protein kinase. Diabetes. 2001 Jul;50(7):1515-21.

Leonard J, Peers B, Johnson T, Ferreri K, Lee S, Montminy MR 1993 Characterization of somatostatin transactivating factor-1, a novel homeobox factor that stimulates somatostatin expression in pancreatic islet cells. Mol Endocrinol 7:1275–1283

Li A, Omura N, Hong SM, Vincent A, Walter K, Griffith M, Borges M, Goggins M. Pancreatic cancers epigenetically silence SIP1 and hypomethylate and overexpress miR-200a/200b in association with elevated circulating miR-200a and miR-200b levels. Cancer Res. 2010 Jul 1;70(13):5226-37. doi: 10.1158/0008-5472.CAN-09-4227.

Li W, Qiao W, Chen L, Xu X, Yang X, Li D, Li C, Brodie SG, Meguid MM, Hennighausen L, Deng CX. Squamous cell carcinoma and mammary abscess formation through squamous metaplasia in Smad4/Dpc4 conditional knockout mice. Development. 2003 Dec;130(24):6143-53.

Li H, Arber S, Jessell TM, Edlund H 1999 Selective agenesis of the dorsal pancreas in mice lacking homeobox gene Hlxb9. Nat Genet 23:67-70

Liang J, Shao SH, Xu ZX, Hennessy B, Ding Z, Larrea M, Kondo S, Dumont DJ, Gutterman JU, Walker CL, Slingerland JM, Mills GB. The energy sensing LKB1-AMPK pathway regulates p27(kip1) phosphorylation mediating the decision to enter autophagy or apoptosis. Nat Cell Biol. 2007 Feb;9(2):218-24.

Lillemoe KD, Yeo CJ, Cameron JL. Cameron Pancreatic cancer: State-of-the-art care CA Cancer J. Clin., 50 (2000), pp. 241–268

Liu C, Kato Y, Zhang Z, Do VM, Yankner BA, He X. 1999. beta-Trcp couples beta-catenin phosphorylation-degradation and regulates Xenopus axis formation. Proc. Natl. Acad. Sci. USA 96:6273–78

Liu C, Li Y, Semenov M, Han C, Baeg GH, Tan Y, Zhang Z, Lin X, He X. 2002. Control of beta-catenin phosphorylation/degradation by a dual-kinase mechanism. Cell 108:837–47

Liu DP, Song H, Xu Y. A common gain of function of p53 cancer mutants in inducing genetic instability. Oncogene. 2010 Feb 18;29(7):949-56.

Liu, C., Y. Li, M. Semenov, C. Han, G.H. Baeg, Y. Tan, Z. Zhang, X. Lin, and X. He. 2002. Control of beta-catenin phosphorylation/degradation by a dual-kinase mechanism. Cell. 108:837–847. doi:10.1016/S0092- 8674(02)00685-2

Liu G, Parant JM, Lang G, Chau P, Chavez-Reyes A, El-Naggar AK, Multani A, Chang S, Lozano G. Chromosome stability, in the absence of apoptosis, is critical for suppression of tumorigenesis in Trp53 mutant mice. Nature Genet. 36, 63–68 (2004).

Liu G, McDonnell TJ, Montes de Oca Luna R, Kapoor M, Mims B, El-Naggar AK, Lozano G.. High metastatic potential in mice inheriting a targeted p53 missense mutation. Proc. Natl Acad. Sci. USA 97, 4174–4179 (2000).

Liu W, Dong X, Mai M, Seelan RS, Taniguchi K, Krishnadath KK, Halling KC, Cunningham JM, Boardman LA, Qian C, Christensen E, Schmidt SS, Roche PC, Smith DI, Thibodeau SN.. Mutations in AXIN2 cause colorectal cancer with defective mismatch repair by activating α-catenin/TCF signalling. *Nature Genet.* **26**, 146–147 (2000).

Liu IM, Schilling SH, Knouse KA, Choy L, Derynck R, Wang XF.TGFbeta-stimulated Smad1/5 phosphorylation requires the ALK5 L45 loop and mediates the pro-migratory TGFbeta switch. EMBO J. 2009 Jan 21;28(2):88-98. doi: 10.1038/emboj.2008.266.

Lizcano JM, Göransson O, Toth R, Deak M, Morrice NA, Boudeau J, Hawley SA, Udd L, Mäkelä TP, Hardie DG, Alessi DR. LKB1 is a master kinase that activates 13 kinases of the AMPK subfamily, including MARK/PAR-1. EMBO J. 2004 Feb 25;23(4):833-43.

Logan CY, Nusse R. The Wnt signaling pathway in development and disease. Annu Rev Cell Dev Biol. 2004;20:781-810.

Lowenfels AB, Maisonneuve P. 2006. Epidemiology and risk factors for pancreatic cancer. Best Pract. Res. Clin. Gastroenterol. 20:197–209

Lu SL, Herrington H, Reh D, Weber S, Bornstein S, Wang D, Li AG, Tang CF, Siddiqui Y, Nord J, Andersen P, Corless CL, Wang XJ. Loss of transforming growth factor-beta type II receptor promotes metastatic head-and-neck squamous cell carcinoma. Genes Dev., 20 (2006), pp. 1331-1342

Lucas Sd Sd, López-Alcorocho JM, Bartolomé J, Carreño V. Nitric oxide and TGF-beta1 inhibit HNF-4alpha function in HEPG2 cells. Biochem Biophys Res Commun. 2004 Aug 27;321(3):688-94.

Lustig B, Jerchow B, Sachs M, Weiler S, Pietsch T, Karsten U, van de Wetering M, Clevers H, Schlag PM, Birchmeier W, Behrens J. (2002) Negative feedback loop of Wnt signaling through upregulation of conductin/axin2 in colorectal and liver tumors. Mol Cell Biol 22:1184–1193.

MacDonald BT, Tamai K, He X. Wnt/beta-catenin signaling: components, mechanisms, and diseases. Dev Cell. 2009 Jul;17(1):9-26. Review.

Maitra, Anirban and Hruban, Ralph H. Pancreatic Cancer Annual Review of Pathology: Mechanisms of Disease 3: 157-188 (Volume publication date February 2008) DOI: 10.1146/annurev.pathmechdis.3.121806.154305

Mani SA, Guo W, Liao MJ, Eaton EN, Ayyanan A, Zhou AY, Brooks M, Reinhard F, Zhang CC, Shipitsin M, Campbell LL, Polyak K, Brisken C, Yang J, Weinberg RA. The epithelial-mesenchymal transition generates cells with properties of stem cells. Cell. 2008 May 16;133(4):704-15.

Manuel Hidalgo, M.D. Pancreatic Cancer N Engl J Med 2010; 362:1605-1617April 29, 201

Mazur, P.K., and Siveke, J.T. (2011). Gut. Genetically engineered mouse models of pancreatic cancer: unravelling tumour biology and progressing translational oncology. Published online August 26 2011. 10.1136/gutjnl- 2011-300756.

Miller CP, McGehee Jr RE, Habener JF 1994 IDX-1: a new homeodomain transcription factor expressed in rat pancreatic islets and duodenum that transactivates the somatostatin gene. EMBO J

Mills SE. Histology for Pathologists. third. Philadelphia: Lippincott Williams & Wilkins; 2007.

Ming Kwan K, Li AG, Wang XJ, Wurst W, Behringer RR. Essential roles of BMPR-IA signaling in differentiation and growth of hair follicles and in skin tumorigenesis. Genesis. 2004 May;39(1):10-25.

Mishina Y, Suzuki A, Ueno N, Behringer RR. 1995a. Bmpr encodes a type I bone morphogenetic protein receptor that is essential for gastrulation during mouse embryogenesis. Genes Dev 9:3027– 3037.

Miura, A., Yamagata, K., Kakei, M., Hatakeyama, H., Takahashi, N., Fukui, K., Nammo, T., Yoneda, K., Inoue, Y., Sladek, F. M., Magnuson, M. A., Kasai, H., Miyagawa, J., Gonzalez, F. J. and Shimomura, I.: Hepatocyte nuclear factor-4alpha is essential for glucose-stimulated insulin secretion by pancreatic beta-cells. J Biol Chem, 281: 5246–5257 (2006).

Mizutani A, Koinuma D, Tsutsumi S, Kamimura N, Morikawa M, Suzuki HI, Imamura T, Miyazono K, Aburatani H. Cell type-specific target selection by combinatorial binding of Smad2/3 proteins and hepatocyte nuclear factor 4alpha in HepG2 cells. J Biol Chem. 2011 Aug 26;286(34):29848-60.

Moreno-Sánchez R, Rodríguez-Enríquez S, Marín-Hernández A, Saavedra E. Energy metabolism in tumor cells. FEBS J. 2007 Mar;274(6):1393-418.

Morin PJ, Sparks AB, Korinek V, Barker N, Clevers H, Vogelstein B, Kinzler KW. Activation of beta-catenin-Tcf signaling in colon cancer by mutations in beta-catenin or APC. Science. 1997;275:1787–1790.

Morita H, Mazerbourg S, Bouley DM, Luo CW, Kawamura K, Kuwabara Y, Baribault H, Tian H, Hsueh AJ. Neonatal lethality of LGR5 null mice is associated with ankyloglossia and gastrointestinal distension. Mol Cell Biol. 2004 Nov;24(22):9736-43.

Morrisey EE, Tang Z, Sigrist K, Lu MM, Jiang F, Ip HS, Parmacek MS. GATA6 regulates HNF4 and is required for differentiation of visceral endoderm in the mouse embryo. Genes Dev. 1998 Nov 15;12(22):3579-90.

Morrone S, Cheng Z, Moon RT, Cong F, Xu W. Crystal structure of a Tankyrase-Axin complex and its implications for Axin turnover and Tankyrase substrate recruitment. Proc Natl Acad Sci U S A. 2012 Jan 31;109(5):1500-5. Epub 2012 Jan 17.

Morton JP, Jamieson NB, Karim SA, Athineos D, Ridgway RA, Nixon C, McKay CJ, Carter R, Brunton VG, Frame MC, Ashworth A, Oien KA, Evans TR, Sansom OJ. LKB1 haploinsufficiency cooperates with Kras to promote pancreatic cancer through suppression of p21-dependent growth arrest. Gastroenterology. 2010 Aug;139(2):586-97, 597.e1-6.

Morton JP, Timpson P, Karim SA, Ridgway RA, Athineos D, Doyle B, Jamieson NB, Oien KA, Lowy AM, Brunton VG, Frame MC, Evans TR, Sansom OJ. Mutant p53 drives metastasis and overcomes growth arrest/senescence in pancreatic cancer. Proc Natl Acad Sci U S A. 2010 Jan 5;107(1):246-51.

Muller PA, Caswell PT, Doyle B, Iwanicki MP, Tan EH, Karim S, Lukashchuk N, Gillespie DA, Ludwig RL, Gosselin P, Cromer A, Brugge JS, Sansom OJ, Norman JC, Vousden KH. Mutant p53 drives invasion by promoting integrin recycling. Cell. 2009 Dec 24;139(7):1327-41. doi: 10.1016/j.cell.2009.11.026

Muñoz NM, Upton M, Rojas A, Washington MK, Lin L, Chytil A, Sozmen EG, Madison BB, Pozzi A, Moon RT, Moses HL, Grady WM. Transforming growth factor beta receptor type II inactivation induces the malignant transformation of intestinal neoplasms initiated by Apc mutation. Cancer Res. 2006 Oct 15;66(20):9837-44.

Murtaugh LC, Melton DA. Genes, signals, and lineages in pancreas development. Annu Rev Cell Dev Biol. 2003;19:71-89. Review.

Nakano H, Yamamoto F, Neville C, Evans D, Mizuno T, Perucho M. Isolation of transforming sequences of two human lung carcinomas: structural and functional analysis of the activated c-K-ras oncogenes. Proc Natl Acad Sci U S A. 1984 Jan;81(1):71-5.

Ning BF, Ding J, Yin C, Zhong W, Wu K, Zeng X, Yang W, Chen YX, Zhang JP, Zhang X, Wang HY, Xie WF.Hepatocyte nuclear factor 4 alpha suppresses the development of hepatocellular carcinoma. Cancer Res. 2010 Oct 1;70(19):7640-51.

Nogueira V, Park Y, Chen CC, Xu PZ, Chen ML, Tonic I, Unterman T, Hay N. Akt determines replicative senescence and oxidative or oncogenic premature senescence and sensitizes cells to oxidative apoptosis. Cancer Cell. 2008 Dec 9;14(6):458-70. doi: 10.1016/j.ccr.2008.11.003.

Odom DT, Zizlsperger N, Gordon DB, Bell GW, Rinaldi NJ, Murray HL, Volkert TL, Schreiber J, Rolfe PA, Gifford DK, Fraenkel E, Bell GI, Young RA. Control of pancreas and liver gene expression by HNF transcription factors. Science. 2004 Feb 27;303(5662):1378-81.

Oesterle EC, Chien WM, Campbell S, Nellimarla P, Fero ML. p27(Kip1) is required to maintain proliferative quiescence in the adult cochlea and pituitary. Cell Cycle. 2011 Apr 15;10(8):1237-48.

Offield MF, Jetton TL, Labosky PA, Ray M, Stein RW, Magnuson MA, Hogan BL, Wright CV.1996. PDX-1 is required for pancreatic outgrowth and differentiation of the rostral duodenum. Development 122:983–95

Oh SP, Seki T, Goss KA, Imamura T, Yi Y, Donahoe PK, Li L, Miyazono K,ten Dijke P, Kim S, Li E (2000) Activin receptor-like kinase 1 modulates transforming growth factor-β 1 signaling in the regulation of angiogenesis. Proc Natl Acad Sci USA 97:2626–2631.

Ohlsson H, Karlsson K, Edlund T 1993 IPF1, a homeodomain-containing transactivator of the insulin gene. EMBO J 12:4251–4259

Ohlsson H, Thor S, Edlund T 1991 Novel insulin promoter- and enhancer-binding proteins that discriminate between pancreatic α- and β-cells. Mol Endocrinol 5:897–904

Olive KP, Jacobetz MA, Davidson CJ, Gopinathan A, McIntyre D, Honess D, Madhu B, Goldgraben MA, Caldwell ME, Allard D, Frese KK, Denicola G, Feig C, Combs C, Winter SP,

Ireland-Zecchini H, Reichelt S, Howat WJ, Chang A, Dhara M, Wang L, Rückert F, Grützmann R, Pilarsky C, Izeradjene K, Hingorani SR, Huang P, Davies SE, Plunkett W, Egorin M, Hruban RH, Whitebread N, McGovern K, Adams J, Iacobuzio-Donahue C, Griffiths J, Tuveson DA.. Inhibition of Hedgehog signalling enhances delivery of chemotherapy in a mouse model of pancreatic cancer. Science 2009;324:1457-61.

Olive KP, Tuveson DA, Ruhe ZC, Yin B, Willis NA, Bronson RT, Crowley D, Jacks T. Mutant p53 gain of function in two mouse models of Li-Fraumeni syndrome. Cell. 2004 Dec 17;119(6):847-60.

Oshima M, Oshima H, Taketo MM. TGF-beta receptor type II deficiency results in defects of yolk sac hematopoiesis and vasculogenesis. Dev Biol. 1996 Oct 10;179(1):297-302.

Ouko, L., Ziegler, T. R., Gu, L. H., Eisenberg, L. M. & Yang, V. W. Wnt11 signaling promotes proliferation, transformation, and migration of IEC6 intestinal epithelial cells. J. Biol. Chem. 279, 26707–26715 (2004).

Pangas SA, Li X, Umans L, Zwijsen A, Huylebroeck D, Gutierrez C, Wang D, Martin JF, Jamin SP, Behringer RR, Robertson EJ, Matzuk MM. Conditional deletion of Smad1 and Smad5 in somatic cells of male and female gonads leads to metastatic tumor development in mice. Mol Cell Biol. 2008 Jan;28(1):248-57.

Pannala R, Leirness JB, Bamlet WR, Basu A, Petersen GM, Chari ST. Prevalence and clinical profi le of pancreatic cancerassociated diabetes mellitus. Gastroenterology 2008; 134: 981–87.

Peshavaria M, Gamer L, Henderson E, Teitelman G, Wright CV, Stein R 1994 XIHbox 8, an endoderm-specific Xenopus homeodomain protein, is closely related to a mammalian insulin gene transcription factor. Mol Endocrinol 8:806–816

Polager, S. & Ginsberg, D. p53 and E2f: partners in life and death. Nature Rev. Cancer 9, 738–748 (2009).

Polakis, P. The many ways of Wnt in cancer. Curr. Opin. Genet. Dev. 17, 45–51 (2007).

Polakis, P. Wnt signaling and cancer. Genes Dev. 14, 1837–1851 (2000).

Potenza N, Vecchione C, Notte A, De Rienzo A, Rosica A, Bauer L, Affuso A, De Felice M, Russo T, Poulet R, Cifelli G, De Vita G, Lembo G, Di Lauro R. Replacement of K-Ras with H-Ras supports normal embryonic development despite inducing cardiovascular pathology in adult mice. EMBO Rep. 2005 May;6(5):432-7.

Pylayeva-Gupta Y, Grabocka E, Bar-Sagi D. RAS oncogenes: weaving a tumorigenic web. Nat Rev Cancer. 2011 Oct 13;11(11):761-74. doi: 10.1038/nrc3106.

Redston MS, Caldas C, Seymour AB, Hruban RH, da Costa L, Yeo CJ, Kern SE. 1994. p53 mutations in pancreatic carcinoma and evidence of common involvement of homocopolymer tracts in DNA microdeletions. Cancer Res. 54:3025–33

Rhee, J., Inoue, Y., Yoon, J. C., Puigserver, P., Fan, M., Gonzalez, F. J. and Spiegelman, B. M.: Regulation of hepatic fasting response by PPARgamma coactivator-1alpha (PGC-1): requirement for hepatocyte nuclear factor 4alpha in gluconeogenesis. Proc Natl Acad Sci USA, 100: 4012–4017 (2003).

Riley T, Sontag E, Chen P, Levine A. Transcriptional control of human p53-regulated genes. Nat Rev Mol Cell Biol. 2008 May;9(5):402-12. Review.

Rinehart J, Adjei AA, Lorusso PM, Waterhouse D, Hecht JR, Natale RB, Hamid O, Varterasian M, Asbury P, Kaldjian EP, Gulyas S, Mitchell DY, Herrera R, Sebolt-Leopold JS, Meyer MB.

Multicenter phase II study of the oral MEK inhibitor, CI-1040, in patients with advanced non-small-cell lung, breast, colon, and pancreatic cancer, J Clin Oncol. 2004 Nov 15;22(22):4456-62.

Rivera F, López-Tarruella S, Vega-Villegas ME, Salcedo M. Treatment of advanced pancreatic cancer: from gemcitabine single agent to combinations and targeted therapy. Cancer Treat Rev. 2009 Jun;35(4):335-9. Epub 2009 Jan 7. Review.

Robertson RP. Chronic oxidative stress as a central mechanism for glucose toxicity in pancreatic islet beta cells in diabetes. J Biol Chem. 2004 Oct 8;279(41):42351-4.

Rollwagen, FM, Yu ZY, Li YY & Pacheco ND. IL-6 rescues enterocytes from hemorrhage induced apoptosis in vivo and in vitro by a bcl-2 mediated mechanism. Clin. Immunol. Immunopathol. 89, 205–213 (1998).

Roth U, Curth K, Unterman TG, Kietzmann T. The transcription factors HIF-1 and HNF-4 and the coactivator p300 are involved in insulin-regulated glucokinase gene expression via the phosphatidylinositol 3-kinase/protein kinase B pathway. J Biol Chem. 2004 Jan 23;279(4):2623-31.

Rozenblum E, Schutte M, Goggins M, Hahn SA, Panzer S, Zahurak M, Goodman SN, Sohn TA, Hruban RH, Yeo CJ, Kern SE. Tumor-suppressive pathways in pancreatic carcinoma. Cancer Res. 1997 May 1;57(9):1731-4

Sansom OJ, Reed KR, Hayes AJ, Ireland H, Brinkmann H, Newton IP, Batlle E, Simon-Assmann P, Clevers H, Nathke IS, Clarke AR, Winton DJ. Loss of Apc in vivo immediately perturbs Wnt signaling, differentiation, and migration. Genes Dev. 2004 Jun 15;18(12):1385-90.

Santos E, Martin-Zanca D, Reddy EP, Pierotti MA, Della Porta G, Barbacid M. Malignant activation of a K-ras oncogene in lung carcinoma but not in normal tissue of the same patient. Science 223, 661–664 (1984).

Satoh S, Daigo Y, Furukawa Y, Kato T, Miwa N, Nishiwaki T, Kawasoe T, Ishiguro H, Fujita M, Tokino T, Sasaki Y, Imaoka S, Murata M, Shimano T, Yamaoka Y, Nakamura Y. AXIN1 mutations in hepatocellular carcinomas, and growth suppression in cancer cells by virus-mediated transfer of AXIN1. *Nature Genet.* **24**, 245–250 (2000).

Scheffzek K, Ahmadian MR, Kabsch W, Wiesmüller L, Lautwein A, Schmitz F, Wittinghofer A. The Ras-RasGAP complex: structural basis for GTPase activation and its loss in oncogenic Ras mutants. Science 277, 333–338 (1997).

Schubbert S, Zenker M, Rowe SL, Böll S, Klein C, Bollag G, van der Burgt I, Musante L, Kalscheuer V, Wehner LE, Nguyen H, West B, Zhang KY, Sistermans E, Rauch A, Niemeyer CM, Shannon K, Kratz CP. Germline KRAS mutations cause Noonan syndrome. Nature Genet. 38, 331–336 (2006).

Sears R, Nuckolls F, Haura E, Taya Y, Tamai K, Nevins JR. Multiple Ras-dependent phosphorylation pathways regulate Myc protein stability. Genes Dev. 2000 Oct 1;14(19):2501-14.

Serrano M, Lin AW, McCurrach ME, Beach D, Lowe SW. Oncogenic ras provokes premature cell senescence associated with accumulation of p53 and p16INK4a. Cell. 1997 Mar 7;88(5):593-602.

Shi, Y. & Massague, J. Mechanisms of TGF-β signaling from cell membrane to the nucleus. Cell 113, 685–700 (2003).

Shih DQ, Screenan S, Munoz KN, Philipson L, Pontoglio M, Yaniv M, Polonsky KS, Stoffel M.. 2001. Loss of HNF-1alpha function in mice leads to abnormal expression of genes involved in pancreatic islet development and metabolism. Diabetes 50:2472–80

Shikata K, Kukita Y, Matsumoto T, Esaki M, Yao T, Mochizuki Y, Hayashi K, Iida M. Gastric juvenile polyposis associated with germline SMAD4 mutation. Am J Med Genet A. 2005; 134:326-9.

Si-Tayeb K, Lemaigre FP, Duncan SA. Organogenesis and development of the liver. Dev Cell. 2010 Feb 16;18(2):175-89.

Sigal, A. & Rotter, V. Oncogenic mutations of the p53 tumor suppressor: the demons of the guardian of the genome. Cancer Res. 60, 6788–6793 (2000).

Sirard C, de la Pompa JL, Elia A, Itie A, Mirtsos C, Cheung A, Hahn S, Wakeham A, Schwartz L, Kern SE, Rossant J, Mak TW. The tumor suppressor gene Smad4/Dpc4 is required for gastrulation and later for anterior development of the mouse embryo. Genes Dev. 1998 Jan 1;12(1):107-19.

Sjöblom T, Jones S, Wood LD, Parsons DW, Lin J, Barber TD, Mandelker D, Leary RJ, Ptak J, Silliman N, Szabo S, Buckhaults P, Farrell C, Meeh P, Markowitz SD, Willis J, Dawson D, Willson JK, Gazdar AF, Hartigan J, Wu L, Liu C, Parmigiani G, Park BH, Bachman KE, Papadopoulos N, Vogelstein B, Kinzler KW, Velculescu VE. (2006). The consensus coding sequences of human breast and colorectal cancers. Science 314, 268–274.

Sladek FM. What are nuclear receptor ligands? Mol Cell Endocrinol. 2011 Mar 1;334(1-2):3-13.

Sladek, FM, Zhong, WM, Lai E, and Darnell JE Jr. (1990) Genes Dev.4, 2353–2365

Smith S, Giriat I, Schmitt A, de Lange T. Tankyrase, a poly (ADP-ribose) polymerase at human telomeres. Science. 1998 Nov 20;282(5393):1484-7.

Smits R, Kielman MF, Breukel C, Zurcher C, Neufeld K, Jagmohan-Changur S, Hofland N, van Dijk J, White R, Edelmann W, Kucherlapati R, Khan PM, Fodde R. Apc1638T: a mouse model delineating critical domains of the adenomatous polyposis coli protein involved in tumorigenesis and development. Genes Dev. 13, 1309–1321 (1999).

Spaderna S, Schmalhofer O, Wahlbuhl M, Dimmler A, Bauer K, Sultan A, Hlubek F, Jung A, Strand D, Eger A, Kirchner T, Behrens J, Brabletz T. The transcriptional repressor ZEB1 promotes metastasis and loss of cell polarity in cancer. Cancer Res. 2008 Jan 15;68(2):537-44.

Starr TK, Allaei R, Silverstein KA, Staggs RA, Sarver AL, Bergemann TL, Gupta M, O'Sullivan MG, Matise I, Dupuy AJ, Collier LS, Powers S, Oberg AL, Asmann YW, Thibodeau SN, Tessarollo L, Copeland NG, Jenkins NA, Cormier RT, Largaespada DA. A transposon-based genetic screen in mice identifies genes altered in colorectal cancer. Science. 2009; 323:1747-50.

Stoffel M, Duncan SA. The maturity-onset diabetes of the young (MODY1) transcription factor HNF4alpha regulates expression of genes required for glucose transport and metabolism. Proc Natl Acad Sci U S A. 1997 Nov 25; 94(24):13209-14.

Stoffers DA, Ferrer J, Clarke WL, Habener JF. 1997. Early-onset type-II diabetes mellitus (MODY4) linked to IPF1. Nat. Genet. 17:138–39

Streeper, R. S., Svitek, C. A., Chapman, S., Greenbaum, L. E., Taub, R., and O'Brien, R. M. (1997) J. Biol. Chem. 272, 11698–11701

Strom A, Bonal C, Ashery-Padan R, Hashimoto N, Campos ML, Trumpp A, Noda T, Kido Y, Real FX, Thorel F, Herrera PL. Unique mechanisms of growth regulation and tumor suppression upon Apc inactivation in the pancreas. Development 134, 2719–2725 (2007).

Subramanian G, Schwarz RE, Higgins L, McEnroe G, Chakravarty S, Dugar S, Reiss M. Targeting endogenous transforming growth factor β receptor signaling in SMAD4-deficient

human pancreatic carcinoma cells inhibits their invasive phenotype. Cancer Res 2004; 64: 5200–11.

Szafranska AE, Doleshal M, Edmunds HS, Gordon S, Luttges J, Munding JB, Barth RJ Jr, Gutmann EJ, Suriawinata AA, Marc Pipas J, Tannapfel A, Korc M, Hahn SA, Labourier E, Tsongalis GJ. Analysis of microRNAs in pancreatic fine-needle aspirates can classify benign and malignant tissues. Clin Chem 2008; 54: 1716–24.

Tada M, Omata M, Kawai S, Saisho H, Ohto M, Saiki RK, Sninsky JJ. Detection of ras gene mutations in pancreatic juice and peripheral blood of patients with pancreatic adenocarcinoma. Cancer Res. 1993 Jun 1;53(11):2472-4.

Takacs CM, Baird JR, Hughes EG, Kent SS, Benchabane H, Paik R, Ahmed Y. Dual positive and negative regulation of wingless signaling by adenomatous polyposis coli. Science. 2008 Jan 18;319(5861):333-6.

Takagi S, Nakajima M, Kida K, Yamaura Y, Fukami T, Yokoi T.MicroRNAs regulate human hepatocyte nuclear factor 4alpha, modulating the expression of metabolic enzymes and cell cycle. J Biol Chem. 2010 Feb 12;285(7):4415-22. doi: 10.1074/jbc.M109.085431.

Takaku K, Oshima M, Miyoshi H, Matsui M, Seldin MF, Taketo MM., 1998 K. Takaku, M. Oshima, H. Miyoshi, M. Matsui, M.F. Seldin, M.M. Taketo. Intestinal tumorigenesis in compound mutant mice of both Dpc4 (Smad4) and Apc genes. Cell, 92 (1998), pp. 645–656

Terzian T, Suh YA, Iwakuma T, Post SM, Neumann M, Lang GA, Van Pelt CS, Lozano G. The inherent instability of mutant p53 is alleviated by Mdm2 or p16INK4a loss. Genes Dev. 2008 May 15;22(10):1337-44.

Thiagalingam S, Lengauer C, Leach FS, Schutte M, Hahn SA, Overhauser J, Willson JK, Markowitz S, Hamilton SR, Kern SE, Kinzler KW, Vogelstein B. Evaluation of candidate tumour suppressor genes on chromosome 18 in colorectal cancers. Nat Genet 1996; 13: 343–6.

Tidyman, W. E. & Rauen, K. A. Noonan, Costello and cardio-facio-cutaneous syndromes: dysregulation of the Ras-MAPK pathway. Expert Rev. Mol. Med. 10, e37 (2008).

Tirona RG, Lee W, Leake BF, Lan LB, Cline CB, Lamba V, Parviz F, Duncan SA, Inoue Y, Gonzalez FJ, Schuetz EG, Kim RB. The orphan nuclear receptor HNF4alpha determines PXR- and CAR-mediated xenobiotic induction of CYP3A4.Nat Med. 2003 Feb;9(2):220-4.

To MD, Wong CE, Karnezis AN, Del Rosario R, Di Lauro R, Balmain A. Kras regulatory elements and exon 4A determine mutation specificity in lung cancer. Nature Genet. 40, 1240–1244 (2008).

Toledo F, Wahl GM. Regulating the p53 pathway: in vitro hypotheses, in vivo veritas. Nat Rev Cancer. 2006 Dec;6(12):909-23.

Tsukazaki T, Chiang TA, Davison AF, Attisano L, Wrana JL. SARA, a FYVE domain protein that recruits Smad2 to the TGFbeta receptor. Cell 1998; 95:779–791.

Tuveson DA, Shaw AT, Willis NA, Silver DP, Jackson EL, Chang S, Mercer KL, Grochow R, Hock H, Crowley D, Hingorani SR, Zaks T, King C, Jacobetz MA, Wang L, Bronson RT, Orkin SH, DePinho RA, Jacks T. Endogenous oncogenic K-ras (G12D) stimulates proliferation and widespread neoplastic and developmental defects. Cancer Cell 2004 5, 375–387.

Umanoff, H., Edelmann, W., Pellicer, A. & Kucherlapati, R. The murine N-ras gene is not essential for growth and development. Proc. Natl Acad. Sci. USA 92, 1709–1713 (1995).

Fantin VR, St-Pierre J, Leder P. Attenuation of LDH-A expression uncovers a link between glycolysis, mitochondrial physiology, and tumor maintenance. Cancer Cell. 2006 Jun;9(6):425-34.

Large genomic deletions of SMAD4, BMPR1A and PTEN in juvenile polyposis.

van Hattem WA, Brosens LA, de Leng WW, Morsink FH, Lens S, Carvalho R, Giardiello FM, Offerhaus GJ.

Gut. 2008 May;57(5):623-7. doi: 10.1136/gut.2007.142927 Vander Heiden MG, Cantley LC, Thompson CB. Understanding the Warburg effect: the metabolic requirements of cell proliferation Science. 2009 May 22;324(5930):1029-33.

Verdeguer F, Le Corre S, Fischer E, Callens C, Garbay S, Doyen A, Igarashi P, Terzi F, Pontoglio M. A mitotic transcriptional switch in polycystic kidney disease. Nat Med. 2010 Jan;16(1):106-10. doi: 10.1038/nm.2068.

Vincent A, Ducourouble MP, Van Seuningen I. Epigenetic regulation of the human mucin gene MUC4 in epithelial cancer cell lines involves both DNA methylation and histone modifi cations mediated by DNA methyltransferases and histone deacetylases. FASEB J 2008; 22: 3035–45.

Vincent, A, Joseph Herman, Rich Schulick, Ralph H Hruban, Michael Goggins; Pancreatic cancer Lancet, Vol 378 August 13, 2011

Viollet B, Andreelli F, Jørgensen SB, Perrin C, Geloen A, Flamez D, Mu J, Lenzner C, Baud O, Bennoun M, Gomas E, Nicolas G, Wojtaszewski JF, Kahn A, Carling D, Schuit FC, Birnbaum MJ, Richter EA, Burcelin R, Vaulont S. The AMP-activated protein kinase alpha2 catalytic subunit controls whole-body insulin sensitivity. J Clin Invest. 2003 Jan;111(1):91-8.

Vogelstein B, Kinzler KW. 2004. Cancer genes and the pathways they control. Nat. Med. 10:789–99

Vousden KH, Lane DP. p53 in health and disease. Nat Rev Mol Cell Biol. 2007 Apr;8(4):275-83.

Wang RH, Li C, Xu X, Zheng Y, Xiao C, Zerfas P, Cooperman S, Eckhaus M, Rouault T, Mishra L, Deng CX. A role of SMAD4 in iron metabolism through the positive regulation of hepcidin expression. Cell Metab. 2005 Dec;2(6):399-409.

Waxman DJ, Holloway MG. Sex differences in the expression of hepatic drug metabolizing enzymes. Mol Pharmacol. 2009 Aug;76(2):215-28.

Weeraratna AT, Jiang Y, Hostetter G, Rosenblatt K, Duray P, Bittner M, Trent JM. Wnt5a signaling directly affects cell motility and invasion of metastatic melanoma. Cancer Cell 1, 279–288 (2002).

Weinhouse S. The Warburg hypothesis fifty years later. Z Krebsforsch Klin Onkol Cancer Res Clin Oncol. 1976;87(2):115-26.

Wellner U, Schubert J, Burk UC, Schmalhofer O, Zhu F, Sonntag A, Waldvogel B, Vannier C, Darling D, zur Hausen A, Brunton VG, Morton J, Sansom O, Schüler J, Stemmler MP, Herzberger C, Hopt U, Keck T, Brabletz S, Brabletz T. The EMT-activator ZEB1 promotes tumorigenicity by repressing stemness-inhibiting microRNAs. Nat Cell Biol. 2009 Dec;11(12):1487-95.

Wilentz RE, Iacobuzio-Donahue CA, Argani P, McCarthy DM, Parsons JL, Yeo CJ, Kern SE, Hruban RH. Loss of expression of Dpc4 in pancreatic intraepithelial neoplasia: evidence that DPC4 inactivation occurs late in neoplastic progression. Cancer Res. 2000;60:2002–2006.

Wilentz RE, Su GH, Dai JL, Sparks AB, Argani P, Sohn TA, Yeo CJ, Kern SE, Hruban RH: Immunohistochemical labeling for dpc4 mirrors genetic status in pancreatic adenocarcinomas : a new marker of DPC4 inactivation. Am J Pathol 2000; 156: 37–43.

Willert K, Brown JD, Danenberg E, Duncan AW, Weissman IL, Reya T, Yates JR 3rd, Nusse R.. Wnt proteins are lipid-modified and can act as stem cell growth factors. Nature 2003 423:448–52

Wingo SN, Gallardo TD, Akbay EA, Liang MC, Contreras CM, Boren T, Shimamura T, Miller DS, Sharpless NE, Bardeesy N, Kwiatkowski DJ, Schorge JO, Wong KK, Castrillon DH.. Somatic LKB1 mutations promote cervical cancer progression. PLoS ONE 4, e5137 (2009).

Wrighton KH, Lin X, Yu PB, Feng XH. Transforming Growth Factor {beta} Can Stimulate Smad1 Phosphorylation Independently of Bone Morphogenic Protein Receptors. J Biol Chem. 2009 Apr 10;284(15):9755-63.

Xu Q, Wang Y, Dabdoub A, Smallwood PM, Williams J, Woods C, Kelley MW, Jiang L, Tasman W, Zhang K, Nathans J. 2004. Vascular development in the retina and inner ear: control by Norrin and Frizzled-4, a high-affinity ligand-receptor pair. Cell 116:883–95

Yachida S, Jones S, Bozic I, Antal T, Leary R, Fu B, Kamiyama M, Hruban RH, Eshleman JR, Nowak MA, Velculescu VE, Kinzler KW, Vogelstein B, Iacobuzio-Donahue CA. Distant metastasis occurs late during the genetic evolution of pancreatic cancer. Nature 2010; 467: 1114–17.

Yagi K, Goto D, Hamamoto T, Takenoshita S, Kato M, Miyazono K. Alternatively spliced variant of SMAD2 lacking exon 3. Comparison with wild-type SMAD2 and SMAD3. J. Biol. Chem. 274, 703–709 (1999).

Yanagawa S, Matsuda Y, Lee JS, Matsubayashi H, Sese S, Kadowaki T, Ishimoto A. 2002. Casein kinase I phosphorylates the Armadillo protein and induces its degradation in Drosophila. EMBO J. 21:1733–42

Yang G, Rosen DG, Zhang Z, Bast RC Jr, Mills GB, Colacino JA, Mercado-Uribe I, Liu J. The chemokine growth-regulated oncogene 1 (Gro-1) links RAS signaling to the senescence of stromal fibroblasts and ovarian tumorigenesis. 2006 Proc. Natl Acad. Sci. USA 103, 16472–16477

Yeh TY, Beiswenger KK, Li P, Bolin KE, Lee RM, Tsao TS, Murphy AN, Hevener AL, Chi NW. Hypermetabolism, hyperphagia, and reduced adiposity in tankyrase-deficient mice. Diabetes. 2009 Nov;58(11):2476-85.

Yonish-Rouach E, Resnitzky D, Lotem J, Sachs L, Kimchi A, Oren M. Wild-type p53 induces apoptosis of myeloid leukaemic cells that is inhibited by interleukin-6. Nature 352, 345–347 (1991).

Yoon, J. C., Puigserver, P., Chen, G., Donovan, J., Wu, Z., Rhee, J., Adelmant, G., Stafford, J., Kahn, C. R., Granner, D. K., Newgard, C. B. and Spiegelman, B. M.: Control of hepatic gluconeogenesis through the transcriptional coactivator PGC-1. Nature, 413: 131–138 (2001).

Yost C, Torres M, Miller JR, Huang E, Kimelman D, Moon RT. 1996. The axis-inducing activity, stability, and subcellular distribution of beta-catenin is regulated in Xenopus embryos by glycogen synthase kinase 3. Genes Dev. 10:1443–54

Yu HM, Jerchow B, Sheu TJ, Liu B, Costantini F, Puzas JE, Birchmeier W, Hsu W. The role of Axin2 in calvarial morphogenesis and craniosynostosis. Development 2005 132:1995–2005.

Yu PB, Deng DY, Lai CS, Hong CC, Cuny GD, Bouxsein ML, Hong DW, McManus PM, Katagiri T, Sachidanandan C, Kamiya N, Fukuda T, Mishina Y, Peterson RT, Bloch KD. BMP

type I receptor inhibition reduces heterotopic [corrected] ossification. Nat Med. 2008b Dec;14(12):1363-9.

Yu PB, Hong CC, Sachidanandan C, Babitt JL, Deng DY, Hoyng SA, Lin HY, Bloch KD, Peterson RT. Dorsomorphin inhibits BMP signals required for embryogenesis and iron metabolism. Nat Chem Biol. 2008 Jan;4(1):33-41.

Z. Chen, E. A. Odstrcil, B. P. Tu, S. L. McKnight, Science 316, 1916 (2007).

Zaninovic V, Gukovskaya AS, I. Gukovsky, M. Mouria and S. J. Pandol (2000). "Cerulein upregulates ICAM-1 in pancreatic acinar cells, which mediates neutrophil adhesion to these cells". Am J Physiol Gastrointest Liver Physiol 279 (4): G666–676. PMID 11005752.1835000

Zaret KS, Grompe M. Generation and regeneration of cells of the liver and pancreas. Science. 2008 Dec 5;322(5907):1490-4. Review.

Zhong W, Sladek FM, Darnell JE Jr. The expression pattern of a Drosophila homolog to the mouse transcription factor HNF-4 suggests a determinative role in gut formation. EMBO J. 1993 Feb;12(2):537-44.

Zhou G, Myers R, Li Y, Chen Y, Shen X, Fenyk-Melody J, Wu M, Ventre J, Doebber T, Fujii N, Musi N, Hirshman MF, Goodyear LJ, Moller DE. Role of AMP-activated protein kinase in mechanism of metformin action. J Clin Invest. 2001 Oct;108(8):1167-74.